Primary T-cell responses against SARS-CoV-2 in patients with hematological disorders

Pothast, C.R.

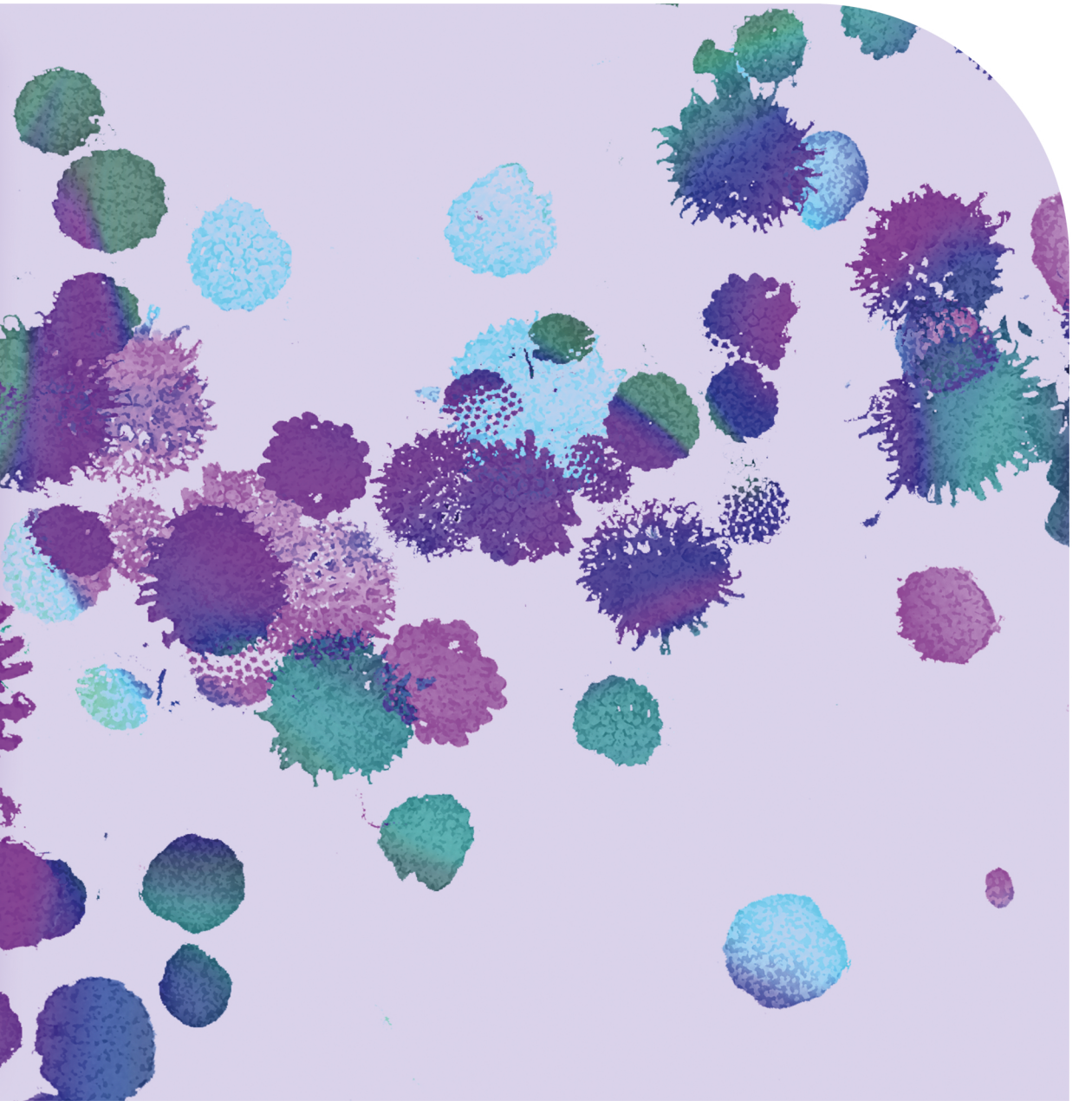

Primary
T-CELL RESPONSES AGAINST SARS-COV-2
in patients with hematological disorders

Cilia Rosan Pothast

PRIMARY T-CELL RESPONSES AGAINST SARS-COV-2 IN PATIENTS WITH HEMATOLOGICAL DISORDERS

Cilia Rosan Pothast

Cover design: Michelle van Andel and Cilia Pothast
Layout: Arul Raja | www.ridderprint.nl
Print: www.ridderprint.nl

ISBN: 978-94-6522-994-2

Primary T-cell responses against SARS-CoV-2 in patients with hematological disorders

Proefschrift

ter verkrijging van

de graad van doctor aan de Universiteit Leiden,

op gezag van rector magnificus prof.dr. S. de Rijcke,

volgens besluit van het college voor promoties

te verdedigen op donderdag 12 februari 2026

klokke 16:00 uur

door

Cilia Rosan Pothast

geboren te Almelo

in 1994

Promotor(es)

Prof. dr. M.H.M. Heemskerk

Prof. dr. J.H.F. Falkenburg

Leden promotiecommissie

Prof. dr. R. Arens

Dr. A.H.E. Roukens

Dr. R. de Vries (Erasmus MC)

Prof. dr. C.A.C.M. van Els (RIVM, universiteit Utrecht)

TABLE OF CONTENTS

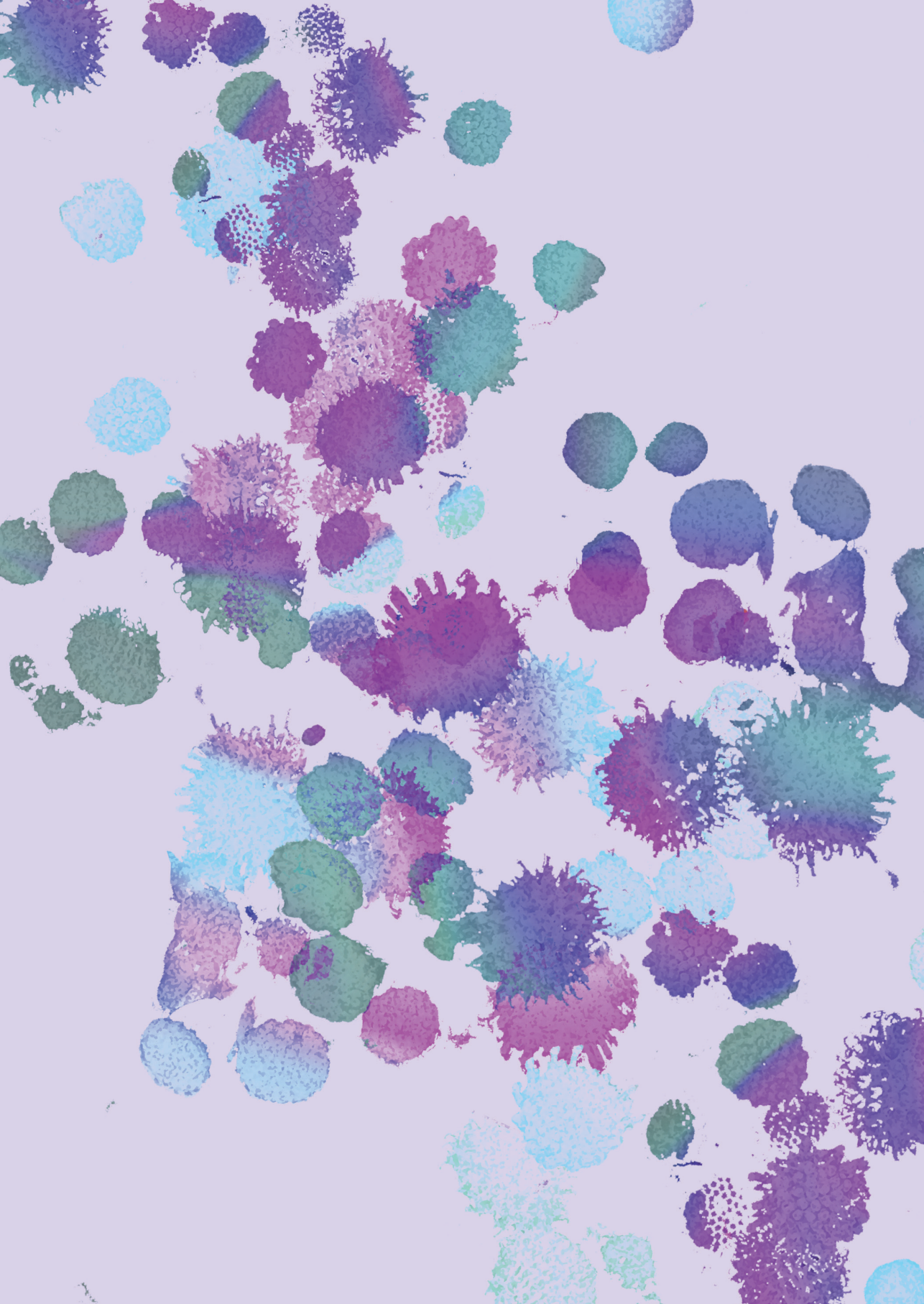

GENERAL INTRODUCTION

Chapter 1

1 SARS-COV-2

1.1 Pandemic

Severe Acute Respiratory Syndrome Coronavirus 2 (SARS-CoV-2) was first identified in December 2019, leading to a pandemic in 2020.[1] The pandemic and the relative severity of symptoms, ranging from asymptomatic to severe coronavirus disease 2019 (COVID-19), induced by SARS-CoV-2 were largely caused by the fact that mankind had never been exposed to this virus and therefore did not possess an existing memory immune response. Since the emergence of SARS-CoV-2, efforts have been made to gain insight into the underlying mechanisms that might explain the large heterogeneity in disease severity. These efforts have been essential to determine which individuals are susceptible to severe disease and who should therefore be prioritized for enhanced protective measures against infection. Fortunately, vaccines against SARS-CoV-2 were quickly developed due to the rapid identification of the full SARS-CoV-2 sequence, availability of mRNA vaccine technology, and parallelization of developmental processes.[1,2] Since 2021, most individuals have developed a memory immune response against SARS-CoV-2 due to vaccination or infection, thereby ending the pandemic.[3] During the pandemic, massive efforts have been made by the scientific community to understand the virus or infection, resulting in the biobanking of samples from before and during the pandemic. These valuable samples offer a unique opportunity to investigate the development of the immune system after an encounter with a new virus.

1.2 Infection

SARS-CoV-2 is part of the beta coronaviruses, which also include the common coronaviruses OC43 and HKU1, as well as SARS-CoV-1 and MERS.[4] The virus comprises a lipid bilayer containing the spike protein, membrane protein, and envelope, which encapsulates the positive, single-stranded ribonucleic acid (RNA) and nucleocapsid protein. The spike protein is essential for viral cell entry as its receptor-binding domain (RBD) directly binds to angiotensin-converting enzyme 2 (ACE-2), which is expressed by, among others, human epithelial cells in the respiratory tract.[5] SARS-CoV-2 therefore predominantly targets the upper and lower respiratory systems. Virus RNA is released inside the cells and translated into polypeptides and enzymes that are needed for transcription and translation of the viral genome. New virus particles are generated and released from the human cell. This process results in rapid replication of new virus particles and severe damage to the cells, leading to pyroptosis.

1.3 Host Immune Response

Infection by SARS-CoV-2 causes pyroptosis of the host cells, causing the release of pathogen-associated molecular patterns (PAMPs) and damage-associated molecular patterns (DAMPs).[6,7] These danger signals are recognized by pattern-recognition receptors (PRRs) expressed by innate immune cells (monocytes, macrophages, neutrophils, dendritic cells, and natural killer cells), which in turn release pro-inflammatory cytokines such as interferon-I/III (IFN-I/III), and chemokines. Pro-inflammatory cytokines and chemokines attract more immune cells including the adaptive immune system (T and B cells), further enhancing the pro-inflammatory environment. Cells of the innate immune system are fast responders and are important for local enhancement of a pro-inflammatory environment, clearing infected cells, and functioning as antigen-presenting cells (APCs) for the adaptive immune system. The adaptive immune system is initially slower but targets the virus specifically.[8] Helper CD4+ T cells have a wide array of functions that include supporting the function of innate cells, B cells, and CD8+ T cells by expressing stimulatory receptors and producing cytokines. Cytotoxic CD8+ T cells recognize cells that are infected by the virus specifically and kill the infected cells. B cells produce antibodies that can neutralize the virus itself, resulting in opsonization and blocking of viral entry. A fast and effective response of the innate and adaptive immune response limits viral spreading and reduces further damage to human cells.

1.4 COVID-19

Most healthy individuals clear SARS-CoV-2 infections with mild respiratory symptoms. However, in contrast to influenza infections, SARS-CoV-2 infections can also lead to gastrointestinal and neurological damage, and a higher percentage of SARS-CoV-2 infections lead to severe disease.[9] Patients with severe disease mainly suffer from pneumonia that can further develop into acute respiratory distress syndrome (ARDS). Autopsies revealed that most patients were indeed deceased due to ARDS (53%), but also multi-organ failure (18%) or heart complications (7%).[10] These complications are caused by tissue damage induced by the virus, but also by overactivation of the immune system. This is caused by delayed viral clearance due to immune-evasion mechanisms of the virus, combined with a delayed immune response and inability to limit overactivation.[8,11] Delayed viral clearance results in a high viral load and therefore an excessive release of PAMPs and DAMPs, which in turn results in highly activated and infiltration of innate immune cells into the lungs.[11] Ineffective initiation of the adaptive immune system further enhances the prolonged presence of the virus. Due to the high viral load, both the innate and adaptive immune responses become overactivated. Subsequently, these patients are unable to dampen this

excessive activation of the immune system. This is a clear hallmark of severe COVID-19 since hyperactivated cells and a cytokine storm can be detected in lung tissues and circulation.[11,12] Therefore, it is proposed that the timing and magnitude of the immune response are mismatched, resulting in excessive tissue damage.[11] Some individuals have trouble fully recovering and develop post-COVID-19 (also known as long COVID-19) with lingering symptoms such as persistent cough, fatigue, and neurological dysfunction.[13] Disease severity varies based on factors that include characteristics of the virus, host factors, and environmental factors.[14] The main host risk factors for severe COVID-19 include factors that enhance symptoms of COVID-19 such as respiratory diseases, cardiovascular diseases, and higher body mass index, or factors that disrupt normal immune function such as diabetes, primary immune deficiencies, or immunosuppressive treatment.[15-17] Another host factor that impacts disease outcome is vaccination, as vaccination results in the initiation of a fast and effective adaptive immune response, thereby limiting viral spread.

1.5 Vaccines

Vaccination is an effective method to induce an immune response against pathogens. Vaccines are designed to activate the adaptive immune system since these cells are pathogen-specific and can result in long-lasting immune memory. Different vaccine types exist for viral infections, which differ in the amount of antigens, protein delivery method, immunogenicity, and adjuvants, which can be roughly subdivided into: live attenuated, inactivated, vector, subunit, or DNA/RNA.[18] Live attenuated vaccines contain the live virus, but the virus is weakened to prevent disease, and initiate a strong immune response. For some vaccines, the virus particles are inactivated or killed, which is called an inactivated vaccine, and often require boosters since they are less effective compared to live attenuated vaccines. Vector vaccines typically consist of a different weak virus (vector) that is genetically modified to express proteins of the virus that the aim is to vaccinate against. Depending on the choice of vector virus, the vaccine might be less effective since individuals may already have developed immunity against the vector virus, or the vector virus is not sufficiently immunogenic. Subunit vaccines do not contain genetic material but are composed of purified proteins, peptides, polysaccharides, or a combination of two subunits (conjugate vaccines). DNA/RNA vaccines contain DNA or RNA that encodes for viral proteins, and are easy to develop but may be less effective. The most commonly administered SARS-CoV-2 vaccines are mRNA-based vaccines. Vaccines based on mRNA technology are not new, as the publication of the first pre-clinical trial dates back to 1993, and the first-in-human clinical trial was in 2017.[19,20] As the name suggests, messenger RNA (mRNA) vaccines consist of mRNA encoding the antigen of interest and are encapsulated by a (ionizable) lipid nanoparticle (LNP). The LNPs ensure efficient delivery of the mRNA

inside cells[21] but also act as an adjuvant.[22] The design of the mRNA and LNP can differ between different vaccines. In the case of the SARS-CoV-2 mRNA vaccines, the mRNA encodes for the full-length stabilized spike protein of the virus, flanked by the 5'- and 3'-untranslated regions. Currently, three companies have developed SARS-CoV-2 mRNA vaccines, but most individuals from the Dutch population have been vaccinated with the BNT162b2 (Pfizer/BioNTech) or mRNA-1273 (Moderna) vaccine. Although they are both LNP-mRNA vaccines, they differ in dosage, design of the LNP, and modifications to the mRNA such as capping method, codon optimizations, and choice of polyadenylation tail.[23]

1.6 mRNA vaccination

The vaccine is injected intramuscularly, causing a local transient infiltration of immune cells and uptake of the LNP-mRNAs mostly by muscle cells, monocytes, and dendritic cells through endocytosis.[24] The mRNA is released from the endosomes and translated into the spike protein. The spike protein is expressed on the cell surface as a protein and degraded into peptides in the cytosol. These peptides are subsequently loaded onto human leukocyte antigen (HLA) molecules and are presented as complexes on the cell surface. The transiently transfected dendritic cells migrate to the draining lymph nodes for presentation of the spike protein to B cells and T cells. Besides expression of the spike antigen, the LNP and mRNA themselves also induce a pro-inflammatory response, such as production of IFN-I by the transfected muscle and immune cells, further enhancing the immune response.[23] Multiple studies have shown that both mRNA vaccines induce long-lived B cells, spike-specific CD4+ and CD8+ T cells in healthy individuals.[25] Both the BNT162b2 and mRNA-1273 induce B-cell and T-cell responses that are detectable in circulation, but the mRNA-1273 induces a more durable humoral response and higher T-cell frequencies.[26] Booster vaccinations, usually meaning a prolonged interval between two vaccinations, enhance the durability of the adaptive immune response. Both vaccines were produced using the ancestral strain of SARS-CoV-2, which resulted in reduced efficacy against new variants of the virus.[27] This was mostly caused by mutations in the RBD, resulting in a reduced ability of neutralizing antibodies to prevent cell entry by binding to the virus.[28] To enhance the efficacy of neutralizing antibodies, both Moderna and BioNTech updated their vaccines to match newer viral variants, resulting in increased vaccine efficacy.[29-32] Interestingly, T-cell responses are less affected by the new variants because T cells typically recognize a wider range of epitopes, making it less likely that viruses can evade T-cell recognition by epitope mutation.[33,34] Furthermore, SARS-CoV-2 mRNA vaccine-induced T-cell responses can persist for a long period and are correlated with protection against severe disease.[34-38]

For these reasons, BioNTech developed a new vaccine (BNT162b4) that focuses on T-cell immunity by including multiple (non-spike) antigens.[39]

1.7 Monitoring

Monitoring of virus-specific immune responses is commonly done by measuring virus-specific antibodies, or immunoglobulins (Ig), titers in the circulation. SARS-CoV-2 infection can lead to antibodies binding to structural, non-structural, and accessory proteins.[40] The current SARS-CoV-2 mRNA vaccines only induce immune responses against the spike protein. For this reason, infection-induced immunity is measured by the presence of anti-nucleocapsid antibodies, whilst vaccine-induced immunity is measured through the presence of anti-spike antibodies in the circulation (in the absence of anti-nucleocapsid antibodies). Furthermore, spike-specific antibodies may be specified based on whether they bind to RBD, as this directly blocks the binding of the virus to human cells. There are five antibody isotypes: IgA, IgD, IgE, IgG, and IgM. For monitoring, IgG concentrations are usually measured because IgG can reach high levels in circulation, is quickly detectable after infection or vaccination, and is highly effective against viruses. Antibodies are measured using qualitative or (semi-)quantitative assays. Qualitative assays only indicate whether antibodies are present, whilst quantitative assays also give a concentration. Semi-quantitative tests give a concentration in a scaling that is specific for the test, whilst quantitative assays give the exact antibody concentration in plasma. The WHO developed International Units IU/ml) for neutralizing antibody levels and binding antibody units per milliliter (BAU/ml) for binding assays, so that the concentration levels are directly comparable between institutes.[41] The focus on antibody monitoring as a proxy for vaccine-induced immunity can be explained by the ease of antibody measurement and that the measurements are standardized between institutes. However, focusing on antibodies ignores the presence of T-cell-mediated immunity. Measuring T cells becomes especially important when realizing that antibodies wane in time, and some individuals might have trouble developing adequate antibody levels, but can induce strong T-cell responses.

2 T CELLS

2.1 Antigen

The antigens recognized by T cells are peptide-HLA complexes on the cell surface of other cells. These complexes consist of peptides presented in the context of HLA class I or II.[42] Intracellular proteins are degraded by the proteasome into peptides and are transported into the endoplasmic reticulum (ER). In the ER, the peptides

are loaded onto the peptide-binding groove of HLA class I and transported through the Golgi apparatus to the cell surface. For HLA class II, this process is slightly different. Exogenous proteins are encapsulated into endosomes, which contain enzymes that degrade the protein into peptides. These endosomes fuse with MHC class II compartments, which contain HLA class II molecules that are stabilized with class II-associated invariant chain peptide (CLIP).[43] The peptide replaces CLIP and the peptide-HLA complex is transported to the cell surface of APCs. Through these processes, peptides from intracellular proteins are presented in HLA class I, whilst peptides that are present extracellularly are typically presented in HLA class II. Which peptide is presented depends on the HLA type. HLA-A, HLA-B, and HLA-C are class I molecules that typically present 8-11 amino acid-long peptides to CD8+ T cells. HLA-DP, HLA-DQ, and HLA-DR are class II molecules that typically present 10-15 amino acid-long peptides to CD4+ T cells. These HLA loci are (highly) polymorphic and consist of different allotypes that differ in amino acids, mainly in the peptide-binding groove. This variation results in differences in which peptides have the highest binding affinity to which HLA isoform. For HLA class I, the peptide-binding motifs typically have an anchor residue at positions 2 and 9, which are essential for binding to the HLA. The peptide-binding motif is less strict for HLA class II, resulting in a larger variability in peptides that can bind to the same HLA. Furthermore, the pockets of HLA class II are open at the ends, resulting in a larger heterogeneity of peptide lengths. Therefore, which peptides are presented in a cell depends on the HLA type of the individual. The more diverse the two alleles for each HLA gene, the wider the diversity of peptides that are presented on a cell. It is therefore generally accepted that a more diverse HLA-type generates a wider T-cell response and therefore enhances protection against pathogens.

2.2 TCR

T cells recognize peptide-HLA complexes through their T-cell receptor (TCR). This interaction (signal 1), together with co-stimulation (signal 2) and cytokines (signal 3), triggers T-cell activation and therefore forms an essential part of T-cell-mediated immunity. Before T cells can exert these functions, they undergo a process of differentiation and selection. T cells originate from hematopoietic stem cells in the bone marrow, from where they travel as lymphoid progenitors to the thymus.[44] In the thymus, the gene encoding for the β-chain of the TCR undergoes rearrangement and pairs with a pre-TCR α-chain to ensure the functionality of the β-chain. After successful β-chain rearrangement, the α-chain starts its rearrangement. Germline *TRB* and *TRA* genes consist of multiple variable and joining segments, and variable segments are rearranged to a joining segment through somatic recombination. The rearrangement of the α-chain and β-chain is not completely the same. *TRA* contains only a single

constant region, whilst *TRB* has two constants. For the α-chain, both *TRA* alleles undergo rearrangement simultaneously, yielding two functional α-chains in ~20% of the cells. This process of rearrangement results in three complementary-determining loops (CDR1-3) in both chains, which are important for binding to the antigen. CDR1 and CDR2 are homologous among TCRs, whilst the CDR3 region is highly diverse due to genetic alterations during joining of segments and therefore is an important factor in dictating TCR specificity and diversity. After the formation of the TCR, the thymocytes undergo selection to eliminate thymocytes that are auto-reactive or lack reactivity at all. This is achieved by programmed apoptosis of thymocytes with TCRs that lack or have a too high binding affinity to peptide-HLA complexes expressed on cortical thymic epithelial cells. Part of the thymocytes with a higher affinity for self-peptide-HLA complexes may be selected to become regulatory T cells. Selected thymocytes are further matured, and cells that weakly recognize a self-peptide in HLA class I will remain single positive for CD8, whilst thymocytes that express a TCR that binds to HLA class II will only express the CD4 co-receptor. Due to the high sequence variability of TCRs, TCRs have a large diversity in binding affinity and specificity towards peptide-HLA combinations. TCRs are considered highly specific given the large diversity of potential peptide–HLA combinations and the limited number of peptide-HLA complexes a single TCR can recognize.[45-48] Recognition of more than one peptide-HLA complex by a single TCR is referred to as cross-reactivity, which can result from multiple mechanisms.[49-56] In most cases, cross-reactivity is caused by peptide-HLA complexes that share sequence or structural homology. Another mechanism is hotspot binding, a phenomenon in which the TCR strongly binds to only a few amino acids of the peptide. TCRs with hotspot binding are therefore more forgiving when amino acids change outside the hotspot. Apart from the reduced footprint of the TCR, cross-reactivity may also be caused by the plasticity of the TCR and peptide-HLA complex. The TCR and peptide-HLA complex may undergo conformational changes upon binding, potentially strengthening the binding. These forms of TCR and peptide-HLA cross-reactivity expand T-cell reactivity towards a wide range of pathogens, called heterologous immunity. However, cross-reactivity may also cause problems, as seen in auto-immune diseases and alloreactivity in allogeneic transplantation settings.

2.2 Differentiation

CD4+ or CD8+ T cells leave the thymus and start circulating in the blood and lymphoid organs. At this stage, they are called naïve T cells and express markers such as CCR7, CD45RA, and CD62L. Upon infection, the pathogen-derived peptides are presented to T cells by antigen-presenting cells (APCs) in lymphoid structures, which triggers T-cell differentiation and proliferation (expansion phase). The T cells leave the lymphoid

structures and recirculate in the blood and migrate to the site of infection.[57,58] After pathogen clearance, most T cells go into apoptosis (contraction phase) and the remaining cells differentiate into central memory (T_{CM}) or effector memory (T_{EM}) cells.[58] Typically, T_{CM} are less capable of producing cytokines but proliferate better compared to T_{EM}. They express lymph node-homing receptors such as CCR7 and CD62L. T_{EM} cells lack the expression of these receptors but express more tissue-homing receptors. Additionally, T_{EM} cells may re-express CD45RA which are then termed terminal effector memories (T_{EMRA}). Memory T cells are present throughout the human body and can respond quickly upon re-infection. They do this by quick upregulation of activation markers such as CD137, CD69, and CD154, and production of cytokines, all within a few hours.

2.3 Function

CD4+ T cells, or T-helper cells, are T cells with a wide range of functions with different phenotypes. Effector memory CD4+ T cells can be subdivided into seven subsets based on transcription factor expression and cytokine profile: Th1, Th2, Th9, Th17, Th22, regulatory T cells (Treg) and follicular helper T cells (Tfh).[58] Th1 cells are most important for protection against viruses and bacteria as they produce cytokines such as IFN-γ and TNF-α/β, and may also produce IL-2. These cytokines promote CD8+ T cell and macrophage function.[57] Th2, Th9, Th17, and Th22 typically play a role in other situations such as tissue repair, protection against parasites, fungi, and allergies. Treg express FoxP3 as well as high levels of CD25 and produce inhibitory cytokines IL-10, TGF-β, and IL-35. Compared to helper T cells, Tregs have a higher affinity for self-peptides and are important for dampening the immune response. Tfh cells express high levels of CXCR5 and PD-1, and are specialized in promoting B-cell isotype switching, affinity maturation, and differentiation through secretion of IL-21 and expression of CD40.[57,59] CD8+ T cells, or cytotoxic T cells, are T cells that are specialized in lysing cells that are infected. Upon antigen encounter, they produce cytokines including IFN-γ and TNF-α, and secrete perforin and granzyme B. Perforin induces cytolysis by forming pores in the cell membrane, and granzyme B induces apoptosis by disrupting essential cellular processes in the targeted cell. These cytokines and enzymes result in the effective clearance of diseased cells.

2.4 Monitoring

Monitoring of antigen-specific T cells is more laborious compared to antibodies because the measurement of living cells is more challenging than that of proteins. Similar to antibodies, assays can differentiate between infection-induced and vaccine-induced T-cell responses, depending on whether the antigen used in the monitoring assay is derived from spike (vaccination and infection) or non-spike

proteins (infection).[60] Antigen selection combined with sampling moment is essential to differentiate between pre-existing immunity, primary T-cell responses, and hybrid immunity in the monitoring assay. Samples frozen down before the pandemic, although SARS-CoV-2-unexposed, may contain SARS-CoV-2-specific T cells. These T cells must have been originally primed by another pathogen, developed into memory T cells, and are cross-reactive towards SARS-CoV-2 antigens. Primary T cell responses can typically be detected in samples frozen down in 2020 or 2021. This is because the virus was first described in December 2019, but most individuals in Europe were exposed to SARS-CoV-2 for the first time from March 2020 onwards. In 2021, the first SARS-CoV-2 vaccines were administered. Combined vaccine- and infection-induced immunity (hybrid immunity) occurs more often in later sampling moments since a large proportion of the population received SARS-CoV-2 vaccination, and time increases the chances of exposure to the virus itself. Apart from antigen selection and sampling moment, the method of detection is essential for the accurate interpretation of measured SARS-CoV-2-specific T cell responses.

2.5 Detection methods

Two distinct methods are being used for the detection of antigen-specific T cells: peptide-HLA tetramer staining which measures the presence of antigen-specific T cells, and peptide-stimulation assays which measure functional antigen-specific T cells.[61] Peptide-HLA tetramers consist of four biotinylated peptide-HLA complexes that are conjugated to a streptavidin-labeled fluorochrome. The peptide-HLA complexes used in these detection methods are composed of HLA prevalent alleles binding earlier identified epitopes from the pathogen of interest. Tetramers are incubated with peripheral blood mononuclear cells (PBMCs), T cells that recognize the peptide-HLA tetramers bind to the tetramer and become fluorochrome-labeled which is subsequently detected using flow cytometry. Setting up such staining is labor-intensive, since for each peptide-HLA combination, new tetramers need to be generated. Since HLA types in the population are diverse and various T-cells target multiple antigens, a large library of peptide-HLA tetramers is needed to cover most individuals and T cells. However, this method is generally highly specific, can detect low frequencies of antigen-specific T cells, and does not rely on cell functionality. Once a library of peptide-HLA tetramers is generated, this tool allows for relatively high-throughput analysis. For peptide-stimulation assays, PBMCs are incubated with peptide pools consisting of 15-amino-acid-long peptides with 11-amino-acid overlap translated from immunogenic proteins. These peptides bind to HLA molecules on the surface of APCs in the sample. T cells that recognize the peptide-HLA complexes become activated, express activation markers, and produce cytokines. These markers and cytokines are then used as a detection method for T cells that are specific for

the peptides that were added to the sample. The most common large-scale, high-throughput, methods are enzyme-linked immunosorbent spot (ELIspot) and the interferon-gamma release assay (IGRA). ELIspot captures the secretion of IFN-γ close to the source, resulting in spots that are counted as an estimate of the number of T cells that produce cytokines. IGRA measures a concentration of IFN-γ in supernatant. These assays are relatively standardized as companies offer specialized kits and protocols. Alternatively, the peptide-stimulated PBMCs are incubated with fluorochrome-labeled antibodies that target phenotypic markers combined with activation markers, and/or intracellular cytokines, and are measured using flow cytometry. This is more informative as it allows the measurement of activation markers, multiple cytokines, and which T-cell subset is the source of cytokine production. For peptide-stimulation assays, epitope prediction and HLA-typing are not necessary because hundreds of peptides are added in an HLA-independent manner. Combined with the large-scale measurement methods, peptide-stimulation assays can be used for high-throughput measurement of antigen-specific T cells. However, this method relies on optimal assay settings to ensure the functionality of the cells, and it can be labor-intensive when using flow cytometry. Therefore, depending on the research question, different tools are available. For high-throughput screening of antigen-specific T cells in a large cohort, IGRA or ELIspot assays are the most convenient. However, for more in-depth analysis (e.g., patient-specific) of epitope-specificity and phenotype, peptide-HLA tetramers are more suitable. To study functionality, peptide-stimulation assays combined with flow cytometry allow the most elaborate analysis of T-cell phenotype combined with functionality.

2.5 Immunity

Healthy individuals typically produce robust immune responses against SARS-CoV-2 after a 2-dose mRNA vaccination.[62] Memory responses are measured by detecting the three components of adaptive immunity: B cells, CD4+ T cells, and CD8+ T cells. Affinity-matured memory B-cell frequencies in circulation gradually increase until a peak moment around 3-6 months after vaccination. Neutralizing antibodies are less long-lived since they gradually wane from their peak concentration around two weeks after vaccination. This is thought to be caused by the induction of short-lived plasma cells instead of long-lived plasma cells derived from germinal center B cells. Due to the relatively short presence of neutralizing antibodies (and the emergence of new variants), booster vaccines are part of the vaccination schedule to enhance humoral and T-cell responses. Spike-specific CD4+ T cells are detected in nearly all individuals with peak frequencies within two weeks after vaccination, followed by a slow reduction. The T cells are of Th1 subtype as they produce IFN-γ and TNF-α, part of some cells produce IL-2, or are circulating follicular helper T cells. Spike-

specific CD8+ T cells are more challenging to measure, but more accurate methods show spike-specific CD8+ T cells in ~80% of healthy individuals. The kinetics of the frequencies in time are highly similar to CD4+ T cells. Both T cells and antibodies provide a layer of protection against disease. Antibodies can neutralize and clear viral particles, thereby preventing or reducing infection. T cells are important for the protection against severe disease by lysing virus-infected cells, and are more durable and more effective against new variants of concern.[63-65] Importantly, the antibody and T-cell responses induced by the mRNA vaccines result in a 94-95% efficacy against symptomatic infection with a good safety profile in healthy individuals.[66,67]

3 DISEASE

The SARS-CoV-2 mRNA vaccines can achieve high efficiencies in healthy individuals. However, the efficacy may be reduced when an individual is immunocompromised, as is often observed for patients with hematological malignancies. In specific cases, the disease itself can directly affect the immune system and result in reduced vaccine efficacy. In most cases, the treatment that these patients receive leaves them in an immunocompromised state. Patients may be treated with lymphocyte-depleting therapies, treated for a long period with immunosuppressive drugs, or treated with (high-dose) chemotherapy. Allogeneic stem cell transplantation is commonly offered to patients with high-risk hematological diseases as a curative option and has a large impact on the patient's immune system. Therefore, allogeneic stem cell transplantation will be discussed first, followed by disease- and treatment-specific characteristics of aplastic anemia and the most common hematological malignancies.

3.1 Allogeneic Stem Cell Transplantation

Allogeneic stem cell transplantation is an option for patients whose initial treatment failed or for patients who are at high risk for relapse.[68] Allogeneic stem cell transplantation is used as a therapy in which the patient's stem cells are replaced by stem cells from a healthy donor, allowing an immune response to take place of donor T cells targeting the (malignant) hematopoietic cells from the patient. The patient is first conditioned to eradicate malignant cells and to suppress the patient's immune system to ensure engraftment of the donor stem cells. Pre-conditioning is typically done using chemotherapy with or without radiation or T cell-depleting therapy, anti-thymocyte globulin (ATG) or alemtuzumab (anti-CD52). Pre-conditioning chemotherapies mostly include melphalan, cyclophosphamide, fludarabine, or busulfan. After transplantation, the patients are immunocompromised due to delayed reconstitution of the immune system. Since transplantation depletes

a large part of the pre-existing immune system, patients are often revaccinated. Revaccination is commonly done approximately six months post-transplant to ensure reconstitution of the immune system before vaccination. It remains unclear whether allogeneic transplantation depletes the complete memory immune responses and whether vaccination shortly after transplantation can induce an immune response. This is important since the immunocompromised state of these patients leaves them vulnerable to a severe course after infection. Although potentially only partially effective, revaccination may still provide a layer of protection. Apart from pre-conditioning, patients can become immunocompromised due to immunosuppressive treatments after transplantation. Allogeneic transplantation can induce (severe) graft-versus-host disease due to alloreactive T cells, which can be prevented or treated using post-transplantation immunosuppressive therapies. However, ongoing treatment with immunosuppressive drugs can hamper the induction of vaccine responses.

3.2 Aplastic Anemia

Aplastic Anemia is a rare and severe disease that is characterized by bone marrow hypocellularity.[69] As a result, these patients develop pancytopenia, which affects the normal function of the immune system. The consensus is that aplastic anemia is caused by auto-reactive immune cells targeting hematopoietic stem and progenitor cells. The majority of aplastic anemia patients are treated with immune-depleting strategies consisting of a short course of anti-thymocyte globulin (ATG), combined with long-term use of cyclosporin.[70] Younger patients may also receive allogeneic stem cell transplantation with cyclophosphamide and ATG pre-conditioning, followed by immunosuppression. The lymphodepleting effect of ATG can result in the depletion of existing memory responses. Vaccination during or shortly before ATG treatment might therefore be ineffective. Furthermore, cyclosporin is immunosuppressive, and long-term use can therefore result in an immunocompromised state of the patient.

3.3 Myelodysplastic syndrome

Myelodysplastic syndrome (MDS) is a group of syndromes that is caused by somatic mutations in hematopoietic stem cells, resulting in bone marrow hypercellularity or hypocellularity and pancytopenia due to ineffective hematopoiesis.[71] MDS is linked to multiple genetic abnormalities and the abnormalities may be present in one or multiple lineages. A subclone in MDS may also develop into AML. Patients with low-grade MDS are often monitored but not treated, whereas patients with high-grade MDS may be treated with chemotherapy, including hypomethylating agents (azacytidine). Hypomethylating agents are immune-modulatory drugs, but are not necessarily known as immunosuppressive.[72,73] Some studies show enhanced efficacy due to hypomethylating agents when vaccinating for anti-leukemic effects.

In contrast, hypomethylating agents preferentially target proliferating cells and could thereby target activated cellular responses during vaccination.[74] Therefore, whether these patients reach an immunocompromised state due to long-term use of hypomethylating agents is unclear.

3.4 Myeloproliferative neoplasm

Myeloproliferative neoplasm (MPN) is a separate group of hematopoietic stem cell disorders that includes primary myelofibrosis, polycythemia vera, and essential thrombocytopenia.[75] MPNs are characterized by somatic mutations in JAK2, CALR, and/or MPL, which are important genes in signal-transduction pathways. These mutations consequently disrupt normal hematopoiesis. Patients may be treated with chemotherapy, ruxolitinib, interferon, or allogeneic stem cell transplantation. Ruxolitinib is a JAK2 inhibitor that inhibits the proliferation of hematopoietic stem cells and cytokine signaling. Ruxolitinib is effectively used as a treatment for graft-versus-host disease to dampen mostly the T-cell responses, which strongly suggests that active ruxolitinib treatment can hamper vaccination-induced T-cell responses. This is supported by the fact that ruxolitinib inhibits the signaling of cytokine receptors, which are essential for effective immune cell function.

3.5 CML

Chronic myeloid leukemia (CML) is an MPN that is characterized by malignant BCR-ABL1-positive stem cells.[68] *BCR-ABL1* is a fusion gene that is caused by the chromosome 9 and 22 translocation in a pluripotent hematopoietic stem cell.[76,77] This fusion gene results in the expression of an active tyrosine kinase that drives the formation of CML cells. CML cells gradually displace healthy hematopoiesis, resulting in bone marrow hypercellularity, anemia, and leukocytosis of immature to mature granulocytes. CML can be effectively treated using tyrosine kinase inhibitors (TKI), resulting in complete responses or minimal disease in most patients.[78] In rare cases, CML may eventually develop into acute leukemia. Since the patients are treated with tyrosine kinase inhibitors that mostly target the BCR::ABL1 protein, the healthy immune cells are thought to be minimally affected.

3.6 AML

Acute myeloid leukemia (AML) is a heterogeneous malignancy of myeloid precursor cells and is diagnosed based on the presence of myeloid blast cells in bone marrow, genetic abnormalities, and differentiation state.[79] Genetic abnormalities are variable but most mutations are in genes involved in signaling, DNA methylation, chromatin modification, and more.[80] Genes *FLT3, NMP1,* and *DNMT3A* are mutated in at least 50% of the AML cases.[80] AML cells accumulate in bone marrow, resulting in bone

marrow hypercellularity, leukocytosis, anemia, and thrombocytopenia. Patients with AML are preferentially treated with remission-induction therapy consisting of high-dose chemotherapy (cytarabine), with or without targeted inhibitors (such as FLT3 or IDH1/2 inhibitors) or hypomethylating agents (azacytidine or decitabine), and venetoclax. Patients are usually treated with several courses of chemotherapy followed by allogeneic stem cell transplantation for high-risk AML. Due to the combination and dosage of these therapies, vaccination during active treatment may result in a hampered immune response.

3.7 ALL

Acute lymphocytic leukemia (ALL) is a malignancy of lymphoid precursor cells (mostly from the B cell lineage). Cells transform into ALL due to multiple different genetic alterations of genes that are involved in self-renewal, proliferation, and survival pathways, from which some of them appear more frequently than others. These alterations include hyperdiploidy, chromosomal translocations resulting in altered expression of tyrosine kinases and transcriptional factors, mutations or deletions, and epigenetic changes. Patients often suffer from anemia, neutropenia, and thrombocytopenia as a result of bone marrow failure due to leukemic blast hypercellularity. Furthermore, symptoms may also be related to infiltration into other organs such as the central nervous system. Patients with ALL are often treated with multiple courses of chemotherapy, tyrosine kinase inhibitors, corticosteroids, and/or immunotherapy. Corticosteroids are known immunosuppressants that can dampen active immune responses and can have a lingering effect. Vaccination during or shortly after corticosteroid therapy may result in reduced efficacy of cellular responses. Immunotherapy for ALL commonly includes rituximab, which binds to CD20 on malignant cells, resulting in depletion of rituximab-bound cells. Healthy B cells also express CD20 and are thereby targeted by rituximab as well, resulting in the depletion of vaccine-induced B-cells during treatment. Similarly, bispecific antibody therapy, such as blinatumomab, which redirects T cells towards CD19-expressing malignant and healthy cells, results in depletion of malignant and healthy B cells, including vaccine-induced B-cells during this therapy. Furthermore, ALL patients who enter remission frequently undergo allogeneic stem cell transplantation as a consolidation treatment, which induces as mentioned above an immune-compromised state.

3.8 CLL

Chronic lymphocytic leukemia (CLL) is an indolent B-cell malignancy that causes lymphocytosis of mature B cells.[81,82] B-cell transformation occurs due to genetic alterations that affect B-cell receptor (BCR) signaling and increased expression of proteins that reduce apoptosis in these cells. CLL cells are present in circulation,

bone marrow, secondary lymphoid organs, and other tissues, where they can affect the normal function of immune cells. Untreated patients often have hypogammaglobulinemia due to weakened function of immune cells in circulation and tissues. CLL treatment includes cytostatic chemotherapy (*e.g.,* fludarabine, cyclophosphamide, bendamustine, or chlorambucil), anti-CD20 monoclonal antibody therapy (rituximab or obinutuzumab), Bruton's tyrosine kinase inhibitors (BTKi), and/or venetoclax. Vaccination responses are likely hampered during active treatment of some of these therapies. For example, the chemotherapies given are known to deplete lymphocytes, thereby hampering existing or the induction of both B and T-cell immune responses. Furthermore, BTKi blocks BCR signaling, and rituximab depletes B cells, thereby hampering humoral immune responses.

3.9 DLBCL

Diffuse large B-cell lymphoma (DLBCL) is the most prevalent aggressive mature B-cell malignancy. Genetic alterations are heterogeneous in DLBCL, which has resulted in subclassifications of DLBCL based on genetic abnormalities that could give a more accurate prognosis such as rearrangements in *MYC, BCL2,* and/or *BCL6*. Most patients have enlarged lymph nodes due to the accumulation of malignant cells. Patients are often treated with a combination of rituximab (anti-CD20 antibody), cyclophosphamide, doxorubicin, vincristine, and prednisone (R-CHOP). Treatment may include radiotherapy or the use of alternative chemotherapies or corticosteroids. R-CHOP compromises the immune system, as rituximab results in short-term depletion of both malignant and healthy B cells, leading to hypogammaglobulinemia. Furthermore, short-term treatment with cyclophosphamide results in depletion of lymphocytes, and long-term corticosteroids result in hampering of immune cell function. In the case of relapsed or refractory DLBCL, cellular therapies can be offered. Patients may be eligible for autologous or allogeneic stem cell transplantation with BEAM (carmustine, etoposide, cytarabine, and melphalan) or carmustine/thiotepa conditioning. A recent advancement in the field is chimeric antigen receptor (CAR) therapy, which includes genetic modification of T cells with a CAR that recognizes surface proteins found on tumor cells.[83] The conditioning regimen consists of fludarabine combined with cyclophosphamide resulting in lymphodepletion. Pre-conditioning regimens for cellular therapies can weaken existing immune responses, and the induction of immune responses during or shortly after treatment may also be hampered. Furthermore, anti-CD19 CAR T-cell therapy leads to hypogammaglobulinemia, since CD19 is expressed on both healthy and malignant B cells.

3.10 Multiple Myeloma

Multiple Myeloma is a malignancy of the post-germinal center plasma cells, which typically includes the accumulation of malignant cells in the bone marrow.[68,84] The malignant cells are monoclonal and therefore produce the same immunoglobulin, referred to as M-protein. Genetic alterations include hyperdiploidy, increased expression of cyclin D1-D3, secondary translocations, mutations, and epigenetic changes. Symptomatic myeloma is characterized by organ or tissue damage: hypercalcemia, renal impairment, anemia, and bone disease (CRAB). Malignant cells can affect normal immune function by repressing healthy immune cells in bone marrow or lymph nodes, or hampering immune cell function by creating an immunosuppressive environment, resulting in hampered cellular immunity and reduced antibody production by non-malignant cells. Patients with symptomatic myeloma who are eligible for autologous transplantation are first treated with intensive induction therapy, which typically includes daratumumab (anti-CD38 antibody), bortezomib/velcade, lenalidomide, and dexamethasone (dara-VRd). Lenalidomide and the other thalidomide analogs are usually referred to as immune modulatory drugs (IMiD) and bind to cereblon, altering protein degradation by the proteasome. This results in alterations in apoptotic pathways, stromal cell and malignant cell interactions, and promotion of T-cell activation by increasing T-cell priming and inhibiting regulatory T cells.[85] Alternatively, patients may be treated with variations on VRd. After Dara-VRd treatment, patients receive high-dose cytostatic melphalan (HDM) followed by autologous stem cell transplantation. Patients ineligible for autologous stem cell transplantation are treated with VRd. Patients with multiple myeloma can become immunocompromised during treatment. Daratumumab can result in short-term partial elimination of the immune system by depleting CD38-expressing plasma cells, activated conventional T cells, and regulatory T cells. Treatment with immune modulatory drugs and corticosteroids is usually long-term, therefore, prior long-term use of the drugs can affect vaccine-induced immune responses during treatment. However, the mode of action of immune modulatory drugs is diverse, and the effect might therefore depend on multiple factors.

4 AIMS

SARS-CoV-2 has circulated in the human population since December 2019 and subsequently caused a pandemic in 2020. Fortunately, vaccines were quickly developed and were effective in limiting the viral spread and hospitalization, thereby ending the pandemic. Due to the urgency of the pandemic, blood samples were bio-banked before and during the vaccination rollout. These precious materials allow us

to study the immune system during the encounter with a new virus or vaccine. First encounter with a virus or vaccine typically results in the induction of T-cell responses from the naïve repertoire, called primary T-cell responses. However, individuals may also exhibit pre-existing immunity: induction of T cells from the memory repertoire that were originally primed by another pathogen. In most healthy individuals, the virus is effectively cleared by the innate and adaptive immune system without causing severe disease. Individuals with a hampered immune system have an increased chance of developing severe COVID-19. Patients with hematological malignancies are often immunocompromised due to the disease itself or the treatment that they receive, causing them to be more susceptible to infections. Typically, vaccine-induced immunity is often measured by the presence of humoral immune responses only, but some patients are unable to produce a humoral response and T cells are important for effective viral clearance as well. As a result, the ability of patients with hematological malignancies to develop effective T-cell responses is unclear. Therefore, this thesis aims to investigate the mRNA vaccine-induced T-cell response in patients who are immunocompromised due to disease or treatment.

The aim of **chapter 2** is to investigate how the T cells of SARS-CoV-2-naïve individuals respond to the virus to get insight into pre-existing T-cell responses. T cells can be cross-reactive towards different viruses, which is usually caused by sequence homology. Therefore, studies investigating T-cell cross-reactivity towards SARS-CoV-2 focus on other common coronaviruses. However, we hypothesize that these T cells could also originate from T cells that recognize cytomegalovirus (CMV). This is because previous reports showed that cross-reactive T cells are present in a large group of individuals, independent of geographical location, and cross-reactive T cells are present in a relatively high percentage in the blood. Both are typical characteristics of CMV. Additionally, CMV-seropositivity has been associated with cross-reactive T cells, and T cells can be cross-reactive between two dissimilar viruses. We will investigate this by randomly selecting PBMCs from healthy individuals that were frozen down before May 2019, to ensure that they are SARS-CoV-2-naïve. We will measure SARS-CoV-2-specific CD4+ and CD8+ T cells and separate the individuals based on CMV serology. SARS-CoV-2-specific T cells will be isolated, and we will aim to identify their peptide-HLA specificity. If successful, we will further aim to understand these T-cell responses by investigating the peptide affinity, T-cell phenotype, and the efficacy of cross-reactive T cells against SARS-CoV-2.

The aim of **chapter 3** is to investigate the SARS-CoV-2 spike-specific humoral and T-cell response following mRNA vaccination in patients with aplastic anemia. Patients with aplastic anemia are often immunocompromised due to therapy,

making them more susceptible to a severe course after infection. However, current guidelines recommend caution with vaccinating against SARS-CoV-2 due to the risk of potential disease relapse and due to the speculation that the vaccine might be ineffective in these patients. These guidelines are given irrespective of whether immunosuppressive treatment is completed. We will investigate whether previous treatment with immunosuppressive therapy can have a lingering effect on the humoral and T-cell responses and whether vaccination may cause aplastic anemia relapse. We will therefore collect blood from patients with aplastic anemia who have been previously treated with immunosuppressive treatment. Spike-specific antibodies and T cells will be measured before and during vaccination, as well as the ability of the T cells to produce IFN-γ, TNF-α, and IL-2. Furthermore, symptoms of aplastic anemia relapse will be monitored.

The aim of **chapter 4** is to investigate the spike-specific humoral and T-cell responses following mRNA vaccination in a selected group of patients with hematological malignancies. Antibody responses are often measured as a proxy for the presence of developed immunity. However, immunity also includes the development of an effective T-cell response. This becomes especially important for patients with hematological malignancies who have a hampered B-cell compartment due to disease or treatment. To investigate this, patients with CLL, lymphoma, or multiple myeloma will be included, and the ability of these patients to develop spike-specific antibodies, CD4+ T cells, or CD8+ T cells will be measured. The developed immune responses will be shown of the patients stratified based on malignancy, but also stratified based on seroconversion. This will be done to investigate whether patients who are unable to seroconvert also lack the ability to mount T-cell responses.

The aim of **chapter 5** is to further extend the patients with hematological malignancies to investigate the spike-specific humoral and T-cell responses in a large cohort of patients, stratified based on disease, but also therapy. Several studies have investigated spike-specific antibodies in a large cohort of patients, but measurement of T cells is more labor-intensive and therefore typically restricted to a smaller group of patients with a specific disease or treatment. As a result, it is challenging to pinpoint whether reduced immune responses are due to disease or therapy and whether these patients have a combined deficient B-cell and T-cell response. Therefore, spike-specific antibodies and CD4+ and CD8+ T cells will be measured during vaccination, and the patients will be stratified based and disease and therapy. Apart from frequencies of spike-specific T cells, the ability to produce cytokines will be measured. Furthermore, these patients often have lymphopenia, and

therefore, we aim to investigate whether reduced T-cell counts or a reduced naïve T-cell pool are associated with a poor T-cell response.

In **chapter 6** the results of the studies will be discussed.

REFERENCES

1. Wu, F. *et al.* A new coronavirus associated with human respiratory disease in China. *Nature* **579**, 265-269, doi:10.1038/s41586-020-2008-3 (2020).
2. Szabo, G. T., Mahiny, A. J. & Vlatkovic, I. COVID-19 mRNA vaccines: Platforms and current developments. *Mol Ther* **30**, 1850-1868, doi:10.1016/j.ymthe.2022.02.016 (2022).
3. Barbier, A. J., Jiang, A. Y., Zhang, P., Wooster, R. & Anderson, D. G. The clinical progress of mRNA vaccines and immunotherapies. *Nat Biotechnol* **40**, 840-854, doi:10.1038/s41587-022-01294-2 (2022).
4. Jamison, D. A., Jr. *et al.* A comprehensive SARS-CoV-2 and COVID-19 review, Part 1: Intracellular overdrive for SARS-CoV-2 infection. *Eur J Hum Genet* **30**, 889-898, doi:10.1038/s41431-022-01108-8 (2022).
5. Khurana, V. & Goswami, B. Angiotensin converting enzyme (ACE). *Clin Chim Acta* **524**, 113-122, doi:10.1016/j.cca.2021.10.029 (2022).
6. Latifi-Pupovci, H. Molecular mechanisms involved in pathogenicity of SARS-CoV-2: Immune evasion and implications for therapeutic strategies. *Biomed Pharmacother* **153**, 113368, doi:10.1016/j.biopha.2022.113368 (2022).
7. Tay, M. Z., Poh, C. M., Renia, L., MacAry, P. A. & Ng, L. F. P. The trinity of COVID-19: immunity, inflammation and intervention. *Nat Rev Immunol* **20**, 363-374, doi:10.1038/s41577-020-0311-8 (2020).
8. Sette, A. & Crotty, S. Adaptive immunity to SARS-CoV-2 and COVID-19. *Cell* **184**, 861-880, doi:10.1016/j.cell.2021.01.007 (2021).
9. Havasi, A. *et al.* Influenza A, Influenza B, and SARS-CoV-2 Similarities and Differences - A Focus on Diagnosis. *Front Microbiol* **13**, 908525, doi:10.3389/fmicb.2022.908525 (2022).
10. Heinrich, F., Mertz, K. D., Glatzel, M., Beer, M. & Krasemann, S. Using autopsies to dissect COVID-19 pathogenesis. *Nat Microbiol* **8**, 1986-1994, doi:10.1038/s41564-023-01488-7 (2023).
11. Paludan, S. R. & Mogensen, T. H. Innate immunological pathways in COVID-19 pathogenesis. *Sci Immunol* **7**, eabm5505, doi:10.1126/sciimmunol.abm5505 (2022).
12. Mehta, P. *et al.* COVID-19: consider cytokine storm syndromes and immunosuppression. *Lancet* **395**, 1033-1034, doi:10.1016/S0140-6736(20)30628-0 (2020).
13. Nalbandian, A., Desai, A. D. & Wan, E. Y. Post-COVID-19 Condition. *Annu Rev Med* **74**, 55-64, doi:10.1146/annurev-med-043021-030635 (2023).
14. Samadizadeh, S. *et al.* COVID-19: Why does disease severity vary among individuals? *Respir Med* **180**, 106356, doi:10.1016/j.rmed.2021.106356 (2021).
15. Dessie, Z. G. & Zewotir, T. Mortality-related risk factors of COVID-19: a systematic review and meta-analysis of 42 studies and 423,117 patients. *BMC Infect Dis* **21**, 855, doi:10.1186/s12879-021-06536-3 (2021).
16. Hu, J. & Wang, Y. The Clinical Characteristics and Risk Factors of Severe COVID-19. *Gerontology* **67**, 255-266, doi:10.1159/000513400 (2021).
17. Stroz, S., Kosiorek, P. & Stasiak-Barmuta, A. The COVID-19 inflammation and high mortality mechanism trigger. *Immunogenetics* **76**, 15-25, doi:10.1007/s00251-023-01326-4 (2024).

18. Pollard, A. J. & Bijker, E. M. A guide to vaccinology: from basic principles to new developments. *Nat Rev Immunol* **21**, 83-100, doi:10.1038/s41577-020-00479-7 (2021).

19. Martinon, F. *et al.* Induction of virus-specific cytotoxic T lymphocytes in vivo by liposome-entrapped mRNA. *Eur J Immunol* **23**, 1719-1722, doi:10.1002/eji.1830230749 (1993).

20. Alberer, M. *et al.* Safety and immunogenicity of a mRNA rabies vaccine in healthy adults: an open-label, non-randomised, prospective, first-in-human phase 1 clinical trial. *Lancet* **390**, 1511-1520, doi:10.1016/S0140-6736(17)31665-3 (2017).

21. Hassett, K. J. *et al.* Optimization of Lipid Nanoparticles for Intramuscular Administration of mRNA Vaccines. *Mol Ther Nucleic Acids* **15**, 1-11, doi:10.1016/j.omtn.2019.01.013 (2019).

22. Alameh, M. G. *et al.* Lipid nanoparticles enhance the efficacy of mRNA and protein subunit vaccines by inducing robust T follicular helper cell and humoral responses. *Immunity* **54**, 2877-2892 e2877, doi:10.1016/j.immuni.2021.11.001 (2021).

23. Verbeke, R., Lentacker, I., De Smedt, S. C. & Dewitte, H. The dawn of mRNA vaccines: The COVID-19 case. *J Control Release* **333**, 511-520, doi:10.1016/j.jconrel.2021.03.043 (2021).

24. Liang, F. *et al.* Efficient Targeting and Activation of Antigen-Presenting Cells In Vivo after Modified mRNA Vaccine Administration in Rhesus Macaques. *Mol Ther* **25**, 2635-2647, doi:10.1016/j.ymthe.2017.08.006 (2017).

25. Dan, J. M. *et al.* Immunological memory to SARS-CoV-2 assessed for up to 8 months after infection. *Science* **371**, doi:10.1126/science.abf4063 (2021).

26. Barbeau, D. J. *et al.* Comparative analysis of human immune responses following SARS-CoV-2 vaccination with BNT162b2, mRNA-1273, or Ad26.COV2.S. *NPJ Vaccines* **7**, 77, doi:10.1038/s41541-022-00504-x (2022).

27. Lin, D. Y. *et al.* Effectiveness of Covid-19 Vaccines over a 9-Month Period in North Carolina. *N Engl J Med* **386**, 933-941, doi:10.1056/NEJMoa2117128 (2022).

28. Mahrokhian, S. H., Tostanoski, L. H., Vidal, S. J. & Barouch, D. H. COVID-19 vaccines: Immune correlates and clinical outcomes. *Hum Vaccin Immunother* **20**, 2324549, doi:10.1080/21645515.2024.2324549 (2024).

29. Modjarrad, K. *et al.* Preclinical characterization of the Omicron XBB.1.5-adapted BNT162b2 COVID-19 vaccine. *NPJ Vaccines* **9**, 229, doi:10.1038/s41541-024-01013-9 (2024).

30. Winokur, P. *et al.* Bivalent Omicron BA.1-Adapted BNT162b2 Booster in Adults Older than 55 Years. *N Engl J Med* **388**, 214-227, doi:10.1056/NEJMoa2213082 (2023).

31. Chalkias, S. *et al.* Original SARS-CoV-2 monovalent and Omicron BA.4/BA.5 bivalent COVID-19 mRNA vaccines: phase 2/3 trial interim results. *Nat Med* **29**, 2325-2333, doi:10.1038/s41591-023-02517-y (2023).

32. Lin, D. Y. *et al.* Effectiveness of Bivalent Boosters against Severe Omicron Infection. *N Engl J Med* **388**, 764-766, doi:10.1056/NEJMc2215471 (2023).

33. Collier, A. Y. *et al.* Immunogenicity of BA.5 Bivalent mRNA Vaccine Boosters. *N Engl J Med* **388**, 565-567, doi:10.1056/NEJMc2213948 (2023).

34. Neale, I. *et al.* CD4+ and CD8+ T cells and antibodies are associated with protection against Delta vaccine breakthrough infection: a nested case-control study within the PITCH study. *mBio* **14**, e0121223, doi:10.1128/mbio.01212-23 (2023).

35. Koutsakos, M. *et al*. SARS-CoV-2 breakthrough infection induces rapid memory and de novo T cell responses. *Immunity* **56**, 879-892 e874, doi:10.1016/j.immuni.2023.02.017 (2023).

36. Guerrera, G. *et al*. BNT162b2 vaccination induces durable SARS-CoV-2-specific T cells with a stem cell memory phenotype. *Sci Immunol* **6**, eabl5344, doi:10.1126/sciimmunol.abl5344 (2021).

37. Hurme, A. *et al*. Long-Lasting T Cell Responses in BNT162b2 COVID-19 mRNA Vaccinees and COVID-19 Convalescent Patients. *Front Immunol* **13**, 869990, doi:10.3389/fimmu.2022.869990 (2022).

38. Kalimuddin, S. *et al*. Early T cell and binding antibody responses are associated with COVID-19 RNA vaccine efficacy onset. *Med* **2**, 682-688 e684, doi:10.1016/j.medj.2021.04.003 (2021).

39. Arieta, C. M. *et al*. The T-cell-directed vaccine BNT162b4 encoding conserved non-spike antigens protects animals from severe SARS-CoV-2 infection. *Cell* **186**, 2392-2409 e2321, doi:10.1016/j.cell.2023.04.007 (2023).

40. Li, Y. *et al*. Antibody landscape against SARS-CoV-2 reveals significant differences between non-structural/accessory and structural proteins. *Cell Rep* **36**, 109391, doi:10.1016/j.celrep.2021.109391 (2021).

41. Kristiansen, P. A. *et al*. WHO International Standard for anti-SARS-CoV-2 immunoglobulin. *Lancet* **397**, 1347-1348, doi:10.1016/S0140-6736(21)00527-4 (2021).

42. Neefjes, J., Jongsma, M. L., Paul, P. & Bakke, O. Towards a systems understanding of MHC class I and MHC class II antigen presentation. *Nat Rev Immunol* **11**, 823-836, doi:10.1038/nri3084 (2011).

43. Roche, P. A. & Furuta, K. The ins and outs of MHC class II-mediated antigen processing and presentation. *Nat Rev Immunol* **15**, 203-216, doi:10.1038/nri3818 (2015).

44. Germain, R. N. T-cell development and the CD4-CD8 lineage decision. *Nat Rev Immunol* **2**, 309-322, doi:10.1038/nri798 (2002).

45. Matzinger, P. & Bevan, M. J. Hypothesis: why do so many lymphocytes respond to major histocompatibility antigens? *Cell Immunol* **29**, 1-5, doi:10.1016/0008-8749(77)90269-6 (1977).

46. Mason, D. A very high level of crossreactivity is an essential feature of the T-cell receptor. *Immunol Today* **19**, 395-404, doi:10.1016/s0167-5699(98)01299-7 (1998).

47. Wooldridge, L. *et al*. A single autoimmune T cell receptor recognizes more than a million different peptides. *J Biol Chem* **287**, 1168-1177, doi:10.1074/jbc.M111.289488 (2012).

48. Sewell, A. K. Why must T cells be cross-reactive? *Nat Rev Immunol* **12**, 669-677, doi:10.1038/nri3279 (2012).

49. Dendrou, C. A., Petersen, J., Rossjohn, J. & Fugger, L. HLA variation and disease. *Nat Rev Immunol* **18**, 325-339, doi:10.1038/nri.2017.143 (2018).

50. Birnbaum, M. E. *et al*. Deconstructing the peptide-MHC specificity of T cell recognition. *Cell* **157**, 1073-1087, doi:10.1016/j.cell.2014.03.047 (2014).

51. Macdonald, W. A. *et al*. T cell allorecognition via molecular mimicry. *Immunity* **31**, 897-908, doi:10.1016/j.immuni.2009.09.025 (2009).

52. Cole, D. K. *et al*. Hotspot autoimmune T cell receptor binding underlies pathogen and insulin peptide cross-reactivity. *J Clin Invest* **126**, 3626, doi:10.1172/JCI89919 (2016).

53. Adams, J. J. *et al*. T cell receptor signaling is limited by docking geometry to peptide-major histocompatibility complex. *Immunity* **35**, 681-693, doi:10.1016/j.immuni.2011.09.013 (2011).

54. Riley, T. P. *et al*. T cell receptor cross-reactivity expanded by dramatic peptide-MHC adaptability. *Nat Chem Biol* **14**, 934-942, doi:10.1038/s41589-018-0130-4 (2018).

55. Piepenbrink, K. H., Blevins, S. J., Scott, D. R. & Baker, B. M. The basis for limited specificity and MHC restriction in a T cell receptor interface. *Nat Commun* **4**, 1948, doi:10.1038/ncomms2948 (2013).

56. Lee, C. H. *et al*. Predicting Cross-Reactivity and Antigen Specificity of T Cell Receptors. *Front Immunol* **11**, 565096, doi:10.3389/fimmu.2020.565096 (2020).

57. Kunzli, M. & Masopust, D. CD4(+) T cell memory. *Nat Immunol* **24**, 903-914, doi:10.1038/s41590-023-01510-4 (2023).

58. Sun, L., Su, Y., Jiao, A., Wang, X. & Zhang, B. T cells in health and disease. *Signal Transduct Target Ther* **8**, 235, doi:10.1038/s41392-023-01471-y (2023).

59. Yoshitomi, H. & Ueno, H. Shared and distinct roles of T peripheral helper and T follicular helper cells in human diseases. *Cell Mol Immunol* **18**, 523-527, doi:10.1038/s41423-020-00529-z (2021).

60. Yu, E. D. *et al*. Development of a T cell-based immunodiagnostic system to effectively distinguish SARS-CoV-2 infection and COVID-19 vaccination status. *Cell Host Microbe* **30**, 388-399 e383, doi:10.1016/j.chom.2022.02.003 (2022).

61. Binayke, A. *et al*. A quest for universal anti-SARS-CoV-2 T cell assay: systematic review, meta-analysis, and experimental validation. *NPJ Vaccines* **9**, 3, doi:10.1038/s41541-023-00794-9 (2024).

62. Sette, A. & Crotty, S. Immunological memory to SARS-CoV-2 infection and COVID-19 vaccines. *Immunol Rev*, doi:10.1111/imr.13089 (2022).

63. Wherry, E. J. & Barouch, D. H. T cell immunity to COVID-19 vaccines. *Science* **377**, 821-822, doi:10.1126/science.add2897 (2022).

64. Goldblatt, D., Alter, G., Crotty, S. & Plotkin, S. A. Correlates of protection against SARS-CoV-2 infection and COVID-19 disease. *Immunol Rev* **310**, 6-26, doi:10.1111/imr.13091 (2022).

65. Wang, L. *et al*. T cell immune memory after covid-19 and vaccination. *BMJ Med* **2**, e000468, doi:10.1136/bmjmed-2022-000468 (2023).

66. Polack, F. P. *et al*. Safety and Efficacy of the BNT162b2 mRNA Covid-19 Vaccine. *N Engl J Med* **383**, 2603-2615, doi:10.1056/NEJMoa2034577 (2020).

67. Baden, L. R. *et al*. Efficacy and Safety of the mRNA-1273 SARS-CoV-2 Vaccine. *N Engl J Med* **384**, 403-416, doi:10.1056/NEJMoa2035389 (2021).

68. Hoffbrand, A. V. & Moss, P. A. H. *Hoffbrand's Essential Haematology*. (Wiley, 2015).

69. Young, N. S. Aplastic Anemia. *New Engl J Med* **379**, 1643-1656, doi:10.1056/NEJMra1413485 (2018).

70. Kulasekararaj, A. *et al*. Guidelines for the diagnosis and management of adult aplastic anaemia: A British Society for Haematology Guideline. *Br J Haematol* **204**, 784-804, doi:10.1111/bjh.19236 (2024).

71. Cazzola, M. Myelodysplastic Syndromes. *N Engl J Med* **383**, 1358-1374, doi:10.1056/NEJMra1904794 (2020).

72. Lindblad, K. E., Goswami, M., Hourigan, C. S. & Oetjen, K. A. Immunological effects of hypomethylating agents. *Expert Rev Hematol* **10**, 745-752, doi:10.1080/17474086.2017.1346470 (2017).

73. Wong, K. K., Hassan, R. & Yaacob, N. S. Hypomethylating Agents and Immunotherapy: Therapeutic Synergism in Acute Myeloid Leukemia and Myelodysplastic Syndromes. *Front Oncol* **11**, 624742, doi:10.3389/fonc.2021.624742 (2021).

74. Sanchez-Abarca, L. I. *et al*. Immunomodulatory effect of 5-azacytidine (5-azaC): potential role in the transplantation setting. *Blood* **115**, 107-121, doi:10.1182/blood-2009-03-210393 (2010).

75. Spivak, J. L. Myeloproliferative Neoplasms. *N Engl J Med* **376**, 2168-2181, doi:10.1056/NEJMra1406186 (2017).

76. Goldman, J. M. & Melo, J. V. Chronic myeloid leukemia--advances in biology and new approaches to treatment. *N Engl J Med* **349**, 1451-1464, doi:10.1056/NEJMra020777 (2003).

77. Chereda, B. & Melo, J. V. Natural course and biology of CML. *Ann Hematol* **94 Suppl 2**, S107-121, doi:10.1007/s00277-015-2325-z (2015).

78. Abruzzese, E. CML 25 Years Later - Poised for Another Breakthrough? *N Engl J Med* **391**, 955-957, doi:10.1056/NEJMe2407913 (2024).

79. Dohner, H., Weisdorf, D. J. & Bloomfield, C. D. Acute Myeloid Leukemia. *N Engl J Med* **373**, 1136-1152, doi:10.1056/NEJMra1406184 (2015).

80. Cancer Genome Atlas Research, N. *et al*. Genomic and epigenomic landscapes of adult de novo acute myeloid leukemia. *N Engl J Med* **368**, 2059-2074, doi:10.1056/NEJMoa1301689 (2013).

81. Burger, J. A. Treatment of Chronic Lymphocytic Leukemia. *N Engl J Med* **383**, 460-473, doi:10.1056/NEJMra1908213 (2020).

82. Herishanu, Y., Katz, B. Z., Lipsky, A. & Wiestner, A. Biology of chronic lymphocytic leukemia in different microenvironments: clinical and therapeutic implications. *Hematol Oncol Clin North Am* **27**, 173-206, doi:10.1016/j.hoc.2013.01.002 (2013).

83. June, C. H. & Sadelain, M. Chimeric Antigen Receptor Therapy. *N Engl J Med* **379**, 64-73, doi:10.1056/NEJMra1706169 (2018).

84. Palumbo, A. & Anderson, K. Multiple myeloma. *N Engl J Med* **364**, 1046-1060, doi:10.1056/NEJMra1011442 (2011).

85. Bird, S. & Pawlyn, C. IMiD resistance in multiple myeloma: current understanding of the underpinning biology and clinical impact. *Blood* **142**, 131-140, doi:10.1182/blood.2023019637 (2023).

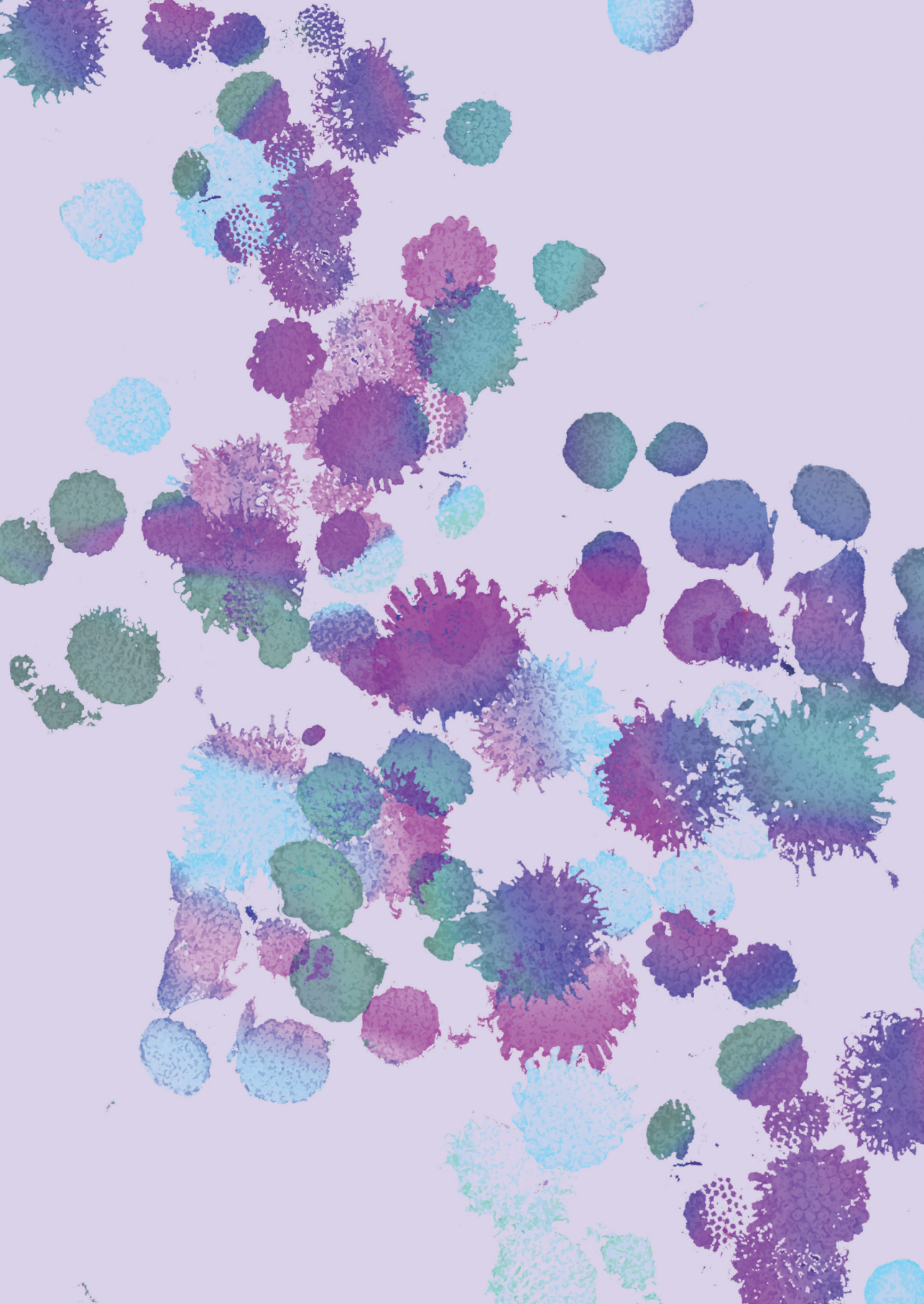

SARS-COV-2-SPECIFIC CD4$^+$ AND CD8$^+$ T CELL RESPONSES CAN ORIGINATE FROM CROSS-REACTIVE CMV-SPECIFIC T CELLS

Pothast, C. R., Dijkland, R. C., Thaler, M., Hagedoorn, R. S., Kester, M. G. D., Wouters, A. K., Hiemstra, P. S., van Hemert, M. J., Gras, S., Falkenburg, J. H. F., & Heemskerk, M. H. M.

(2022). *Elife*. DOI: 10.7554/eLife.82050

Chapter 2

ABSTRACT

Detection of SARS-coronavirus-2 (SARS-CoV-2) specific $CD4^+$ and $CD8^+$ T cells in SARS-CoV-2-unexposed donors has been explained by the presence of T cells primed by other coronaviruses. However, based on the relative high frequency and prevalence of cross-reactive T cells, we hypothesized CMV may induce these cross-reactive T cells. Stimulation of pre-pandemic cryo-preserved PBMCs with SARS-CoV-2 peptides revealed that frequencies of SARS-CoV-2-specific T cells were higher in CMV-seropositive donors. Characterization of these T cells demonstrated that membrane-specific $CD4^+$ and spike-specific $CD8^+$ T cells originate from cross-reactive CMV-specific T cells. Spike-specific $CD8^+$ T cells recognize SARS-CoV-2 spike peptide FVSNGTHWF (FVS) and dissimilar CMV pp65 peptide IPSINVHHY (IPS) presented by HLA-B*35:01. These dual IPS/FVS-reactive $CD8^+$ T cells were found in multiple donors as well as severe COVID-19 patients and shared a common T cell receptor (TCR), illustrating that IPS/FVS-cross-reactivity is caused by a public TCR. In conclusion, CMV-specific T cells cross-react with SARS-CoV-2, despite low sequence homology between the two viruses, and may contribute to the pre-existing immunity against SARS-CoV-2.

INTRODUCTION

The effectiveness of the innate and adaptive immune system is an important factor for disease outcome during infection with severe acute respiratory syndrome coronavirus 2 (SARS-CoV-2) [1]. $CD4^+$ and $CD8^+$ T cells are important components of the adaptive immune system as $CD4^+$ T cells promote antibody production by B cells and help cytotoxic $CD8^+$ T cells to mediate cytotoxic lysis of SARS-CoV-2 infected cells [2]. Whilst immunity is commonly measured solely based on antibody titers, research into coronavirus disease (COVID-19) pathophysiology and vaccination effectiveness has associated an effective T cell response with less severe COVID-19 [2-8]. Additionally, SARS-CoV-2-specific T cell responses have been shown to be present in most individuals 6 months after infection or vaccination and remain largely unaffected by emerging variants of concern, illustrating their importance in generating durable immune responses [9-17].

Besides *de novo* SARS-CoV-2-specific T cell responses in infected individuals, SARS-CoV-2-specific T cells have also been identified in unexposed individuals [18-22]. This finding indicates that T cells which were initially primed against other pathogens are able to cross-recognize SARS-CoV-2 antigen. This phenomenon is called heterologous immunity and can often be explained by genomic sequence homology between pathogens. Highly homologous DNA sequences are translated into similar proteins which can be processed and presented as epitopes with high sequence similarity in human leukocyte antigen (HLA). For this reason, most research has focused on cross-reactive T cells that are potentially primed by other human coronaviruses (HCoVs) since they share around 30% amino acid sequence homology with SARS-CoV-2 [21-27]. However, it has been postulated that SARS-CoV-2-specific T cells in unexposed individuals could also conceivably be primed by other, non-HCoVs [22,28-30]. Furthermore, previous studies, although limited, have demonstrated the occurrence of cross-reactivity between two epitopes with relatively low sequence homology [31-36]. This form of heterologous immunity is poorly understood and, therefore, predicting such cross-reactivity remains a challenge [37].

Pre-pandemic SARS-CoV-2-specific T cells are reportedly present in a relatively high proportion of the population, independent of geographical location, indicating that a highly prevalent pathogen could be the initial trigger of these cross-reactive T cells [5,18-23,38]. Furthermore, these cross-reactive T cells should be present in relatively high frequencies, as they are detectable in antigen-induced stimulation assays without additional amplification steps [5,18,19,22,23]. Cytomegalovirus (CMV) is a highly prevalent pathogen and usually induces high T cell frequencies, making CMV a potential trigger

for cross-reactive SARS-CoV-2-specific T cells [39,40]. This is supported by the finding that SARS-CoV-2 cross-reactive CD8$^+$ T cells were increased in CMV-seropositive (CMV$^+$) donors, and that previous CMV infection has been associated with severe COVID-19 [41-43]. Studies so far indicate that cross-reactive T cells can play a role in COVID-19 immunity but whether they are protective or pathogenic is unclear [24,26]. Taken together, we hypothesized that cross-reactive SARS-CoV-2-specific T cells might originate from the CMV-specific memory population.

In the present study, we aimed to identify SARS-CoV-2-specific cross-reactive CD4$^+$ and CD8$^+$ T cells in SARS-CoV-2-unexposed individuals. We found an increased presence of cross-reactive T cells in CMV$^+$ donors and upon isolation and clonal expansion of the spike-reactive CD8$^+$ and membrane-reactive CD4$^+$ T cells we confirmed that these T cells were reactive against both SARS-CoV-2 and CMV. Interestingly, isolated CD8$^+$ T cells recognizing a previously described CMV epitope IPSINVHHY presented by HLA-B*35:01 were cross-reactive with dissimilar SARS-CoV-2 spike peptide FVSNGTHWF presented by HLA-B*35:01, demonstrating that cross-reactivity does not solely depend on peptide sequence homology. The T cell receptor (TCR) isolated from these CD8$^+$ T cells was found in multiple donors showing that pre-pandemic spike-reactive CD8$^+$ T cells can be caused by a public CMV-specific TCR. Based on the reduced activation status compared to other SARS-CoV-2 specific T cells in severe COVID-19 patients, we hypothesize that these cross-reactive T cells are not important for clearing the virus at this late stage of the disease. However, these cross-reactive CD8$^+$ T cells were shown to reduce spreading of SARS-CoV-2 infection *in vitro*, and in 2 out of 2 CMV$^+$ severe COVID-19 patients these cross-reactive T cells were detected. This indicates that early in infection at the stage that no SARS-CoV-2 specific T cells are present yet, these cross-reactive T cells may play a role in preventing SARS-CoV-2 infection or reducing the severity of COVID-19.

RESULTS

SARS-CoV-2-specific T cell responses in SARS-CoV-2-unexposed PBMCs correlate with CMV seropositivity

To investigate whether SARS-CoV-2-specific CD4$^+$ and CD8$^+$ T cell responses in SARS-CoV-2-unexposed donors correlate with previous CMV infection, pre-pandemic cryopreserved PBMCs from CMV seropositive (CMV$^+$, N=28) and CMV seronegative (CMV$^-$, N=39) healthy individuals were stimulated overnight using SARS-CoV-2 15-mer peptide pools. These pools included 3 spike peptide pools that together overlap the entire spike gene (S, S1 and S+), membrane (M) and nucleocapsid (N) antigens from

SARS-CoV-2. To confirm that CMV$^+$ individuals have CMV-specific T cells, reactivity against the most immunogenic CMV antigen, pp65, was also tested. Memory SARS-CoV-2-specific CD4$^+$ T cells were characterized as CD154$^+$CD137$^+$ and memory SARS-CoV-2-specific CD8$^+$ T cells were identified based on expression of CD137 and IFN-y (**Figure 1A-B** and **Figure 1 – figure supplement 1**). As expected, all CMV$^+$ donors displayed a CD4$^+$ and/or CD8$^+$ T cell response upon stimulation with pp65 (**Figure 1C-E**). No marked increase of CD4$^+$ T cell responses were observed after SARS-CoV-2 spike and nucleocapsid stimulation in the CMV$^+$ group compared to CMV$^-$. However, 6 donors in the CMV$^+$ group displayed a CD4$^+$ T cell response against the membrane peptide pool which was not observed in the CMV$^-$ group (**Figure 1C**). Furthermore, CD4$^+$ T cell response against the membrane pool was accompanied by a CD4$^+$ T cell response against pp65 (**Figure 1D**). In addition, CD8$^+$ T cell responses were detected against spike peptides in two CMV$^+$ donors which were not detected in CMV$^-$ donors (**Figure 1E**). Interestingly, donors with a high CD8$^+$ T cell response against SARS-CoV-2 spike peptides additionally displayed strong reactivity against pp65 (**Figure 1F**). Taken together, these results show that SARS-CoV-2-unexposed CMV$^+$, but not CMV$^-$, individuals had detectable CD4$^+$ T cell responses against membrane peptides and CD8$^+$ T cells targeting spike peptides. These SARS-CoV-2 responses were accompanied by T cell responses against pp65 and thus may indicate that SARS-CoV-2 T cell responses in pre-pandemic samples potentially are memory T cells targeting pp65.

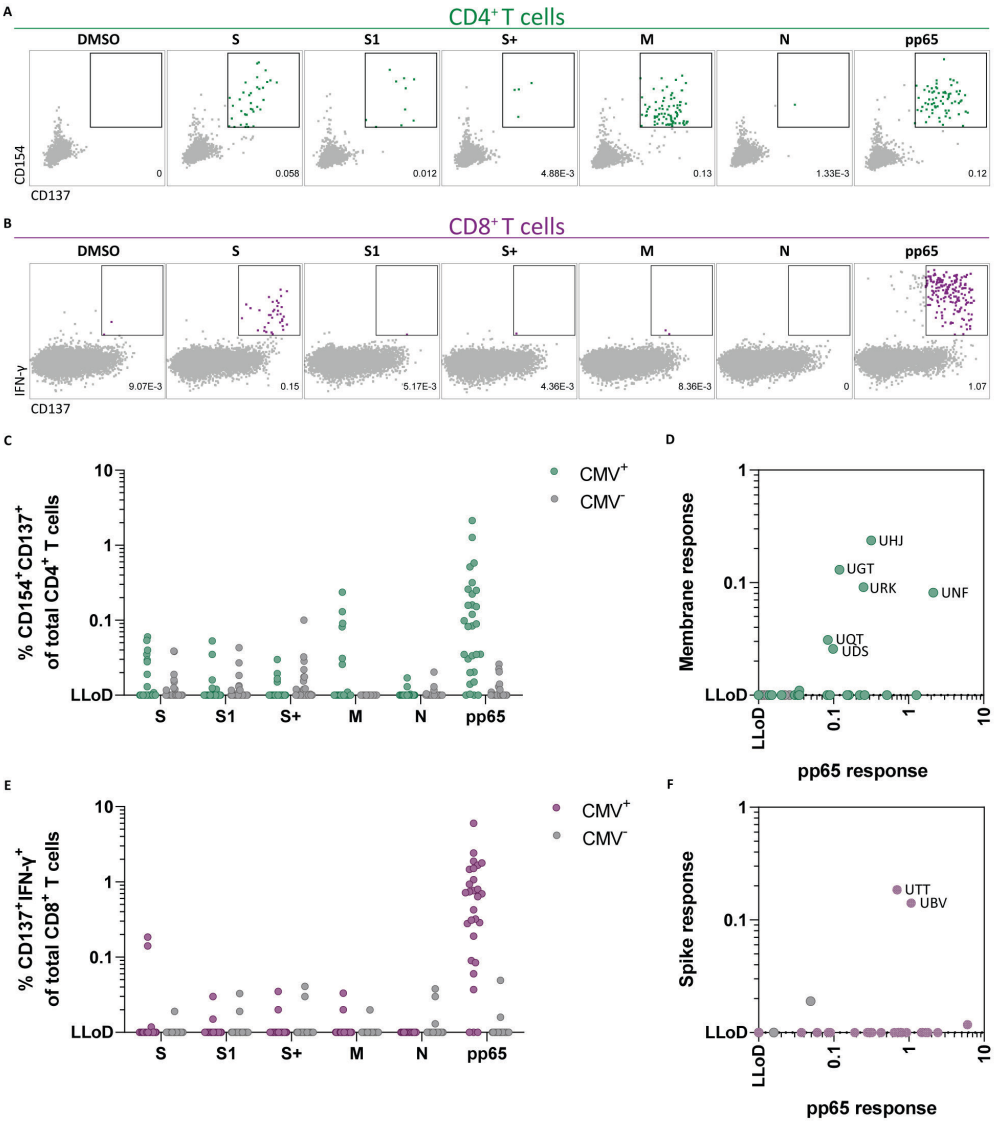

Figure 1 *Ex vivo* SARS-CoV-2-specific CD4⁺ and CD8⁺ T-cell responses in CMV-positive and –negative unexposed donors

Pre-pandemic cryo-preserved PBMCs were stimulated using SARS-CoV-2 spike (S, S1 and S+), membrane (M), nucleocapsid (N) and CMV pp65 peptide pools or not stimulated (DMSO). A) A representative flow cytometry example of a CD4⁺ T cell response in a SARS-CoV-2-unexposed donor. Numbers in plot represent frequencies of CD137⁺CD154⁺ cells of total CD4⁺ T cells. B) A representative flow cytometry example of a CD8⁺ T cell response in a SARS-CoV-2-unexposed donor. Numbers in plot represent frequencies of CD137⁺IFN-γ⁺ cells of total CD8⁺ T cells. C) Scatter plot showing frequencies of CD137⁺CD154⁺ cells of total CD4⁺ T cells of CMV⁺ (green, N=28) and CMV⁻ (grey, N=39) donors. D) Frequencies of CD137⁺CD154⁺ cells of total CD4⁺ T cells in the membrane-stimulated condition (membrane response) plotted against pp65-stimulated condition (pp65 response). 3 letter codes

are anonymized codes of CMV$^+$ (green) and CMV$^-$ (grey) donors. E) Scatter plot showing frequencies of CD137$^+$ IFN-γ^+ cells of total CD8$^+$ T cells of CMV$^+$ (green, N=28) and CMV$^-$ (grey, N=39) donors. F) Frequencies of CD137$^+$IFN-γ^+ cells of total CD8$^+$ T cells in the spike-stimulated condition (spike response) plotted against pp65-stimulated condition (pp65 response).

Pre-pandemic SARS-CoV-2-specific CD4$^+$ and CD8$^+$ T cells recognize pp65 peptides from CMV

To confirm that pre-pandemic SARS-CoV-2-specific T cells are able to recognize peptides from pp65, these SARS-CoV-2-specific T cells were isolated and clonally expanded. SARS-CoV-2-unexposed (pre-pandemic cryopreserved) PBMCs from a CMV$^+$ individual showing a CD4$^+$ T cell response against SARS-CoV-2 membrane protein (donor UGT) were stimulated with the membrane peptide pool and single cell sorted based on CD137 upregulation (**Figure 2 – figure supplement 1**). After clonal expansion, 20 out of 27 screened T cell clones produced IFN-γ when stimulated with membrane peptide pool compared to no peptide stimulation (data not shown). T cell clones 4UGT5, 4UGT8 and 4UGT17, all three expressing a different TCR, were used for further experiments (**Figure 2 – figure supplement 2A**). As hypothesized, the T cell clones were reactive against both SARS-CoV-2 membrane antigen and CMV pp65 when loaded on HLA-matched Epstein-Barr virus lymphoblastoid cell lines (EBV-LCLs) (**Figure 2A**). Interestingly, IFN-γ production by the T cell clones was significantly increased when stimulated with pp65 peptides compared to membrane peptides indicating higher avidity for CMV compared to SARS-CoV-2 (**Figure 2B**). To identify which peptide in pp65 is recognized, reactivity of T cell clone 4UGT8 against a pp65 library was measured which resulted in recognition of three sub pools which contained peptide AGILARNLVPM (**Figure 2 – figure supplement 2B-C**). HLA-mismatched EBV-LCLs were retrovirally transduced with HLA Class II molecules that were commonly shared between donors that had a detectable CD4$^+$ T cell response against the membrane and pp65 peptide pool (**Figure 1D**). T cell clone 4UGT8 recognized both peptide pools and the AGI peptide only when presented in HLA-DRB3*02:02 (**Figure 2C and figure 2 – figure supplement 2D**). The SARS-CoV-2 membrane protein epitope recognized by these cross-reactive T cells remains unidentified as *in vitro* experiments and *in silico* prediction methods failed to identify the epitope. A similar approach was applied for CD8$^+$ T cells in which T cell clones were generated after SARS-CoV-2 spike peptide pool stimulation of PBMCs from CMV$^+$ donor UTT (**Figure 2 – figure supplement 1**). The isolated CD8$^+$ T cell clones were screened for their reactivity with SARS-CoV-2 spike which showed that 23 out of the 28 T cell clones produced IFN-γ upon spike peptide pool stimulation (data not shown). TCR sequencing revealed that all 23 T cell clones expressed the same TCR (**Figure 2 – figure supplement 3A**). T cell clone 8UTT6 was selected for further testing and analyzed for its cross-reactivity towards SARS-CoV-2 spike and CMV pp65 peptide pools Additionally, the HLA restriction of T cell clone 8UTT6 was hypothesized to be HLA-B*35:01 as the

unexposed donors with a $CD8^+$ T cell response against SARS-CoV-2 spike (UTT and UBV) both expressed HLA-B*35:01. The results confirmed that T cell clone 8UTT6 recognized spike as well as pp65 peptide pool presented by K562 cells transduced with HLA-B*35:01 but not transduced with HLA-A*11:01 (**Figure 2D**). To identify the spike epitope, reactivity of clone 8UTT6 against the 15-mer spike peptide library was measured. For the identification of the CMV epitope, an unbiased approach was performed using the nonamer combinatorial peptide library (CPL) assay. Recognition patterns were analyzed using netMHC 4.0 analysis for predicted binding to HLA-B*35:01, which revealed SARS-CoV-2 spike peptide FVSNGTHWF (FVS, $S_{1094\text{-}1103}$) and CMV pp65 IPSINVHHY (IPS, $pp65_{112\text{-}121}$) as the most likely epitopes (**Figure 2 – figure supplement 3B-E**). The FVS and IPS peptides were indeed recognized by clone 8UTT6 (**Figure 2E**). Importantly, the IPS peptide was recognized with higher avidity compared to the FVS peptide by clone 8UTT6 (**Figure 2F**). Supporting these findings, the same TCRβ chain was already described and demonstrated to be specific for IPS in HLA-B*35:01 [44]. Taken together, SARS-CoV-2 reactive $CD4^+$ and $CD8^+$ T cells in pre-pandemic samples cross-reacted with CMV and SARS-CoV-2 peptides.

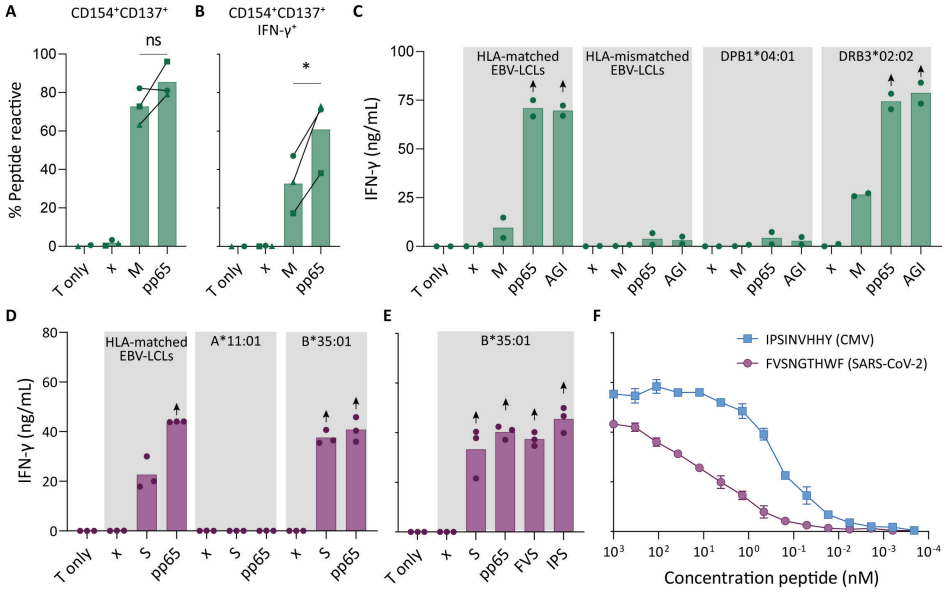

Figure 2 Recognition of SARS-CoV-2 and CMV by pre-existing CD4⁺ and CD8⁺ T cells
Clonally expanded CD4⁺ T cells from donor UGT and CD8⁺ T cells from donor UTT were overnight co-cultured with peptide-pulsed stimulator cells. A-B) Percentages of CD154⁺, CD137⁺ and/or IFN-γ⁺ cells of cross-reactive CD4⁺ T cell clones after overnight culture (T only) or after overnight co-culture with HLA-matched EBV-LCLs that were not peptide pulsed (x) or loaded with membrane (M) or pp65 peptide pool, measured by flow cytometry. Dots represent the mean of experimental repeats of 4UGT5 (square, 1 repeat), 4UGT8 (circles, 4 repeats) and 4UGT17 (triangle, 2 repeats). Significance was tested by a paired *t*-test. C) Bar graphs showing ELISA measurement of secreted IFN-γ after co-culturing of a representative clone, 4UGT8 clone, with HLA-matched or HLA-mismatched EBV-LCLs. HLA-mismatched EBV-LCLs were retrovirally transduced with HLA class II molecule as depicted in figure. Stimulator cells were peptide-pulsed with membrane (M) peptide pool, pp65 peptide pool or AGILARNLVPM (AGI) peptide. Data points are experimental duplicates. Black arrows indicate that values were above plateau value of the ELISA calibration curve. D-E) Bar graphs showing ELISA measurement of secreted IFN-γ after co-culturing of a representative clone, 8UTT6 clone, with HLA-matched EBV-LCLs or K562s transduced with HLA-B*35:01 or HLA-A*11:01. Stimulator cells were peptide-pulsed with spike (S) peptide pool, pp65 peptide pool, IPSINVHHY (IPS) peptide or FVSNGTHWF (FVS) peptide. Data points are technical triplicates. F) Peptide titration of IPS peptide (blue) and FVS peptide (purple) in a co-culture assay with 8UTT6 clone.

Similarity at the C-terminal part of the peptides could drive T cell cross-reactivity

To understand the molecular basis of T cell cross-reactivity between dissimilar peptides FVS and IPS, we modelled the FVS structure based on the solved structure of the IPS peptide bound to HLA-B*35:01 (**Figure 3**) [45]. The two peptides share 2 residues (P3-S and P7-H) and have 2 similar residues (P6-T/V and P9-F/Y) based on similar biochemical properties and size. Residue substitutions from the IPS to FVS peptide were possible without major steric clashes with the HLA or peptide residues. The lack of secondary anchor residue at position 5 in the FVS peptide (P5-N/G) might change the conformation of the central part of the peptide, that could be similar to the

one observed in the spike-derived peptide IPF ($S_{896-904}$) in complex with HLA-B*35:01 (**Figure 3 – figure supplement 1**) [46]. The primary anchor in the FVS peptide are P2-V and P9-F, both within the favored residues at those positions for HLA-B35-restricted peptide [47]. Overall, the FVS peptide might adopt a similar backbone conformation compared to the IPS peptide, which would place in both peptides a small hydrophobic residue at position 6 (P6-T/V), a histidine at position 7, and a residue with a large side-chain at position 8 (P8-W/H).

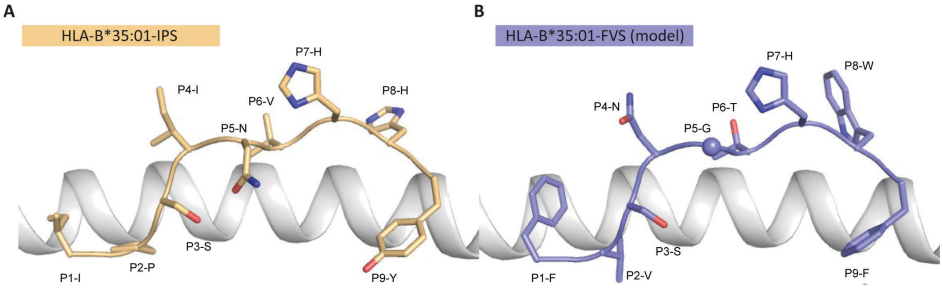

Figure 3 Model of the HLA-B*35:01-FVS structure
A) Crystal structure of the HLA-B*35:01-IPS complex with the HLA in white cartoon and the IPS peptide in clear orange cartoon and stick. B) Model of the HLA-B*35:01-FVS complex with the HLA in white cartoon and the FVS peptide in blue cartoon and stick. The sphere represents the Cα atom of the FVS peptide P5-G residue.

IPS/FVS-specific cross-reactive CD8$^+$ T cells are detectable in multiple individuals

To investigate the prevalence and phenotype of IPS/FVS cross-reactive T cells, HLA-B*35:01$^+$ CMV$^+$ healthy donors were screened for IPS/FVS-specific T cells using tetramers consisting of HLA-B*35:01-FVS (B*35/FVS-tetramer) and HLA-B*35:01-IPS (B*35/IPS-tetramer) (**Figure 4 - figure supplement 1**). Tetramer staining of PBMCs from donor UTT demonstrated that not all T cells that bound to B*35/IPS-tetramer were able to bind to the B*35/FVS-tetramer as well. However, all T cells that bound to B*35/FVS-tetramer were also binding to the B*35/IPS-tetramer (**Figure 4A**). This observation indicates that IPS/FVS cross-reactivity is dictated by specific TCR sequences which was further supported by the lack of binding to B*35/FVS-tetramer by an IPS-specific T cell clone with a different TCR (**Figure 4B**). Screening of SARS-CoV-2-unexposed, CMV$^+$ and HLA-B*35(:01) donors (N=37) showed that nearly all CMV$^+$ donors had IPS-specific T cells with frequencies above background level and, interestingly, three of the analyzed donors (UTT, UBV and SFW) presented with clearly detectable IPS/FVS-specific T cells (**Figure 4C**). Furthermore, IPS/FVS-specific T cells displayed an effector memory phenotype (CCR7$^-$CD45RA$^-$), confirming a memory repertoire origin and, interestingly, a less differentiated phenotype compared to IPS-specific T cells (**Figure 4D**). In summary, IPS/FVS cross-reactivity is dependent on the TCR clonotype and these cross-reactive T cells are detected in multiple donors.

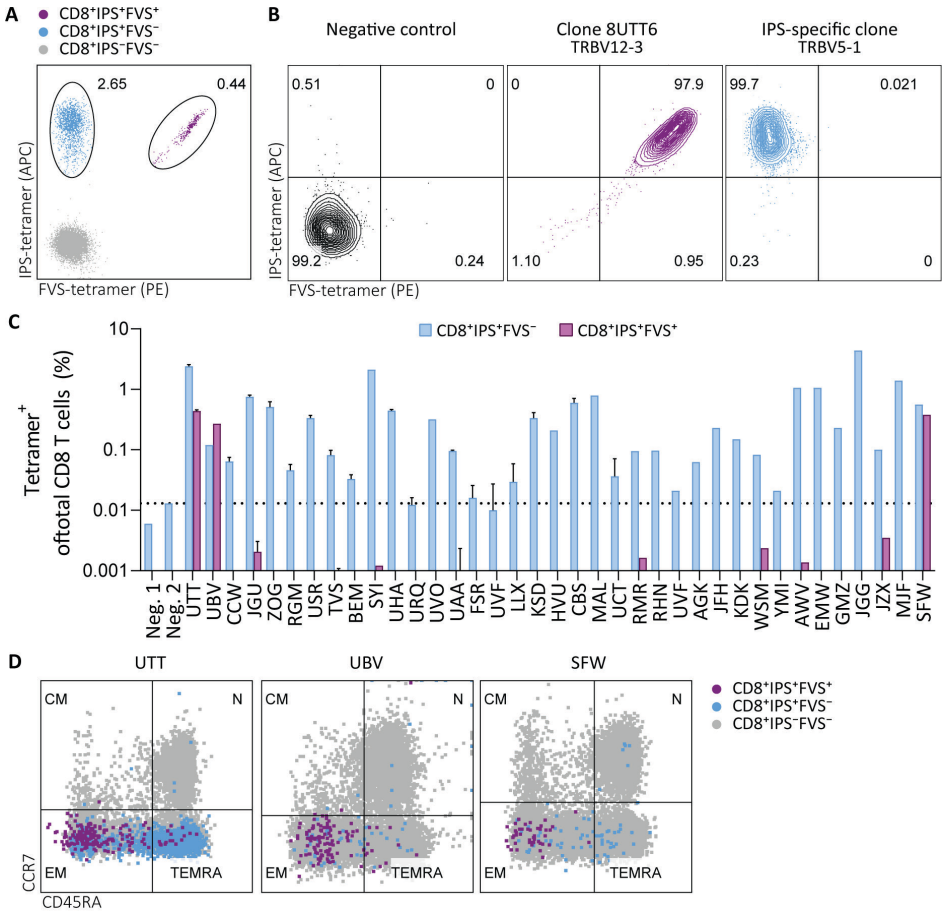

Figure 4 Tetramer detection of IPS/FVS-specific CD8⁺ T cells in CMV⁺ and HLA-B*35:01⁺ donors

Flow cytometry measurement of PBMCs or T cell clones that are binding to B*35/IPS-tetramer (blue), B*35/FVS-tetramer (purple) or to neither (grey). A) Flow cytometry dot plot showing percentages of tetramer-binding cells of total CD8⁺ T cells in PBMCs from donor UTT. B) Dot plot showing percentages of tetramer-binding of 8UTT6 clone and an IPS-specific clone with their IMGT variable region of T cell receptor β-chain (TRBV) depicted. As a negative control (neg. ctrl.), a T cell clone recognizing a non-relevant peptide in HLA-B*35:01 was included. C) Bar graph showing frequencies of tetramer-binding of total CD8⁺ from PBMCs of healthy CMV⁺ and HLA-B*35(:01)⁺ donors. Error bars represent standard deviation of experimental duplicates. Dotted line represents background level which was based on HLA-B*35:01⁻ donors (neg.). D) Dot plot showing expression of CCR7 and CD45RA by total CD8⁺ T cells and tetramer-binding T cells in PBMCs from UTT, UBV and SFW. Quadrants separates differentiation subsets into naïve (N), central memory (CM), effector memory (EM) and terminally differentiated effector memory (TEMRA).

IPS/FVS cross-reactivity is underpinned by a public TCR

To investigate whether the IPS/FVS-specific CD8⁺ T cells found in multiple donors expressed a similar TCR, B*35/FVS-tetramer-binding T cells were isolated and the

TCR α and β chains sequenced (**Figure 5 - figure supplement 1**). Sequencing was performed for samples with clear detection of IPS/FVS-specific T cells (UTT, UBV, SFW) and one donor with detectable, but below the limit of accurate detection of B*35/FVS-tetramer^{+} T cells (JZX) (**Figure 4C**). Interestingly, B*35/FVS-isolated T cells from all donors displayed amino acid identical dominant complementary-determining region 3 (CDR3) of the α-chain, CAGNQGGKLIF (CDR3α^{CAGNQG}), and β-chain, CASSLALDEQFF (CDR3β^{CASSLA}) (**Figure 5A**). This observation thereby shows that IPS/FVS cross-reactivity is caused by a public TCR. These identical CDR3s were not a result of sequencing artefact as nucleotide alignment revealed minor differences between samples (**Figure 5 – figure supplement 2**). In addition to B*35/FVS-isolated T cells, T cells that bound B*35/IPS-tetramer were isolated and sequenced in parallel. Both CDR3α^{CAGNQG} and CDR3β^{CASSLA} were identified in all samples and shown to be among the most dominant TCRs. Remarkably, this was also observed in donor JZX which showed IPS/FVS-tetramer^{+} T cells below background level, indicating that in more than 3 out of 37 donors this public TCR is present. (**Figure 5C**). Taken together, IPS/FVS-specific T cells express an identical TCR, found in multiple donors, indicating that public TCRs can exhibit cross-reactive properties.

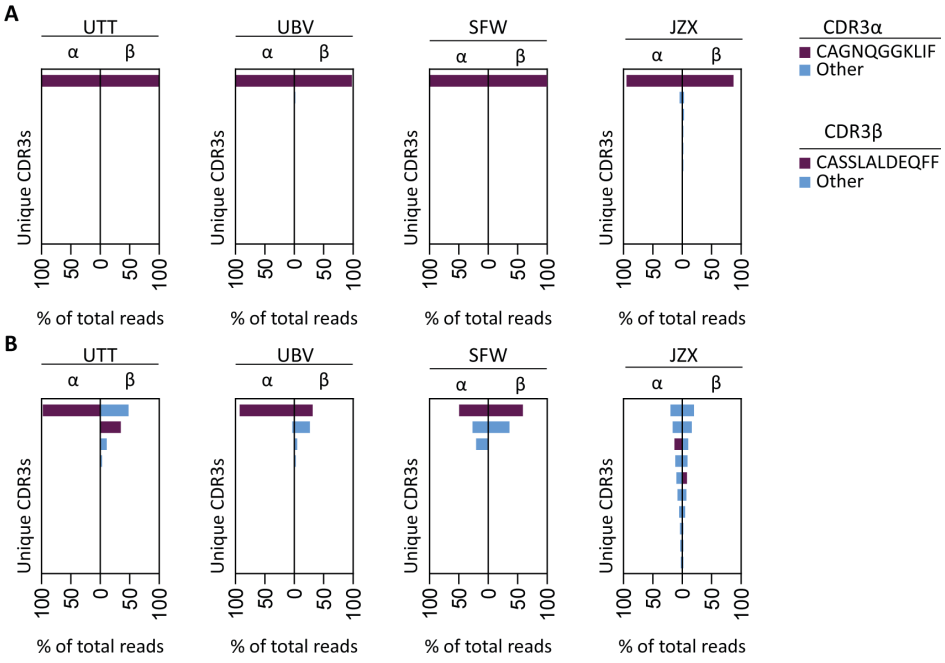

Figure 5 TCR sequencing of IPS/FVS-specific T cells
PBMCs from healthy CMV$^+$ and HLA-B*35:01$^+$ donors were sorted on B*35/IPS- or B*35/FVS-tetramer binding and directly sequenced for their TCR alpha and beta chain. Unique CDR3 sequences are depicted in two-sided bar graphs in which the left side shows abundance of CDR3 sequences from the TCR α-chain (CDR3α) and the right side shows abundance of CDR3 sequences from the TCR β-chain (CDR3β). Bar graphs are purple if the CDR3α has the CAGNQGGKLIF sequence or the CDR3β has the CASSLALDEQFF sequence, all other found sequences are depicted in blue. CDR3s with less than 1% abundance were excluded from the figure. A) Two-sided bar graphs showing abundances of unique CDR3 sequences of samples sorted on binding to B*35/FVS-tetramer. B) Two-sided bar graphs showing abundances of unique CDR3 sequences of samples sorted on binding to B*35/IPS-tetramer.

IPS/FVS cross-reactive CD8$^+$ T cells are able to recognize SARS-CoV-2 infected cells but do not show an activated phenotype during acute disease

To investigate whether IPS/FVS-specific CD8$^+$ T cells can play a role during SARS-CoV-2 infection, the function of IPS/FVS-specific T cells in an *in vitro* model and the activation state of these T cells during acute SARS-CoV-2 infection in severe COVID-19 patients was assessed. Firstly, the reactivity of IPS/FVS-specific T cells against K562 transduced with the spike gene was measured which showed that the T cells were able to recognize endogenously processed and presented peptide (**Figure 6A**). To investigate whether the IPS/FVS-specific T cells can recognize SARS-CoV-2-infected cells and thereby limit viral spread, Calu-3 airway epithelial cells were infected with live SARS-CoV-2 virus (wildtype) and incubated for 6 hours before co-culturing with CD8$^+$ T cells. SARS-CoV-2 spike-specific CD8$^+$ T cells from a SARS-CoV-2 vaccinated donor were able to reduce intracellular SARS-CoV-2 RNA copies at both 0.05 and 0.5

multiplicity of infection (MOI) 24 hours post infection (**Figure 6B-C**). Interestingly, IPS/FVS-specific CD8$^+$ T cells were able to reduce SARS-CoV-2 intracellular RNA copies in Calu-3 cells infected with 0.05 MOI (MOI (**Figure 6B**). Incubating with 10-fold more virus (0.5 MOI) resulted in no difference in RNA copies compared to the no T cell control (**Figure 6C**). To further investigate the function of IPS/FVS-specific CD8$^+$ T cells *ex vivo*, the activation state of these T cells was evaluated during severe COVID-19 disease in two CMV$^+$ HLA-B*35:01$^+$ patients. The activation state was measured by expression of activation markers CD38 and HLA-DR as these markers are highly expressed on SARS-CoV-2-specific CD8$^+$ T cells during severe COVID-19 (**Figure 6D**) [5]. Interestingly, IPS/FVS-cross-reactive T cells were detected in 2 out of 2 CMV$^+$ HLA-B*35:01$^+$ patients suffering from severe COVID-19, whereas the cross-reactive T cells were detected in 3 out of 37 healthy CMV$^+$ HLA-B*35:01$^+$ donors (**Figure 4C and 6E**). The expression of CD38 and HLA-DR was lower compared to the SARS-CoV-2-specific CD8$^+$ T cells and not considerably increased compared to IPS-specific T cells that were not cross-reactive with FVS (**Figure 6D-E**). These results indicate that IPS/FVS-specific CD8$^+$ T cells recognize SARS-CoV-2-infected cells and are able to limit SARS-CoV-2 replication at low virus titers. However, IPS/FVS-specific T cells did not show an activated phenotype during acute severe SARS-CoV-2 infection.

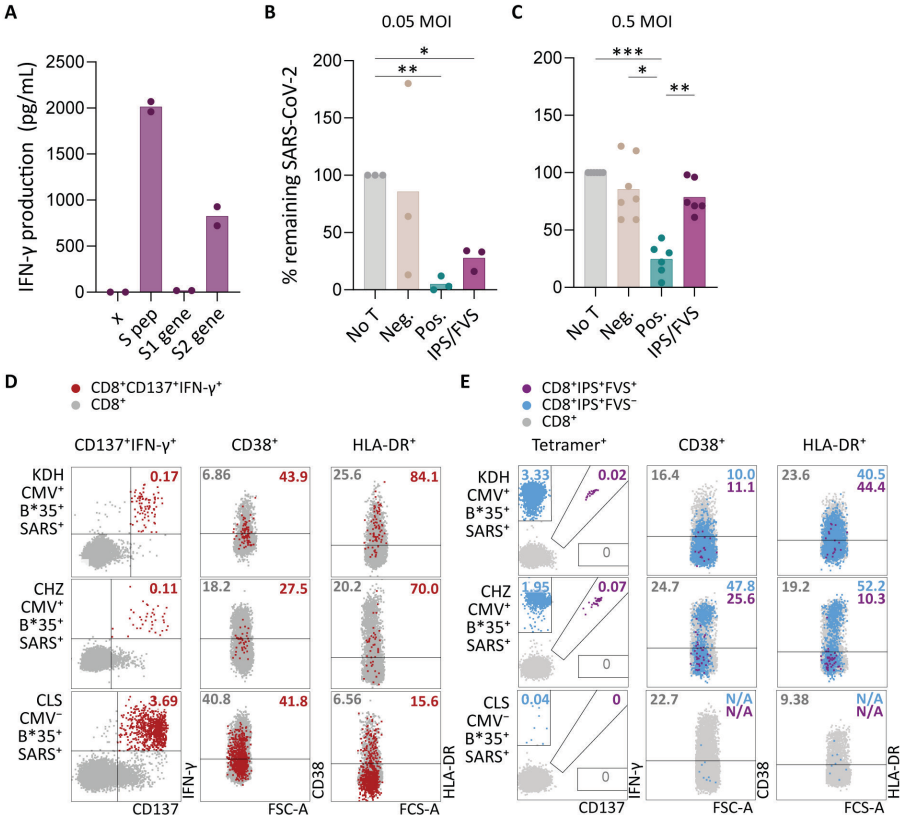

Figure 6 *Ex vivo* and *in vitro* evaluation of IPS/FVS-specific T cells

A) IFN-γ release of IPS/FVS-specific CD8⁺ T cells after co-incubation with K562 that were untransduced (x), loaded with spike peptide pool (S pep), or transduced with nucleotide 1 to 2082 (S1 gene) or nucleotide 2052 to 3822 (S2 gene) of the spike gene. B-C) Calu-3 cells were transduced to express HLA-B*35:01 and infected with the wildtype SARS-CoV-2 virus. 6 hours post infection, IPS/FVS-specific CD8⁺ T cells were added in a 10:1 effector to target ratio. SARS-CoV-2 spike-specific T cells, isolated from COVID-19 vaccinated individuals, that recognize VASQSIIAY presented in HLA-B*35:01 or YLQPRTFLL presented in HLA-A*02:01 functioned as a positive control (pos.) or negative control (neg.), respectively. Cells were harvested 24 hpi to measure intracellular viral RNA. Bar graphs show the means of percentage reduction in SARS-CoV-2 intracellular RNA copies compared to the no T cell condition (no T) as measured by RT-qPCR, at 24 hpi post infection using a MOI of 0.05 or 0.5. One-way ANOVA was applied test statistical differences between conditions and only comparisons with $p<0.05$ are shown. (D-E) Flow cytometry analysis of CD38 and HLA-DR expression on CD8⁺ T cells in PBMCs from severe COVID-19 patients that were CD137⁺IFN-γ⁺ after SARS-CoV-2 nucleocapsid peptide stimulation (red), only bound to B*35/IPS-tetramer (blue) or bound to both B*35/IPS- and B*35/FVS-tetramer (purple). All other CD8⁺ T cells are grey. Two patients were HLA-B*35:01⁺CMV⁺ (KDH and CHZ) and, as a control, one patient was HLA-B*35:01⁺CMV⁻ (CLS). Detection of B*35/IPS- and B*35/FVS-specific T cells and expression of the activation markers were measured and compared within the same sample.

DISCUSSION

SARS-CoV-2-specific T cells in pre-pandemic cryo-preserved samples have been reported in several studies. The majority of these studies describe T cell immunity against other HCoVs as the main source of these T cells [21-27]. However, some studies have postulated that pre-pandemic SARS-CoV-2-specific T cells could be derived from other sources [22,28-30]. Our findings demonstrate that CMV pp65-specific $CD4^+$ T cells cross-react with the membrane protein from SARS-CoV-2 and CMV pp65-specific $CD8^+$ T cells are able to cross-react with SARS-CoV-2 spike protein. The cross-reactive $CD8^+$ T cells recognized known CMV epitope IPSINVHHY in HLA-B*35:01 and cross-reacted with the SARS-CoV-2 epitope FVSNGTHWF in HLA-B*35:01. These IPS/FVS-specific $CD8^+$ T cells were detected in multiple donors all expressing an identical T cell receptor, indicating that cross-reactivity with SARS-CoV-2 can be caused by a CMV-specific public TCR. Functional and phenotypic assessment of the IPS/FVS-specific $CD8^+$ T cells indicated their capacity to reduce low concentrations of SARS-CoV-2 *in vitro* but these cross-reactive T cells detected in two severe COVID-19 patients were not activated based on phenotypic characterization.

To our knowledge this is the first study to identify CMV-specific T cells that are cross-reactive with SARS-CoV-2. The cross-reactive $CD4^+$ T cells recognized CMV pp65 epitope AGILARNLVPM in HLA-DRB3*02:02 and were able to cross-react with an as of yet unidentified, SARS-CoV-2 membrane epitope in HLA-DRB3*02:02. [42]Previous studies have reported the presence of membrane-specific $CD4^+$ T cell responses in SARS-CoV-2-unexposed donors utilizing the same commercially available membrane peptide pool, yet these studies did not aim to identify the peptide-HLA restriction [5,26]. AGI-specific $CD4^+$ T cells have been described to be cross-reactive towards SARS-CoV-2 spike which is in contrast to our finding [42]. The cross-reactive $CD8^+$ T cells recognize the CMV epitope IPSINVHHY and SARS-CoV-2 epitope FVSNGTHWF presented in HLA-B*35:01. IPS/FVS-specific T cells were possibly detected previously but never further investigated or characterized [48,49]. Both cross-reactive $CD4^+$ and $CD8^+$ T cells displayed a higher avidity for the CMV epitope compared to the epitope derived from SARS-CoV-2. In contrast, other studies have reported an equal or even higher avidity for the SARS-CoV-2 epitope compared to the epitopes derived from the HCoV for which the T cells were hypothesized to be primed against [21,23,27,50]. This appears to be contradictive since it has been shown that repeated exposure results in selection of high avidity T cell clonotypes which are able to clear viral infection and protect against reinfection [51-54]. Cross-reactive T cells would therefore most likely display a higher avidity for the source pathogen compared to the avidity for SARS-CoV-2, as reported in this study. This discrepancy could be caused by the fact that previous

studies focused on other HCoVs since they share high sequence homology with SARS-CoV-2, thereby potentially missing the true source of these particular T cells [21-27]. Alternatively, samples frozen down during the pandemic were considered unexposed if the donors displayed neither SARS-CoV-2-specific antibodies nor a history of COVID-19-like symptoms [23,26,50]. However, SARS-CoV-2 infection does not necessarily lead to symptoms nor a detectable antibody response [55,56]. The described reduced avidity for HCoV therefore could imply that these cross-reactive T cells were derived from the SARS-CoV-2-induced repertoire. Taken together, whereas cross-reactive T cells recognizing SARS-CoV-2 have been primarily described to be derived from other HCoVs, the contribution of these other HCoVs as initial primers of the T cell response may have been over-estimated due to experimental design. Further studies are required to identify other potential sources of cross-reactivity with low sequence homology yet high prevalences such as CMV, EBV, influenza or non-viral pathogens.

The identified cross-reactive CD8$^+$ T cells appeared to recognize CMV peptide IPSINVHHY and a dissimilar peptide FVSNGTHWF derived from SARS-CoV-2. *Ex vivo* detected heterologous CD8$^+$ T cell immunity against two pathogens caused by dissimilar epitopes presented in the same HLA is rarely reported [31,36]. Nevertheless, ample studies have investigated the underlying mechanisms of such T cell-mediated cross-reactivity. Heterologous immunity can be caused by the expression of a dual TCR which means that two TCR α- or β-chains are expressed simultaneously, resulting in two distinctive TCRs within one T cell [57]. However, here we identified a single TCR in cross-reactive T cells excluding this hypothesis. Recognition of two distinct epitopes by a single TCR can be explained by shape similarity once the peptides are bound to the HLA molecule, and this shape similarity, or molecular mimicry, can underpin T cell cross-reactivity [58]. Possible other underlying mechanisms are reduced footprint of the TCR with peptide [59,60], an altered TCR-docking angle [61], or plasticity of the peptide-MHC complex [32,61] or TCR [62]. Here, similarity between the IPS and FVS peptides in backbone conformation and the C-terminal part might underpin the T cell cross-reactivity observed, as the majority of TCR docks preferentially towards the C-terminal of the peptide [63]. Solving the crystal structure of the IPS/FVS-TCR binding to HLA-B*35:01-FVS and -IPS would be necessary to provide insight in the binding properties of the public TCR.

IPS/FVS-specific CD8$^+$ T cells were able to reduce SARS-CoV-2 spread *in vitro* when exposed to a low virus concentration, which is supported by our finding that two out of two tested severe COVID-19 patients had clearly detectable IPS/FVS-specific CD8$^+$ T cells while the prevalence in healthy donors was 3 out of 37. The presence of these cross-reactive memory T cells in circulation may be an advantage during

initial SARS-CoV-2 infection as rapid T cell responses were associated with less severe COVID-19 [2,7,25]. However, the cross-reactive CD8⁺ T cells were less efficient compared to SARS-CoV-2-specific, vaccination-primed T cells in limiting viral spread *in vitro* which can be explained by the reduced avidity of the cross-reactive T cells for the spike protein compared to CMV. This study also demonstrated that IPS/FVS-specific CD8⁺ T cells did not display the same degree of activation as observed for the SARS-CoV-2-specific T cells during severe COVID-19. Additionally, despite the presence of the cross-reactive CD8⁺ T cells, these individuals developed severe disease. These observations together indicate that IPS/FVS-specific CD8⁺ T cells might be able to reduce SARS-CoV-2 spread at initial infection, but likely do not play a significant role in the pathogenesis of severe COVID-19. One limitation is that our study focused on circulating T cells, and we cannot exclude the possibility that cross-reactive CD8⁺ T cells present in lung tissue did display an activated phenotype. Another limitation of this study is the small severe COVID-19 cohort that was investigated and literature describing the role of cross-reactive T cells is scarce [24,26]. In summary, additional studies using larger cohorts are required to fully elucidate the potential role of cross-reactive CD8⁺ T cells in disease.

In conclusion, pre-pandemic SARS-CoV-2-specific T cells can derive from non-homologous pathogens such as CMV. This expands the potential origin of these pre-pandemic SARS-CoV-2-specific CD4⁺ and CD8⁺ T cell beyond other HCoVs. The cross-reactive CD8⁺ T cells were reactive towards dissimilar epitopes and this cross-reactivity was caused by a public TCR, which has been rarely observed so far. Our data points towards a role of the cross-reactive T cells in reducing SARS-CoV-2 viral load in the early stages of infection, prior to priming of SARS-CoV-2 specific T cells. Altogether, these results aid in further understanding heterologous T cell immunity beyond common cold coronaviruses and facilitates the investigation into the potential role of cross-reactive T cells in COVID-19.

METHODS

Key Resourced Table

Key Resources Table				
Reagent type (species) or resource	**Designation**	**Source or reference**	**Identifiers**	**Additional information**
Peptide, recombinant protein	SARS-CoV-2 Spike (S), 15-mers, 11aa overlapping peptide pool	Miltenyi	130-126-701	1 µg/mL
Peptide, recombinant protein	SARS-CoV-2 Spike (S1), 15-mers, 11aa overlapping peptide pool	Miltenyi	130-127-041	1 µg/mL
Peptide, recombinant protein	SARS-CoV-2 Spike (S+), 15-mers, 11aa overlapping peptide pool	Miltenyi	130-127-312	1 µg/mL
Peptide, recombinant protein	SARS-CoV-2 Membrane (M), 15-mers, 11aa overlapping peptide pool	Miltenyi	130-126-703	1 µg/mL
Peptide, recombinant protein	SARS-CoV-2 Nucleocapsid (N), 15-mers, 11aa overlapping peptide pool	Miltenyi	130-126-699	1 µg/mL
Peptide, recombinant protein	CMV pp65, 15-mers, 11aa overlapping peptide pool	JPT	Custom-made	1 µg/mL
Peptide, recombinant protein	CMV pp65 peptide library, 15-mers, 11aa overlapping	JPT	Custom-made	1 µg/mL
Peptide, recombinant protein	SARS-CoV-2 Spike peptide library, 15-mers, 11aa overlapping	SB Peptides	SB043	1 µg/mL

Key Resourced Table *Continued*

Key Resources Table				
Reagent type (species) or resource	**Designation**	**Source or reference**	**Identifiers**	**Additional information**
Peptide, recombinant protein	CMV, VFTWPPWQAGILARN	LUMC	Custom-made	1 µg/mL
Peptide, recombinant protein	CMV, PPWQAGILARNLVPM	LUMC	Custom-made	1 µg/mL
Peptide, recombinant protein	CMV, AGILARNLVPMVATV	LUMC	Custom-made	1 µg/mL
Peptide, recombinant protein	CMV, ARNLVPMVATVQGQN	LUMC	Custom-made	1 µg/mL
Peptide, recombinant protein	CMV, VPMVATVQGQNLKYQ	LUMC	Custom-made	1 µg/mL
Peptide, recombinant protein	CMV, AQGDDDVWTSGSDSD	LUMC	Custom-made	1 µg/mL
Peptide, recombinant protein	CMV, SSATACTSGVMTRGR	LUMC	Custom-made	1 µg/mL
Peptide, recombinant protein	CMV, PKRRRHRQDALPGPC	LUMC	Custom-made	1 µg/mL
Peptide, recombinant protein	SARS-CoV-2, FVSNGTHWF	LUMC	Custom-made	1 µg/mL
Peptide, recombinant protein	CMV, IPSINVHHY	LUMC	Custom-made	1 µg/mL
Antibody	rat monoclonal anti-human CCR7 (BV711)	BD Biosciences	Cat.#563712 RRID:AB_2738386	FC (1:100)
Antibody	mouse monoclonal anti-human CD137 (APC)	BD Biosciences	Cat.#550890 RRID:AB_398477	FC (1:75)

Key Resources Table				
Reagent type (species) or resource	**Designation**	**Source or reference**	**Identifiers**	**Additional information**
Antibody	mouse monoclonal anti-human CD14 (FITC)	BD Biosciences	Cat.#555397 RRID:AB_395798	FC (1:100)
Antibody	mouse monoclonal anti-human CD154 (Pacific Blue)	Biolegend	Cat.#310820 RRID:AB_830699	FC (1:300)
Antibody	mouse monoclonal anti-human CD19 (FITC)	BD Biosciences	Cat.#555412 RRID:AB_395812	FC (1:100)
Antibody	mouse monoclonal anti-human CD4 (PE-Cy7)	Beckham Coulter	Cat.#737660 RRID:AB_2922769	FC (1:300)
Antibody	mouse monoclonal anti-human CD4 (FITC)	BD Biosciences	Cat.#555346 RRID:AB_395751	FC (1:30)
Antibody	mouse monoclonal anti-human CD4 (BV510)	BD Biosciences	Cat.#562970 RRID:AB_2744424	FC (1:300)
Antibody	mouse monoclonal anti-human CD45RA (PE-Texas-Red)	Invitrogen	Cat.#MHCD45RA17 RRID:AB_10372222	FC (1:200)
Antibody	mouse monoclonal anti-human CD8 (APC-H7)	BD Biosciences	Cat.#560179 RRID:AB_1645481	FC (1:100)
Antibody	mouse monoclonal anti-human CD8 (PE-Cy7)	BD Biosciences	Cat.#557746 RRID:AB_396852	FC (1:320)
Antibody	mouse monoclonal anti-human CD8 (Pacific Blue)	BD Biosciences	Cat.#558207 RRID:AB_397058	FC (1:500)
Antibody	mouse monoclonal anti-human IFN-γ (Alexa-Fluor 700)	Sony	Cat.#3112600 RRID:AB_2922770	FC (1:120)
Antibody	mouse monoclonal anti-human IFN-γ (BV711)	BD Biosciences	Cat.#564039 RRID:AB_2738557	FC (1:300)

Key Resourced Table *Continued*

Key Resources Table				
Reagent type (species) or resource	**Designation**	**Source or reference**	**Identifiers**	**Additional information**
Antibody	mouse monoclonal anti-human HLA-DR (Alexa-Fluor 700)	BD Biosciences	Cat.#560743 RRID:AB_1727526	FC (1:150)
Antibody	mouse monoclonal anti-human CD38 (BV605)	BD Biosciences	Cat.#740401 RRID:AB_2740131	FC (1:120)
Antibody	rat monoclonal anti-mouse CD19 (Mouse)	Biolegend	Cat.#557399 RRID:AB_396682	FC (1:250)
Other	Zombie-Red	Biolegend	Cat.#423109	FC (1:1000)
Other	Zombie-Aqua	BD Biosciences	Cat.#423101	FC (1:1000)
Other	Brilliant Violet Staining Buffer Plus	Beckham Coulter	Cat.#566385	FC (1:10)
Cell line (*Homo Sapiens)*	K-562	ATCC	CCL-342	
Cell line (*Homo Sapiens)*	Calu-3	ATCC	HTB-55	
Biological sample (*Homo Sapiens*)	PBMCs from 67 healthy donors	LUMC Biobank		Cryo-preserved before May 2019
Biological sample (*Homo Sapiens*)	PBMCs from critical COVID-19 patient (KDH)	LUMC BEAT-COVID consortium	Clinical trial #: NL8589	Male, 61 years, 31 days ICU
Biological sample (*Homo Sapiens*)	PBMCs from critical COVID-19 patient (CHZ)	LUMC BEAT-COVID consortium	Clinical trial #: NL8589	Male, 76 years, 40 days ICU
Biological sample (*Homo Sapiens*)	PBMCs from critical COVID-19 patient (CLS)	LUMC BEAT-COVID consortium	Clinical trial #: NL8589	Male, 71 years, 107 days ICU

Study samples and cell lines

Bio-banked PBMCs were cryopreserved after informed consent from the respective donors, in accordance with the declaration of Helsinki. The samples from COVID-19 patients were part of a trial (NL8589) registered in the Dutch Trial Registry and approved by Medical Ethical Committee Leiden-Den Haag-Delft (NL73740.058.20). All three patients suffered from critical COVID-19 as categorized according to World Health Organization guidelines (WHO ref#: WHO/2019-nCoV/clinical/2020.4) (see **Supplementary file 1** for patient details). Bio-banked PBMCs from CMV-seropositive (N=28) and CMV-seronegative (N=39) donors that were frozen down before May 2019 were randomly selected to assure that the samples are SARS-CoV-2 naïve and represent the European population (**Supplementary file 2**). Prior to cryopreservation, PBMCs were isolated from fresh whole blood using Ficoll-Isopaque. PBMCs were thawed in culture medium consisting of Iscove Modified Dulbecco Medium (IMDM; Lonza, Basel, Switserland) supplemented with 10% heat-inactivated fetal bovine serum (FBS; Sigma-Aldrich, Saint Louis, Missouri), 2.7 mM L-glutamine (Lonza), 100 U/mL penicillin (Lonza) and 100 µg/mL streptomycin (Lonza) (1% p/s), and subsequently treated with 1.33 mg/ml DNAse to minimize cell clumping. K562 cells *(CCL-243;* American Type Culture Collection (ATCC)) and Calu-3 lung carcinoma cells (*HTB-55;* ATCC) were regularly checked for the presence of mycoplasma. K562s were regularly checked to ensure (lack of) HLA expression and calu-3 cells were authenticated by STR sequencing.

Intracellular cytokine staining assay

Thawed PBMCs were stimulated in culture medium supplemented with 1 µg/mL SARS-CoV-2 peptides pools covering the entire spike (Miltenyi, Keulen, Germany), membrane (Miltenyi), or nucleocapsid (Miltenyi) proteins for one hour at 37°C + 5% CO_2. The peptides of the spike gene were by the manufacturer divided over a "S", "S1" and "S+" pool, wherein "S" covers the most immunogenic parts of the gene, "S1" mostly covers S1 domain and "S+" mostly covers S2 domain. An additional peptide pool containing 11 amino acid overlapping 15-mer peptides covering the pp65 antigen from CMV (JPT Peptide Technologies) was included (see **Supplementary file 3** for peptide details). After one hour stimulation, 5 µg/mL Brefeldin A (Sigma-Aldrich) was added and the samples were incubated for an additional 15 hours at 37°C + 5% CO_2. The samples were subsequently stained with the viability dye Zombie-Red (Biolegend, San Diego, California) for 25 minutes at room temperature (RT) after which the cells were washed in PBS containing 0.8 mg/mL albumin (FACS buffer) and stained with antibodies against CD4 and CD8 in FACS buffer for 30 minutes at 4°C. Cells were washed in PBS and fixed in 1% paraformaldehyde for 8 minutes RT followed by a wash and a permeabilization step for 30 minutes at 4°C in FACS

buffer supplemented with 1% p/s and 0.1% saponin (permeabilization buffer). After permeabilization, the cells were stained using an antibody cocktail directed against CD14, CD19, CD137, CD154 and IFN-γ in permeabilization buffer (see **Supplementary file 4** for antibody details) for 30 minutes at 4°C. After staining, the samples were washed, resuspended in permeabilization buffer and measured on a 3-laser aurora (Cytek Biosciences, Fremont, California).

Isolation of SARS-CoV-2-specific T cells

Thawed PBMCs were stimulated for 16 hours at 37°C + 5% CO_2 using 1 µg/mL of spike (Miltenyi) or membrane (Miltenyi) peptide pool in culture medium (see **Supplementary file 7** for peptide details). After stimulation, the cells were washed and stained with antibodies directed against CD4, CD8 and CD137 in phenol-red free IMDM (Gibco, Waltham, Massachusetts) containing 2% FBS (Sigma-Aldrich), 1% p/s (Lonza) (sort medium) (see **Supplementary file 4** for antibody details) for 30 minutes at 4°C. The cells were subsequently washed and resuspended in sort medium. $CD4^+$ or $CD8^+$ and $CD137^+$ cells were single-cell sorted using an Aria III cell sorter (BD Biosciences, Franklin Lakes, New Jersey) into a 96-well round-bottom plate containing $1x10^5$ 35-Gy-irradiated PBMCs, 50-Gy-irradiated EBV-LCL-JYs and 0.8 µg/mL phytohemagglutinin (PHA) (Thermo Fisher, Waltham, Massachusetts) in 100 µL T cell medium (TCM) consisting of IMDM (Lonza) supplemented with 2.7 mM L-glutamine (Lonza), 100 U/mL penicillin (Lonza) and 100 µg/mL streptomycin (Lonza), 5% FBS (Sigma-Aldrich), 5% human serum (Sanquin, Amsterdam, The Netherlands) and 100 IU/mL recombinant human IL-2 (Novartis, Basel, Switzerland). Sorted T cells were clonally expanded to generate T cell clones. T cell clones were restimulated between day 14-20 post stimulation using PHA, PBMCs and EBV-LCL-JYs as described above and used for assays between day 7-20 post stimulation.

Co-culture assays

To test peptide and HLA restriction, T cell clones were washed and co-cultured with stimulator cells in a 1:6 effector to stimulator ratio. Stimulator cells consisted of either autologous or HLA-matched EBV-LCLs or retrovirally transduced K562s. K562 were transduced with a pZLRS or MP71 vector containing a HLA gene of interested linked to a marker gene, transduction was performed as previously described [64]. Cells were enriched for marker gene expression using magnetic activated cell sorting (MACS; Miltenyi) or fluorescent activated cell sorting (FACS) on an Aria III cell sorter (BD Biosciences). Stimulator cells were loaded with peptides through pre-incubation for 30 minutes at 37°C with 0.01-1 µM peptide (**Supplementary file 3** for peptide details). To identify the pp65 epitope of the $CD4^+$ T cell clones, a co-culture assay was performed using a pp65 peptide library. The pp65 library consisted of 15-mere

peptides with 11 amino acid overlap, spanning the whole pp65 gene. The peptides are divided into matrix pools with horizontal and vertical sub pools so that each pool has an unique peptide combination and each peptide is in one horizontal and one vertical sub pool. To identify the HLA-restriction of the $CD4^+$ T cell clones, the peptides were not washed away during the co-culture incubation period and HLA class II was knocked out in the T cell clones as previously described [65]. However, the protocol was adapted to knock-out Class II Major histocompatibility complex transactivator (CIITA) by designing two reverse guide RNAs: 5'-AGTCGCTCACTGGTCCCACTAGG-3' and 5'-CCGTGGACAGTGAATCCACTGGG-3' (Integrated DNA technologies Inc., Coralville, Iowa). Co-culture assays were incubated overnight and secreted IFN-γ was measured as an indicator of T cell activity by ELISA (Diaclone, Besançon, France) as described by the manufacturer.

To identify the peptide recognition signature of the CD8 T cell clones, a co-culture assay was performed using a nonamer combinatorial peptide library (CPL) [35]. The 9-mer CPL scan contains 180 peptide pools with each pool consisting of a mixture of peptides with one naturally-occurring amino acid fixed at one position [66]. Co-culture assay was performed as described above with small changes; $2x10^4$ K562 transduced with HLA-B*35:01 were pre-incubated with 100 µM CPL peptides for 1 hour at 37°C before $5x10^3$ T cell clones were added. After overnight incubation, secreted IFN-γ was measured by an IFN-γ-ELISA (Diaclone) and results were analyzed using WSBC PI CPL for viruses [67,68]. Identified peptides following peptide libraries or CPL were analyzed for predicted binding to HLA-B*35:01 using netMHC 4.0 [69]. Alternatively, peptide recognition by T cell clones was measured using ICS assay as described above.

Peptide-HLA modelling

The binding of FVS in HLA-B*35:01 was modelled based on the solved crystal structure of the HLA-B*35:01-IPS [45]. Each residue of the IPS peptide was mutated to their corresponding residues in the FVS peptide using the mutagenesis wizard in PyMOL [70]. The residues were mutated into the most favorable rotamer to avoid steric clashes. No major steric clashes with the peptide or HLA were observed.

Tetramer staining

$1\text{-}2x10^6$ PBMCs or $5x10^4$ T cell clones were incubated with in-house generated, PE- or APC-conjugated tetramers for 30 minutes at RT [53]. After tetramer incubation, the cells were washed and incubated with an antibody mix targeting CD4, CD8, CD45RA, CCR7, CD38 and/or HLA-DR. After incubation, cells were washed and resuspended in FACS buffer and immediately measured on a 3-laser Aurora (Cytek Biosciences).

TCR sequencing

PBMCs were thawed and 10-50x10^6 cells directly stained with PE-conjugated HLA-B*35:01-FVS or HLA-B*35:01-IPS tetramers. Tetramers were labelled to beads using anti-PE MicroBeads (Miltenyi) and enriched through magnetic-activated cell sorting (Miltenyi). The tetramer-enriched cells were washed and incubated with an antibody cocktail targeting CD4 and CD8 (see **Supplementary file 4** for antibody details) in sort medium. Stained samples were washed in sort medium and bulk-sorted on an Aria III cell sorter (BD Biosciences) (see **Fig S6B** for a gating example). RNA isolation and TCR sequencing was performed as previously described [71]. In short, cells were directly collected in lysis buffer for RNA isolation using the ReliaPrep RNA cell Miniprep system (Promega, Madison, Wisconsin). The total RNA yield of each sample was converted to cDNA using a template-switch oligo primer (TSO) (Eurogentec, Seraing, Belgium), RNAsin (Promega) and SMARTScribe reverse transcriptase (Takara Bio, Kusatsu, Japan) [72]. cDNA was pre-amplified via an IS region in the Oligo dT primer prior to barcoding on samples containing cDNA from 500 or fewer cells [73]. Barcoded TCR PCR product was generated in two rounds of PCR: in the first PCR reaction, *TRA* and *TRB* product was generated in separate PCR reactions using Phusion Flash (Thermo Fisher Scientific), Smartseq2modified PCR primer (Eurogentec) and TRAC or TRBC1/2 specific primers (Eurogentec) (see **Supplementary file 5** for primer list). The PCR product was then purified using the Wizard SV 96 PCR Clean-Up System (Promega) and barcoded in a second PCR using two-sided six-nucleotide barcoded primers to discriminate between TCRs of different T cell populations. PCR products of different T cell populations were pooled, after which TCR sequences were identified by NovaSeq (GenomeScan, Leiden, The Netherlands).

SARS-CoV-2 infection assay

Calu-3 lung carcinoma cells (*HTB-55;* ATCC) were cultured in Eagle's minimum essential medium (EMEM, Lonza), supplemented with 9% fetal calf serum (FCS; CapriCorn Scientific, USA), 1% NEAA (Sigma-Aldrich), 2 mM L-glutamine (Sigma-Aldrich), 1 mM sodium pyruvate (Sigma-Aldrich) and 100 U/ml of penicillin/streptomycin (P/S; Sigma-Aldrich). Calu-3 cells were retrovirally transduced with a pLZRS vector containing the HLA-B*35:01 molecule linked via an internal ribosome entry site (IRES) sequence to mouse CD19, transduction was performed as previously described [64]. Mouse CD19 was used as a marker gene to enrich for successfully transduced cells by adding antibodies directed against mouse CD19 and enriching for stained cells by MACS (Miltenyi) followed by FACS on an Aria III cell sorter (BD Biosciences) (see **Supplementary file 4** for antibody details). For the infection assay, Calu-3 cells were seeded in 96-well cell culture plates at a density of 3x10^4 cells per well in 100 µl culture medium. Infections were done with clinical isolate SARS-CoV-2/Leiden-0008,

which was isolated from a nasopharyngeal sample collected at the LUMC during the first wave of the Corona pandemic in March 2020 (GenBack: MT705206.1). Cells were infected with SARS-CoV-2 at a multiplicity of infection (MOI) of 0.05 or 0.5 in 50 µl infection medium. After 1.5h, cells were washed three times with medium and 100 µl of medium was added. At 6 hours post infection (hpi) medium was removed again and 100 µl of T cell medium with $3x10^5$ T cells per well was added. At 24 hpi cells were harvested to collect intracellular RNA by lysing the cells in 100 µl GITC reagent (3M GITC, 2% sarkosyl, 20 mM Tris, 20 mM EDTA) per well. Intracellular RNA was isolated using magnetic beads and viral RNA was quantified by internally controlled multiplex TaqMan RT-qPCR as described previously [74].

Statistics

Flow cytometry data was unmixed using Spectroflo (Cytek Biosciences) and analyzed using FlowJo v10.7.1. (BD Biosiences) to set gates on the samples based on the DMSO negative control in ICS assays or adapted to positive control for tetramer staining (see **Figure 1 – figure supplement 1, figure 2 – figure supplement 1, figure 4 – figure supplement 1** and **figure 5 – figure supplement 1**)me for a gating example). Samples were excluded from the analysis if less than 10,000 events in $CD4^+$ or $CD8^+$ gate was measured or if after further testing they appeared not to be $\alpha\beta$ T cells. For the SARS-CoV-2 infection assays, experiments were excluded from the analysis if the positive control had higher SARS-CoV-2 intracellular RNA copies compared to no T cell condition. Statistical analysis and generation of figures was conducted using GraphPad Prism 9.0.1 (GraphPad Software). Data was tested for significance using an one-way ANOVA with *p*-values below 0.05 considered as significant. *p*-values are categorized in the figures as: ns=not significant; $*p<0.05$; $**p<0.01$ or $***p<0.001$.

TCR sequence data were analysed using MiXCR software (v3.0.13) to determine the Vα and Vβ family and CDR3 regions using annotation of the IMGT library (http://www.imgt.org; v6) [75]. CDR3 regions were analysed in RStudio and CDR3 sequences that were non-functional or had ⩽50 reads were excluded from the analysis.

Acknowledgements

The authors like to thank Joost M. Lambooij for critically editing the manuscript. Flow cytometry was performed at the Flow cytometry Core Facility (FCF) of Leiden University Medical Center (LUMC) in Leiden, Netherlands (https://www.lumc.nl/research/facilities/fcf).

REFERENCES

1. Brodin, P. Immune determinants of COVID-19 disease presentation and severity. *Nat Med* **27**, 28-33, doi:10.1038/s41591-020-01202-8 (2021).
2. Sette, A. & Crotty, S. Adaptive immunity to SARS-CoV-2 and COVID-19. *Cell* **184**, 861-880, doi:10.1016/j.cell.2021.01.007 (2021).
3. Liao, M. *et al*. Single-cell landscape of bronchoalveolar immune cells in patients with COVID-19. *Nat Med* **26**, 842-844, doi:10.1038/s41591-020-0901-9 (2020).
4. Rydyznski Moderbacher, C. *et al*. Antigen-Specific Adaptive Immunity to SARS-CoV-2 in Acute COVID-19 and Associations with Age and Disease Severity. *Cell* **183**, 996-1012 e1019, doi:10.1016/j.cell.2020.09.038 (2020).
5. Sekine, T. *et al*. Robust T Cell Immunity in Convalescent Individuals with Asymptomatic or Mild COVID-19. *Cell* **183**, 158-168 e114, doi:10.1016/j.cell.2020.08.017 (2020).
6. Bange, E. M. *et al*. CD8(+) T cells contribute to survival in patients with COVID-19 and hematologic cancer. *Nat Med* **27**, 1280-1289, doi:10.1038/s41591-021-01386-7 (2021).
7. Tan, A. T. *et al*. Early induction of functional SARS-CoV-2-specific T cells associates with rapid viral clearance and mild disease in COVID-19 patients. *Cell Rep* **34**, 108728, doi:10.1016/j.celrep.2021.108728 (2021).
8. Bertoletti, A., Le Bert, N., Qui, M. & Tan, A. T. SARS-CoV-2-specific T cells in infection and vaccination. *Cell Mol Immunol* **18**, 2307-2312, doi:10.1038/s41423-021-00743-3 (2021).
9. Gao, Y. *et al*. Ancestral SARS-CoV-2-specific T cells cross-recognize the Omicron variant. *Nat Med*, doi:10.1038/s41591-022-01700-x (2022).
10. Keeton, R. *et al*. T cell responses to SARS-CoV-2 spike cross-recognize Omicron. *Nature*, doi:10.1038/s41586-022-04460-3 (2022).
11. Liu, J. *et al*. Vaccines Elicit Highly Conserved Cellular Immunity to SARS-CoV-2 Omicron. *Nature*, doi:10.1038/s41586-022-04465-y (2022).
12. GeurtsvanKessel, C. H. *et al*. Divergent SARS CoV-2 Omicron-reactive T- and B cell responses in COVID-19 vaccine recipients. *Sci Immunol*, eabo2202, doi:10.1126/sciimmunol.abo2202 (2022).
13. Tarke, A. *et al*. SARS-CoV-2 vaccination induces immunological T cell memory able to cross-recognize variants from Alpha to Omicron. *Cell*, doi:10.1016/j.cell.2022.01.015 (2022).
14. Chiuppesi, F. *et al*. Vaccine-induced spike- and nucleocapsid-specific cellular responses maintain potent cross-reactivity to SARS-CoV-2 Delta and Omicron variants. *iScience* **25**, 104745, doi:10.1016/j.isci.2022.104745 (2022).
15. Choi, S. J. *et al*. T cell epitopes in SARS-CoV-2 proteins are substantially conserved in the Omicron variant. *Cell Mol Immunol* **19**, 447-448, doi:10.1038/s41423-022-00838-5 (2022).
16. Jung, M. K. *et al*. BNT162b2-induced memory T cells respond to the Omicron variant with preserved polyfunctionality. *Nature Microbiology* **7**, 909-917 (2022).
17. Redd, A. D. *et al*. Minimal Crossover between Mutations Associated with Omicron Variant of SARS-CoV-2 and CD8(+) T-Cell Epitopes Identified in COVID-19 Convalescent Individuals. *mBio* **13**, e0361721, doi:10.1128/mbio.03617-21 (2022).

18. Grifoni, A. *et al*. Targets of T Cell Responses to SARS-CoV-2 Coronavirus in Humans with COVID-19 Disease and Unexposed Individuals. *Cell* **181**, 1489-1501 e1415, doi:10.1016/j.cell.2020.05.015 (2020).

19. Weiskopf, D. *et al*. Phenotype and kinetics of SARS-CoV-2-specific T cells in COVID-19 patients with acute respiratory distress syndrome. *Sci Immunol* **5**, doi:10.1126/sciimmunol.abd2071 (2020).

20. Nelde, A. *et al*. SARS-CoV-2-derived peptides define heterologous and COVID-19-induced T cell recognition. *Nat Immunol* **22**, 74-85, doi:10.1038/s41590-020-00808-x (2021).

21. Mateus, J. *et al*. Selective and cross-reactive SARS-CoV-2 T cell epitopes in unexposed humans. *Science* **370**, 89-94, doi:10.1126/science.abd3871 (2020).

22. Le Bert, N. *et al*. SARS-CoV-2-specific T cell immunity in cases of COVID-19 and SARS, and uninfected controls. *Nature* **584**, 457-462, doi:10.1038/s41586-020-2550-z (2020).

23. Braun, J. *et al*. SARS-CoV-2-reactive T cells in healthy donors and patients with COVID-19. *Nature* **587**, 270-274, doi:10.1038/s41586-020-2598-9 (2020).

24. Kundu, R. *et al*. Cross-reactive memory T cells associate with protection against SARS-CoV-2 infection in COVID-19 contacts. *Nat Commun* **13**, 80, doi:10.1038/s41467-021-27674-x (2022).

25. Loyal, L. *et al*. Cross-reactive CD4(+) T cells enhance SARS-CoV-2 immune responses upon infection and vaccination. *Science* **374**, eabh1823, doi:10.1126/science.abh1823 (2021).

26. Bacher, P. *et al*. Low-Avidity CD4(+) T Cell Responses to SARS-CoV-2 in Unexposed Individuals and Humans with Severe COVID-19. *Immunity* **53**, 1258-1271 e1255, doi:10.1016/j.immuni.2020.11.016 (2020).

27. Johansson, A. M. *et al*. Cross-reactive and mono-reactive SARS-CoV-2 CD4+ T cells in prepandemic and COVID-19 convalescent individuals. *PLoS Pathog* **17**, e1010203, doi:10.1371/journal.ppat.1010203 (2021).

28. Tan, C. C. S. *et al*. Pre-existing T cell-mediated cross-reactivity to SARS-CoV-2 cannot solely be explained by prior exposure to endemic human coronaviruses. *Infect Genet Evol* **95**, 105075, doi:10.1016/j.meegid.2021.105075 (2021).

29. Peng, Y. *et al*. Broad and strong memory CD4(+) and CD8(+) T cells induced by SARS-CoV-2 in UK convalescent individuals following COVID-19. *Nat Immunol* **21**, 1336-1345, doi:10.1038/s41590-020-0782-6 (2020).

30. Stervbo, U., Rahmann, S., Roch, T., Westhoff, T. H. & Babel, N. Epitope similarity cannot explain the pre-formed T cell immunity towards structural SARS-CoV-2 proteins. *Sci Rep* **10**, 18995, doi:10.1038/s41598-020-75972-z (2020).

31. Clute, S. C. *et al*. Cross-reactive influenza virus-specific CD8+ T cells contribute to lymphoproliferation in Epstein-Barr virus-associated infectious mononucleosis. *J Clin Invest* **115**, 3602-3612, doi:10.1172/JCI25078 (2005).

32. Riley, T. P. *et al*. T cell receptor cross-reactivity expanded by dramatic peptide-MHC adaptability. *Nat Chem Biol* **14**, 934-942, doi:10.1038/s41589-018-0130-4 (2018).

33. Su, L. F. & Davis, M. M. Antiviral memory phenotype T cells in unexposed adults. *Immunol Rev* **255**, 95-109, doi:10.1111/imr.12095 (2013).

34. Cameron, B. J. *et al*. Identification of a Titin-derived HLA-A1-presented peptide as a cross-reactive target for engineered MAGE A3-directed T cells. *Sci Transl Med* **5**, 197ra103, doi:10.1126/scitranslmed.3006034 (2013).

35. Bijen, H. M. *et al*. Preclinical Strategies to Identify Off-Target Toxicity of High-Affinity TCRs. *Mol Ther* **26**, 1206-1214, doi:10.1016/j.ymthe.2018.02.017 (2018).

36. Cornberg, M. *et al*. CD8 T cell cross-reactivity networks mediate heterologous immunity in human EBV and murine vaccinia virus infections. *J Immunol* **184**, 2825-2838, doi:10.4049/jimmunol.0902168 (2010).

37. Lee, C. H. *et al*. Predicting Cross-Reactivity and Antigen Specificity of T Cell Receptors. *Front Immunol* **11**, 565096, doi:10.3389/fimmu.2020.565096 (2020).

38. Meckiff, B. J. *et al*. Imbalance of Regulatory and Cytotoxic SARS-CoV-2-Reactive CD4(+) T Cells in COVID-19. *Cell* **183**, 1340-1353 e1316, doi:10.1016/j.cell.2020.10.001 (2020).

39. Zuhair, M. *et al*. Estimation of the worldwide seroprevalence of cytomegalovirus: A systematic review and meta-analysis. *Rev Med Virol* **29**, e2034, doi:10.1002/rmv.2034 (2019).

40. Sylwester, A. W. *et al*. Broadly targeted human cytomegalovirus-specific CD4+ and CD8+ T cells dominate the memory compartments of exposed subjects. *J Exp Med* **202**, 673-685, doi:10.1084/jem.20050882 (2005).

41. Alanio, C. *et al*. Cytomegalovirus latent infection is associated with an increased risk of COVID-19-related hospitalization. *J Infect Dis*, doi:10.1093/infdis/jiac020 (2022).

42. Weber, S. *et al*. CMV seropositivity is a potential novel risk factor for severe COVID-19 in non-geriatric patients. *PLoS One* **17**, e0268530, doi:10.1371/journal.pone.0268530 (2022).

43. Jo, N. *et al*. Aging and CMV Infection Affect Pre-existing SARS-CoV-2-Reactive CD8+ T Cells in Unexposed Individuals. *Frontiers in Aging* **2**, doi:10.3389/fragi.2021.719342 (2021).

44. Klarenbeek, P. L. *et al*. Deep sequencing of antiviral T-cell responses to HCMV and EBV in humans reveals a stable repertoire that is maintained for many years. *PLoS Pathog* **8**, e1002889, doi:10.1371/journal.ppat.1002889 (2012).

45. Pellicci, D. G. *et al*. The molecular bases of delta/alphabeta T cell-mediated antigen recognition. *J Exp Med* **211**, 2599-2615, doi:10.1084/jem.20141764 (2014).

46. Nguyen, A. T. *et al*. SARS-CoV-2 Spike-Derived Peptides Presented by HLA Molecules. *Biophysica* **1**, 194-203 (2021).

47. Escobar, H. *et al*. Large scale mass spectrometric profiling of peptides eluted from HLA molecules reveals N-terminal-extended peptide motifs. *J Immunol* **181**, 4874-4882, doi:10.4049/jimmunol.181.7.4874 (2008).

48. Tarke, A. *et al*. Comprehensive analysis of T cell immunodominance and immunoprevalence of SARS-CoV-2 epitopes in COVID-19 cases. *Cell Rep Med* **2**, 100204, doi:10.1016/j.xcrm.2021.100204 (2021).

49. Shomuradova, A. S. *et al*. SARS-CoV-2 Epitopes Are Recognized by a Public and Diverse Repertoire of Human T Cell Receptors. *Immunity* **53**, 1245-1257 e1245, doi:10.1016/j.immuni.2020.11.004 (2020).

50. Lineburg, K. E. *et al*. CD8(+) T cells specific for an immunodominant SARS-CoV-2 nucleocapsid epitope cross-react with selective seasonal coronaviruses. *Immunity* **54**, 1055-1065 e1055, doi:10.1016/j.immuni.2021.04.006 (2021).

51. Price, D. A. *et al*. Avidity for antigen shapes clonal dominance in CD8+ T cell populations specific for persistent DNA viruses. *J Exp Med* **202**, 1349-1361, doi:10.1084/jem.20051357 (2005).

52. Abdel-Hakeem, M. S., Boisvert, M., Bruneau, J., Soudeyns, H. & Shoukry, N. H. Selective expansion of high functional avidity memory CD8 T cell clonotypes during hepatitis C virus reinfection and clearance. *PLoS Pathog* **13**, e1006191, doi:10.1371/journal.ppat.1006191 (2017).

53. Hombrink, P. *et al*. Mixed functional characteristics correlating with TCR-ligand koff -rate of MHC-tetramer reactive T cells within the naive T-cell repertoire. *Eur J Immunol* **43**, 3038-3050, doi:10.1002/eji.201343397 (2013).

54. Schober, K., Buchholz, V. R. & Busch, D. H. TCR repertoire evolution during maintenance of CMV-specific T-cell populations. *Immunol Rev* **283**, 113-128, doi:10.1111/imr.12654 (2018).

55. Gao, Z. *et al*. A systematic review of asymptomatic infections with COVID-19. *J Microbiol Immunol Infect* **54**, 12-16, doi:10.1016/j.jmii.2020.05.001 (2021).

56. Steiner, S. *et al*. Reactive T Cells in Convalescent COVID-19 Patients With Negative SARS-CoV-2 Antibody Serology. *Front Immunol* **12**, 687449, doi:10.3389/fimmu.2021.687449 (2021).

57. Cusick, M. F., Libbey, J. E. & Fujinami, R. S. Molecular mimicry as a mechanism of autoimmune disease. *Clin Rev Allergy Immunol* **42**, 102-111, doi:10.1007/s12016-011-8293-810.1007/s12016-011-8294-7 (2012).

58. Macdonald, W. A. *et al*. T cell allorecognition via molecular mimicry. *Immunity* **31**, 897-908, doi:10.1016/j.immuni.2009.09.025 (2009).

59. Cole, D. K. *et al*. Hotspot autoimmune T cell receptor binding underlies pathogen and insulin peptide cross-reactivity. *J Clin Invest* **126**, 3626, doi:10.1172/JCI89919 (2016).

60. Birnbaum, M. E. *et al*. Deconstructing the peptide-MHC specificity of T cell recognition. *Cell* **157**, 1073-1087, doi:10.1016/j.cell.2014.03.047 (2014).

61. Adams, J. J. *et al*. T cell receptor signaling is limited by docking geometry to peptide-major histocompatibility complex. *Immunity* **35**, 681-693, doi:10.1016/j.immuni.2011.09.013 (2011).

62. Piepenbrink, K. H., Blevins, S. J., Scott, D. R. & Baker, B. M. The basis for limited specificity and MHC restriction in a T cell receptor interface. *Nat Commun* **4**, 1948, doi:10.1038/ncomms2948 (2013).

63. Szeto, C., Lobos, C. A., Nguyen, A. T. & Gras, S. TCR Recognition of Peptide-MHC-I: Rule Makers and Breakers. *Int J Mol Sci* **22**, doi:10.3390/ijms22010068 (2020).

64. Jahn, L. *et al*. Therapeutic targeting of the BCR-associated protein CD79b in a TCR-based approach is hampered by aberrant expression of CD79b. *Blood* **125**, 949-958, doi:10.1182/blood-2014-07-587840 (2015).

65. Morton, L. T. *et al*. Simultaneous Deletion of Endogenous TCRalphabeta for TCR Gene Therapy Creates an Improved and Safe Cellular Therapeutic. *Mol Ther* **28**, 64-74, doi:10.1016/j.ymthe.2019.10.001 (2020).

66. Wooldridge, L. *et al*. CD8 controls T cell cross-reactivity. *J Immunol* **185**, 4625-4632, doi:10.4049/jimmunol.1001480 (2010).

67. Szomolay, B. *et al*. Identification of human viral protein-derived ligands recognized by individual MHCI-restricted T-cell receptors. *Immunol Cell Biol* **94**, 573-582, doi:10.1038/icb.2016.12 (2016).

68. Wooldridge, L. Individual MHCI-Restricted T-Cell Receptors are Characterized by a Unique Peptide Recognition Signature. *Front Immunol* **4**, 199, doi:10.3389/fimmu.2013.00199 (2013).

69. Andreatta, M. & Nielsen, M. Gapped sequence alignment using artificial neural networks: application to the MHC class I system. *Bioinformatics* **32**, 511-517, doi:10.1093/bioinformatics/btv639 (2016).

70. Schrodinger, LLC. *The PyMOL Molecular Graphics System, Version 1.8* (2015).

71. Roukens, A. H. E. *et al*. Prolonged activation of nasal immune cell populations and development of tissue-resident SARS-CoV-2-specific CD8(+) T cell responses following COVID-19. *Nat Immunol* **23**, 23-32, doi:10.1038/s41590-021-01095-w (2022).

72. Koning, M. T. *et al*. ARTISAN PCR: rapid identification of full-length immunoglobulin rearrangements without primer binding bias. *Br J Haematol* **178**, 983-986, doi:10.1111/bjh.14180 (2017).

73. Picelli, S. *et al*. Smart-seq2 for sensitive full-length transcriptome profiling in single cells. *Nat Methods* **10**, 1096-1098, doi:10.1038/nmeth.2639 (2013).

74. Salgado-Benvindo, C. *et al*. Suramin Inhibits SARS-CoV-2 Infection in Cell Culture by Interfering with Early Steps of the Replication Cycle. *Antimicrob Agents Ch* **64**, doi:ARTN e00900-2010.1128/AAC.00900-20 (2020).

75. Bolotin, D. A. *et al*. MiXCR: software for comprehensive adaptive immunity profiling. *Nat Methods* **12**, 380-381, doi:10.1038/nmeth.3364 (2015).

SUPPLEMENTARY FIGURES

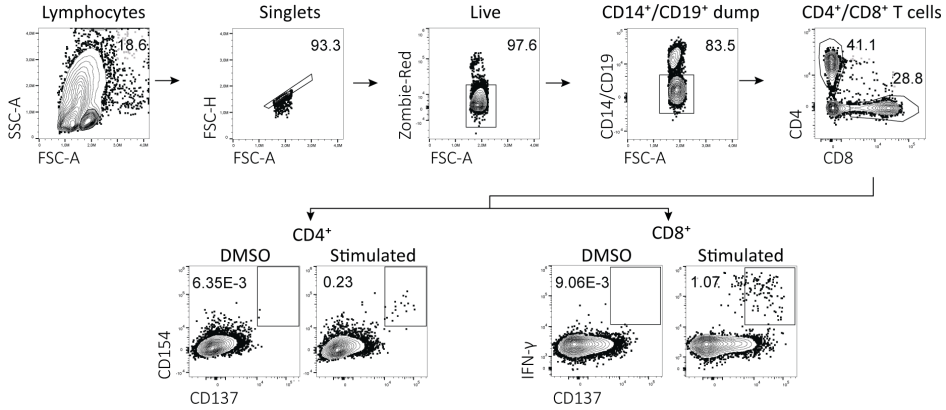

Figure 1 - figure supplement 1 Flow cytometry gating example for peptide stimulation assays

Representative example of flow cytometry gating strategy for peptide-reactive CD4+ and CD8+ T cells. All events were gated on lymphocytes, single cells, viable cells, CD14 and CD19 negative and either CD4 or CD8 positive. For CD4+ T cells, activation was measured by upregulation of CD137 and CD154 compared to DMSO. For CD8+ T cells, activation was measured by upregulation of CD137 and IFN-γ production compared to DMSO.

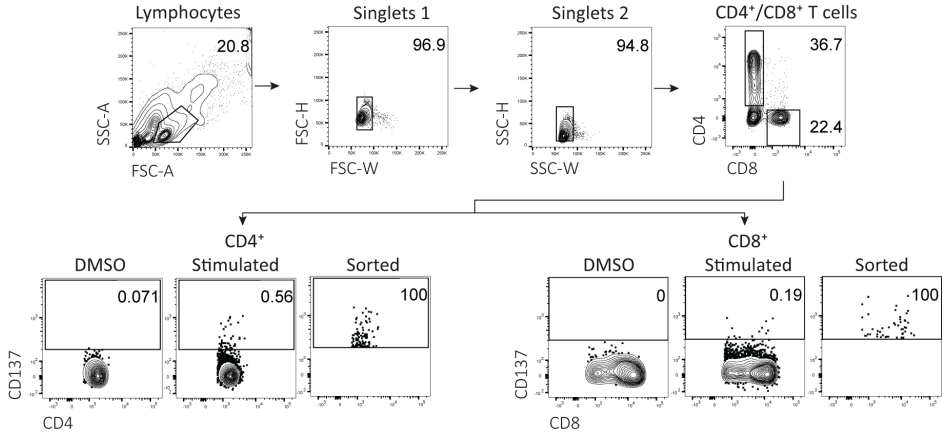

Figure 2 - figure supplement 1 Flow-activated cell sorting gating example for peptide stimulation assays

Representative example of fluorescent-activated cell sorting for peptide-reactive CD4+ and CD8+ T cells. All events were gated on lymphocytes, single cells and subsequently selected for CD4 positive or CD8 positive cells. Activated CD4+ or CD8+ T cells were sorted based on increased expression of CD137 compared to DMSO.

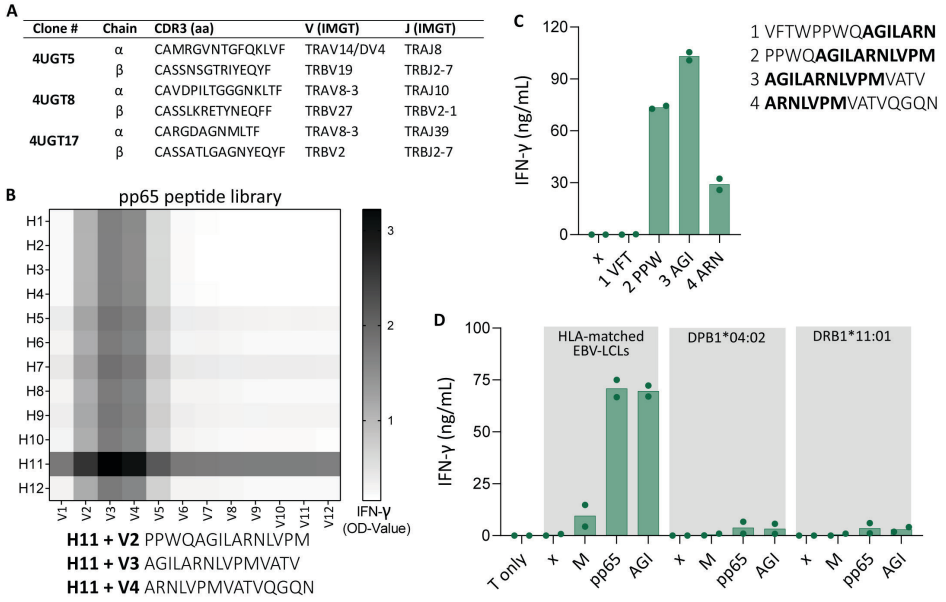

Figure 2 - figure supplement 2 TCR sequence and pp65 peptide identification of 4UGT8 clone

A) Figure showing T cell receptor sequencing of 3 cross-reactive CD4⁺ T cell clones. B) Heatmap showing reactivity of 4UGT8 clone after co-culturing with HLA-matched EBV-LCLs and CMV pp65 peptide library which consisted of 12 horizontal (H1-H12) and 12 vertical sub pools (V1-V12). Reactivity was measured by IFN-γ ELISA of the supernatant, depicted as OD-value. Peptides that were present in the sub pools with highest reactivity are shown below the figure. C) Bar graphs showing IFN-γ secretion after co-culturing 4UGT8 clone with single peptides. Peptide sequences are depicted next to the figure with amino acid overlap between the peptides in bold. Data points are technical duplicates. D) Bar graphs showing ELISA measurement of secreted IFN-γ after co-culturing of 4UGT8 clone with HLA-matched EBV-LCLs, or HLA-mismatched EBV-LCLs transduced with HLA-DPB1*04:02 or DRB1*11:01. Stimulator cells were peptide-pulsed with membrane (M) peptide pool, pp65 peptide pool or AGILARNLVPM (AGI) peptide. Data points are experimental duplicates. Black arrows indicate that values were above plateau value of the ELISA calibration curve.

A

Chain	CDR3 (aa)	V (IMGT)	J (IMGT)
α	CAGNQGGKLIF	TRAV21*02	TRAJ23*01/2
β	CASSLALDEQFF	TRBV12-3/4*01	TRBJ2-1*01

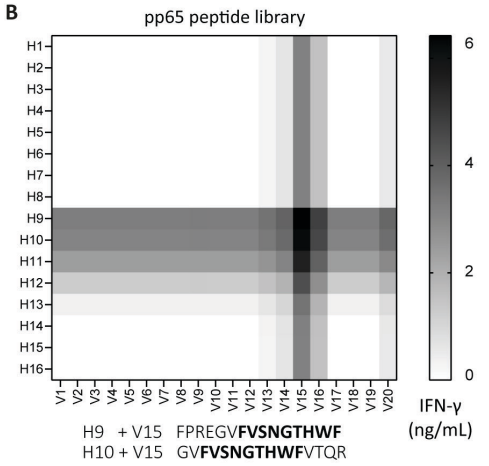

C

Peptide	Affinity(nM)
FVSNGTHWF	17.28 ←
VFVSNGTHWF	3416.18
GVFVSNGTH	14798.68
GVFVSNGTHWF	15539.73
VSNGTHWF	23385.28
VFVSNGTHW	26065.08
FVSNGTHW	27437.91
GVFVSNGTHW	35804.39
VFVSNGTH	35937.91
GVFVSNGT	42011.96

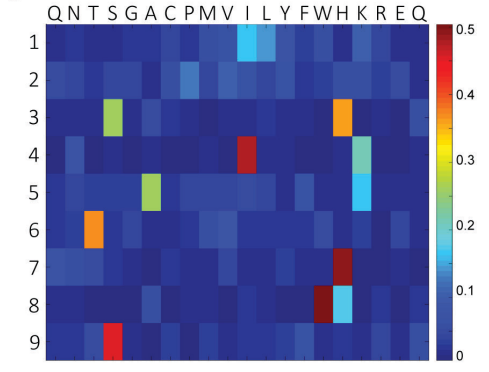

E

CPL score	Peptide	Affinity(nM)
-15,2522	KPSIGEHWS	10598.08
-17,0164	LISKQTHWY	163.63
-17,1607	LNSIVTHLS	23849.06
-17,5175	IPSINVHHY	33.76 ←
-17,8196	LEQIKTHWL	27394.30
-17,8927	KPPIGEHWS	18294.40
-17,9177	VPSIGEHWD	8368.07
-17,9652	LDSIAPHHF	8964.47
-18,0241	KPHIGTVDS	6409.98
-18,0418	LLHILTQIS	19051.95

Figure 2 - figure supplement 3 TCR sequence and peptide identification of 8UTT6 clone
A) Figure showing T cell receptor sequencing result of UTT clones (N=23). B) Heatmap showing reactivity of a representative clone, 8UTT6 clone, against sub pools of SARS-CoV-2 spike peptide library loaded on K562s transduced with HLA-B*35:01. Reactivity was measured by IFN-γ ELISA. Peptides that induced highest IFN-γ production were depicted under the figure with amino acid overlap between the peptides in black. C) Figure showing NetMHC 4.0-predicted binding to HLA-B*35:01 of peptides that were recognized in the spike peptide library. The 10 peptides with highest binding to HLA-B*35:01 are shown and strong binders are indicated by an arrow. D) Heatmap demonstrating peptide recognition signature of 8UTT6 clone using the CPL assay. 8UTT6 clone was co-cultured with peptide-loaded K562 cells transduced HLA-B*35:01. Secreted IFN-γ was measured by ELISA and corrected per row. Y-axis shows peptide position and x-axis shows the fixed amino acid. E) Figure showing the 10 peptides with highest CPL score, their binding affinity to HLA-B*35:01 and strong binders are indicated by an arrow, as predicted by netMHC 4.0.

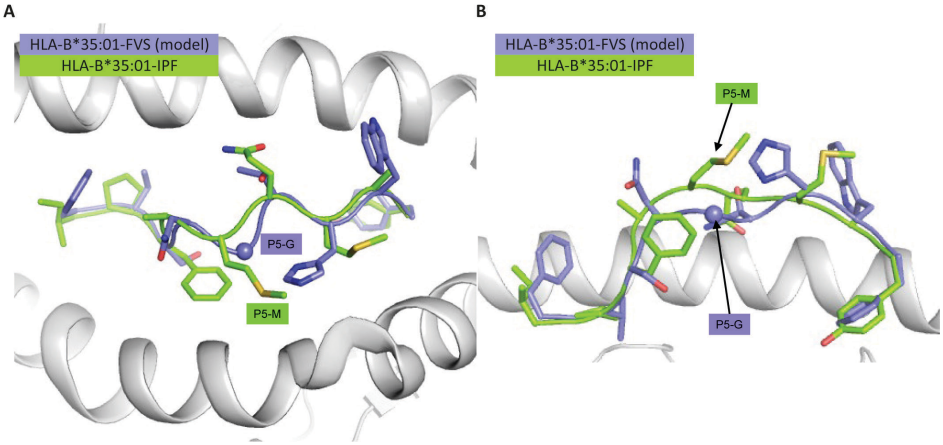

Figure 3 - figure supplement 1 Structural overlay of HLA-B*35:01-IPF structure with the model of the HLA-B*35:01-FVS

(A) Top view of the HLA-B*35:01-IPF (peptide in chartreuse) and HLA-B*35:01-FVS (peptide in blue) aligned on the HLA cleft (white cartoon). B) Side view of the same structural overlay as panel A, with the same colour scheme. The sphere represents the Cα atom of the FVS peptide P5-G residue.

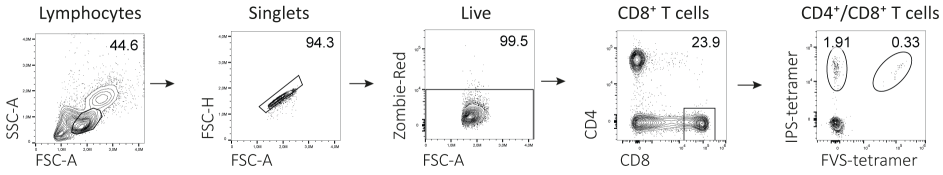

Figure 4 - figure supplement 1 Flow cytometry gating example for tetramer staining assays

Representative example of flow cytometry gating strategy for tetramer positive CD8⁺ T cells. All events were gated on lymphocytes, single cells, viable cells, CD8 positive and subsequently separated for binding to tetramer consisting of HLA-B*35:01 with IPS peptide or FVS peptide.

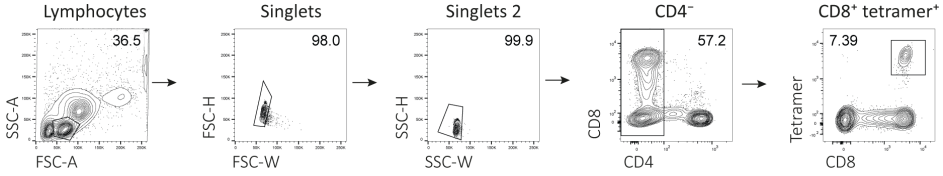

Figure 5 - figure supplement 1 Flow activated cell sorting gating example

Representative example of fluorescent-activated cell sorting for tetramer positive CD8⁺ T cells. All events were gated on lymphocytes, single cells, CD4⁻ and subsequently on CD8⁺tetramer⁺.

A

	TRAV (IMGT)	TRAJ (IMGT)	CDR3 (aa)	CDR3α (nt)
UTT	TRAV21*02	TRAJ23*01	CAGNQGGKLIF	TGTGCTGGGGAACCAGGGAGGAAAGCTTATCTTC
UBV	TRAV21*01	TRAJ23*01	CAGNQGGKLIF	TGTGCTGGGAAACCAGGGAGGAAAGCTTATCTTC
JZX	TRAV21*02	TRAJ23*01	CAGNQGGKLIF	TGTGCTGGGGAACCAGGGAGGAAAGCTTATCTTC
SFW	TRAV21*02	TRAJ23*01	CAGNQGGKLIF	TGTGCTGGGGAACCAGGGAGGAAAGCTTATCTTC

B

	TRBV (IMGT)	TRBV (IMGT)	CDR3 (aa)	CDR3β (nt)
UTT	TRBV12-3*01	TRBJ2-1*01	CASSLALDEQFF	TGTGCCAGCAGTTTAGCGCTGGATGAGCAGTTCTTC
UBV	TRBV12-3*01	TRBJ2-1*01	CASSLALDEQFF	TGTGCCAGCAGTTTAGCGCTGGATGAGCAGTTCTTC
JZX	TRBV12-3*01/TRBV12-4*01	TRBJ2-1*01	CASSLALDEQFF	TGTGCCAGCAGTTTAGCGCTCGATGAGCAGTTCTTC
SFW	TRBV12-3*01/TRBV12-4*01	TRBJ2-1*01	CASSLALDEQFF	TGTGCCAGCAGTTTAGCGCTTGATGAGCAGTTCTTC

Figure 5 - figure supplement 2 TCR sequencing of B*35/FVS-sorted samples

Nucleotide alignment of the CDR3 α and β sequence of PBMCs sorted on B*35/FVS-tetramer binding. Segment numbering is depicted according to the international immunogenetics information system (IMGT) nomenclature. A) Nucleotide alignment of the CDR3α sequences. B) Nucleotide alignment of the CDR3β sequences.

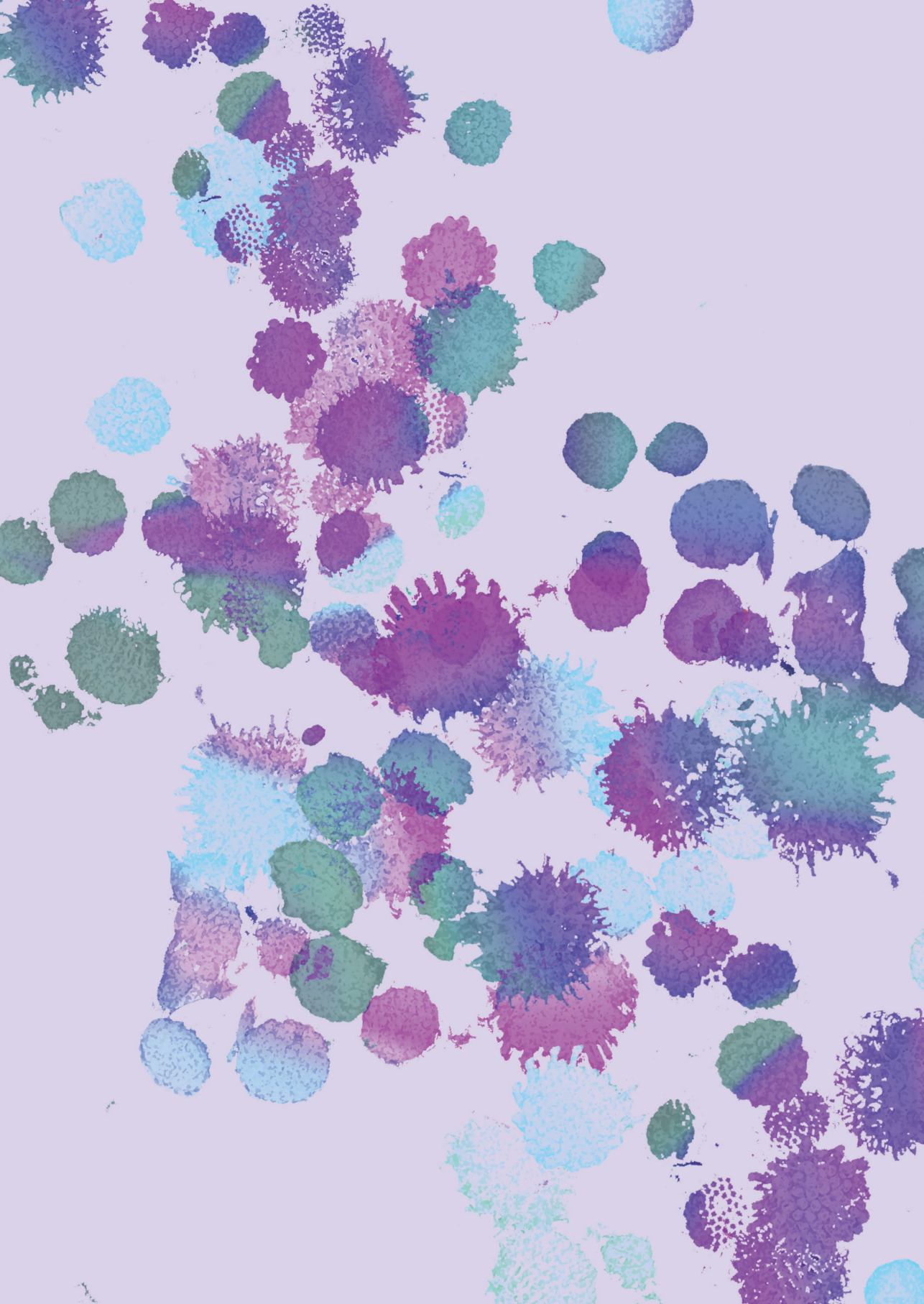

SARS-COV-2 MRNA VACCINATION OF APLASTIC ANEMIA PATIENTS IS SAFE AND EFFECTIVE

Pothast, C. R.*, van Dijk, K.*, Pool, E. S., Halkes, C. J. M., Heemskerk, M. H. M., & Tjon, J. M.

(2022). *Am J Hematol*. DOI: 10.1002/ajh.26780

Chapter 3

To the editor,
Vaccines are an essential part of the fight against the COVID-19 pandemic. Especially immunocompromised patients at risk for a severe or fatal course of SARS-CoV-2 infection are expected to benefit from vaccination. While studies on SARS-CoV-2 mRNA vaccines have shown that healthy subjects are able to mount both effective humoral and cellular immune responses to these vaccines,(1) the effectiveness and safety of SARS-CoV-2 vaccines for immunocompromised patients remains unclear. Acquired aplastic anemia (AA) is an example of a disease that results in an immunocompromised state. AA patients are immunocompromised either due to the disease itself which is characterized by profound pancytopenia caused by immune mediated bone marrow failure, or due to the immunosuppressive treatment (IST) consisting of horse-derived anti-thymocyte globulin (hATG) in combination with cyclosporine A (CsA) that they received.(2) This immunocompromised state of AA patients argues that it is important to vaccinate these patients with a SARS-CoV-2 mRNA vaccine in order to prevent severe COVID-19. However, anecdotal case studies have reported AA relapse after vaccination and therefore the international guidelines recommend caution when vaccinating AA patients after IST irrespective of the time between last IST and vaccination.(3) Furthermore, it is not known whether previous IST affects the ability to mount an adequate immune response to a vaccine in these patients. These considerations create a dilemma whether to vaccinate AA patients after IST with SARS-CoV-2 mRNA vaccines.

In this study we investigated the occurrence of relapse as well as the ability to mount both a humoral and T-cell response to SARS-CoV-2 mRNA vaccination in 18 AA patients treated with IST at a median time of 11.1 years (range 0.3-39) before SARS-CoV-2 vaccination (**Table S1**). At the time of vaccination, 14 AA patients were transfusion-independent and successfully tapered from IST. Three patients were transfusion-independent but IST-dependent, and one patient was both transfusion- and IST-dependent. All IST-dependent patients (N=4) received CsA at time of vaccination. The AA patients and healthy controls (HCs; N=9) received two SARS-CoV-2 mRNA vaccines (mRNA-1273 (Moderna) or BNT162b2 (Pfizer-BioNtech) vaccines). Whole blood was sampled prior and post vaccination to measure blood counts, and to isolate serum and peripheral blood mononuclear cells (PBMCs) to measure SARS-CoV-2-specific IgG antibodies and T-cells (see **supplementary material and methods**).

To investigate whether AA patients relapsed after SARS-CoV-2 mRNA vaccination, hemoglobin (Hb), thrombocyte, and neutrophil values were determined in peripheral blood. Samples were taken pre-vaccination, post-vaccination (median 27 days after the second vaccination) and at follow-up (median 9.1 months after the first vaccination).

The blood values were stable post-vaccination and remained stable without the need for transfusion during the follow-up period in all 17 patients that were transfusion-independent at start of the study (**Figure 1A**). The transfusion-frequency remained stable in the patient that was transfusion-dependent at the start of the study. These results indicate that no signs of AA relapse are present up to 9 months after first vaccination, which is in accordance with a previous study investigating mRNA vaccination in 16 AA patients.(4) This suggests that the case reports describing AA relapse observed after vaccination may be rare incidents or incidents unrelated to vaccination.

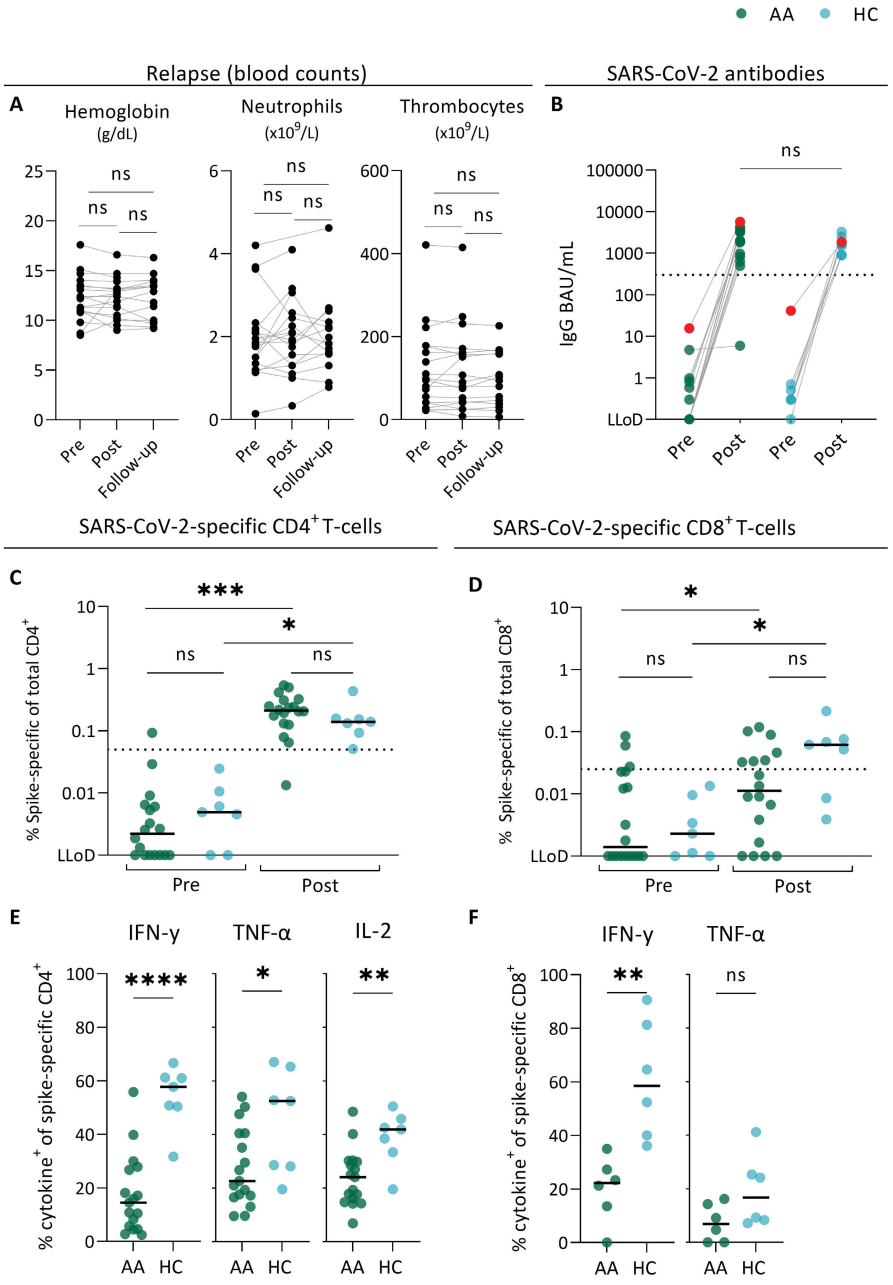

Figure 1 Blood counts, humoral responses and T-cell responses following SARS-CoV-2 mRNA vaccination in aplastic anemia patients and healthy controls

(A) Hemoglobin, neutrophils and thrombocytes shown pre-vaccination, post vaccination (median 27.1 days after second vaccination) and at follow-up (median 9.1 months after start vaccination). Blood value data at follow-up was not available for 3 patients, therefore the statistical comparisons of pre/post with follow-up blood values was only performed for the 15 AA patients for whom data was available. (B) SARS-CoV-2 spike IgG response according to WHO standardization of AA patients (green; n=18) and HCs (light blue; n=9). The red dots correspond to individuals that were positive for SARS-CoV-2 IgG before vaccination. Post-vaccination SARS-CoV-2 spike IgG levels were determined in serum of AA patients (median 27.1 days (range 11-49)) and HCs (median 21.4 days (range 18-24)) after second vaccination. Dotted line shows threshold of an adequate IgG response of 300 BAU/mL. (C) Percentage of SARS-CoV-2 spike-specific $CD4^+$ T-cells of total $CD4^+$ T-cells pre- and post-vaccination in AA patients (green) and HC (light blue). Dotted line shows a threshold for a $CD4^+$ T-cell response of 0.05%. (D) Percentage of SARS-CoV-2 spike-specific $CD8^+$ T-cells of total $CD8^+$ T-cells pre- and post-vaccination in AA patients (green) and HC (light blue). The percentage of SARS-CoV-2 spike-specific CD4+ and CD8+ T-cells was corrected for the background signal in the negative control (DMSO). Dotted line shows a threshold for a $CD8^+$ T-cell response of 0.025%. (E) The percentages of IFN-γ, TNF-α and IL-2 producing spike-specific CD4+ T-cells in AA patients (green) and HC (light blue). (F) The percentages of IFN-γ and TNF-α producing spike-specific $CD8^+$ T-cells in AA patients (green) and HC (light blue). Horizontal bars in figures C-F represent the median. ns: $p>0.05$, *: $p\leq0.05$, **: $p\leq0.01$, ***: $p\leq0.001$
Abbreviations: AA, aplastic anemia; HC, healthy controls; ns, not significant; LLoD, Lowest limit of detection; BAU, binding antibody units; DMSO, dimethyl sulfoxide; TNF-α, tumor necrosis factor alpha; IFN-γ, interferon gamma; IL-2, interleukin 2.

The humoral immune response of AA patients to SARS-CoV-2 mRNA vaccination was measured by determining SARS-CoV-2 anti-Spike IgG levels pre- and post-vaccination. 17 of 18 AA patients had an adequate SARS-CoV-2 IgG antibody response (defined as >300 BAU/ml) after vaccination which was similar to HCs (**Figure 1B**). The patient with antibody levels below threshold had recently received hATG, still received CsA, and was the oldest person (79 years) in the AA patient cohort. An inversed correlation between age and Spike-IgG was found (**Table S2**), indicating that the amount of Spike-IgG decreased with increasing age. For other factors, such as time between IST (hATG treatment) and vaccination, absolute number of B-cells, absolute number of $CD4^+$ and $CD8^+$ T-cells, no significant correlations were observed (**Table S2**). In short, the majority of AA patients is able to generate an adequate antibody response and which is accordance with previous literature.(4)

Spike-specific $CD4^+$ and $CD8^+$ T cell responses were measured by incubating PBMCs with a SARS-CoV-2 spike peptide pool, followed by intracellular cytokine staining for flow cytometry. The frequency of SARS-CoV-2 spike-specific $CD4^+$ and $CD8^+$ T -cells was determined before and after vaccination which showed a significant increase in both AA patients and healthy controls (**Figure 1C-D**). The SARS-CoV-2 spike-specific $CD4^+$ and $CD8^+$ T-cell frequencies between AA patients and HCs were not significantly different after vaccination, although a trend towards a lower frequency of SARS-CoV-2 specific $CD8^+$ T-cells in AA patients could be observed (**Figure 1C-D**). As expected, the $CD4^+$ and $CD8^+$ T-cell responses directed against the broad cytomegalovirus, Epstein-barr virus, influenza and extended peptide pool (CEFX) did not differ pre- and post-vaccination in AA patients and HCs, and frequencies of CEFX-specific $CD4^+$ and $CD8^+$

T-cell were comparable for both cohorts (**Figure S1A-B**). Percentages of SARS-CoV-2 spike-specific $CD4^+$ and $CD8^+$ T-cells that produce interferon-γ (IFN-γ), tumour necrosis factor-α (TNF-α) or interleukin-2 (IL-2) were significantly lower in the AA patients than in healthy controls (**Figure 1E-F**). Interestingly, this trend of reduced cytokine production was also observed for the CEFX-specific $CD4^+$ T-cells in AA patients that produced significantly reduced levels of TNF-α and IL-2 compared to healthy controls (**Figure S1C-D**). In conclusion, spike-specific $CD4^+$ and $CD8^+$ T cell frequencies were comparable between AA patients and healthy controls. However, the percentage of spike-specific $CD4^+$ and $CD8^+$ T cells that produced IFN-γ, TNF-α or IL-2 was lower in AA patients compared to healthy controls.

Reduced T-cell cytokine production can be caused by multiple factors. Age, time between IST (hATG treatment) and vaccination and absolute numbers of the $CD4^+$ and $CD8^+$ T-cell compartment at the time of vaccination were not significantly correlated to the reduced cytokine production seen after IST (**Table S2**). Since CsA is a known inhibitor of T-cell proliferation and cytokine production, we investigated whether CsA could be responsible for the decreased cytokine production of the SARS-CoV-2 specific T-cells. Although the frequency of $CD4^+$ and $CD8^+$ SARS-CoV-2 spike-specific T-cells was comparable between AA patients who received CsA at time of vaccination and AA patients who did not receive CsA at time of vaccination, we observed that 3 AA patients who received CsA at time of vaccination tended to have lower percentages of IFN-γ, TNF-α and IL-2 producing SARS-CoV-2 spike-specific $CD4^+$ T-cells (**Figure S2A**). Interestingly, these AA patients tended to have higher spike-IgG antibody levels (median: 3431 BAU/mL) compared to patients who no longer received CsA (median: 1912 BAU/mL) at the time of vaccination (**Figure S2B**). Due to the low number of patients that received CsA at time of vaccination (n=3) both trends could not be statistically confirmed.

For the AA patients that did not receive CsA during vaccination we cannot fully explain the lower percentage of cytokine producing SARS-CoV-2 spike-specific T-cells in comparison to HCs. We cannot exclude the possibility that the reduced cytokine production is the result of a lingering effect of the disease or the IST these patients have received. Although no correlation was found between the spike-specific T-cell response and time that patients last received hATG or CsA, hATG or CsA may have had a permanent effect on the repertoire of the T lymphocytes. Based on the analyses of the major T lymphocyte subsets, no obvious difference could be detected (**Figure S3**). However, it is also possible that the difference is more subtle and could therefore not be detected based on the T-cell markers used in this study and the sample size of the study population. Importantly, it is not known whether the reduced cytokine

production influences the effectiveness of vaccines in AA patients and whether this might increase by additional vaccination doses.

In summary, no indications of AA relapse was observed up to 9 months after the first mRNA vaccination. Additionally, 17 of 18 AA patients were able to mount an adequate humoral response and demonstrated comparable magnitudes of spike-specific $CD4^+$ T-cells and spike-specific $CD8^+$ T-cells. Our study sheds another light on the current view on the risk/benefit discussion for vaccination of AA patients as the results indicate that SARS-CoV-2 mRNA vaccines are more beneficial to AA patients than potentially harmful. The reduced cytokine production by the T-cells further underlines the importance of vaccinating AA patients to protect against a possible severe course of SARS-CoV-2 infection. Larger cohort studies are needed to further study the chance of AA relapse after SARS-CoV-2 mRNA vaccination and vaccine efficacy in AA patients not only after successfully tapered IST but also in AA patients recently treated with hATG who are still using CsA. Furthermore, it has to be determined whether additional vaccination doses result in improved cytokine production by spike-specific T-cells which could affect the vaccination scheme for AA patients.

ACKNOWLEDGEMENTS

Flow cytometry was performed at the Flow cytometry Core Facility (FCF) of Leiden University Medical Center (LUMC) in Leiden, the Netherlands.

REFERENCES

1. Painter MM, Mathew D, Goel RR, Apostolidis SA, Pattekar A, Kuthuru O, et al. Rapid induction of antigen-specific CD4(+) T cells is associated with coordinated humoral and cellular immunity to SARS-CoV-2 mRNA vaccination. Immunity. 2021;54(9):2133-42 e3.
2. Young NSJNEJoM. Aplastic anemia. 2018;379(17):1643-56.
3. Killick SB, Bown N, Cavenagh J, Dokal I, Foukaneli T, Hill A, et al. Guidelines for the diagnosis and management of adult aplastic anaemia. 2016;172(2):187-207.
4. Walter J, Kricheldorf K, Isfort S, Brümmendorf TH, Panse J, Beier F. Antibody titers after SARS-CoV-2 mRNA vaccination in patients with aplastic anemia - a single center study. Eur J Haematol. 2022.
5. Oosting SF, van der Veldt AAM, GeurtsvanKessel CH, Fehrmann RSN, van Binnendijk RS, Dingemans AC, et al. mRNA-1273 COVID-19 vaccination in patients receiving chemotherapy, immunotherapy, or chemoimmunotherapy for solid tumours: a prospective, multicentre, non-inferiority trial. Lancet Oncol. 2021;22(12):1681-91.
6. Boerenkamp LS, Pothast CR, Dijkland RC, van Dijk K, van Gorkom GNY, van Loo IHM, et al. Increased CD8 T-cell immunity after COVID-19 vaccination in lymphoid malignancy patients lacking adequate humoral response: An immune compensation mechanism? Am J Hematol. 2022.

SUPPLEMENTARY MATERIAL AND METHODS

Patients and healthy controls

18 patients with AA and 9 healthy controls (HC) were recruited. AA patients were diagnosed and treated with first-line IST consisting of hATG (either ATGAM (Pfizer) or lymphoglobulin (Sanofi)) in combination with CsA according to the Dutch guidelines. Peripheral blood samples were collected after informed consent was given in accordance to local ethical guidelines and the Declaration of Helsinki. This study was approved by the Medical Ethical Committee of the Leiden University Medical Center (Protocol number: B22.029). Patients and HCs below 18 years of age were excluded. The patients received two SARS-CoV-2 mRNA vaccines (either the mRNA-1273 (Moderna) or the BNT162b2 (Pfizer-Biontech)) vaccines. The AA patients and the HCs were age- and sex-matched as much as possible. See Table S1 for patient characteristics.

SARS-CoV-2-specific IgG

Peripheral blood mononuclear cells (PBMCs) were isolated using Ficoll-Isopaque and cryo-preserved until further use. Serum was collected from fresh blood and subsequently stored at -80°C. The humoral response to the SARS-CoV-2 mRNA vaccination was measured in serum using a commercial chemiluminescent microparticle immunoassay (CMIA); AdviseDx SARS-CoV-2 Spike immunoglobulin G (IgG) II (Abbott Alinity). An adequate antibody response was defined as a result above >300 BAU/ml anti-spike IgG which was based on neutralization capacity in a previous study.(5)

SARS-CoV-2-specific T-cells

SARS-CoV-2-specific $CD4^+$ and $CD8^+$ T-cells were measured as previously described. (6) In short, PBMCs were overnight incubated with a 15-mer with 11 amino acid overlapping SARS-CoV-2 spike peptide pool (SB-peptide) or a CEFX peptide pool (JPT/LUMC) consisting of peptides from cytomegalovirus (CMV), Epstein-barr virus (EBV), influenza and other common pathogens(**Table S3-4**). After overnight incubation in the presence of Brefeldin A (Sigma), the cells were intracellularly stained for activation markers and cytokines for flow cytometry measurement (**Table S5**). SARS-CoV-2-specific $CD4^+$ T-cells were detected by increased expression of CD137 and/or CD154 compared to negative control (DMSO), and SARS-CoV-2-specific $CD8^+$ T-cells as increased CD137 and CD69 expression compared to negative control (**Figure S4**). In parallel, PBMCs were incubated without the presence of stimulators to measure differentiation state of the T-cells (CD45RA and/or CCR7 expression). A $CD4^+$ T-cell response was considered positive above 0.05% and a $CD8^+$ T-cell response above 0.025%. These percentages were based on the healthy cohort in this study.

SUPPLEMENTARY FIGURES

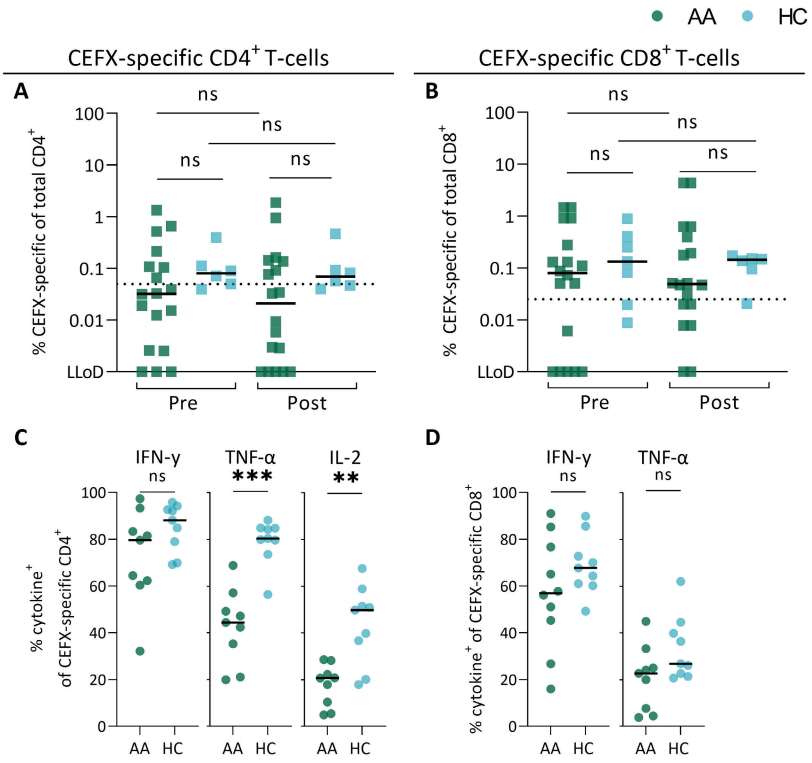

Figure S1 CEFX-specific T-cell responses in aplastic anemia patients and healthy controls

(A) Percentage of CEFX-specific $CD4^+$ T-cells of total $CD4^+$ T-cells pre- and post-vaccination in AA patients (green) and HC (light blue). Dotted line shows a threshold for a $CD4^+$ T-cell response of 0.05%. (B) Percentage of CEFX-specific $CD8^+$ T-cells of total $CD8^+$ T-cells pre- and post-vaccination in AA patients (green) and HC (light blue). The percentages of CEFX-specific CD4+ and CD8+ T-cells were corrected for the background signal in the negative control (DMSO). Dotted line shows a threshold for a $CD8^+$ T-cell response of 0.025%. (C) The percentages of IFN-γ, TNF-α and IL-2 producing CEFX-specific CD4+ T-cells in AA patients (green) and HC (light blue). (D) The percentages of IFN-γ and TNF-α producing CEFX-specific $CD8^+$ T-cells in AA patients (green) and HC (light blue). Horizontal bars in figures C-F represent the median. ns: $p>0.05$, *: $p\leq0.05$, **: $p\leq0.01$, ***: $p\leq0.001$

Abbreviations: AA, aplastic anemia; HC, healthy controls; ns, not significant; LLoD, Lowest limit of detection; DMSO, dimethyl sulfoxide; CEFX: Cytomegalovirus, Epstein-barr virus, influenza and extended peptide pool; TNF-α, tumor necrosis factor alpha; IFN-γ, interferon gamma; IL-2, interleukin 2.

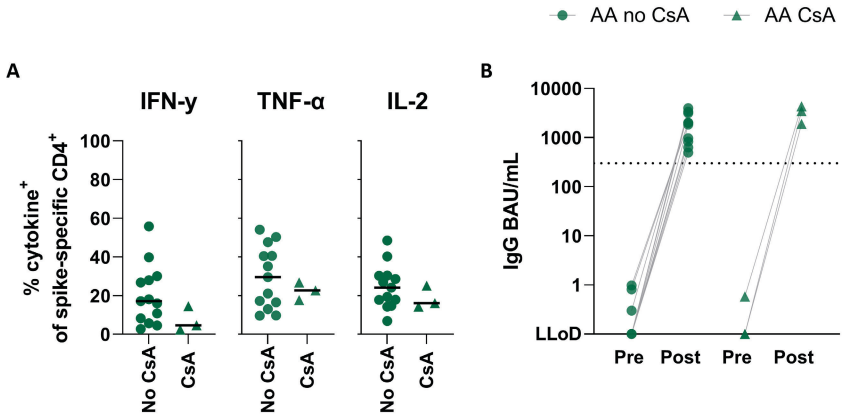

Figure S2 Humoral and T-cell response during SARS-CoV-2 vaccination in AA patients treated with Csa compared to patients not treated with CsA

(A) The percentages of type 1 cytokine (TNF-α, IFN-γ, IL-2) producing SARS-CoV-2 spike-specific $CD4^+$ T-cells of AA patients who did not receive CsA (No CsA: green circle) and AA patients who received CsA (CsA; green triangle) at time of vaccination. (B) SARS-CoV-2 spike IgG response of AA patients who did not receive CsA and who received CsA at time of vaccination. AA patients who were Spike-IgG positive pre-vaccination were excluded from these comparisons. Percentages of cytokine-producing $CD4^+$ T-cells and antibody titers were determined at median 27.1 days (11-49 days) after the second vaccination. Dotted line shows threshold of an adequate IgG response of 300 BAU/ml.

Abbreviations: AA, aplastic anemia; CsA, cyclosporin A; TNF-α, tumor necrosis factor alpha; IFN-γ, interferon gamma; IL-2, interleukin 2; LLoD, lower limit of detection.

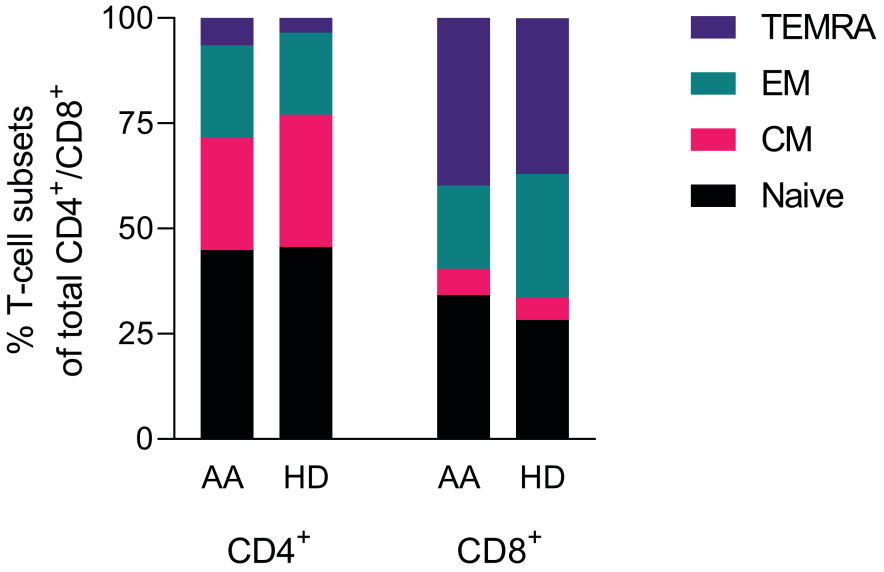

Figure S3 CD4⁺ and CD8⁺ T-cell subset frequencies in AA patients (n=18) and HC's (n=8) before vaccination

Median T-cell subset frequencies are shown. No significant differences between AA patients and HCs in the T-cell subsets could be found. Naïve T-cell subset is defined as $CCR7^{+}CD45RA^{+}$. CM T-cell subset is defined as $CCR7^{+}CD45RA^{-}$. EM T-cell subset is defined as $CCR7^{-}CD45RA^{-}$. TEMRA T-cell subset is defined as $CCR7^{-}CD45RA^{+}$.

Abbreviations: AA, aplastic anemia; HC, healthy controls; CM, central memory; EM, effector memory; TEMRA, terminally differentiated effector memory.

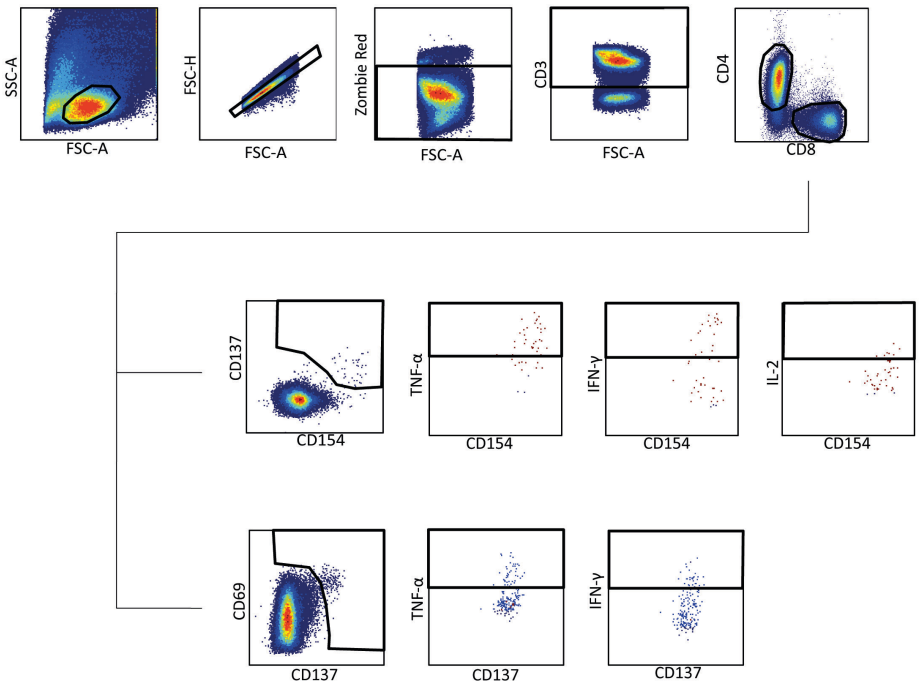

Figure S4 Representative example of gating strategy used to identify peptide-specific CD4⁺ and CD8⁺ T-cells

Cells were first gated using the side scatter area (SSC-A) and forward scatter area (FSC-A) parameters. Subsequently, doublets were excluded using the forward scatter height (FSC-H) and FSC-A parameters. Dead cells were then removed using the Zombie Red-A live dead marker. Next, CD3⁺ cells were selected and CD4⁺ and CD8⁺ T-cells were identified within the CD3⁺ gate. Peptide specific CD4⁺ T-cells and CD8⁺ T-cells were subsequentially gated using CD137⁺ and CD154⁺ and CD69⁺ and CD137⁺, respectively. Finally, cytokine-producing peptide-specific CD4⁺ and CD8⁺ T-cells were gated based on TNF-α, and IFN-γ positivity. The gating strategy on a representative AA patient sample is shown.

Abbreviations: SSC-A, side scatter area; FSC-A, forward scatter area; TNF-α, tumor necrosis factor alpha; IFN-γ, interferon gamma; IL-2, interleukin 2.

SUPPLEMENTARY TABLES

Table S1 List of patient characteristics

	Aplastic anemia patients (n=18)	**Healthy controls (n=9)**
Age (median, range in years)	52 (21-80)	44 (33-59)
Gender (N, male:female)	8:10	5:4
Disease status at vaccination N (%)		
Transfusion-independent and IST-independent (%)	14 (77.8)	N/A
Transfusion-independent and IST dependent* (%)	3 (16.7)	N/A
Transfusion-dependent and IST dependent* (%)	1 (5.6)	N/A
Time between hATG and vaccination in years (median, range in years)	11.1 (0.3-39.0)	N/A
Sample time post second vaccination (median, range in days)	27.1 (11-49)	21.2 (18-24)
Follow-up time after first vaccination (median, range in months) n=15	9.1 (4.7-12.7)	N/A

*IST-dependent patients received cyclosporin A at the time of vaccination

Table S2 Spearman's rank sum testing to correlate spike-specific T-cell responses to patient characteristics

Correlation	**R value**	**P value**
% spike-specific $CD4^+$ T-cells *versus*		
Absolute # of $CD4^+$ T-cells pre vaccination	-0.44	0.08
% Naïve $CD4^+$ T-cells	-0.46	0.06
Age	-0.08	0.77
Date of last hATG administration	0.36	0.15
% spike-specific $CD8^+$ T-cells *versus*		
Absolute # of $CD8^+$ T-cells pre vaccination	0.11	0.69
% Naïve $CD8^+$ T-cells	0.15	0.56
Age	-0.09	0.73
Date of last hATG administration	-0.01	0.98
% TNF-α^+ spike-specific $CD4^+$ T-cells *versus*		
Absolute # of $CD4^+$ T-cells pre vaccination	-0.03	0.91
Age	-0.27	0.33

Correlation	R value	P value
Date of last hATG administration	0.12	0.67
% IFN-γ^+ spike-specific CD4$^+$ T-cells *versus*		
Absolute # of CD4$^+$ T-cells pre vaccination	-0.34	0.21
Age	-0.23	0.40
Date of last hATG administration	0.22	0.43
% IL-2$^+$ spike-specific CD4$^+$ T-cells *versus*		
Absolute # of CD4$^+$ T-cells pre vaccination	-0.06	0.83
Age	-0.30	0.27
Date of last hATG administration	0.40	0.14
SARS-CoV-2 IgG antibodies (BAU/mL) *versus*		
Age	-0.67	0.020
Date of last hATG administration	0.26	0.41
Activated CD4$^+$ T-cells	0.33	0.29
Activated CD8$^+$ T-cells	-0.10	0.76
Absolute # CD4$^+$ T-cells	0.39	0.24
Absolute # CD8$^+$ T-cells	0.60	0.06
Absolute # B-cells	0.25	0.45

Table S3 List of peptides used in the CEFX peptide pool mix

Pathogen	Antigen	Supplier	Cat #	Peptide characteristics
CMV	pp65	JPT	Custom-made	15-mers, 11 aa overlapping
Influenza A	NP1	JPT	N/A	15-mers, 11 aa overlapping, NCBI: ABB79814
EBV	BZLF1	JPT	PM-EBV-BZLF1	15-mers, 11 aa overlapping
EBV Class I	Pool	LUMC	Custom made	9-mers, known epitopes (Table S2)
Pool	Pool	JPT	PM-CEFX-2	15-mers, 11 aa overlapping

Table S4 List of EBV class I peptides used for the CEFX peptide pool

Antigen	Amino Acid Sequence	HLA Restriction	Supplier	Peptide Characteristics
LMP2	ESEERPPTPY	A*01:01	LUMC	9-mer
BMLF1	GLCTLVAML	A*02:01	LUMC	9-mer
LMP2	CLGGLLTMV	A*02:01	LUMC	9-mer
LMP2	FLYALALLL	A*02:01	LUMC	9-mer
BRLF1	RVRAYTYSK	A*03:01	LUMC	9-mer
EBNA3A	RLRAEAQVK	A*03:01	LUMC	9-mer
EBNA3B	IVTDFSVIK	A*11:01	LUMC	9-mer
EBNA3B	AVFDRKSDAK	A*11:01	LUMC	9-mer
BRLF1	DYCNVLNKEF	A*24:02	LUMC	9-mer
EBNA3A	RPPIFIRRL	B*07:02	LUMC	9-mer

Table S5 List of staining reagent and antibodies used for flow cytometry

Antigen	Fluorochrome	Clone ID	Company	Cat#
Zombie-Red			Biolegend	423110
CD8	APC-H7	SK1	BD Biosciences	560179
CD3	PE-Texas-Red	7D6	Invitrogen	MHCD0317
CD69	FITC	L78	BD Biosciences	347823
CD137	APC	4B4-1	BD Biosciences	550890
CD154	Pacific blue	24-31	Biolegend	310820
IL-2	PE	SCPL1362	BD Biosciences	130-091-646
IL-4	PERCPCY5.5	MP4-25D2	Biolegend	500822
FOXP3	AF700	PCH101	Thermo Fisher	56-4776-41
CXCR5	Pe-Vio770	REA103	Miltenyi	130-117-358
PD-1	BV786	EH12.1	BD Biosciences	563789
IL-17	BV650	N49-653	BD Biosciences	563746
IFN-γ	BV711	B27	BD Biosciences	564039
TNF-α	BV421	Mab11	BD Biosciences	562783
CD4	BV510	SK3	BD Biosciences	562970
CD45RA	PE-Texas-Red	MEM-56	Invitrogen	MHCD45RA17
CCR7	BV711	3D12	BD Biosciences	563712

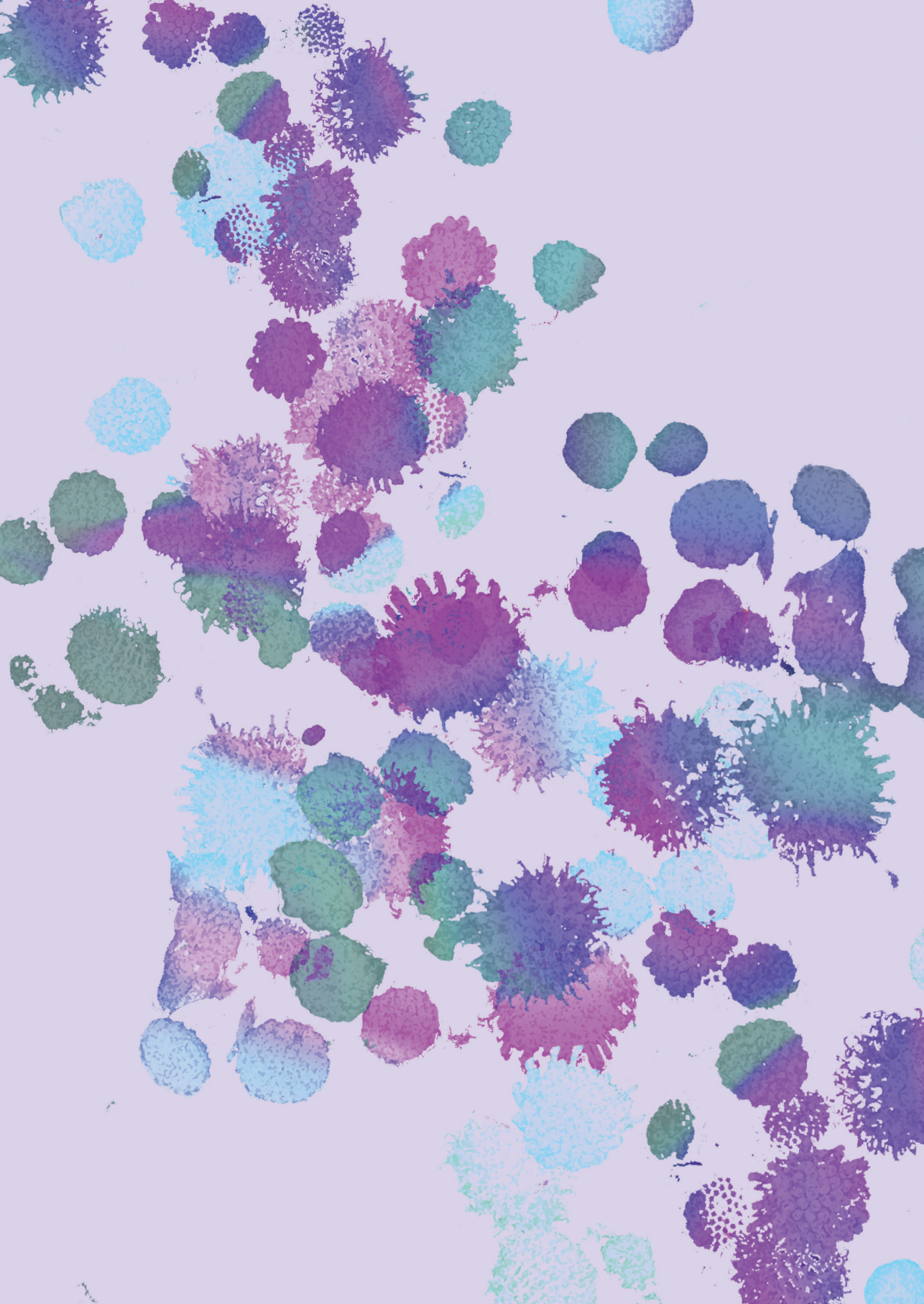

INCREASED CD8 T-CELL IMMUNITY AFTER COVID-19 VACCINATION IN LYMPHOID MALIGNANCY PATIENTS LACKING ADEQUATE HUMORAL RESPONSE: AN IMMUNE COMPENSATION MECHANISM?

Boerenkamp, L. S.*, Pothast, C. R.*, Dijkland, R. C., van Dijk, K., van Gorkom, G. N. Y., van Loo, I. H. M., Wieten, L., Halkes, C. J. M., Heemskerk, M. H. M., & Van Elssen, C.

(2022). *Am J Hematol*. DOI: 10.1002/ajh.26729

Chapter 4

TO THE EDITOR

SARS-CoV-2 vaccine immunogenicity is commonly evaluated by measuring antibody titers against the SARS-CoV-2 Spike (S) protein. Previously, inferior humoral vaccination responses in patients with lymphoid malignancies have been shown.[1] This can be attributed to immune defects caused by disease or treatment. NHL and CLL treated with CD20- and MM with CD38-directed therapies lead to long-lasting B- or plasma-cell depletion, respectively. CLL and MM are associated with hypogammaglobulinemia and aberrations in T-cell function. T-cell immunity is vital for viral clearance and long-lasting protection against COVID-19 after vaccination.[2] Moreover, high CD8+ T-cells contribute to COVID-19 survival in hematological patients.[3] Studies investigating T-cell responses after vaccination in patients with lymphoid malignancies are, however, scarce and results are conflicting. This leaves a knowledge gap, underlining the urgency of an in-depth and reproducible analysis of functional SARS-CoV-2-specific T-cell responses following vaccination in hematological patients.

Patients. Adult patients diagnosed with CLL, NHL, or MM at two tertiary care centers in the Netherlands undergoing SARS-CoV-2 vaccination were included in the study. Serological and T-cell responses were evaluated pre-vaccination and 2 weeks, 3- and 6-months post-vaccination. Patients were included between March and June 2021. All participants gave written informed consent and all procedures performed were in accordance with the ethical standards of the national research committee and the 1964 Helsinki declaration (NL76863.068.21/METC 21-014).

Vaccination responses. Antibody levels were measured with an anti-SARS-CoV-2 S immunoassay (Elecsys, Roche Diagnostics International Ltd). Adequate seroconversion was defined as an Ig serum concentration ≥250 BAU/ml. CD4+ and CD8+ T-cell responses were evaluated by stimulation of PBMCs using a 15-mer with 11 amino acid overlapping SARS-CoV-2 spike peptide pool (SB-peptide). T-cell activation and phenotype were measured by flow cytometry: CD154, CD137, CD69, IFN-γ, TNF-α, IL-2, IL-4, PD-1, IL-17, CXCR5, and FOXP3. In parallel, SARS-CoV-2-specific CD8+ T-cells were detected using spike peptide-HLA tetramer (spike/HLA-tetramer) staining combined with differentiation markers (CD45RA and CCR7). Stimulation with CEFX peptide pool (JPT/LUMC), containing peptides of CMV and other common pathogens, was used as a positive control. A response was considered to be positive if ≥0.05% of all CD4+ T-cells are spike reactive and if ≥0.005% of all CD8+ T-cells are spike reactive or binding spike-specific human leukocyte antigen (HLA)-peptide tetramers. These thresholds were based on the CD4 and CD8 T-cell responses measured in nine healthy individuals (data not shown). Additional information is provided in Supplemental Methods.

Statistics. Continuous variables are described as median (IQR) and categorical variables as number and percentage of total. Antibody and T-cell responses of diagnostic subgroups were compared to population proportions using one-sample binomial testing. Missing data varied across timepoints; therefore, the number of included measurements is mentioned in the figures and confidence intervals are provided. To evaluate factors associated with humoral and cellular responses, univariable logistic regression was performed. To compare groups Chi square, Wilcoxon or Mann–Whitney U tests were used when applicable. All tests were two-sided with an α of 0.05. Analyses were performed using IBM SPSS Statistics (version 25.0.0.2) and Graphpad Prism (version 9.3.1).

One hundred and sixty patients diagnosed with CLL (n = 31), aggressive NHL (n = 39), indolent NHL (n = 57), MM (n = 30), and other (acute lymphoblastic leukemia n = 2, autoimmune pancytopenia n = 1) were included (Table S1). All patients received two doses of an mRNA vaccine. Eight patients with pre-vaccination positive anti-SARS-CoV-2 S Ig were excluded from the analysis.

Adequate seroconversion rates 2 weeks post-vaccination were 31% in CLL, 62% in aggressive NHL, 60% in indolent NHL, and 93% in MM patients (Figure 1A). Compared to an age-adjusted population proportion of 99%, this was significantly lower in patients with all disease categories, except MM. Recent treatment with anti-CD20 containing regimens significantly reduces adequate seroconversion rate (Figure S1A). However, when treatment was >12 months before vaccination, this seroconversion rate increased significantly to 87% (Figure S1B), indicating that sufficient B-cell recovery to elicit seroconversion takes at least 12 months after B-cell depleting therapy. Next to disease and treatment, univariable logistic regression analysis showed that only a lymphocyte count below 1*109/L was a significant predictor of humoral outcome (Figure S2A), which is related to B-cell-depleting therapy. These findings are in line with previous studies.[1]

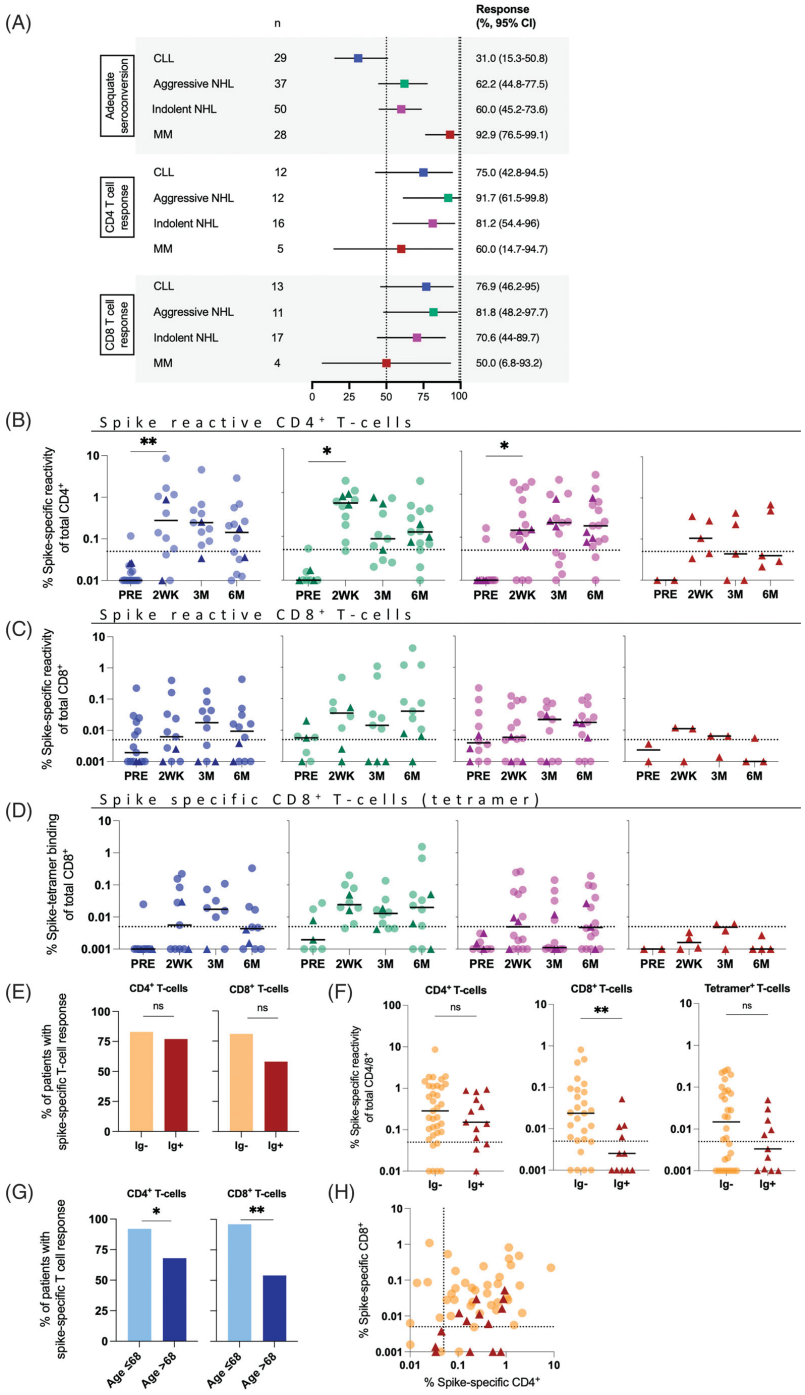
(A)
n
Response (%, 95% CI)
Adequate seroconversion
CLL 29 31.0 (15.3-50.8)
Aggressive NHL 37 62.2 (44.8-77.5)
Indolent NHL 50 60.0 (45.2-73.6)
MM 28 92.9 (76.5-99.1)
CD4 T cell response
CLL 12 75.0 (42.8-94.5)
Aggressive NHL 12 91.7 (61.5-99.8)
Indolent NHL 16 81.2 (54.4-96)
MM 5 60.0 (14.7-94.7)
CD8 T cell response
CLL 13 76.9 (46.2-95)
Aggressive NHL 11 81.8 (48.2-97.7)
Indolent NHL 17 70.6 (44-89.7)
MM 4 50.0 (6.8-93.2)
0 25 50 75 100
(B)
Spike reactive CD4+ T-cells
% Spike-specific reactivity of total CD4+
PRE 2WK 3M 6M
(C)
Spike reactive CD8+ T-cells
% Spike-specific reactivity of total CD8+
(D)
Spike specific CD8+ T-cells (tetramer)
% Spike-tetramer binding of total CD8+
(E)
CD4+ T-cells
CD8+ T-cells
% of patients with spike-specific T-cell response
ns
Ig- Ig+
(F)
CD4+ T-cells
CD8+ T-cells
Tetramer+ T-cells
% Spike-specific reactivity of total CD4/8+
(G)
CD4+ T-cells
CD8+ T-cells
% of patients with spike-specific T cell response
Age ≤68
Age >68
(H)
% Spike-specific CD8+
% Spike-specific CD4+

Figure 1 Humoral and spike-specific CD4+ and CD8+ T-cell responses after mRNA vaccination in patients with CLL (purple), aggressive NHL (green), indolent NHL (pink) or MM (red).

Response evaluation at different time points (2 weeks, 3 months, and 6 months) after initial complete vaccination, which for mRNA-1273 and BNT162b consisted of two vaccination doses, administered within a 4–5 week interval. Data for patients with CLL are shown in blue, for aggressive NHL in green, for indolent NHL in purple and, for MM in red. Anti-SARS-CoV-2 Spike antibodies were measured using anti-SARS-CoV-2 S immunoassay. Spike-specific T-cell responses were measured by thawing PBMCs and stimulating them with a spike peptide pool for 16 h, and afterwards, samples were analyzed by flow cytometry using various markers. Values were corrected for background measured in DMSO. In (B–H), each dot represents a patient; seronegative patients are depicted as circles and seropositive patients are depicted as darker triangles. (A) Response rates 2 weeks after complete vaccination, serological response rate was based on the percentage of patients with adequate anti-SARS-CoV-2 spike Ig (>250 BAU/ml). CD4+ T-cell response was the percentage of patients with >0.05% of spike-specific CD4+ T-cells (CD137+ and/or CD154+) within the total CD4+ population and CD8+ T-cell response was the percentage of patients with >0.005% of spike-specific CD8+ T-cells (CD69+ and/or CD137+ and IFN-γ+ and/or TNF-α+) and/or Spike/HLA-tetramer positive CD8+ T-cells within the total CD8+ population. All proportions were stratified based on hematological disorder and compared to expected population proportions of 99% for serological response, 100% for CD4+ T-cell response, and 50% for CD8+ T-cell response (shown as dotted lines in the figure) using one sample binomial testing. Clopper-Pearson method was used to estimate 95% confidence intervals. (B) Percentage of spike-specific CD4+ T-cells of total CD4+ T-cells measured before and after vaccination. Spike-specific CD4+ T-cells were defined as CD4+ T-cells expressing CD137+and/or CD154+ after stimulation with SARS-CoV-2 Spike peptides. Dotted line represents threshold of 0.05%. Black horizontal line represents median. Kruskal–Wallis testing does not show significant difference between hematologic disorders at 2 weeks, 3, or 6 months (p = .526, p = .319, .227). Wilcoxon test shows a significant increase in percentage of spike-specific CD4+ T-cells 2 weeks after vaccination for CLL, aggressive NHL and indolent NHL (p = .0078, .0156, .0313) compared to pre vaccination, MM was not tested due to lack of sufficient samples. (C) Percentage of spike-specific CD8+ T-cells of total CD8+ T-cells measured before and after vaccination. Spike-specific CD8+ T-cells were defined as CD8+ T-cells having a expressing CD69+and/or CD137+ and IFN-γ+ and/or TNF-α+ after SARS-CoV2 spike peptide stimulation. Dotted line represents threshold of 0.005%. Black horizontal line represents median. Kruskal–Wallis testing does not show significant difference between hematologic disorders at 2 weeks, 3, or 6 months (p = .369, .921, .082). Wilcoxon test shows no significant increase in spike-specific CD8+ T-cell response 2 weeks after vaccination for CLL, aggressive and indolent NHL (p = .195, .250, .922) compared to pre-vaccination, MM was not tested due to lack of sufficient samples. (D) Percentage of Spike/HLA-tetramer positive CD8+ T-cells of total CD8+ T-cells measured before and after vaccination. Dotted line represents threshold of 0.005%. Black horizontal line represents median. Kruskal–Wallis testing does not show significant difference between hematologic disorders at 2 weeks, 3, or 6 months (p = .146, .225, .188). Wilcoxon test shows no significant increase in tetramer positive CD8+ T-cell responses 2 weeks after vaccination for CLL, aggressive and indolent NHL (p = .063, .063, .094) compared to pre-vaccination, MM was not tested due to lack of sufficient samples. (E) Percentage of patients with spike-specific CD4+ or CD8+ T-cell responses in adequately seroconverted (Ig+) or seronegative (Ig–) patients. Significance was tested by Chi square test (CD4+ p = .640, CD8+ p = .143). (F) Frequency of spike-specific CD4+ or CD8+ T-cells in adequately seroconverted (Ig+) or seronegative (Ig–) patients. Significance was tested by Mann–Whitney U tests (CD4+ p = .332, CD8+ p = .007, tetramer p = .21). (G) Percentage of patients with a spike-specific CD4+ or CD8+ T-cell response split by age under or above 68 years. Significance was tested by Chi square test (CD4+ p = .033, CD8+ p = .001). (H) Percentage of spike-specific CD8+ T-cells (CD69+and/or CD137+ and IFN-γ+ and/or TNF-α+) of total CD8+ T-cells (y-axis) plotted against percentage of spike-specific CD4+ T-cells (CD137+and/or CD154+) of total CD4+ T-cells (x-axis). All patients at timepoint 2 weeks or 3 months, independent of cohort, are shown in the figure and dark triangles depict patients with an adequate anti-spike antibody response. Dotted lines either represent threshold for spike-specific CD8+ T-cell response on y-axis of 0.005% or spike-specific CD4+ T-cell response on x-axis of 0.05%. ns, not significant; *p < .05; **p < .01 or ***p < .001. PRE, before vaccination; 2W, 2 weeks after complete vaccination; 3M, 3 months after complete vaccination; 6M, 6 months after complete vaccination.

T-cell responses were measured in 49 patients lacking and 14 patients with adequate seroconversion (Table S2). Spike-specific CD4+ T-cell responses significantly increased in all disease cohorts 2 weeks after mRNA vaccination, whilst control CEFX-specific T-cells remained stable pre- and post-vaccination (Figures 1B and S3A). Spike-specific CD8+ T-cell responses based on reactivation with Spike peptides (Figure 1C) and spike/HLA-tetramer staining (Figure 1D) were increased in CLL and both NHL cohorts 2 weeks after vaccination. Most spike-specific CD4+ and CD8+ T-cell responses remained present over time with fluctuations (Figure 1B–D) and demonstrated to exhibit a type 1 cytokine profile (Figure S4). No clear effect of a third vaccination was seen at 6 months post-initial vaccination; however, only 62% of patients received a third vaccination and this was at various time points before the 6-month time point (median: 46 days, range: 1–70). Expression of PD-1, an early T-cell activation marker, was most prominent 2 weeks after vaccination (Figure S4D,K). In the subset of Spike-specific CD4+ T-cells, both T follicular helper cells and regulatory T-cells were present, though low in number (Figure S4G–H). Spike-specific CD8+ T-cells were mostly effector memory phenotype (Figure S4L). These results were in line with the phenotype observed in a healthy control cohort (n = 9) and previous studies in healthy cohorts (data not shown).[4]

Our in-depth T-cell analysis demonstrated induction of Spike-specific CD4+ responses in 75%, 92%, 81%, and 60% of CLL, aggressive NHL, indolent NHL, and MM, respectively (Figure 1A). Induction of Spike-specific CD8+ responses (presence of Spike-specific and/or Spike/HLA-tetramer+ CD8+ T-cells) were 77%, 82%, 71%, and 50%, respectively (Figure 1A). These data collectively indicate that induction of T-cell responses does not seem to be affected by disease. However, it is important to note that, though low in number of patients analyzed, T-cell responses seem to be hampered in MM. Possible explanation is the use of dexamethasone and/or anti-CD38 therapy, which are known to negatively affect T-cells and their function.

When comparing the Spike-specific T-cell responses between patients with and without adequate seroconversion, no significant differences were observed in the percentage of patients that generated a CD4+ T-cell response nor the percentage of Spike-specific CD4+ T-cells in individual patients (Figures 1E,F and S2B), indicating that the lack of humoral responses was not caused by lack of CD4+ T-cell help (Figure 1A). Furthermore, no difference was observed in the percentage of patients that generated a CD8+ T-cell response (Figures 1E and S2C); however, the frequency of

Spike-specific CD8+ T-cells was significantly higher in patients lacking serological response (Figure 1F) 2 weeks post-vaccination, which could represent an immune compensation mechanism that might contribute to a survival advantage in case of severe COVID-19.[3]

T-cell immunity is known to decline with advanced age. In this study, age was the only significant predictor of Spike-specific T-cell responses (CD4+ OR: 0.18, CD8+ OR: 0.05). (Figure S2B,C), both Spike-specific CD4+ and CD8+ T-cell responses decline significantly for patients aged over 68 years (Figure 1G).

Though cellular responses after SARS-COV-2 vaccination in patients with lymphoid malignancies have been suggested,5 we for the first time show with a highly specific and reproducible technique that nearly all lymphoid malignancy patients exhibit a good Spike-specific CD4+ and CD8+ T-cell response 2 weeks to 3 months after vaccination (Figure 1H).

Limitations of this study include a limited sample size, making it difficult to perform subgroup analysis especially within disease cohorts. Therefore, analyzing specific treatment-related effects is not possible. However, this cohort does represent a real-world situation for patients in two secondary-/tertiary-care centers in the Netherlands. In addition, the peptide pools used in the T-cell assays were based on the ancestral Wuhan strain sequence which is not the current circulating variant. However, it is important to note that it has been shown that T-cell responses induced by mRNA-1273 and BNT162b2 are minimally affected by the mutations found in omicron.[6]

In conclusion, this study demonstrates that the majority of patients lacking adequate seroconversion following SARS-CoV-2 mRNA vaccination were able to generate a cellular immune response. Moreover, a hampered humoral response is compensated by a stronger cellular response, which indicates that vaccination is of significance also in patients lacking seroconversion.

ACKNOWLEDGEMENTS

The authors would like to thank all patients and colleagues from Maastricht University Medical Center and Leiden University Medical Center who made this study possible. Flow cytometry was performed at the Flow cytometry Core Facility (FCF) of Leiden University Medical Center (LUMC) in Leiden, Netherlands (https://www.lumc.nl/research/facilities/fcf).

REFERENCES

1. Jiménez M, Roldán E, Fernández-Naval C, et al. Cellular and humoral immunogenicity of the mRNA-1273 SARS-CoV-2 vaccine in patients with hematologic malignancies. Blood Adv. 2022; 6(3): 774-784.
2. Moss P. The T cell immune response against SARS-CoV-2. Nat Immunol. 2022; 23(2): 186
3. Bange EM, Han NA, Wileyto P, et al. CD8+ T cells contribute to survival in patients withCOVID-19 and hematologic cancer. Nat Med. 2021; 27(7): 1280-1289.
4. Sahin U, Muik A, Derhovanessian E, et al. COVID-19 vaccine BNT162b1 elicits human antibody and TH1 T cell responses. Nature. 2020; 586(7830): 594-599.
5. Marasco V, Carniti C, Guidetti A, et al. T-cell immune response after mRNA SARS-CoV-2 vaccines is frequently detected also in the absence of seroconversion in patients with lymphoid malignancies. Br J Haematol. 2022; 196(3): 548-558.
6. Tarke A, Coelho CH, Zhang Z, et al. SARS-CoV-2 vaccination induces immunological T cell memory able to cross-recognize variants from Alpha to Omicron. Cell. 2022; 185: 847-859.e11.

SUPPLEMENTAL METHODS

Antibody measurement

For quantitative anti-SARS-CoV-2 Spike RBD antibody measurement the Roche Elecsys anti-SARS-CoV-2 S (Roche Diagnostics GmbH, Mannheim, Germany) was used. This test is an electrochemiluminescence assay (ECLIA) detecting total antibodies (IgG, IgA, and IgM) against the receptor binding protein of the SARS-CoV-2 Spike protein.

The test is standardized against an internal anti-RBD monoclonal antibody mixture and is expressed as units/mL (U/ml), with a measuring range of 0-250 U/ml). U/ml corresponds in a 1:1,0288 ratio with BAU/ml. The test was performed according to the manufacturer's instruction. Values higher than 0.8 BAU/ml were considered positive and values higher than 250 BAU/ml were considered as adequate response, as healthy individuals all have a value of 250 BAU/ml or higher. (1) Expected seroconversion rate using the Roche Elecsys assay after COVID-19 vaccination in comparable older individuals is 99% (prefrail category in Semelka et al.) (2).

1. Elecsys anti-SARS-CoV-2 S Method sheet [internet]. 2020 [cited 2022-03-17]. Available from: https://www.fda.gov/media/144037/download.
2. Semelka CT, DeWitt ME, Callahan KE, Herrington DM, Alexander-Miller MA, Yukich JO, Munawar I, McCurdy LH, Gibbs MA, Weintraub WS, Sanders JW; COVID-19 Community Research Partnership. Frailty and COVID-19 mRNA Vaccine Antibody Response in The COVID-19 Community Research Partnership. J Gerontol A Biol Sci Med Sci. 2022 Apr 21.

DETECTION OF SARS-COV-2 SPECIFIC T CELLS

PBMCs were isolated from fresh whole blood using Ficoll-Isopaque and cryo-preserved (in RPMI medium + 10% dimethyl sulfoxide (DMSO)) until further use. Upon thawing, the PBMCs were slowly diluted in culture medium consisting of Iscove Modified Dulbecco Medium (IMDM; Lonza) supplemented with 10% heat-inactivated fetal bovine serum (FBS; Sigma-Aldrich), 2.7mM L-glutamine (Lonza), 100 U/mL penicillin (Lonza) and 100 µg/mL streptomycin (Lonza) (1% p/s). After thawing and washing, PBMCs were treated with 1.33 mg/ml DNAse to minimize cell clumping, counted, and used for T-cell stimulation assay as well as for peptide-HLA tetramer staining. For the T-cell stimulation assay, up to $2x10^6$ PBMCs were seeded in 100 µL culture medium and stimulated with 15-mer peptides with 11 amino acid overlap which cover the whole SARS-CoV-2 spike antigen (sb-PEPTIDE) in 96-well round bottomed plates. The peptides were dissolved in 20% DMSO in ddH_2O and added to the wells

in a 1 µg/mL final concentration. As a negative control, DMSO and ddH_2O in the same concentration was added. As a positive control, a pool of peptides from CMV, EBV, Flu etcetera (CEFX) was dissolved in 20% DMSO in ddH_2O and in a final concentration of 0.25 µg/mL (see **Table S3** for CEFX peptide pool details). After one hour incubation (37°C, 5% CO_2), 5 µg/mL Brefeldin A was added to the well and the plate was further incubated for 15 hours. The stimulation reaction was stopped by washing the cells in PBS followed by viability staining using Zombie-Red. After a PBS wash, cells were fixated and permeabilized using the FOXP3 buffer kit (Thermo Fisher). 20 µL antibody staining mix was added containing 0.8 mg/mL albumin, Brilliant Stain Buffer Plus and antibodies directed against CD3, CD4, CD8, CD154, CD137, CD69, IFN-γ, TNF-α, IL-2, IL-4, IL-17, PD-1, FOXP3 and CXCR5 (see **Table S4** for product details). After incubation for 30 minutes at room temperature (RT), the cells were washed in PBS containing 0.8 mg/mL albumin (FACS buffer) and dissolved in 100 µL FACS buffer for measurement on a 3-laser aurora (Cytek Biosciences).

For the tetramer staining, up to $2x10^6$ PBMCs were incubated for 16 hours in 100 µL culture medium. The cells were washed in FACS buffer and stained in two steps. First, 10 µL of an antibody cocktail directed against CD4, CCR7, CD45RA, PD-1 was added together with a tetramer pool in FACS buffer and incubated for 15 minutes at RT. Second, 10 µL of FACS buffer containing CD8 APC-H7 was incubated for an additional 15 minutes at RT (see **Table S3** for product details). The tetramer pool contained 23 in-house-made tetramers, consisting of spike peptides and HLAs (spike/HLA-tetramers), conjugated to PE as well as APC (see **Table S5** for tetramer details). Cells were washed and dissolved in 100 µL FACS buffer for measurement on a 3-laser aurora (Cytek Biosciences).

For flow cytometry analysis, OMIQ (http://www.omiq.ai) was used to set gates and retrieve percentages (see **Fig. S3** for gating strategy). Due to optimal reference controls used for unmixing on the 3-laser Cytek Aurora, no compensation was needed. The same gate was applied to all samples within one donor and as much as possible between donors. Percentage SARS-CoV-2 spike reactive $CD4^+$ T-cells was identified as $CD137^+$ and/or $CD154^+$ cells of total $CD4^+$ T-cells, corrected for background in DMSO. Percentage SARS-CoV-2-spike reactive $CD8^+$ T-cells was identified as $CD137^+$ and/or $CD69^+$ and IFN-γ^+ and/or TNF-α^+ of total $CD8^+$ T-cells. The same $CD137^+$ and/or $CD154^+$ or $CD137^+$ and/or $CD69^+$ was applied to all samples unless the background in DMSO was 0.1% or higher. Then the gate was adapted and applied to all samples of that donor.

Percentage SARS-CoV-2-spike $CD4^+$ T-cells was removed from analysis if there were less than 10.000 events in CD4 gate and percentage SARS-CoV-2-spike $CD8^+$ T-cells was removed from analysis if there were less than 10.000 events in CD8 gate. For CLL this was diminished to 5.000 events within the $CD4^+$ T-cell gate and the $CD8^+$ T-cell gate, because of the large B-cell population. A threshold was set on 0.05% for frequency $CD154^+$ and/or $CD137^+$ of total $CD4^+$ T-cells, 0.005% for frequency $CD137^+$ and/or $CD69^+$ AND IFN-γ^+ and/or TNF-α^+ of total CD8 T-cells and 0.005% for frequency of spike/HLA-tetramer$^+$ of total $CD8^+$ T-cells. Further gating to calculate percentage of spike-specific cells that are IFN-γ, TNF-α, IL-2, IL-4, IL-17, Tfh (T follicular helper cells; $CXCR5^+PD\text{-}1^+$), PD-1 ($CXCR5^-PD\text{-}1^+$) or Treg ($FOXP3^+$IFN-γ^- TNF-α^-) positive was only done if frequency threshold was met and if there were more than 25 events in the $CD154^+$ and/or $CD137^+$ gate for $CD4^+$ T-cells and $CD137^+$ and/or $CD69^+$ for the $CD8^+$ T-cells. Percentage of naïve (CCR7+CD45RA+), central memory (CM; CCR7+CD45RA-), effector memory (EM; CCR7-CD45RA-) or terminal effector memory (TEMRA; CCR7-CD45RA+) was measured of spike/HLA-tetramer$^+$ $CD8^+$ T-cells and only calculated if the frequency of spike/HLA-tetramer$^+$ $CD8^+$ T-cells was above threshold and contained at least 10 events. The percentages were exported and further analyzed in Graphpad Prism 9.0.1. All timepoints of the same patient were measured simultaneously to minimize technical variance within one patient. Patients were measured and analyzed in random order to minimize technical variance and bias between cohorts. In the last analysis step the data was separated for the different cohorts to prevent bias during analysis.

SUPPLEMENTARY FIGURES

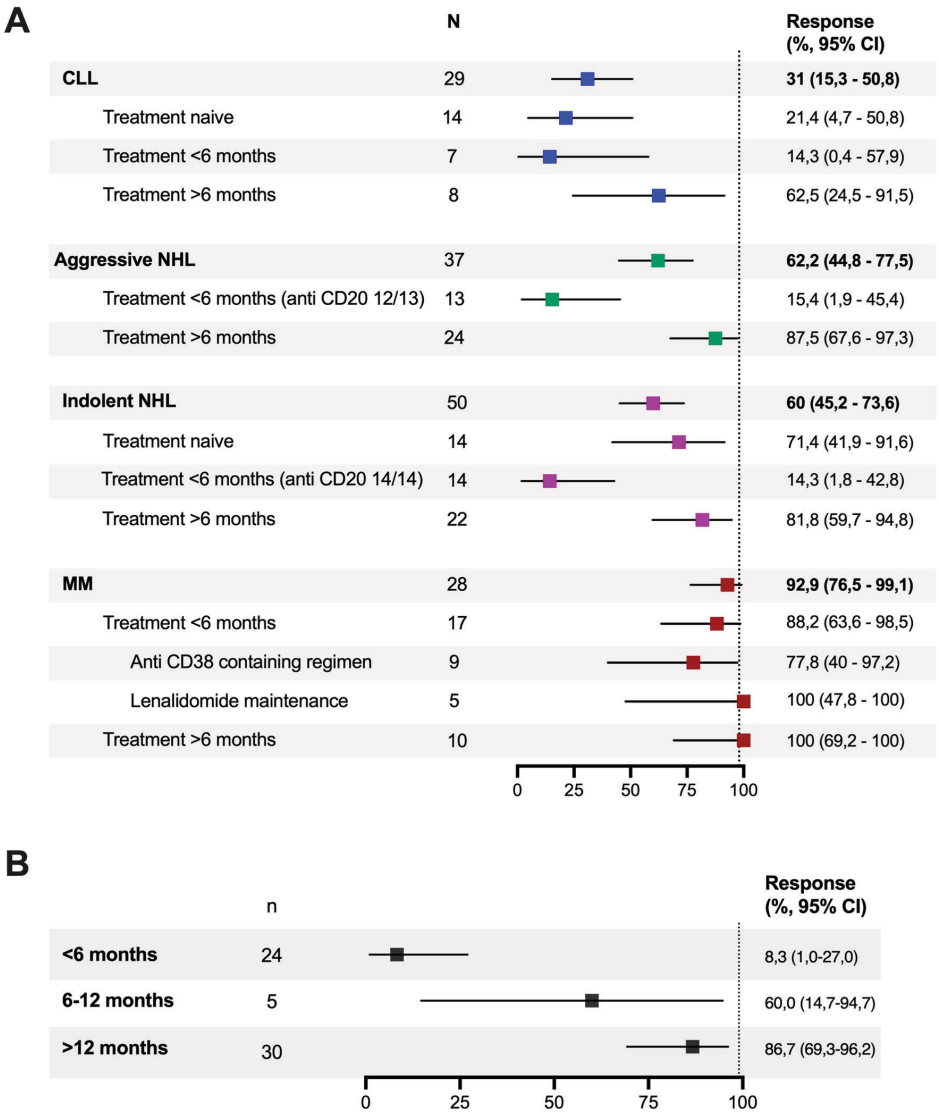

Figure S1 Serological response rates 2 weeks after SARS-CoV-2 mRNA vaccination.
Serological response rate was based on the percentage of patients with adequate anti-SARS-CoV-2 Spike antibodies (>250 BAU/ml). All proportions were compared to the expected population proportion of 99%, using one sample binomial testing. Clopper-Pearson method was used to estimate 95% confidence intervals. A) Data stratified to hematological disorder, time since treatment and if applicable type of treatment. Subgroups with n<5 were excluded from this figure. B) Data stratified to time since anti-CD20 containing regimen treatment.

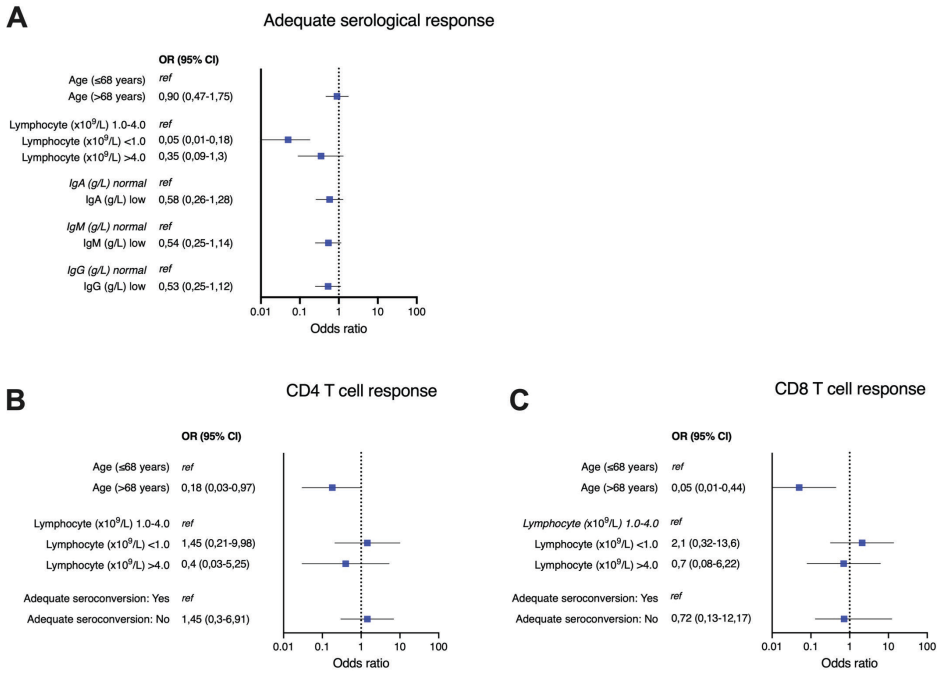

Figure S2 Potential predictive factors for serological CD4⁺ or CD8⁺ T-cell response.
Univariable logistic regression for possible outcome predictors of adequate serological (A), CD4⁺ (B) and CD8⁺ T-cell response (C). Showing odds ratios (OR) including 95% confidence interval. An OR <1 indicates a negative impact on the outcome and an OR >1 indicates a positive impact on the outcome. CD4⁺ T-cell response was defined as >0.05% of SARS-CoV-2 Spike-specific CD4⁺ T-cells, CD8⁺ T-cell response was defined as <0.005% of SARS-CoV-2 Spike-specific or spike/HLA-tetramer binding CD8⁺ T-cells.

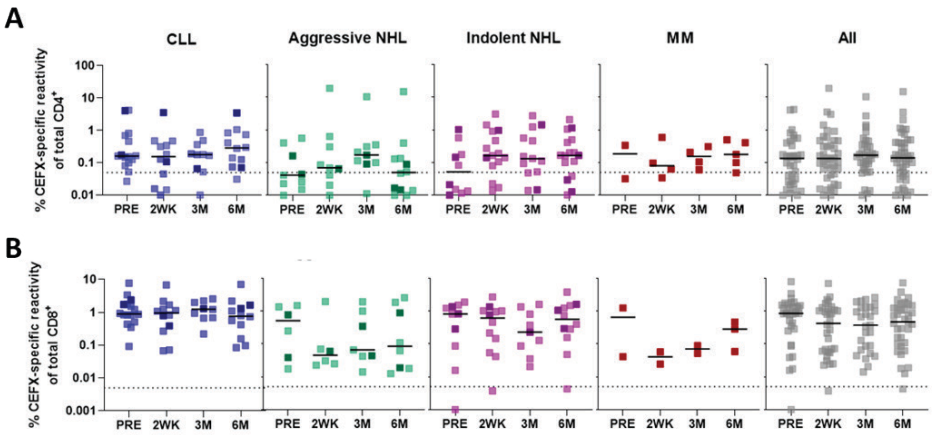

Figure S3 CD4⁺ and CD8⁺ T-cell responses after stimulation with CEFX peptide pool.
PBMCs from patients with CLL (blue), aggressive NHL (green), indolent NHL (purple) and MM (red) were isolated and stimulated with a CEFX peptide pool, after which flowcytometric analysis was performed to investigate CEFX-specific T-cell responses before vaccination (PRE), 2 weeks after vaccination (2WK), 3 months after vaccination (3M) and 6 months after vaccination (6M). Patients with adequate seroconversion following SARS-CoV-2 vaccination are depicted as dark squares while patients lacking adequate seroconversion are depicted as lightly colored squares. CD4⁺ T-cell response was defined as the percentage of CD4⁺ T-cells that express CD137⁺ and/or CD154⁺ phenotype after stimulation with CEFX peptide pool. CD8⁺ T-cell response was defined as the percentage of CD8⁺ T-cells that express CD69⁺ and/or CD137⁺ and IFNγ⁺ and/or TNFα⁺ phenotype after stimulation with the CEFX peptide pool. Values were corrected for background measured in DMSO. Each dot represents a patient. Horizontal black line shows the median. A) Percentage of CEFX-specific CD4⁺ T-cells of total CD4⁺ T-cells measured before vaccination and after vaccination. Dotted line represents a threshold of 0.05%. B) Percentage of CEFX-specific CD8⁺ T-cells of total CD8⁺ T-cells measured before vaccination and after vaccination. Dotted line represents a threshold of 0.005%.

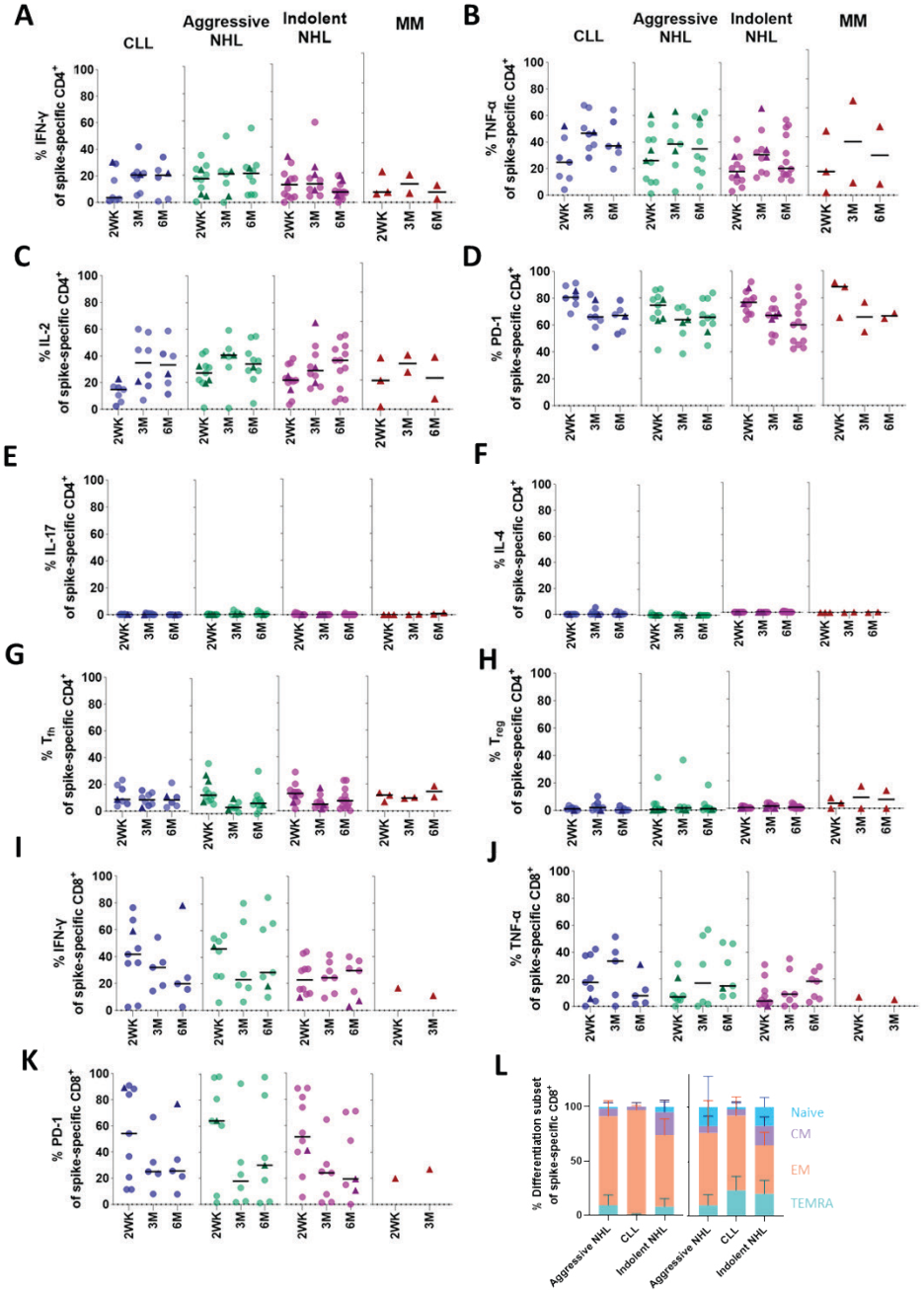
A
CLL
Aggressive NHL
Indolent NHL
MM
% IFN-γ of spike-specific CD4+
B
% TNF-α of spike-specific CD4+
C
% IL-2 of spike-specific CD4+
D
% PD-1 of spike-specific CD4+
E
% IL-17 of spike-specific CD4+
F
% IL-4 of spike-specific CD4+
G
% Tfh of spike-specific CD4+
H
% Treg of spike-specific CD4+
I
% IFN-γ of spike-specific CD8+
J
% TNF-α of spike-specific CD8+
K
% PD-1 of spike-specific CD8+
L
% Differentiation subset of spike-specific CD8+
Naive
CM
EM
TEMRA
2WK
3M
6M
Aggressive NHL
CLL
Indolent NHL

Figure S4 Cytokine production and marker expression of spike-specific $CD4^+$ and $CD8^+$ T-cells.

PBMCs from patients with CLL (blue), aggressive NHL (green), indolent NHL (purple) and MM (red) were isolated and stimulated with SARS-CoV-2 Spike peptides followed by flowcytometry. Percentage of spike-specific T-cells that are cytokine or marker positive 2 weeks (2WK), 3 months (3M) and 6 months (6M) after vaccination was analyzed for each disease group.Patients with adequate antibody responses following SARS-CoV-2 vaccination are depicted as dark triangles while patients lacking an adequate antibody response are depicted as circles. Each dot represents a patient. Horizontal black line shows the median. A) Percentage of IFNγ production by spike-specific CD4+ T-cells, shown per disease group. B) Percentage of TNFα production by spike-specific CD4+ T-cells, shown per disease group. C) Percentage of IL-2 production by spike-specific CD4+ T-cells, shown per disease group. D) Percentage of PD-1 expression by spike-specific CD4+ T-cells, shown per disease group. E) Percentage of IL-17 production by spike-specific CD4+ T-cells, shown per disease group. F) Percentage of IL-4 production by spike-specific CD4+ T-cells, shown per disease group. G) Percentage of Tfh cells of total spike-specific CD4+ T-cells, shown per disease group. H) Percentage of Treg cells of total spike-specific CD4+ T-cells, shown per disease group. I) Percentage of IFNγ production by spike-specific CD8+ T-cells, shown per disease group. J) Percentage of TNFα production by spike-specific CD8+ T-cells, shown per disease group. K) Percentage of PD-1 expression by spike-specific CD4+ T-cells, shown per disease group. L) Percentage of spike/HLA-specific CD8+ T-cells which are naïve (blue; CCR7+CD45RA+), central memory (CM; purple; CCR7+CD45RA-), effector memory (EM; orange; CCR7-CD45RA-) or terminal effector memory (TEMRA; green; CCR7-CD45RA+).

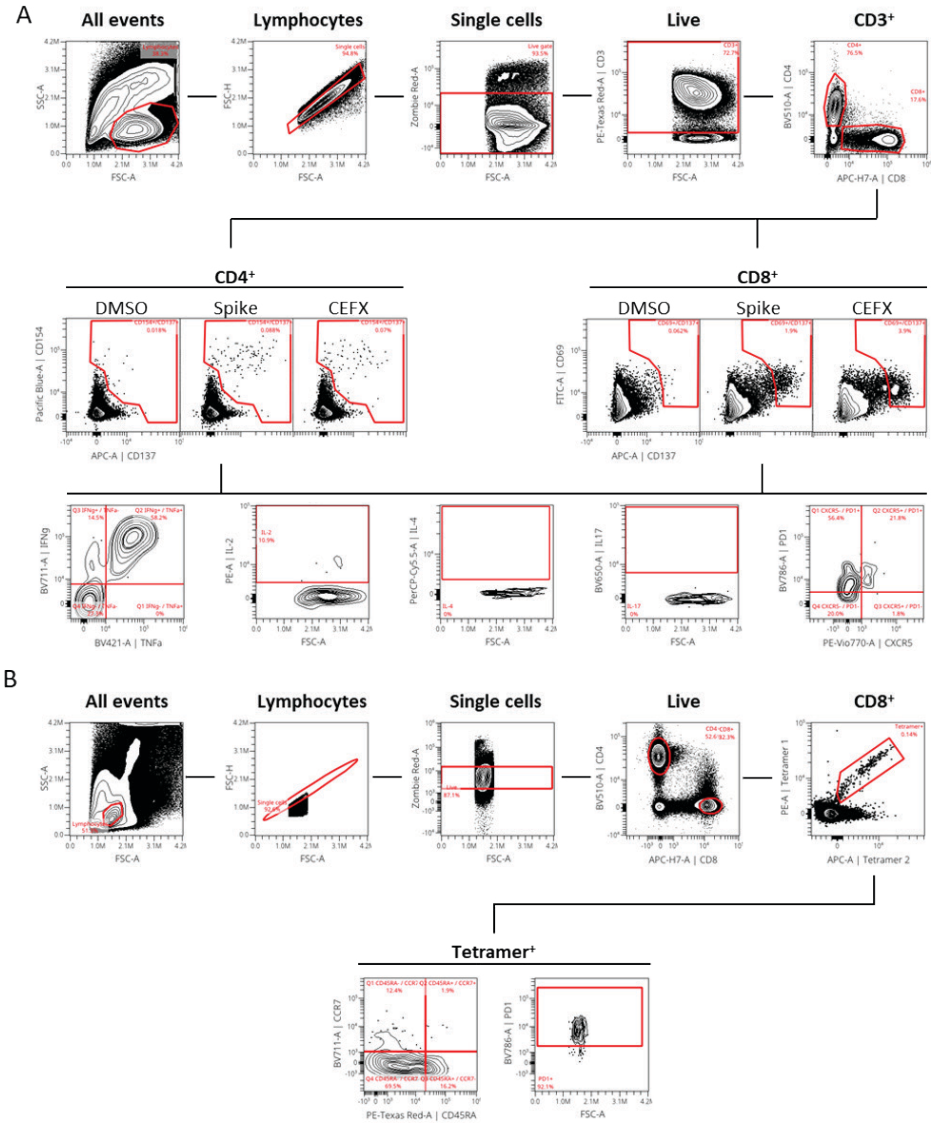

Figure S5 Flow cytometry gating example for peptide stimulation assays and tetramer staining.

A) Representative example of flow cytometry gating strategy for peptide-specific CD4+ and CD8+ T-cells. All events were gated on lymphocytes, single cells, viable cells, CD3 positive and subsequently either CD4 or CD8 positive. For CD4+ T-cells, activated cells were gated on CD137 and/or CD154 positive whilst for CD8+ T-cells CD137 and/or CD69 and IFN-γ and/or TNF-α positive cells were gated. DMSO functioned as a negative control and CEFX functioned as a positive control. From the activated cell gate onwards, cytokine production and marker expression were calculated. B) Representative example of flow cytometry gating strategy for spike/HLA-tetramer positive CD8+ T-cells. All events were gated on lymphocytes, single cells, viable cells, CD8 positive and spike/HLA-tetramer positive. Tetramer positive events were subsequently gated on CCR7, CD45RA or PD-1.

Table S1 Baseline characteristics

Characteristic	N (%) / median [IQR]
Sex	
Male	93 (58)
Female	67 (42)
Age (years)	68 [60-73]
Haematological diagnosis	
CLL	31 (19)
Treatment naïve	16 (52)
Treatment <6M	7 (23)
• Anti CD20 containing regimen	1 (14)
• Ibrutinib	4 (57)
• Venetoclax	2 (29)
Treatment >6M	8 (26)
Aggressive NHL	39 (24)
Treatment <6M*	13 (33), 2/13 (15)
• Anti CD20 containing regimen	12 (92)
• Chemotherapy	1 (8)
Treatment >6M	26 (67)
Indolent NHL	57 (36)
Treatment naïve	15 (26)
Treatment <6M**	19 (33)
• Anti CD20 containing regimen	14 (74)
• Ibrutinib	2 (11)
• Other	3 (16)
Treatment >6M	22 (39)
MM	30 (19)
Treatment naïve	2 (7)
Treatment <6M***	18 (60)
• Anti CD38 containing regimen	10 (56)
• Lenalidomide maintenance	5 (28)
• Other	3 (17)
Treatment >6M	10 (33)
Other	3 (2)
Presence of anti SARS-CoV-2 RBD prevaccination	8 (5)
Vaccine type (initial vaccination)	127 (80)
• mRNA-1273	25 (16)
• BNT162b	8 (5)
• Unknown	

Table S1 *Continued*

Characteristic	N (%) / median [IQR]
Booster vaccination**	110 (69)
• Received	29 (18)
• Not received	21 (13)
• Unknown	
Leukocytes (*10^9/L)	5,9 [4,6-8,7]
Leukocytes (*10^9/L)	
Total IgA (g/L)	1,08 [0,56-1,87]
Total IgG (g/L)	7,65 [5,26-10,50]
Total IgM (g/L)	0,38 [0,21-0,67]

* 2 patients have also received an autologous stem cell transplant <6 months ago
** 1 patient has also received an autologous stem cell transplant <6 months ago
*** 3 patients have also received an autologous stem cell transplant <6 months ago
**** Patients that have received a third/booster vaccination before the 6 months timepoint

Table S2 Baseline characteristics T-cell subset

Characteristic	N (%) / median [IQR]	Anti SARS-CoV-2 Ig pos/ neg (n)
Age (years)	69 [62-74]	
CLL	20 (32)	18/2
Treatment naïve	10 (16)	
Treatment <6M	6 (10)	
• Anti CD20 containing regimen	1 (2)	
• Ibrutinib	4 (6)	
• Venetoclax	1 (2)	
Treatment >6M	4 (6)	
Aggressive NHL	16 (25)	13/3
Treatment <6M	12 (19)	
• Anti CD20 containing regimen	12 (19)	
Treatment >6M	4 (6)	
Indolent NHL	19 (30)	15/4
Treatment naïve	6 (10)	
Treatment <6M	13 (21)	
• Anti CD20 containing regimen	12 (19)	
• Ibrutinib	1 (2)	
MM	5 (8)	0/5
Treatment <6M	5 (8)	
• Anti CD38 containing regimen	5 (8)	
Other	3 (5)	3/0

Characteristic	N (%) / median [IQR]	Anti SARS-CoV-2 Ig pos/ neg (n)
Booster vaccination*	39 (62)	
• Received	12 (19)	
• Not received	12 (19)	
• Unknown		
Leukocytes (*10^9/L)	5.6 [4.1-10.2]	
Lymphocytes (*10^9/L)	1.4 [0.8-5.8]	

*Patients that have received a third/booster vaccination before the 6 months timepoint

Table S3 List of peptides used in this study

Peptide pools				
Pathogen	**Antigen**	**Supplier**	**Catalogous #**	**Peptide characteristics**
CMV	PP65	JPT	Custom-made	15-mer, 11aa overlapping
Pool	Pool	JPT	PM-CEFX-3	15-mer, 11aa overlapping
EBV	BZLF1	JPT	PM-EBV-BZLF1	15-mer, 11aa overlapping
EBV class I	Mix	LUMC	Custom-made	9-mer, known epitopes (see below)
Influenza A	NP1	JPT	N/A	15-mer, 11aa overlapping, NCBI: ABB79814

EBV class I peptide pool				
Antigen	**Sequence (aa)**	**HLA restriction**	**Supplier**	**Peptide characteristics**
LMP2	ESEERPPTPY	A*01:01	LUMC	9-mer
BMLF1	GLCTLVAML	A*02:01	LUMC	9-mer
LMP2	CLGGLLTMV	A*02:01	LUMC	9-mer
LMP2	FLYALALLL	A*02:01	LUMC	9-mer
BRLF1	RVRAYTYSK	A*03:01	LUMC	9-mer
EBNA3A	RLRAEAQVK	A*03:01	LUMC	9-mer
EBNA3B	IVTDFSVIK	A*11:01	LUMC	9-mer
EBNA3B	AVFDRKSDAK	A*11:01	LUMC	9-mer
BRLF1	DYCNVLNKEF	A*24:02	LUMC	9-mer
EBNA3A	RPPIFIRRL	B*07:02	LUMC	9-mer
BZLF1	RAKFKQLL	B*08:01	LUMC	9-mer
EBNA3A	QAKWRLQTL	B*08:01	LUMC	9-mer
EBNA3A	FLRGRAYGL	B*08:01	LUMC	9-mer
EBNA3A	YPLHEQHGM	B*35:01	LUMC	9-mer

Table S4 List of antibodies and reagents used for flow cytometry

Antibodies				
Antigen	**Format**	**Clone ID**	**Supplier**	**Catalogous #**
CD4	BV510	SK3	BD Biosciences	562970
CD8	APC-H7	SK1	BD Biosciences	560179
CD3	Pe-Texas-Red	7D6	Invitrogen	MHCD0317
CD69	FITC	Clone L78	BD Biosciences	347823
CD137	APC	4B4-1	BD Biosciences	550890
CD154	Pacific blue	24-31	Biolegend	310820
IFNγ	BV711	B27	BD Biosciences	564039
TNFα	BV421	MAb11	BD Biosciences	562783
IL2	PE	SCPL1362	BD Biosciences	560436
IL4	PERCPCY5.5	MP4-25D2	Biolegend	500822
FOXP3	AF700	PCH101	Thermo Fisher	56-4776-41
CXCR5	PE-Vio770	REA103	Miltenyi	130-117-358
PD1	BV786	EH12.1	BD Biosciences	563789
IL17	BV650	N49-653	BD Biosciences	563746
CCR7	BV711	3D12	BD Biosciences	563712
CD45RA	Pe-Texas-Red	MEM-56	Invitrogen	MHCD45RA17

Other reagents		
Product	**Supplier**	**Catalogous #**
Brilliant Violet Stain Buffer Plus	BD Biosciences	566385
FOXP3 buffer kit	Thermo fisher	00-5521-00
Zombie-red	Biolegend	423110

Table S5 List of peptide-HLA tetramers used for flow cytometry

Tetramers		
Peptide sequence (aa)	**HLA allele**	**Supplier**
LTDEMIAQY	A*01:01	LUMC
FLPFFSNV	A*02:01	LUMC
RLNEVAKNL	A*02:01	LUMC
RLQSLQTYV	A*02:01	LUMC
VLNDILSRL	A*02:01	LUMC
YLQPRTFLL	A*02:01	LUMC
GTHWFVTQR	A*03:01/A*11:01	LUMC
KCYGVSPTK	A*03:01/A*11:01	LUMC
IYKTPPIKDF	A*24:02	LUMC
QYIKWPWYI	A*24:02	LUMC
RFDNPVLPF	A*24:02	LUMC
TQDLFLPFF	A*24:02	LUMC
TYVPAQEKNFT	A*24:02	LUMC
LPQGFSAL	B*07:02	LUMC
MIAQYTSAL	B*07:02	LUMC
SPRRARSVA	B*07:02	LUMC
CVADYSVLY	B*15:01	LUMC
LVKNKCVNF	B*15:01	LUMC
VASQSIIAY	B*15:01	LUMC
IYKTPPIKDF	B*35:01	LUMC
QPTESIVRF	B*35:01	LUMC

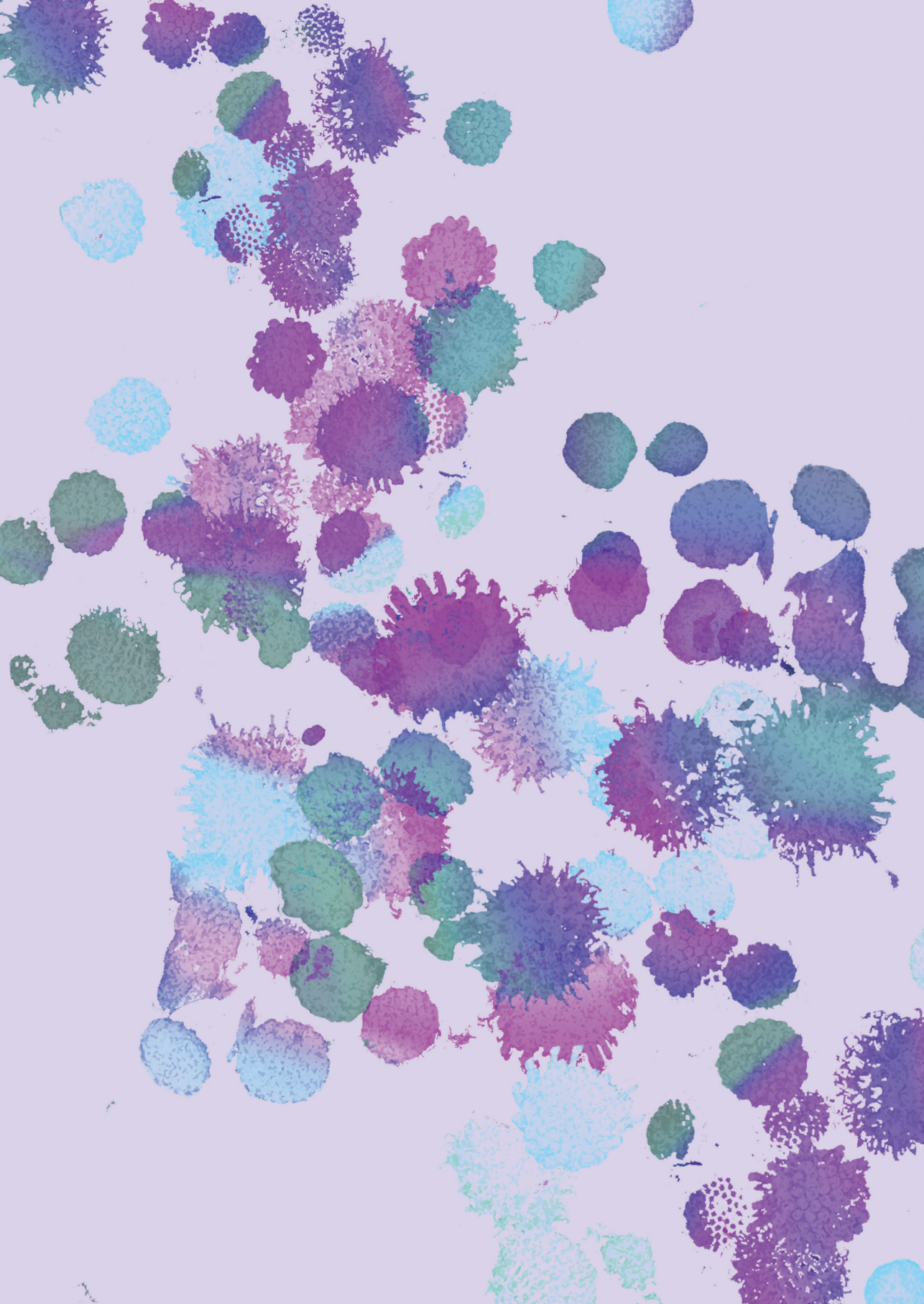

T-CELL AND ANTIBODY RESPONSES IN IMMUNOCOMPROMISED PATIENTS WITH HEMATOLOGIC MALIGNANCIES INDICATE STRONG POTENTIAL OF SARS-COV-2 MRNA VACCINES

Pothast, C. R.*, Hofsink, Q.*, Haggenburg, S., Dijkland, R.C., van de Meent, M., van Dijk, K., Bhoekhan, M.S., Haverkate, N.J.E., van Meerloo, J., Falkenburg, J.H.F., de Groen, R.A.L., Broers, A.E.C., van Doesum, J.A., van Binnendijk, R.S., den Hartog, G., Lissenberg-Witte, B.I., Kater, A.P., Smits, G.P., Wouters, D., van Leeuwen, E.M.M., Bontkes, H.J., Kootstra, N.A., Vogels-Nooijen, S., van Baarle, D., de Vries, R.D., van Meerten, T., Mutsaers, P.G.N.J., Goorhuis, A., Nijhof, I.S., Hazenberg, M.D., Heemskerk, M.H.M., Rutten, C.E., & COBRA KAI study team

Adapted version of:
(2025) *Haematologica*. DOI: 10.3324/haematol.2024.287136

Chapter 5

SARS-CoV-2 emergence combined with new mRNA vaccination provided a unique opportunity to investigate *de novo* mRNA vaccine-induced immune responses. In healthy individuals (HI) SARS-CoV-2 mRNA vaccines are effective, but immunocompromised patients are often understudied. In particular, patients with hematological malignancies are rarely stratified based on disease and treatment. Furthermore, the focus is usually on antibodies whilst T cells are underreported and seldom studied in detail by flow cytometry. We therefore aimed to investigate the SARS-CoV-2 mRNA vaccine-induced humoral and T cell responses in patients with hematological malignancies in a side-by-side comparison of different malignancies and treatments. We enrolled and categorized 723 patients with hematologic diseases in 16 pre-defined cohorts based on malignancy and therapy.[1] For the current study, we randomly selected 173 patients, representative for each cohort with respect to age, absolute baseline CD4+ and CD8+ T cell numbers, and S1 IgG concentrations. HI were age-matched to the overall patient cohort, except for patients treated with hypomethylating agents (HMA) where the median age was 71 years (**Table 1 Figure S1**). We performed an in-depth, combined analysis of the frequency, phenotype and functionality of spike-specific CD4+ and CD8+ T cells and spike (S1)-specific antibody responses before and four weeks after each mRNA-1273 vaccination (**Figure S2**). Methods are described previously.[2, 3] Study protocols were approved by the institutional review board of all participating centers.

Table 1 Patient characteristics, stratified by disease and treatment at time of first COVID-19 vaccination

	Included for T cell analyses	**Years of age**	**Female sex*[1]**	**WHO PS 0-1**
	n	***Median (IQR)***	***%***	***%***
All participants	193	61 (53-67)	44	96
Lymphoma				
During anti-CD20 therapy (αCD20)	13	64 (41-73)	46	100
Anti-CD20 therapy <12mo (< αCD20)	11	65 (51-73)	64	100
BEAM-autologous HCT <12mo (BEAM)	11	65 (58-66)	55	91
CD19 CAR T cell therapy (CAR T)	9	63 (57-67)	44	100
CLL				
Watch and wait (W&W)	10	64 (59-70)	60	100

	Included for T cell analyses	Years of age	Female sex*[1]	WHO PS 0-1
	n	*Median (IQR)*	*%*	*%*
Ibrutinib (BTKi)	11	67 (61-69)	64	100
Multiple myeloma (MM)				
Induction therapy (VTD)	17	59 (54-68)	35	94
Daratumumab (αCD38)	10	65 (57-71)	40	90
Immunomodulatory drug (IMiD)	8	60 (56-62)	13	100
HDM-autologous HCT <9mo (HDM)	9	63 (58-69)	11	100
AML and high-risk MDS (AML)				
High-dose chemotherapy (chemo)	14	58 (48-62)	29	92
Hypomethylating agents (HMA)*[2]	11	71 (65-73)	27	91
MPN				
Ruxolitinib (JAK2i)	9	55 (45-65)	33	100
CML				
Tyrosine kinase inhibitor (TKI)	10	51 (41-61)	60	90
Allogeneic HCT (alloHCT)				
<6 months (<6 mo)	11	59 (57-68)	36	91
Chronic graft-versus-host disease (GvHD)	9	52 (49-64)	22	100
Healthy individuals (HI)	20	58 (50-63)	70	N/A

All patients are part of the COBRA KAI study and received a three-dose mRNA-1273 vaccination series, according to the Dutch National Institute for Public Health and the Environment (RIVM) guidelines. SARS-CoV-2-naïve patients were randomly selected from each cohort, with SARS-CoV-2-naïve defined as spike protein S1 subunit (S1) immunoglobulin G (IgG) concentration <10 binding antibody units (BAU)/mL before vaccination, nucleocapsid (N) antibodies <14.3 BAU/mL in all measurements, and absence of patient-reported SARS-CoV-2 infection. Patients were compared to healthy individuals matched on age, type and number of vaccinations. For T cell assays, these were healthy participants of the RECOVAC study (NCT04741386), or healthcare workers from Erasmus MC (MEC 2020 0264). For spike-specific antibody concentrations, data from healthy participants from the PIENTER Corona (PICO) cohort (Clinical Trial Registration TR8473) were used. All participants involved provided written informed consent.

*[1]All patients were female or male. *[2]Patients received HMA as monotherapy, one patient also received venetoclax. WHO PS = World Health Organization Performance Status. BEAM = carmustine-etoposide-cytarabine-melphalan. HDM = high dose melphalan. CAR = chimeric antigen receptor. BTKi = Bruton's tyrosine kinase inhibitor. VTD = bortezomib-thalidomide-dexamethasone. HCT = hematopoietic cell transplantation. MDS = myelodysplastic syndrome. BEAM = carmustine-etoposide-cytarabine-melphalan.

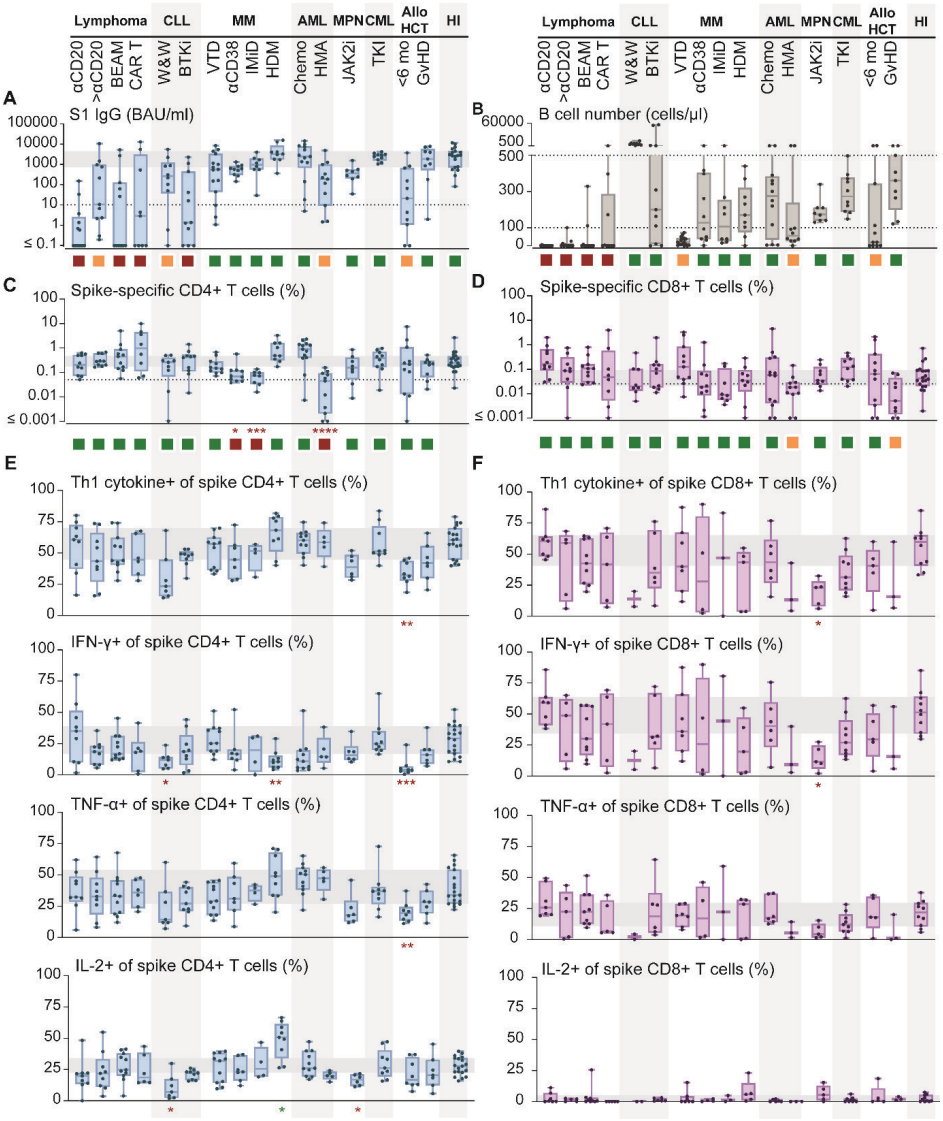

Figure 1 Vaccination-induced spike-specific antibody and T cell responses in patients with hematologic malignancies

Before and four weeks after each mRNA-1273 vaccination, serum and PBMCs were collected to measure antibodies and T cells. **A**) S1 IgG antibody concentrations after two SARS-CoV-2 mRNA vaccinations, categorized as no seroconversion (red; median S1 IgG <10 BAU/mL), low concentration (orange; median S1 IgG 10-300 BAU/mL), or adequate concentration (green; median S1 IgG >300 BAU/mL). Dotted line indicates seroconversion threshold. S1 IgG >300 BAU/mL was considered an adequate antibody response against the ancestral SARS-CoV-2, since this IgG concentration corresponded with a 50% plaque reduction neutralization titer of 40 or higher in two independent prospective Dutch mRNA-1273 vaccination cohorts. Concentrations of S1 and N IgG were quantified in BAU/mL according to the WHO International Standard for COVID-19 serological tests. **B**) Number of B cells per microliter blood at start of vaccination (baseline). Dotted lines indicate range in healthy individuals (100-500 cells/

microliter blood). Squares indicate categorization of the cohorts based on the median. Cohorts with a median value below the arbitrary threshold of 10 cells/microliter are depicted as red, with a median between 10 and 100 are depicted as orange, and with a median above 100 as green. **C-D**) Frequency of spike-specific CD4+ or CD8+ T cells after two SARS-CoV-2 mRNA vaccinations as determined by activation-induced marker (AIM) assay and, for CD8+ T cells, in combination with peptide-HLA tetramer staining. For the AIM assay, 2 million thawed PBMCs were incubated with 15-mer spike peptides (SB peptide, France), DMSO negative control, or a CMV, EBV, Flu and extra (CEFX) peptide pool (JPT). After 1 hour, brefeldin A was added. All time points of one patient were measured simultaneously to minimize technical variance within one patient. Patients were measured and analyzed in random order across cohorts to minimize technical variance and bias between cohorts. 15 hours after adding brefeldin A, cells were stained for viability, fixated, permeabilized and incubated with antibodies directed against CD3, CD4, CD8, CD154, CD137, CD69, IFN-γ, TNF-α, IL-2, IL-4, IL-17, PD-1, FOXP3 and CXCR5. In parallel, PBMCs were incubated with a viability dye, peptide-HLA tetramers and antibodies directed against CD4, CD8, CCR7 and CD45RA. Dotted lines indicate response positivity threshold (0.05% for CD4+, 0.025% for CD8+). **E-F**) Frequency of spike-specific CD4+ (E) or CD8+ (F) T cells that produce IFN-γ, TNF-α and/or IL-2. Th1 cytokine-positive frequency was calculated by subtracting the frequency of cells that do not produce any of these cytokines from 100%. For all panels, grey horizontal area corresponds to interquartile range in healthy individuals. T cell frequencies from each cohort are compared to those in HI by Mann-Whitney U tests and significance corrected for multiple testing (times 16) is shown (ns: $p>0.05$; *: $p\leq0.05$; **: $p\leq0.01$; ***: $p\leq0.001$; ****: $p\leq0.0001$). Squares indicate categorization of the T cell responses based on p-value prior to and after correction for multiple testing (green when not significantly lower prior to correction; orange when significantly lower before, but not after correction; red when significantly lower after correction). αCD20 = during anti-CD20 therapy, > αCD20 = within 12 months after anti-CD20 therapy, BEAM = BEAM-autologous HCT within 12 months, CAR T = CD19 CAR T cell therapy, CLL = chronic lymphocytic leukemia, W&W = watch and wait, BTKi = ibrutinib, MM = multiple myeloma, VTD = induction therapy, αCD38 = daratumumab, IMiD = immunomodulatory drugs, HDM = HDM-autologous HCT within 9 months, AML = acute myeloid leukemia and high-risk MDS, chemo = high-dose chemotherapy, HMA = hypomethylating agents, MPN = myeloproliferative neoplasms, JAK2i = ruxolitinib, CML = chronic myeloid leukemia, TKI = tyrosine kinase inhibitors, alloHCT = allogeneic hematopoietic cell transplantation, GvHD = chronic graft-versus-host disease, HI = healthy individuals.

Generally, SARS-CoV-2 mRNA vaccination induced S1 IgG concentrations similar to HI in most patients except for patients that were B-cell depleted (**Figure 1A-B**). Spike-specific CD4+ and CD8+ T cells increased upon each vaccination, whilst other T cell specificities (CEFX; CMV, EBV, flu and more) remained constant in time (**Figure S3-7**). As antigen-specific CD8+ T cells are challenging to detect, we performed activation-induced marker assays and peptide-HLA tetramer staining. Both methods correlated closely and were combined for further analysis (**Figure S28**). Most patients developed spike-specific CD4+ (85%) and CD8+ (65%) T cell frequencies including Th1 cytokine production comparable to HI after the second vaccination (**Figure 1C-F**). Control CEFX-specific CD4+ and CD8+ T cell responses including Th1 cytokine production were comparable to HI in most cohorts (**Figure S9**). Interestingly, patients with reduced antibody concentrations mostly did not have reduced T cell frequencies, although antibody concentration and CD4+ T cell frequency did positively correlate (**Figure 1A-D, S310A**). Furthermore, reduced absolute T cell numbers or lower percentage of naïve T cells at baseline were not associated with reduced spike-specific CD4+ or CD8+ T cell frequencies (**Figure 1C-D, 2B-C, S310B-E**). Although counterintuitive,

it demonstrates that limited baseline naïve T cell frequencies could proliferate to adequate spike-specific frequencies. Since low numbers of circulating T cells can bias spike-specific frequencies, we calculated the absolute number of circulating spike-specific T cells per microliter blood, which showed comparable results (**Figure 2D**).

Figure 2 Baseline parameters, number of spike-specific T cells, and integrated analysis of cellular and humoral immune responses

A) Categorization of spike-specific CD4+ or CD8+ T cell frequencies as shown in figure 1. **B**) CD4+ or CD8+ T cell numbers directly measured in blood as cells per microliter. Absolute numbers of lymphocyte subsets were determined using fresh whole EDTA blood with Multitest 6-color reagents (BD Biosciences, San Jose, California) according to the manufacturer's instructions. The dotted lines indicate the clinically-accepted normal ranges in healthy individuals. **C**) Frequency of naïve (CCR7+CD45RA+) CD4+ or CD8+ T cells. Grey horizontal area corresponds to interquartile range in healthy individuals. **D**) Number of spike-specific CD4+ or CD8+ T cells in peripheral blood, calculated by multiplying the percentage of spike-specific T cells by the number of T cells in peripheral blood. **E**) Categorization of mRNA vaccine-induced B and T cell immune responses, and number of circulating B cells at start of vaccination per cohort. Categorization was based on median (S1 IgG), clinically accepted threshold (B cells), or statistics (T cell responses). T cell responses are categorized based on significance before and after correction for multiple testing (green when not significantly lower before correction; orange when significantly lower before, but not after correction; red when significantly lower after correction). Categorization of cytokine-producing spike-specific CD8+ T cells frequencies is not depicted due to limited availability of data points. **F**) Summary heatmap of the data gathered from six variables of all cohorts, generated using RStudio (R-4.3.0, packages: circlize-0.4.15, ComplexHeatmap-2.15.4). Each vertical line represents the same individual. However, S1 IgG concentrations were obtained from an independent HI cohort (blue box), therefore, the vertical lines of the S1 IgG in HI do not represent the same vertical lines as the HI cohort of the T cell data. Values are color-coded by relative abundance within each variable. The minimum value (red) was set to zero, the maximum (dark green) to the highest measured value, and the median (light green) to the median value in healthy individuals. B cells were not measured in healthy individuals and therefore the light-green median is set to the clinically-accepted minimal normal value of 100 cells/μL. Unavailable data are shown as white-colored bars. Cytokine+ frequency of spike CD4/8+ indicates frequency of spike-specific CD4/8+ T cells that produce IFN-γ, TNF-α and/or IL-2.

αCD20 = during anti-CD20 therapy, > αCD20 = within 12 months after anti-CD20 therapy, BEAM = BEAM-autologous HCT within 12 months, CAR T = CD19 CAR T cell therapy, CLL = chronic lymphocytic leukemia, W&W = watch and wait, BTKi = ibrutinib, MM = multiple myeloma, VTD = induction therapy, αCD38 = daratumumab, IMiD = immunomodulatory drugs, HDM = HDM-autologous HCT within 9 months, AML = acute myeloid leukemia and high-risk MDS, chemo = high-dose chemotherapy, HMA = hypomethylating agents, MPN = myeloproliferative neoplasms, JAK2i = ruxolitinib, CML = chronic myeloid leukemia, TKI = tyrosine kinase inhibitors, alloHCT = allogeneic hematopoietic cell transplantation, GvHD = chronic graft-versus-host disease, HI = healthy individuals.

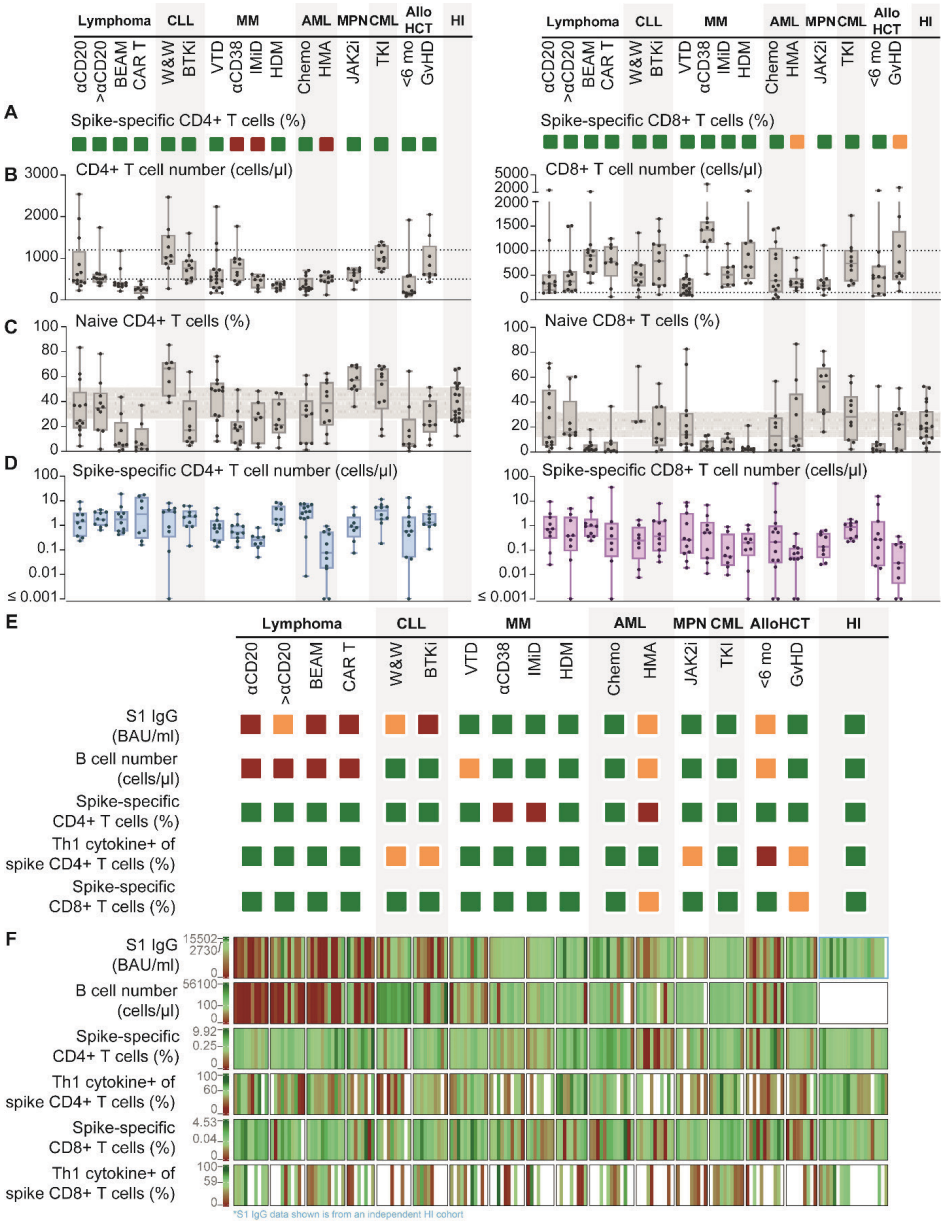
Lymphoma
CLL
MM
AML
MPN
CML
Allo HCT
HI
αCD20
>αCD20
BEAM
CAR T
W&W
BTKi
VTD
αCD38
IMiD
HDM
Chemo
HMA
JAK2i
TKI
<6 mo
GvHD
A
Spike-specific CD4+ T cells (%)
Spike-specific CD8+ T cells (%)
B
CD4+ T cell number (cells/µl)
CD8+ T cell number (cells/µl)
C
Naive CD4+ T cells (%)
Naive CD8+ T cells (%)
D
Spike-specific CD4+ T cell number (cells/µl)
Spike-specific CD8+ T cell number (cells/µl)
≤ 0.001
E
S1 IgG (BAU/ml)
B cell number (cells/µl)
Spike-specific CD4+ T cells (%)
Th1 cytokine+ of spike CD4+ T cells (%)
Spike-specific CD8+ T cells (%)
F
S1 IgG (BAU/ml)
B cell number (cells/µl)
Spike-specific CD4+ T cells (%)
Th1 cytokine+ of spike CD4+ T cells (%)
Spike-specific CD8+ T cells (%)
Th1 cytokine+ of spike CD8+ T cells (%)
*S1 IgG data shown is from an independent HI cohort

Analyzing the cohorts separately, the median S1 IgG concentration was <300 BAU/mL in patients with lymphoma receiving B-cell depleting therapy, patients with chronic lymphocytic leukemia (CLL), patients treated with HMA for acute myeloid leukemia (AML) or myelodysplastic syndrome (MDS), and patients who had received allogeneic hematopoietic cell transplantation (alloHCT) <6 months before vaccination (**Figure 1A**). Despite the absence or low seroconversion, patients in the lymphoma groups had adequate spike-specific T cell responses, as described previously (**Figure 1C-D**).[4, 5] These cohorts included patients on active anti-CD20 therapy, shortly after anti-CD20 therapy, post BEAM-autologous HCT (autoHCT) or after chimeric antigen receptor (CAR) T cell therapy (**Table 1**). These T cell responses may explain our previous observation that vaccination in B cell-depleted patients was associated with rapid antibody maturation in future humoral responses once B cells are reconstituted.[6] Patients with untreated (watch&wait; W&W) CLL or treated with BTK inhibitors (BKTi) also showed spike-specific CD4+ and CD8+ T cell frequencies comparable to HI, which is in contrast to other reports and could be related to vaccine type.[7, 8] In patients treated with BTKi, S1 IgG concentrations were lower compared to patients with untreated CLL, possibly related to impairment of non-malignant B cells induced by BTKi.[9] Furthermore, spike-specific CD4+ T cells showed significantly lower production of IFN-γ and IL-2 compared to HI, which was partially reversed in CLL-depleted samples (**Figure 1E, S11**). In patients with multiple myeloma treated with induction therapy (VTD), daratumumab (α-CD38), immune modulatory drugs (IMiD) or high-dose melphalan (HDM) humoral and cellular spike-specific immune responses were generally detected. However, S1 IgG concentrations were reduced in patients treated with daratumumab, probably caused by depletion of plasma cells by daratumumab. Patients treated with daratumumab or IMiD had reduced spike-specific CD4+ T cell frequencies compared to HI. Interestingly, patients treated with HDM demonstrated a skewing towards IL-2- and TNF-α-producing CD4+ T cells with reduced IFN-γ production, indicating a change in cytokine profile. Patients with AML/MDS treated with HMA had both low S1 IgG concentrations and low frequencies of spike-specific CD4+ and CD8+ T cells which is consistent with previous reports of impaired vaccine responses in patients with AML/MDS.[10] The observation that patients with AML receiving high-dose chemotherapy were able to generate immune responses comparable to HI suggests that the therapy, rather than disease, hampered the vaccination responses. Since HMA preferentially targets replicating cells, it may suppress active, vaccine-induced T cells rather than resting T cells.[11] Indeed, CEFX-specific T cells were unaffected (**Figure S39**). Notably, the reduced immune responses may also be related to the higher median age of patients in the HMA cohort. Patients with MPN, including chronic myeloid leukemia (CML), showed humoral- and T cell responses similar to HI. However, patients with MPN treated with JAK2-inhibitors

demonstrated a lower frequency of IL-2-producing spike-specific CD4+ T cells and IFN-γ-producing spike-specific CD8+ T cells (**Figure 1E-F**). CEFX-specific CD8+ T cells showed a similar trend (**Figure S9D**). Patients who underwent alloHCT <6 months before vaccination had variable S1 IgG levels and spike-specific CD4+ T cell frequencies, and production of IFN-γ and TNF-α by the CD4+ T cells was reduced. Others have suggested that impaired mRNA vaccination-induced T cell responses after alloHCT could be related to corticosteroid use.[12] Patients that had developed chronic graft-versus-host-disease (cGvHD) after alloHCT tended to have reduced spike-specific CD8+ T cell frequencies compared to HI, while this was not observed for antibody concentrations and spike-specific CD4+ T cell frequencies. In patients who were vaccinated shortly after autologous (autoHCT), spike-specific antibodies (HDM) and T cell frequencies (BEAM and HDM) were comparable to HI.

Since cellular therapy can affect T cell counts and function, we investigated the correlation between time since therapy and spike-specific CD4+ T cell frequencies. The frequency of spike-specific CD4+ T cells was negatively correlated with time since CAR T cell therapy (**Figure S12A**). This correlation, although not significant, was also observed when calculating the absolute number of spike-specific CD4+ T cells (**Figure S12B**). Patients treated with alloHCT within 6 months before vaccination had variable S1 IgG levels and spike-specific CD4+ T cell frequencies, which did not correlate with time since alloHCT (**Figure S12C**).

The SARS-CoV-2 mRNA vaccines are designed to especially induce Th1 responses, indeed, IL-4 or IL-17 was not produced by spike-specific CD4+ T cells (**Figure 13**). Frequencies of circulating spike-specific follicular helper T cells (Tfh; PD-1+CXCR5+) were significantly increased in patients with lymphoma shortly after anti-CD20 therapy and in patients with multiple myeloma treated with VTD (**Figure S14A**). Frequencies of FOXP3+CD4+ T cells at the start of vaccination were low for all cohorts, yet in patients with MM who had received HDM, significantly increased frequencies were detected (**Figure S14B**).

A third vaccination significantly increased S1 IgG concentrations and frequencies of spike-specific T cells but the T cell frequencies of non-responders remained low (**Figure S20A-D**).[13] Seven patients received an auto-HCT between the second and third vaccination. Frequencies of spike-specific CD4+ T cells in these patients increased further after the third vaccination, suggesting that pre-existing immunity was not fully eliminated by autoHCT (**Figure S20E**). A similar pattern was observed for humoral responses in these patients.[13]

This study showed that humoral and cellular immune responses to SARS-CoV-2 vaccination, summarized per cohort (**Figure 2E**) or per individual (**Figure 2F**), were differently affected depending on the hematological malignancy and treatment. A limitation of our study is the small size per cohort, which especially applies to the cohorts where heterogeneous responses were found. Yet our results depict some patient cohorts that may respond inadequately to mRNA vaccination which warrants further research. Importantly, it remains to be determined to what extent humoral and cellular responses correlate to protection against severe disease. A large, population-based COVID-19 outcome study, including patients with comparable immunodeficiency states, is ongoing and may identify cohorts that are more susceptible to severe disease.[14] Both studies combined may provide further insight in the contribution of each component of the immune system in the protection against severe COVID-19. In conclusion, most patients with hematologic malignancies receiving immunosuppressive therapies generated antibody and/or T cell responses after two-dose SARS-CoV-2 mRNA vaccination. While all study participants were considered immunodeficient, the combination of reduced cellular and humoral SARS-CoV-2-specific immune responses was rare. These findings emphasize the potential of mRNA vaccines in generating humoral and cellular immune responses in patients with hematologic malignancies.

ACKNOWLEDGEMENTS

The authors are greatly indebted to the patients who participated in the study. The authors would also like to thank the COBRA KAI study team, staff of Leiden UMC (LUMC), Amsterdam UMC (AMC), Erasmus MC (EMC), UMC Groningen (UMCG), Dutch National Institute for Public Health and the Environment (RIVM), and the Netherlands Comprehensive Cancer Organization (IKNL) for their help with patient inclusion and data collection. The COBRA KAI study team includes Iris M.J. Kant, Thecla Graas, Belle Toussaint, Sterre de Jong, Shahan Darwesh, Sandjiv S. Mahes, Dora Kamminga, Matthijs Koelewijn, Gino Faber, Guus Beaumont, Marije D. Engel, R. Cheyenne N. Pierie, Suzanne R. Janssen, Kazimierz Groen, Judith A. Burger, Joey H. Bouhuijs, Paul A. Baars, Marit J. van Gils, Edith van Dijkman, Jarom Heijmans, Yara Y. Witte, Rogers A. Nahui Palomino, Said Z. Omar, Sonja Zweegman, Caya van den Vegt, Ilonka Arends-Halbesma, Emma de Pater, Margriet J. Dijkstra, Nynke Y. Rots, Esther Siteur-van Rijnstra, Dennis M. de Rooij, Rogier W. Sanders, Meliawati Poniman, Wouter Olijhoek, Jacqueline van Rijswijk, Tim Beaumont, Lusia Çetinel, Louis Schellekens, Yvonne M. den Hartogh, Jacqueline Cloos, Suzanne S. Weijers, Saïda Tonouh-Aajoud, Selime Avci, Elianne Roelandse-Koop, and Willem A. Dik. Flow cytometry was performed at

the Flow cytometry Core Facility (FCF) of Leiden University Medical Center (LUMC) in Leiden, Netherlands (https://www.lumc.nl/research/facilities/fcf). The COBRA KAI study is funded by ZonMW.

STUDY REGISTRATION

EudraCT 2021-001072-41

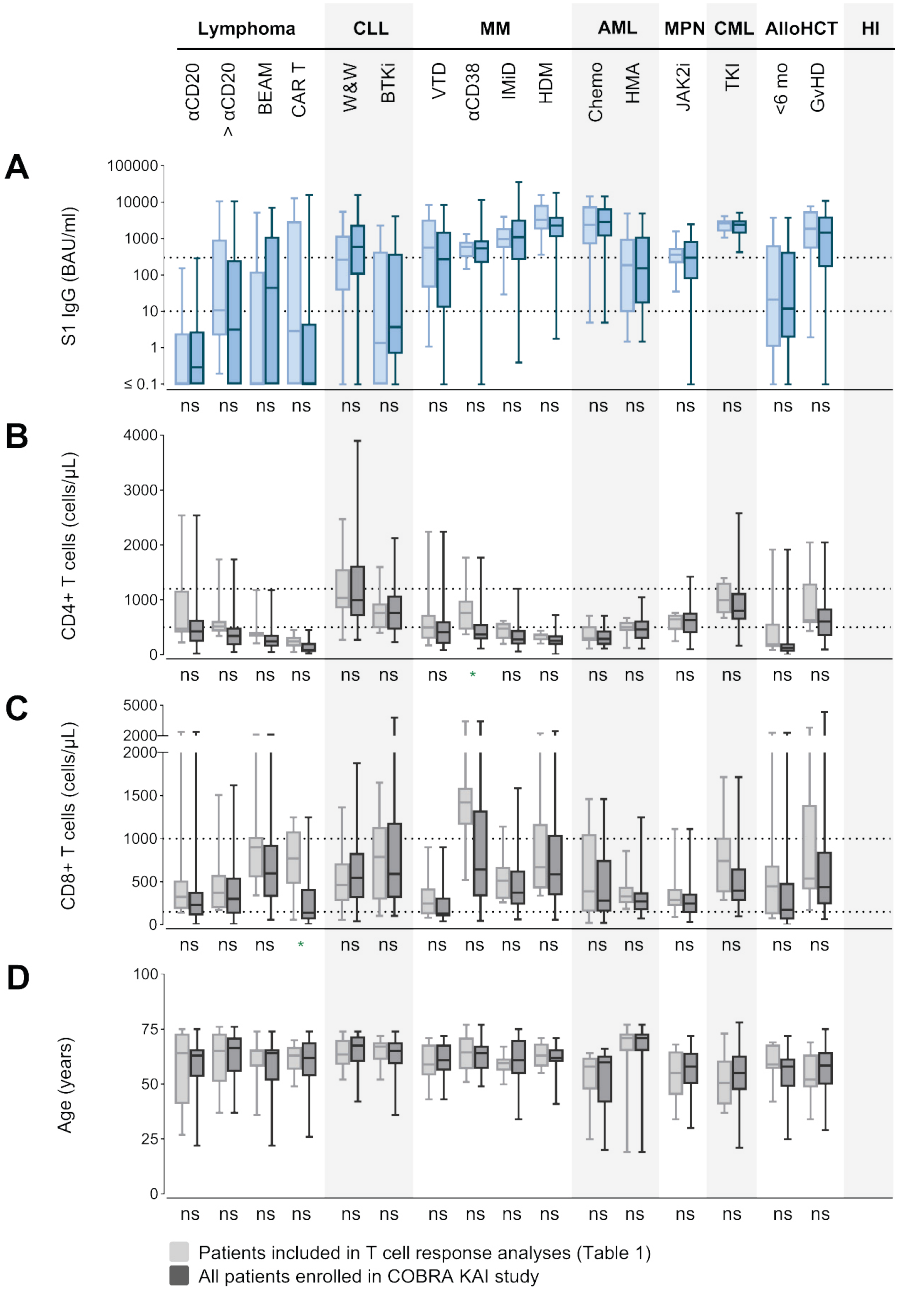

Supplementary figure 1 Clinical characteristics of patients included in T cell analyses in relation to full COBRA KAI study cohorts.

A) S1 IgG concentrations following the second mRNA vaccination. B) Number of CD4+ T cells per microliter blood. C) Number of CD8+ T cells per microliter blood. D) Age of the patients at start of vaccination. In A-D, values are compared to those in HI by Mann-Whitney U tests and significance corrected for multiple testing (times 16) is shown (ns: p>0.05; *: p≤0.05; **: p≤0.01; ***: p≤0.001; ****: p≤0.0001).

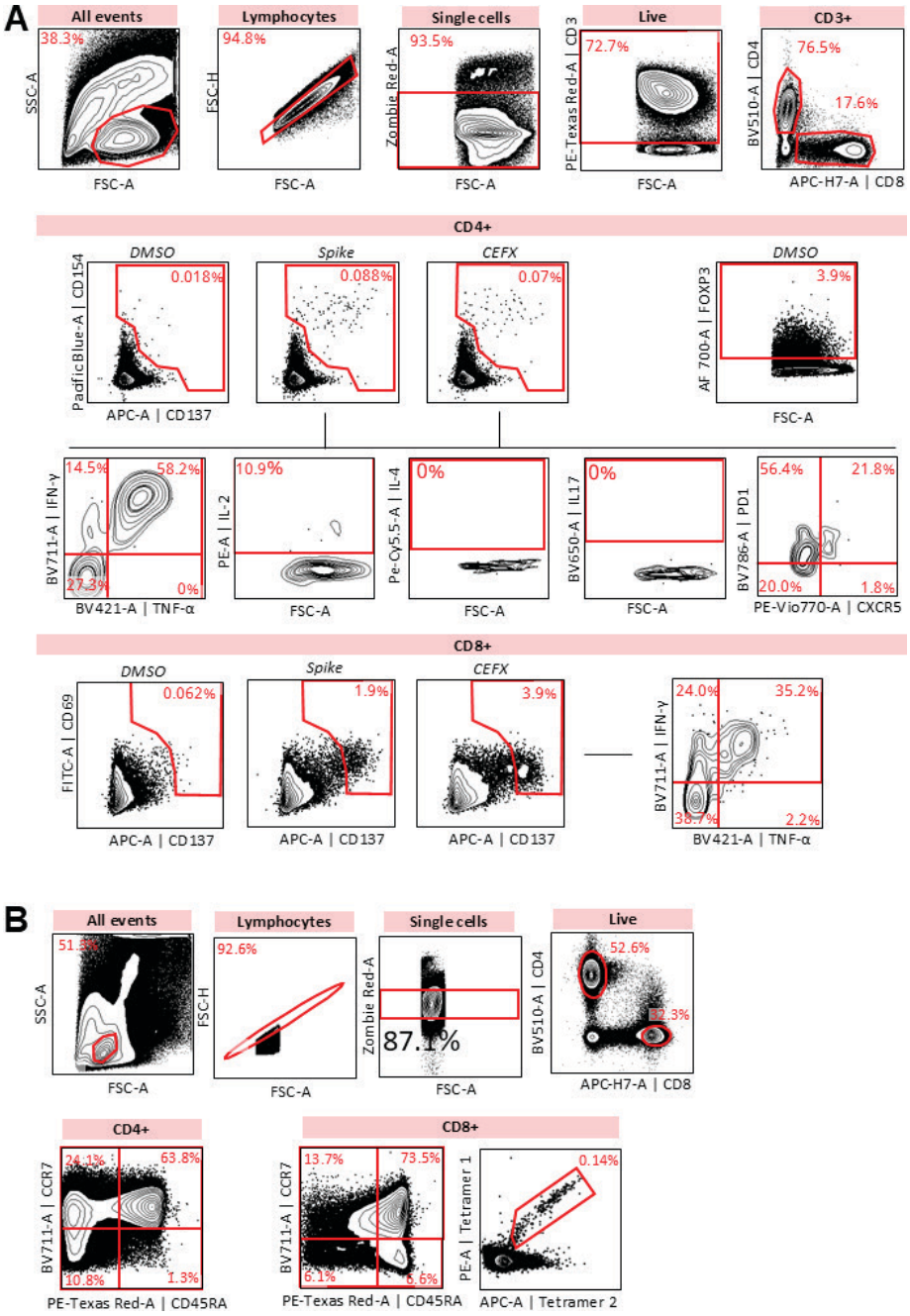

Supplementary figure 2 Flow cytometry gating example for the detection of antigen-specific T cells

Supplementary figure 2 *Continued*

A) Representative example of flow cytometry gating strategy for antigen-reactive CD4+ and CD8+ T cells. Samples were measured on a three-laser Aurora (Cytek Biosciences) and analyzed using OMIQ (www.omiq.ai). All events were gated on lymphocytes, single cells, viable cells, CD3-positive, and either CD4- or CD8-positive. Only samples with more than 5,000 events in the CD4+ or CD8+ gates were analyzed. Activation was measured by upregulation of CD137 and CD154 by CD4+ T cells and CD137 and CD69 by CD8+ T cells, compared to DMSO. Response positivity thresholds were set at 0.05% for CD4+ T cells and 0.025% for CD8+ T cells based on results of an independent previous healthy cohort. Analysis of cytokine-producing spike-specific cells (IFN-γ, TNF-α, IL-2, IL-4, IL-17) and spike-specific Tfh cells (CD4+CXCR5+PD-1+) was only performed if the response positivity threshold was met and more than 25 events were measured in the CD154+/CD137+ gate for CD4+ T cells and in the CD137+CD69+ gate for CD8+ T cells. FOXP3+ cells were gated within total CD4+ T cell population in DMSO condition. B) Representative example of flow cytometry gating strategy for differentiation status of CD4+ and CD8+ T cells and for spike-specific CD8+ T cells using peptide- HLA tetramer technology. In addition to peptide-stimulation, 2 million unstimulated PBMCs were stained with a fixed pool of peptide-HLA tetramers to detect spike-specific CD8+ T cells. The tetramers consist of 23 peptides that were previously reported spike epitopes with strong (predicted) binding to 8 HLA-types common in The Netherlands. Tetramer staining was combined with antibodies directed against CD4, CCR7, and CD45RA followed by anti-CD8 staining. Samples were measured on a three-laser Aurora (Cytek Biosciences) and analyzed using OMIQ (www.omiq.ai). Only samples with more than 5,000 events in the CD4+ or CD8+ gates were analyzed, whilst 10,000 events were required in the CD8+ gate for the frequency of peptide-HLA tetramer-binding cells. All events were gated on lymphocytes, single cells, viable cells and CD4- or CD8-positive. Subsequently, the percentage of CD4+ or CD8+ T cells that express CCR7/CD45RA was determined. CD8+ T cells were gated on double positive tetramer binding for the detection of spike-specific CD8+ T cells.

Supplementary figure 3 Kinetics of spike-specific CD4+ T cell frequencies before and during the three-dose vaccination schedule

PBMC isolated prior to vaccination (Pre), four weeks after first vaccination (1st), four weeks after second vaccination (2nd) and four weeks after third vaccination (3rd) were incubated with SARS-CoV-2 spike peptide pool. Frequencies of CD4+ T cells positive for CD154 or CD137, corrected for DMSO, were plotted over time. Dotted line indicates response positivity threshold (0.05%). Each line represents one individual (ns: $p>0.05$; *: $p\leq0.05$; **: $p\leq0.01$; ***: $p\leq0.001$; ****: $p\leq0.0001$).

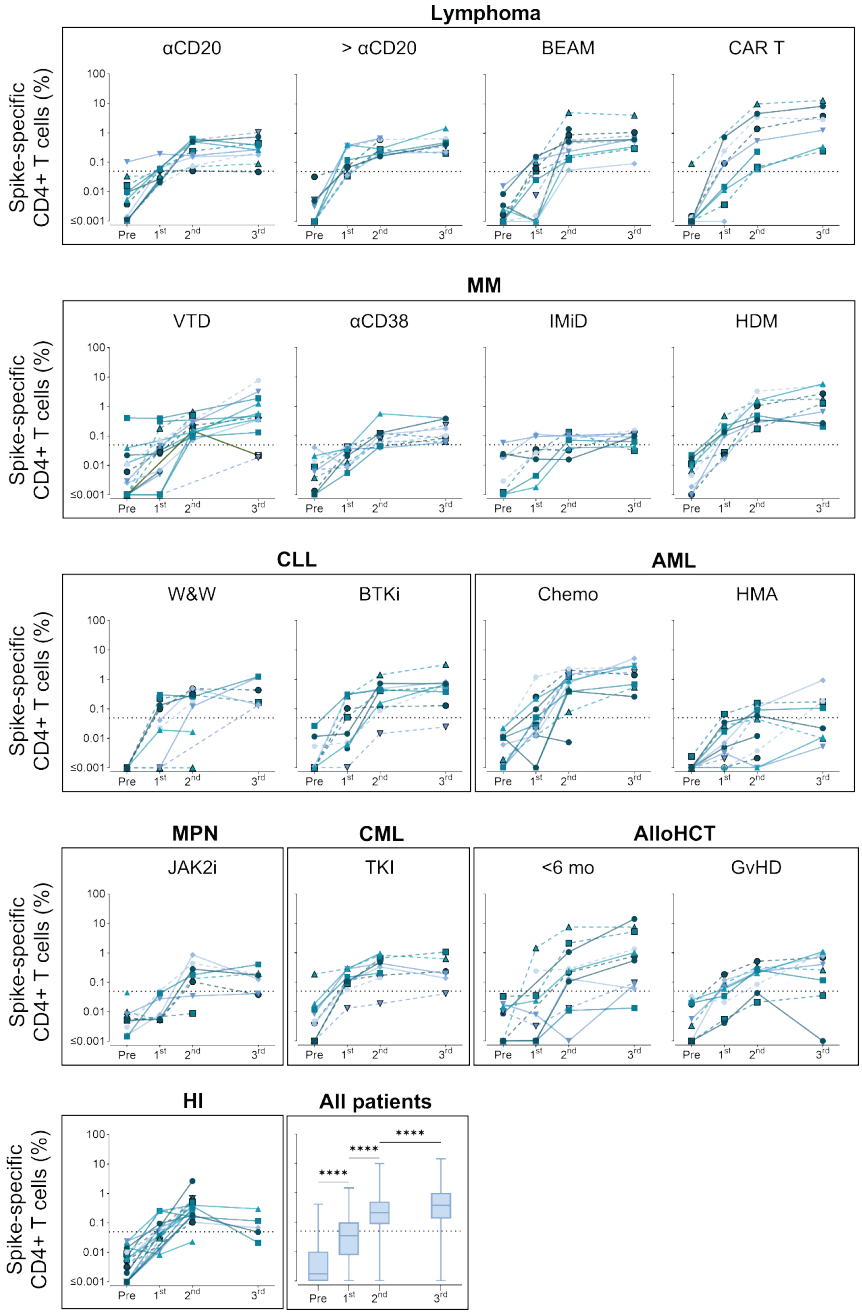
Lymphoma
αCD20
> αCD20
BEAM
CAR T
MM
VTD
αCD38
IMiD
HDM
CLL
W&W
BTKi
AML
Chemo
HMA
MPN
JAK2i
CML
TKI
AlloHCT
<6 mo
GvHD
HI
All patients
Spike-specific CD4+ T cells (%)
100
10
1
0.1
0.01
≤0.001
Pre
1st
2nd
3rd
****

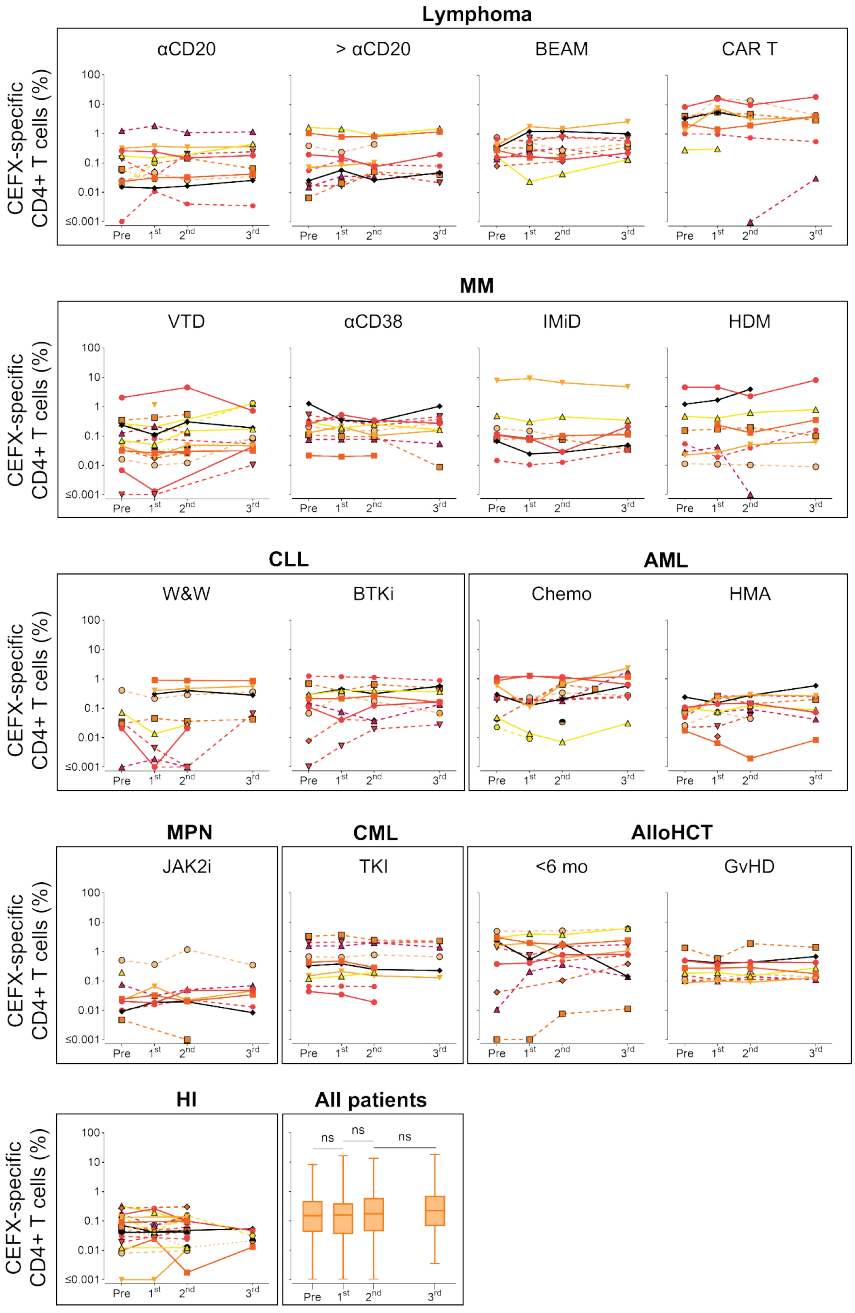

Supplementary figure 4 Kinetics of CEFX-specific CD4+ T cell frequencies before and during the three-dose vaccination schedule

PBMC isolated prior to vaccination (Pre), four weeks after first vaccination (1st), four weeks after second vaccination (2nd) and four weeks after third vaccination (3rd) were incubated with a CEFX peptide pool. Frequencies of CD4+ T cells positive for CD154 or CD137, corrected for DMSO, were plotted over time. Each line represents one individual (ns: p>0.055).

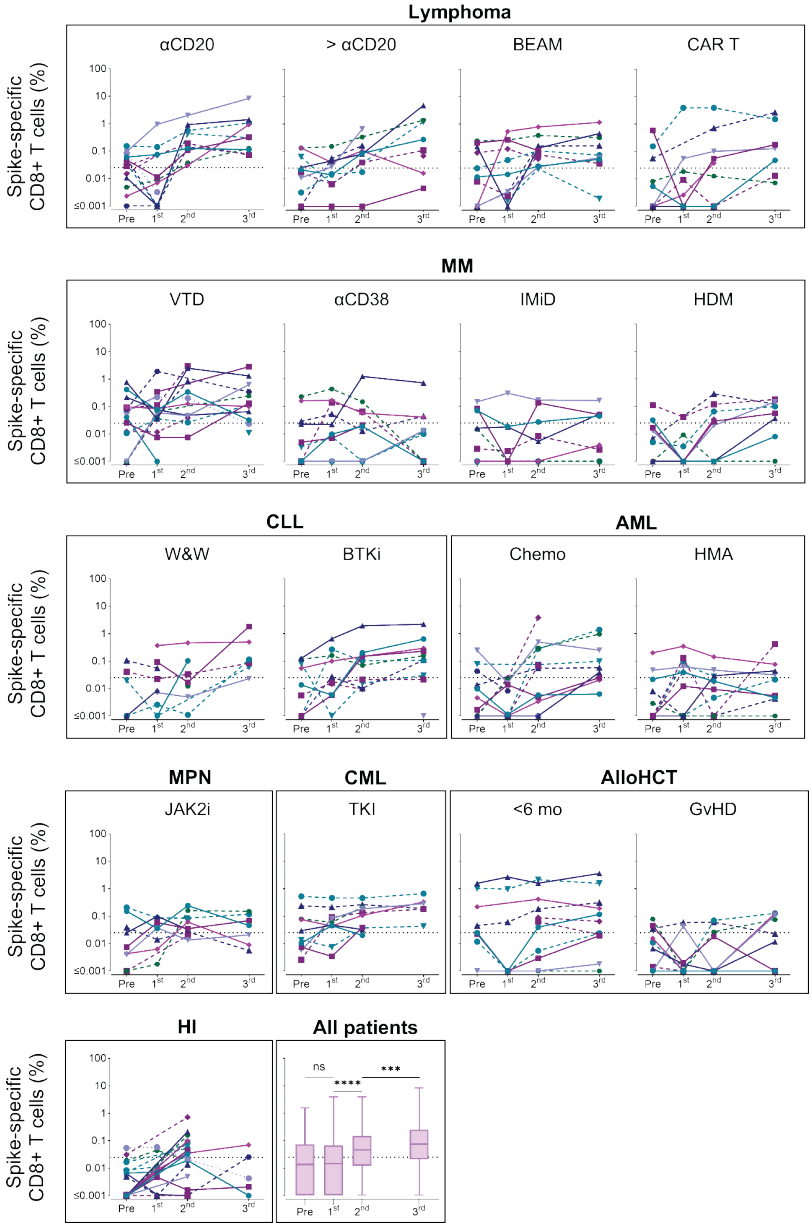

Supplementary figure 5 Kinetics of spike-specific CD8+ T cell frequencies before and during the three-dose vaccination schedule, determined by AIM

PBMC isolated prior to vaccination (Pre), four weeks after first vaccination (1st), four weeks after second vaccination (2nd) and four weeks after third vaccination (3rd) were incubated with SARS-CoV-2 spike peptide pool. Frequencies of CD8+ T cells positive for CD137 and CD69, corrected for DMSO, were plotted over time. Dotted line indicates response positivity threshold (0.025%). Each line represents one individual. Bottom right figure shows data points of all patients combined. Difference in frequency after each vaccination was tested by a Wilcoxon matched-pairs Signed-Rank test (ns: $p>0.05$; *: $p\leq0.05$; **: $p\leq0.01$; ***: $p\leq0.001$; ****: $p\leq0.0001$).

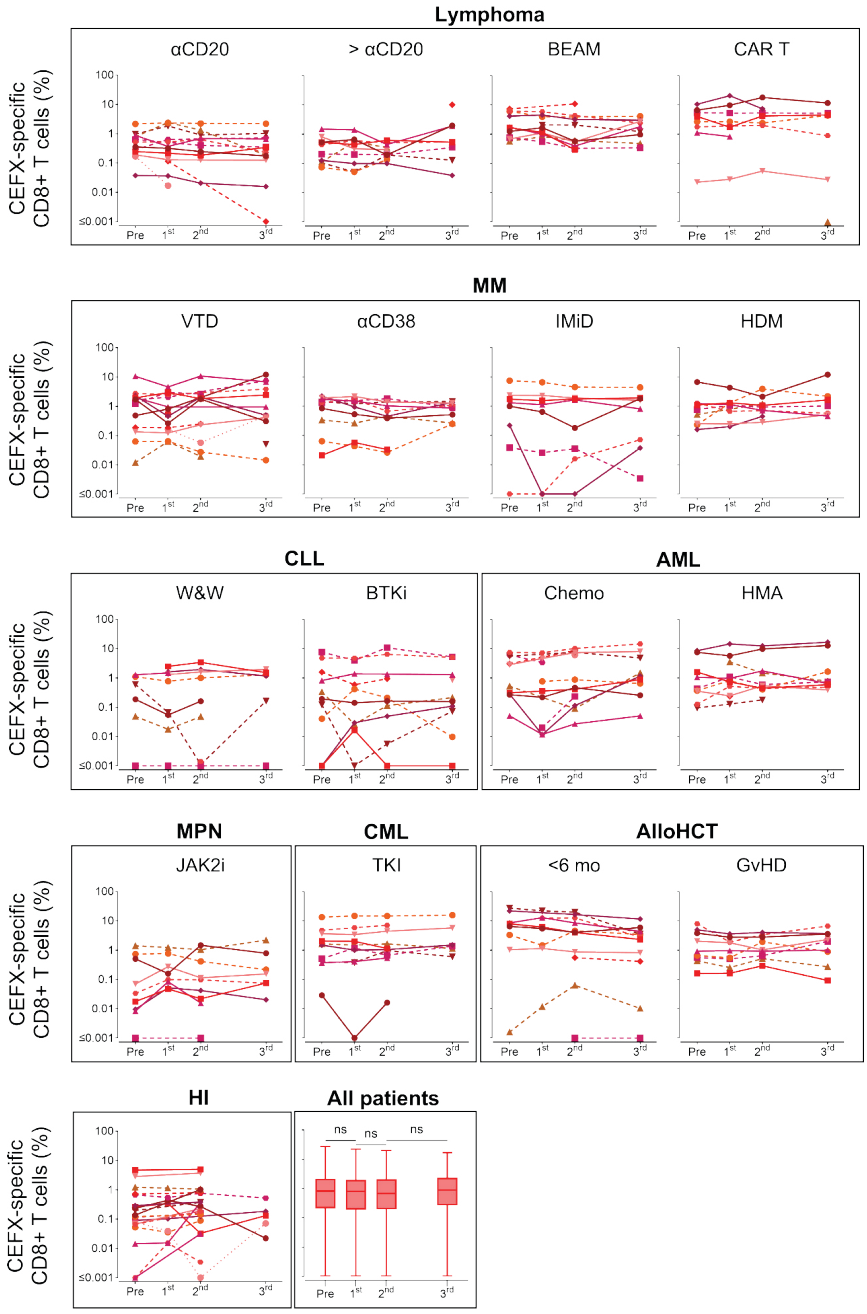

Supplementary figure 6 Kinetics of CEFX-specific CD8+ T cell frequencies before and during the three-dose vaccination schedule

PBMC isolated prior to vaccination (Pre), four weeks after first vaccination (1st), four weeks after second vaccination (2nd) and four weeks after third vaccination (3rd) were incubated with a CEFX peptide pool. Frequencies of CD8+ T cells positive for CD137 and CD69, corrected for DMSO, were plotted over time. Each line represents one individual. Difference in frequency after each vaccination was tested by a Wilcoxon matched-pairs Signed-Rank test (ns: $p>0.05$; *: $p\leq0.05$; **: $p\leq0.01$; ***: $p\leq0.001$; ****: $p\leq0.0001$).

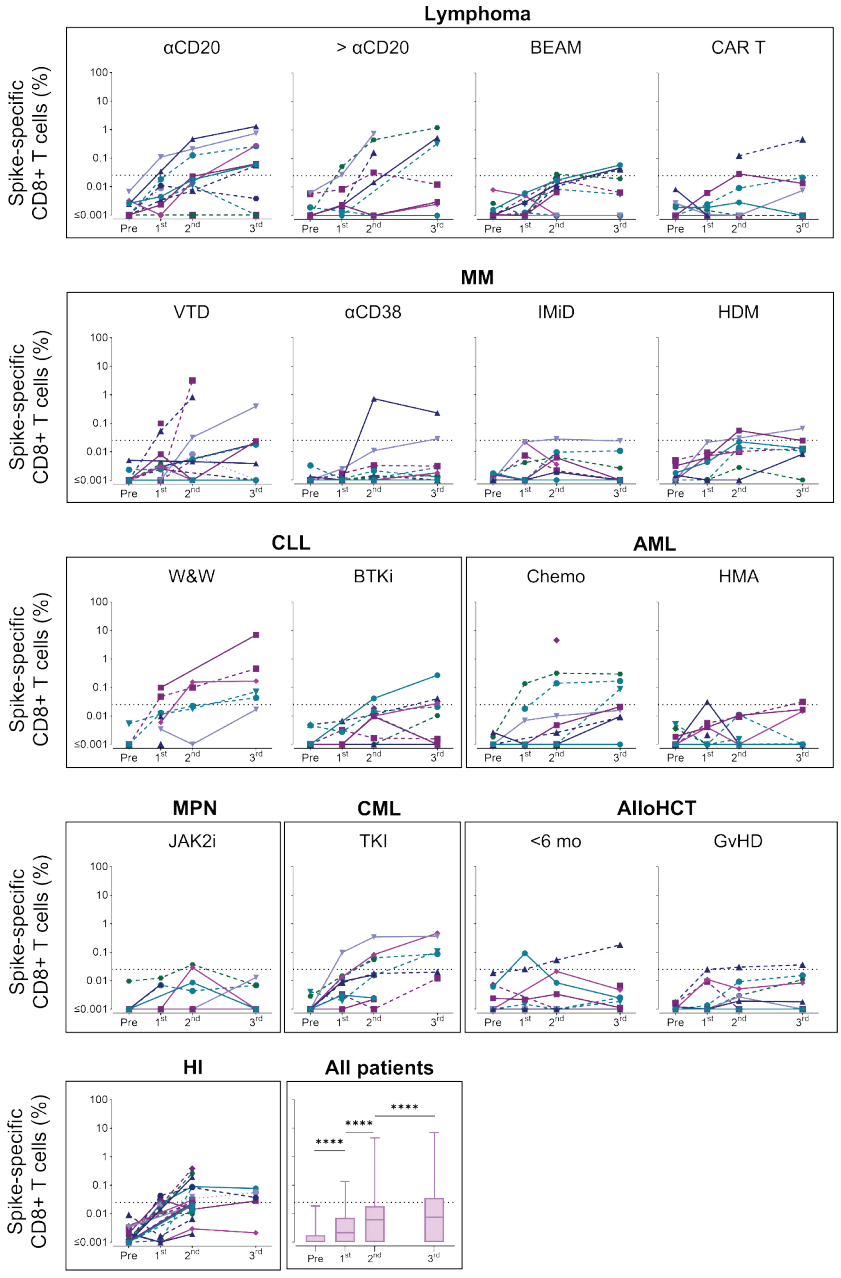

Supplementary figure 7 Supplementary figure 10: Kinetics of spike-specific CD8+ T cell frequencies before and during the three-dose vaccination schedule, determined by peptide-HLA tetramer technology PBMC isolated prior to vaccination (Pre), 4 weeks after first vaccination (1st), 4 weeks after second vaccination (2nd) and 4 weeks after

Supplementary figure 7 *Continued*

third vaccination (3rd) were incubated with peptide-HLA tetramers containing SARS-CoV-2 spike peptides bound to common HLA-types. Frequency of CD8+ T cells that bound to the tetramers were plotted over time. Dotted line indicates response positivity threshold (0.025%). Each line represents one individual. Difference in frequency after each vaccination was tested by a Wilcoxon matched-pairs Signed-Rank test (ns: p>0.05; *: p≤0.05; **: p≤0.01; ***: p≤0.001; ****: p≤0.0001).

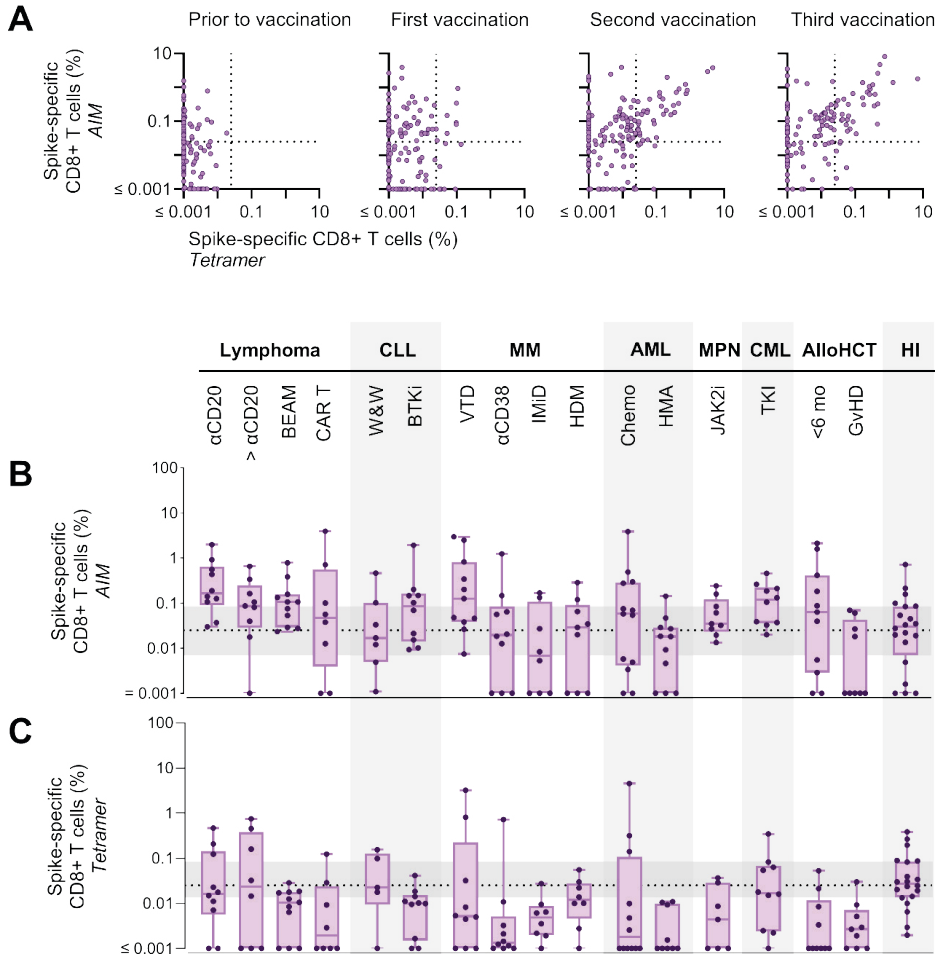

Supplementary figure 8 Supplementary figure 8: Detection of spike-specific CD8+ T cells through peptide-stimulation assays and peptide-HLA tetramer staining

A) Frequency of spike-specific CD8+ T cells measured by activation induced markers (AIM) plotted against frequency of spike-specific CD8+ T cells measured by peptide-HLA tetramer technology. Spike-specific CD8+ T cell frequencies are shown before vaccination and four weeks after the first, second, and third mRNA vaccine dose. B) Frequency of spike-specific CD8+ T cells measured by AIM assay four weeks after the second mRNA vaccination. C) Frequency of spike-specific CD8+ T cells measured by peptide-HLA tetramer technology four weeks after the second mRNA vaccination. In B and C, horizontal grey area shows interquartile range of HI. Dotted line indicates response positivity threshold (0.025%). Each dot represents one individual.

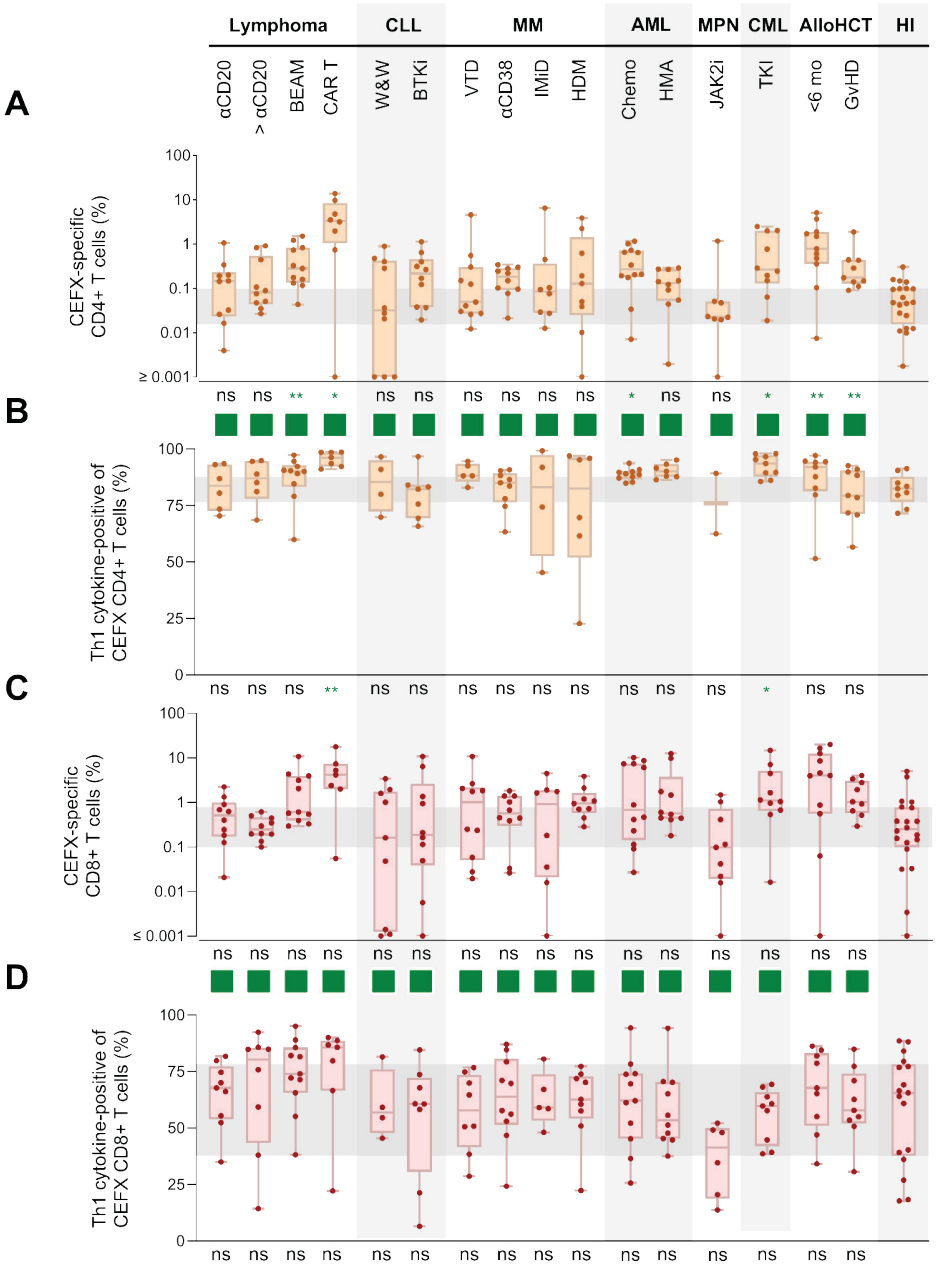

Supplementary figure 9 Supplementary figure 7: Frequency of CEFX-specific CD4+ and CD8+ T cells

A) Frequency of CEFX-specific CD4+ T cells after two COVID-19 mRNA vaccinations. B) Frequency of CEFX-specific CD4+ T cells that produce IFN-γ, TNF-α and/or IL-2. Frequency was calculated by subtracting the frequency of cells that do not produce any cytokines from 100%. C) Frequency of CEFX-

Supplementary figure 9 *Continued*

specific CD8+ T cells after two COVID-19 mRNA vaccinations. D) Frequency of CEFX-specific CD8+ T cells that produce IFN-γ, TNF-α and/or IL-2. Frequency was calculated by subtracting the frequency of cells that do not produce any cytokines from 100%. The grey horizontal area corresponds to interquartile range in healthy individuals. Each dot represents one individual. T cell frequencies are compared to those in HI by Mann-Whitney U tests and significance corrected for multiple testing (times 16) is shown (ns: p>0.05; *: p≤0.05; **: p≤0.01; ***: p≤0.001; ****: p≤0.0001). T cell responses are categorized based on p value prior to and after correction for multiple testing (green when not significantly lower prior to correction; orange when significantly lower prior to, but not after correction; red when significantly lower after correction).

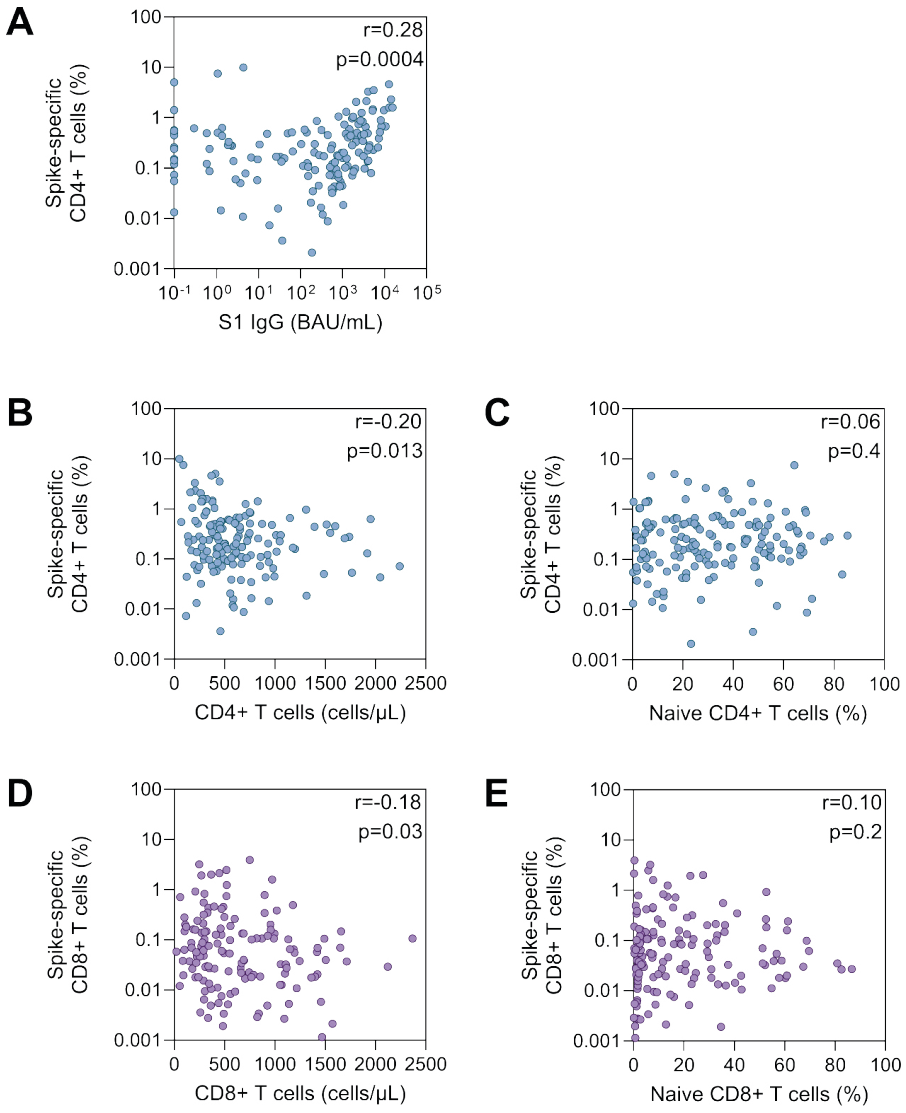

Supplementary figure 10 Supplementary figure 5: Correlations between spike-specific T cell frequencies and other immune parameters

A) Correlation between spike-specific CD4+ T cell frequencies and S1 IgG concentration after two

vaccinations. B) Correlation between spike-specific CD4+ T cell frequencies after two vaccinations and CD4+ T cell numbers in blood at start of vaccination. C) Correlation between spike-specific CD4+ T cell frequencies after two vaccinations and naïve CD4+ T cell frequencies (CCR7+CD45RA+) at start of vaccination. D) Correlation between spike-specific CD8+ T cell frequencies after two vaccinations and CD8+ T cell numbers in blood at start of vaccination E) Correlation between spike-specific CD8+ T cell frequencies after two vaccinations and naïve CD8+ T cell frequencies (CCR7+CD45RA+) at start of vaccination. Each dot represents one individual. Statistics show result of Spearman's correlation.

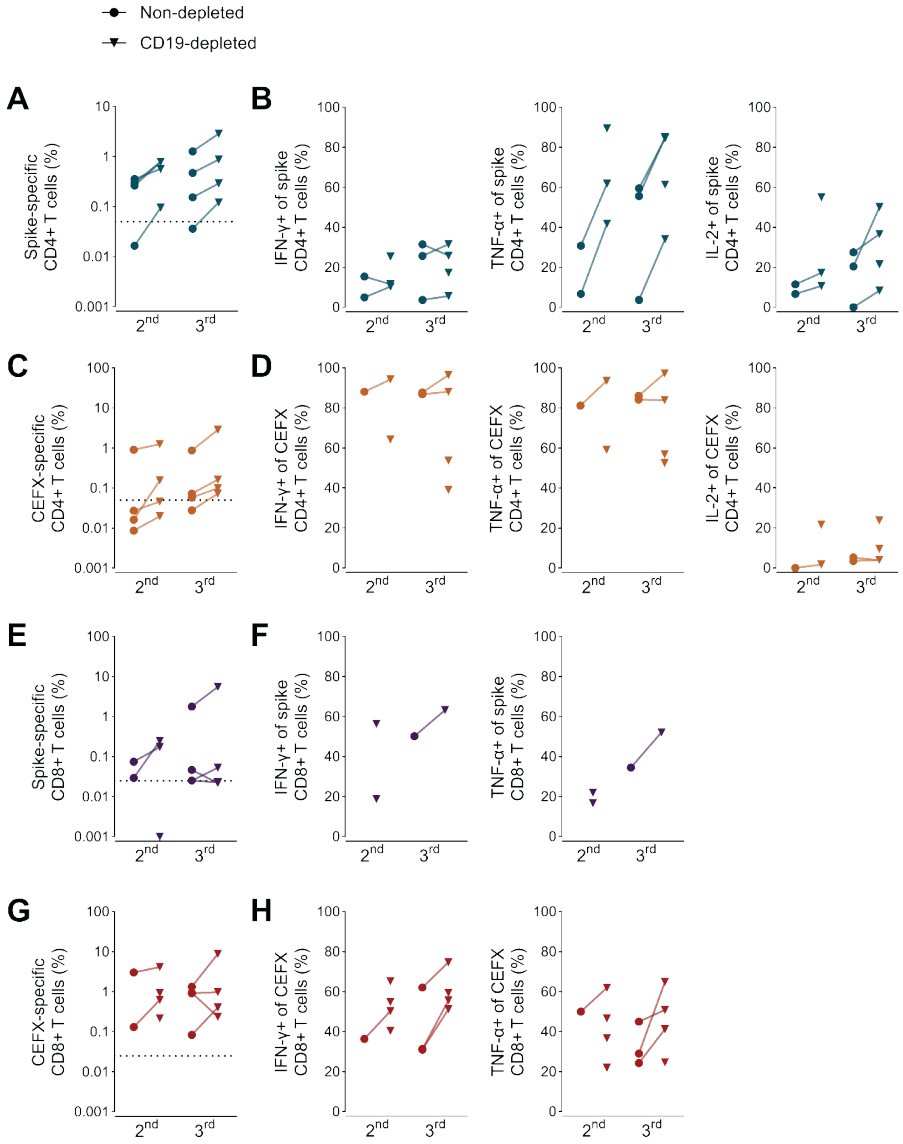

Supplementary figure 11 Supplementary figure 13: Spike-specific T cell frequencies, including cytokine production, in CD19-depleted and non-depleted PBMC from patients with CLL

Supplementary figure 11 *Continued*

PBMCs from four patients with CLL with B cell counts >5000/μl were randomly selected and depleted from CD19+ cells using QuadroMACS™ (Miltenyi) before incubation with peptides and measurement. A) Spike-specific CD4+ T cells frequencies. B) Frequency of spike-specific CD4+ T cells positive for IFN-γ, TNF-α or IL-2. C) CEFX-specific CD4+ T cells frequencies. D) Frequency of CEFX-specific CD4+ T cells positive for IFN-γ, TNF-α or IL-2. E) Spike-specific CD8+ T cells frequencies. F) Frequency of spike-specific CD8+ T cells positive for IFN-γ or TNF-α. G) CEFX-specific CD8+ T cell frequencies. H) Frequency of CEFX-specific CD4+ T cells positive for IFN-γ or TNF-α. In A-H, PBMC were either non-depleted (circles) or depleted from CD19+ cells (triangles). Dotted line indicates response positivity threshold. Each line or dot represents one individual.

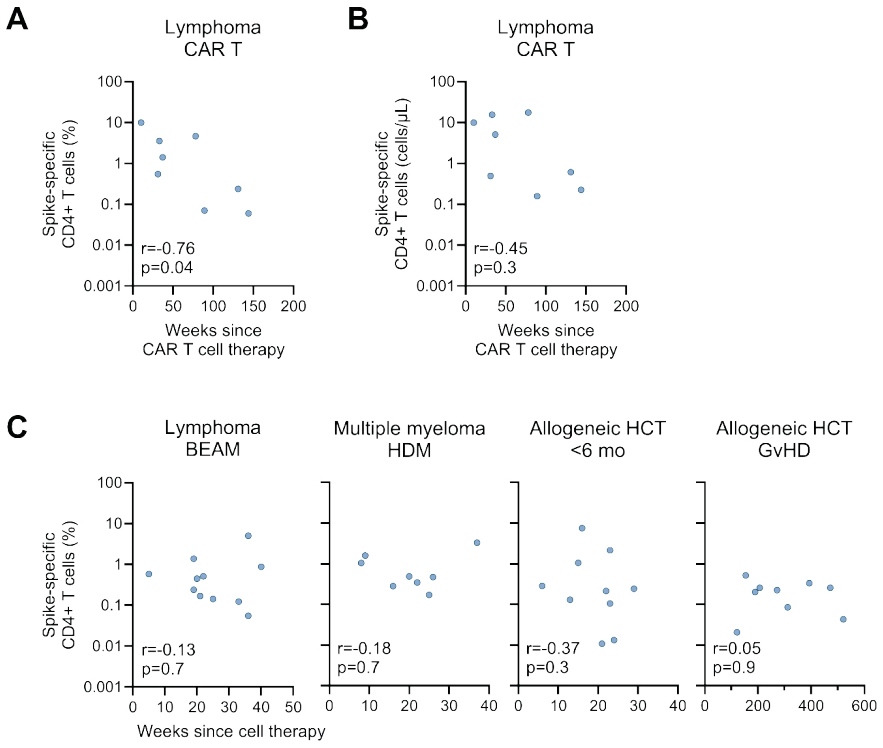

Supplementary figure 12 Supplementary figure 6: Correlation between spike-specific CD4+ T cell frequencies/numbers and duration since cell therapy

A) Correlation between spike-specific CD4+ T cell frequency and weeks since CAR T cell infusion. B) Correlation between number of spike-specific T cells per microliter blood and weeks since CAR T cell infusion. C) Correlation between spike-specific T cell frequency and weeks since hematopoietic cell transplantation. Each dot represents one individual. Statistics are shown for Spearman's correlation test.

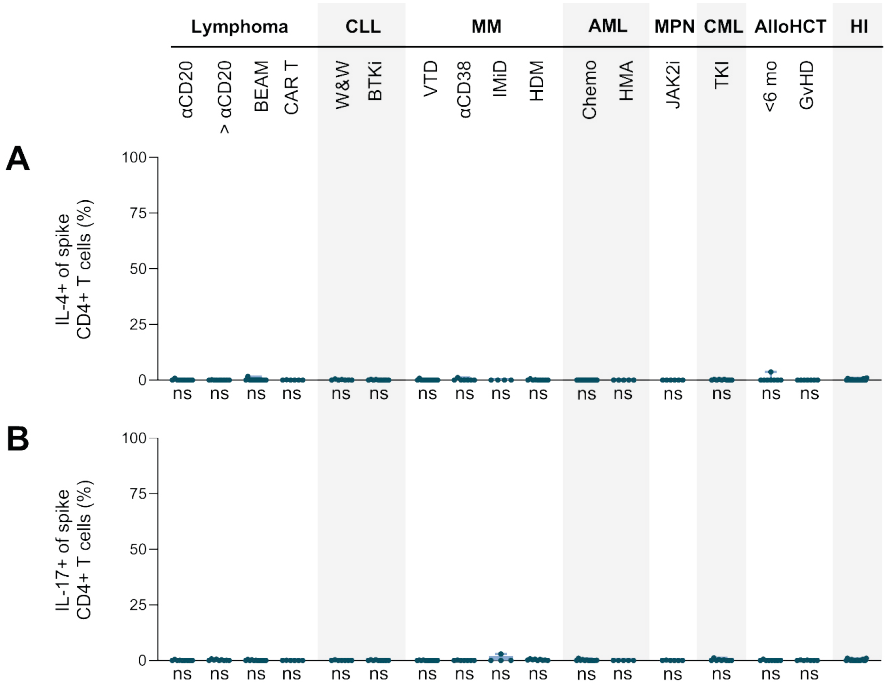

Supplementary figure 13 Supplementary figure 12: IL-4 and IL-17 production by spike-specific CD4+ T cells

A) Frequency of spike-specific CD4+ T cells that produce IL-4. B) Frequency of spike-specific CD4+ T cells that produce IL-17. Each dot represents one individual. Frequencies from each cohort are compared to those in HI by Mann-Whitney U tests and significance corrected for multiple testing (times 16) is shown (ns: p>0.05; *: p≤0.05; **: p≤0.01; ***: p≤0.001; ****: p≤0.0001).

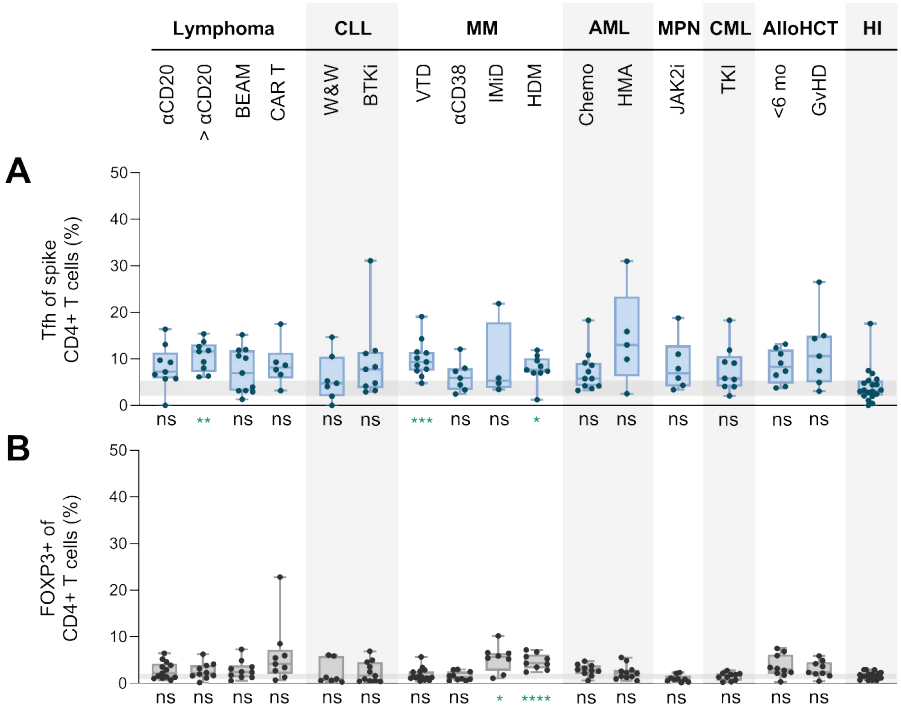

Supplementary figure 14 Supplementary figure 18: FOXP3+ expression by CD4+ T cells, and PD-1+CXCR5+ expression by spike-specific CD4+ T cells

A) Frequency of FOXP3+ CD4+ T cells at start of vaccination. B) Frequency of spike-specific CD4+ T cells that are follicular helper T cells (Tfh; CXCR5+PD-1+) after two mRNA vaccinations. In A and B, horizontal grey area indicate interquartile range of HI. Each dot represents one individual. T cell frequencies from each cohort are compared to those in HI by Mann-Whitney U tests and significance corrected for multiple testing (times 16) is shown (ns: p>0.05; *: p≤0.05; **: p≤0.01; ***: p≤0.001; ****: p≤0.0001).

Supplementary figure 15 Supplementary figure 20: Spike-specific CD4+ and CD8+ T cell frequencies after second and third vaccination.

A) Spike-specific CD4+ T cell frequencies after two (light blue) or three (dark blue) COVID-19 mRNA vaccinations. B) Spike-specific CD8+ T cell frequencies after two (light purple) or three (dark purple) COVID-19 mRNA vaccinations. C) Spike-specific CD4+ T cell frequencies from all patients, separated in responders and non-responders based on spike-specific CD4+ T cell frequencies above (responders) or below (non-responders) the response positivity threshold (0.05%) after two vaccinations. D) Spike-specific CD8+ T cell frequencies from all patients, separated in responders and non-responders based on spike-specific CD8+ T cell frequencies above (responders) or below (non-responders) the response positivity threshold (0.025%) after two vaccinations. E) Comparing the spike-specific CD4+ T cell frequencies after the second and third vaccination of patients that received an autoHCT between second and third vaccination. Dotted lines indicate response positivity thresholds. T cell frequencies are compared between four weeks after second and third vaccination using a paired t-test and p values are shown (ns: p>0.05; *: p≤0.05; **: p≤0.01; ***: p≤0.001; ****: p≤0.0001). Correction for multiple testing was performed (p-value times 16).

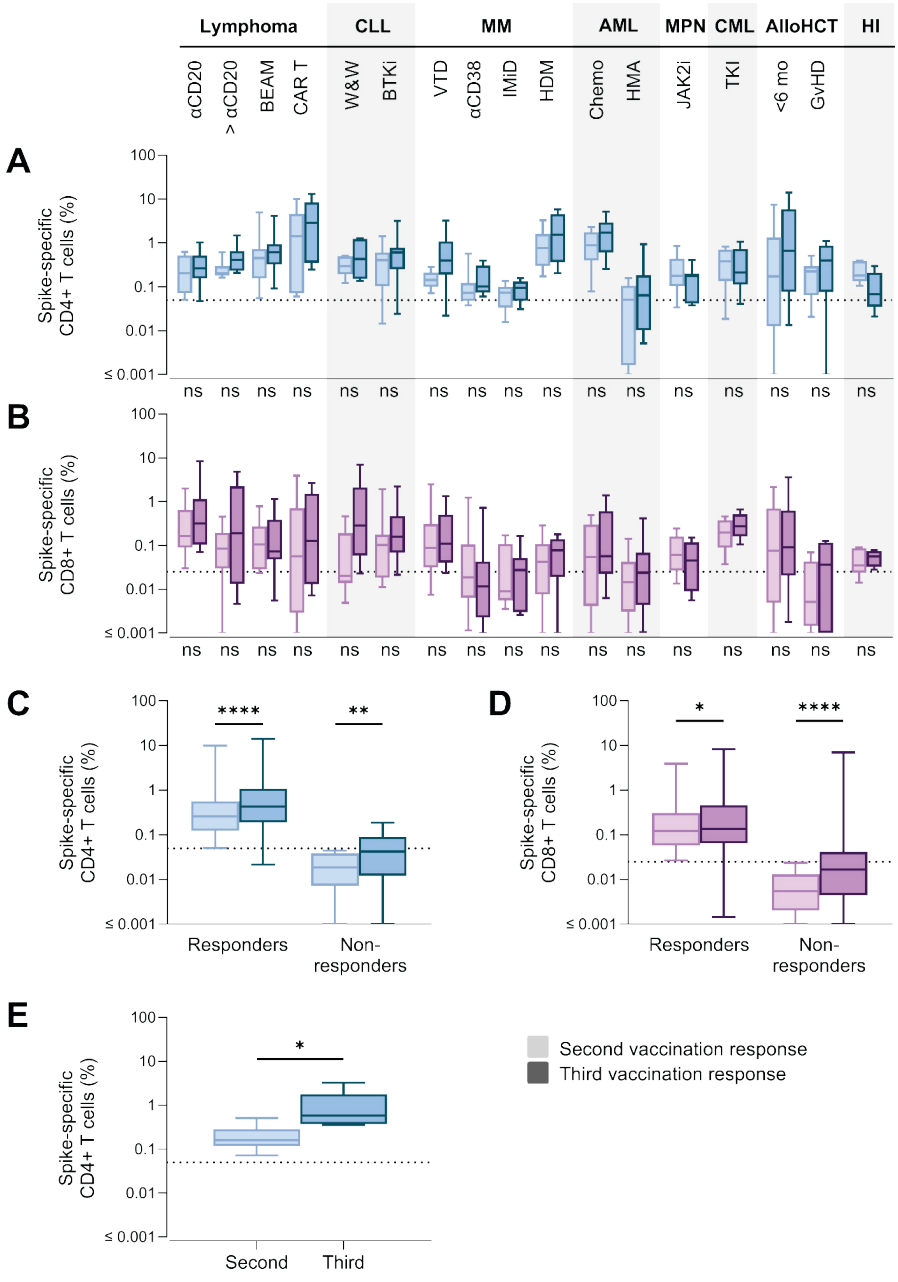
Lymphoma
CLL
MM
AML
MPN
CML
AlloHCT
HI
αCD20
> αCD20
BEAM
CAR T
W&W
BTKi
VTD
αCD38
IMiD
HDM
Chemo
HMA
JAK2i
TKI
<6 mo
GvHD
A
Spike-specific CD4+ T cells (%)
B
Spike-specific CD8+ T cells (%)
100
10
1
0.1
0.01
≤ 0.001
ns
C
D
****
**
*
Responders
Non-responders
E
Second
Third
Second vaccination response
Third vaccination response

REFERENCES

1. Haggenburg S, Lissenberg-Witte BI, van Binnendijk RS, et al. Quantitative analysis of mRNA-1273 COVID-19 vaccination response in immunocompromised adult hematology patients. Blood Adv. 2022;6(5):1537-1546.
2. den Hartog G, Schepp RM, Kuijer M, et al. SARS-CoV-2-Specific Antibody Detection for Seroepidemiology: A Multiplex Analysis Approach Accounting for Accurate Seroprevalence. J Infect Dis. 2020;222(9):1452-1461.
3. Prins MLM, Roozen GVT, Pothast CR, et al. Immunogenicity and reactogenicity of intradermal mRNA-1273 SARS-CoV-2 vaccination: a non-inferiority, randomized-controlled trial. NPJ Vaccines. 2024;9(1):1.
4. Boerenkamp LS, Pothast CR, Dijkland RC, et al. Increased CD8 T-cell immunity after COVID-19 vaccination in lymphoid malignancy patients lacking adequate humoral response: An immune compensation mechanism? Am J Hematol. 2022;
5. Zonozi R, Walters LC, Shulkin A, et al. T cell responses to SARS-CoV-2 infection and vaccination are elevated in B cell deficiency and reduce risk of severe COVID-19. Sci Transl Med. 2023;15(724):eadh4529.
6. Hofsink Q, Haggenburg S, Lissenberg-Witte BI, et al. Fourth mRNA COVID-19 vaccination in immunocompromised patients with haematological malignancies (COBRA KAI): a cohort study. EClinicalMedicine. 2023;61(102040.
7. Gao Y, Cai C, Wullimann D, et al. Immunodeficiency syndromes differentially impact the functional profile of SARS-CoV-2-specific T cells elicited by mRNA vaccination. Immunity. 2022;55(9):1732-1746 e1735.
8. Zhang Z, Mateus J, Coelho CH, et al. Humoral and cellular immune memory to four COVID-19 vaccines. Cell. 2022;185(14):2434-2451 e2417.
9. Solman IG, Blum LK, Burger JA, et al. Impact of long-term ibrutinib treatment on circulating immune cells in previously untreated chronic lymphocytic leukemia. Leuk Res. 2021;102(106520.
10. Loke J, Upasani V, Gaskell C, et al. Defective T-cell response to COVID-19 vaccination in acute myeloid leukaemia and myelodysplastic syndromes. Br J Haematol. 2023;202(3):498-503.
11. Sanchez-Abarca LI, Gutierrez-Cosio S, Santamaria C, et al. Immunomodulatory effect of 5-azacytidine (5-azaC): potential role in the transplantation setting. Blood. 2010;115(1):107-121.
12. Mackova J, Hainz P, Krystofova J, et al. Specific immune response to mRNA vaccines against COVID-19 in patients receiving allogeneic stem cell transplantation for myeloid malignancy was altered by immunosuppressive therapy. Leuk Res. 2023;130(107314.
13. Haggenburg S, Hofsink Q, Lissenberg-Witte BI, et al. Antibody Response in Immunocompromised Patients With Hematologic Cancers Who Received a 3-Dose mRNA-1273 Vaccination Schedule for COVID-19. Jama Oncol. 2022;8(10):1477-1483.
14. Hofsink Q, Haggenburg S, Lissenberg-Witte BI, et al. Risk of Severe Sars-Cov-2 Infections in COVID-19 Vaccinated Individuals with Hematologic Malignancies (SAVE HEM): A Nationwide Cohort Study in the Netherlands. Blood. 2023;142(Supplement 1):546-546.

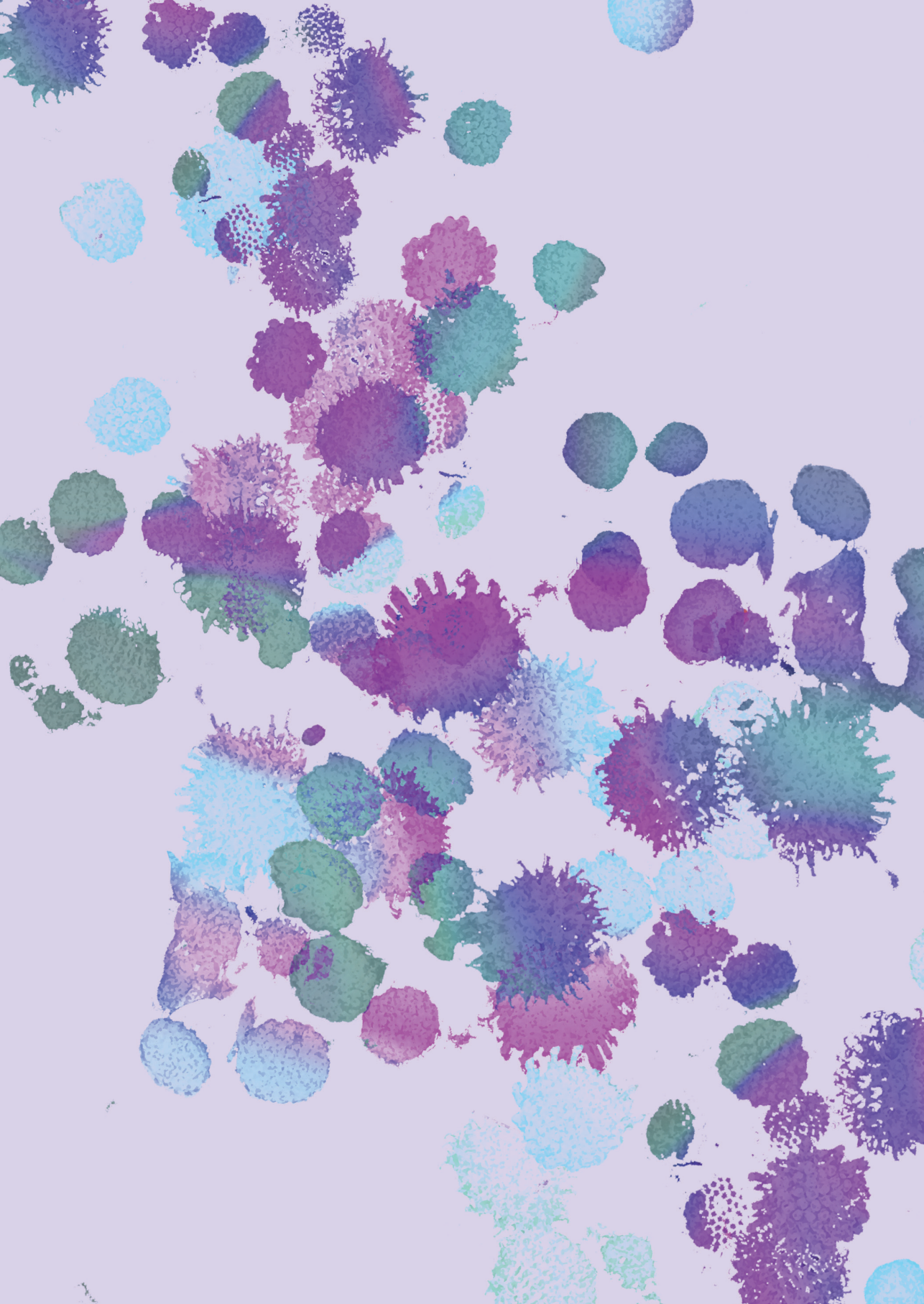

SUMMARY

Chapter 6

The severe acute respiratory syndrome coronavirus 2 (SARS-CoV-2) mRNA vaccines induce effective humoral and T-cell responses in healthy individuals. Antibodies are important for preventing the entry of viral particles into cells. T cells can support other immune cells or directly lyse virus-infected cells. However, patients with hematological malignancies are often immunocompromised due to their disease or treatment. Understanding the specifics of the immunocompromised state of these patients is vital to adapting vaccination strategies or vaccine designs to improve protection against severe disease in these patients. However, vaccine-induced T-cell responses are rarely measured, as they are more laborious and complicated to interpret compared to antibodies. Therefore, in this thesis, we aimed to identify vaccine-induced SARS-CoV-2-specific T cells and antibodies in a large group of patients. The detection of vaccine-induced T cells is challenged by cross-reactive T cells since vaccine-induced T-cell responses are commonly measured using peptide-stimulation assays, which also result in the activation of cross-reactive T cells. We found that some individuals exhibit SARS-CoV-2-specific T cells even before exposure to the virus, and these T cells can originate from cytomegalovirus (CMV)-specific T cells. However, it seems that these cross-reactive T cells are not highly effective in SARS-CoV-2-infected cells, indicating that these pre-existing cells may not be able to change the course of the disease. The SARS-CoV-2 mRNA vaccines can induce antibody and T-cell responses in most individuals. Patients with aplastic anemia induced immune responses, although their cytokine production may be reduced compared to healthy individuals. In patients with hematological malignancies, it is known that the humoral response can be quite variable due to B-cell-targeting therapies that many patients receive. Despite this, most of these patients were able to develop SARS-CoV-2-specific T-cell responses. The magnitude of the CD4+ or CD8+ T-cell response and their cytokine profile did vary in some cohorts. Interestingly, poor T-cell counts or naïve T cells did not predict the vaccine-induced T-cell response. We demonstrated that, despite being immunocompromised, most patients with hematological malignancies can mount T-cell responses and therefore may have a layer of protection through these cells.

T cells can be cross-reactive against different peptide-human leukocyte antigen (HLA) complexes. By chance, individuals may have memory T cells that are reactive against a virus that they have never been exposed to. This is typically caused by sequence-homologous viruses. For this reason, most studies focused on whether pre-existing SARS-CoV-2-specific CD4+ and CD8+ T cells originate from other coronaviruses. However, in **chapter 2,** we showed that pre-existing SARS-CoV-2-reactive T cells can also originate from CMV-specific CD4+ or CD8+ T cells. Individuals who were seropositive for CMV had more measurable cross-reactive T cells. Upon isolation of these T cells, we confirmed their reactivity towards pp65, which is the most

immunogenic protein of CMV. The avidity of these cross-reactive T cells towards the CMV peptide was higher than for SARS-CoV-2 confirming that the T cells were primed and developed against CMV. The cross-reactive CD8+ T cells were detectable in multiple individuals. However, in an *in vitro* infection model, cross-reactive CD8+ T cells were less effective in limiting spread compared to vaccine-induced CD8+ T cells. Furthermore, we detected the cross-reactive CD8+ T cells in two patients with severe coronavirus disease 2019 (COVID-19) but these T cells showed a less activated phenotype compared to infection-induced T cells. This indicated that cross-reactive T cells appeared to be less functional compared to infection- or vaccine-induced T-cell responses.

Vaccination typically induces effective humoral and T-cell responses, resulting in improved viral clearance and thereby improved protection against severe disease. Vaccination is particularly important for individuals with a compromised immune system, such as patients with aplastic anemia. However, current guidelines recommend caution when it comes to vaccinating due to the potential risk of relapse of the aplastic anemia based on case reports, combined with the expectation that vaccinating might be less effective. Surprisingly, these guidelines also apply to patients who are in remission and years after immunosuppressive treatment. This is surprising considering that viral infections can trigger relapse. In **chapter 3**, we showed that this group of patients was able to mount SARS-CoV-2-specific antibodies and T-cell responses comparable to healthy individuals although cytokine production by the T cells appeared to be lower. Importantly, none of the patients showed signs of aplastic anemia relapse. In summary, the results from this chapter showed that the SARS-CoV-2 mRNA vaccine effectively induced antibody and T-cell responses in patients with aplastic anemia who were in remission and after immunosuppressive treatment, without inducing relapse.

Patients with hematological malignancies are often immunocompromised due to disease or treatment. For this reason, vaccination is prioritized for this group to minimize the severe course of COVID-19. However, the expected severity of the immunocompromised state of these patients is not clear, as immunity is often solely measured by the presence of antigen-specific antibodies. In **chapter 4**, we investigated whether patients who did not seroconvert following mRNA vaccination also lacked vaccine-induced T-cell responses. Spike-specific antibodies and CD4+ and CD8+ T cells were measured in patients with chronic lymphocytic leukemia (CLL), indolent or aggressive B-cell lymphoma, or multiple myeloma, which we stratified based on lacking (n=49) or with adequate seroconversion (n=14). We found that antibody levels can be variable among the patients and were especially low in patients with CLL.

Spike-specific CD4+ and CD8+ T cells were detected in almost all patients. Frequencies of spike-specific T cells appeared to reduce with age, as patients above 68 had lower frequencies of spike-specific CD4+ and CD8+ T cells compared to patients below 68. Interestingly, patients who did not seroconvert had higher frequencies of spike-specific CD8+ T cells. Therefore, the absence of antibodies is not a predictive measure of a lack of immunity in patients with CLL, lymphoma or multiple myeloma.

In **chapter 5**, we extended the group of patients with hematological malignancies (n=173) and stratified based on malignancy or treatment, resulting in 16 cohorts. These 16 cohorts included patients with lymphoma treated with rituximab or chemotherapy, untreated or BTK-inhibitors-treated CLL, multiple myeloma treated with chemotherapy, daratumumab or immunomodulatory drugs, acute myeloid leukemia (AML, including myelodysplastic syndrome) treated with chemotherapy or hypomethylating agents, myeloproliferative neoplasm (MPN) treated with JAK2-inhibitors, chronic myeloid leukemia (CML) treated with tyrosine-kinase-inhibitor (TKI), or patients treated with allogeneic stem cell transplantation. mRNA-induced spike-specific antibodies, CD4+ and CD8+ T cells, as well as the cytokine production and phenotype of the T cells were measured before and four weeks after each vaccine dose. Firstly, we found that in this extended cohort, most patients can generate spike-specific CD4+ and/or CD8+ T cells, also in the absence of antibodies. Combined antibody and T-cell deficiency was rare, although in patients treated with hypomethylating agents both antibodies and T cells were reduced but not absent. For patients treated with allogeneic stem cell transplantation, the antibody and T-cell responses were variable. Spike-specific CD4+ T cells showed lower frequencies in patients with multiple myeloma treated with daratumumab or immune-modulatory drugs. Cytokine production by spike-specific CD4+ T cells was reduced in patients with untreated CLL, MPN treated with JAK2 inhibitors, and allogeneic stem cell transplantation. Interestingly, lower frequencies of spike-specific T cells did not seem to be a result of the lack of availability of a large pool of naïve T cells, since T-cell counts or the percentage of naïve T cells at the start of vaccination did not correlate with vaccine-induced CD4+ or CD8+ T-cell frequencies. In summary, the immune response to mRNA vaccination was variable in the patient cohorts, but most patients developed humoral and/or T-cell responses. This shows that the SARS-CoV-2 mRNA vaccination can induce immune responses in these immunocompromised patients and thereby can protect against severe COVID-19.

GENERAL DISCUSSION

The circulation of SARS-CoV-2 and the introduction of vaccination in a previously unexposed (naïve) population, combined with bio-banking of samples, have created a unique opportunity to investigate both pre-existing immunity and primary immune responses. For this reason, our understanding of immune responses towards SARS-CoV-2 and mRNA vaccination has been widely expanded. This thesis aimed to contribute to this understanding by performing an in-depth analysis of SARS-CoV-2-specific CD4+ and CD8+ T cells in different contexts. A detailed investigation of antigen-specific T cells is often lacking due to its labor-intensive nature.[1] By employing advanced methods, this thesis aimed to expand the possible origins of pre-existing SARS-CoV-2-specific T cells and to provide novel insights into the vaccine-induced humoral and T-cell responses in immunocompromised patients. The results show the importance of in-depth analysis of antigen-specific T cells, especially considering the critical role T cells can play in protecting against severe disease.[2-6]

Detection of antigen-specific T cells

Following vaccination, each component of the adaptive immune response provides a layer of protection that is important to prevent a severe course of disease.[2] However, patients with hematological malignancies are often immunocompromised due to impaired antibody, CD4+ T-cell, and/or CD8+ T-cell responses. Assessments of vaccine-induced immune responses are usually focused on seroconversion, underreporting cellular responses.[7-11] As a result, vaccination recommendations are often based solely on antibody titers, with a lack of antibody presence being interpreted as an absence of immunity.[12-15] This may result in advice against or delayed vaccination in vulnerable individuals who are unable to seroconvert, despite evidence that T cells can provide protection against severe disease and are more effective against variants of concern compared to antibodies.[2-6,12] This issue of underreported cellular responses and vaccination recommendations solely based on antibody titers is not specific for SARS-CoV-2 vaccination but also extends to other vaccinations.[16] The main cause of the limited attention on T-cell responses is the lack of high-throughput and standardized detection methods, underscoring an urgent need for improved detection of antigen-specific T cells.[6]

The current most standardized methods for measuring antigen-specific T cells are the interferon gamma release assay (IGRA) and the enzyme-linked immunosorbent spot (ELIspot) assay. These techniques were commonly used during the SARS-CoV-2 pandemic to measure T-cell responses in patients with hematological malignancies.[1,6] In these assays, whole blood or peripheral blood mononuclear cells (PBMCs)

are co-incubated with peptides, and the release of IFN-γ is measured either as a concentration in the supernatant (IGRA) or as spot-forming units captured directly upon cytokine release from individual cells (ELIspot). These spots are then counted as a measurement of the number of interferon-γ (IFN-γ)-producing cells. Although these assays can quickly provide insights into the number of T cells per unit of PBMCs or whole blood, these assays appear to be variable between studies and generally underestimate the true magnitude of the T-cell response.[17-19] This issue is probably related to differences in peptide selection, culturing conditions, analysis methods, IFN-γ-exclusive measurement, and inconsistent PBMC input across samples. This issue is further complicated in patients with hematological malignancies, where due to lymphopenia or a high burden of malignant cells, abnormal PBMC composition can distort the results. Because these assays do not correct for the actual amount of T cells present in the samples, the chance of missing antigen-specific T cells is high when T-cell frequencies fall outside the normal range.[20] Therefore, while ELISA-based assays are highly valuable for large-scale measurement of T-cell responses in healthy individuals, they may be less optimal for patients with hematological malignancies. In such cases, flow cytometry would be a more accurate and informative approach. This is because flow cytometry gives more insight into the frequencies of antigen-specific T cells, independent of the amount of other immune cells, and can also provide more insight into cytokine-producing cell subsets. However, flow cytometry is more labor-intensive and less standardized. Potential solutions to improve feasibility could be circumventing permeabilization steps using optimized cytokine-capture-based assays or simplifying analysis using artificial intelligence.[21-23] Accordingly, there is a need to optimize and standardize flow cytometry protocols for high-throughput detection of antigen-specific T cells.[1]

As mentioned before, flow cytometry allows for a more accurate and specific detection of antigen-specific T cells. However, elaborate studies on antigen-specific T-cell responses following SARS-CoV-2 vaccination using flow cytometry are scarce and mainly focused on CD4+ T cells. This is partly caused by the challenges that come with the detection of antigen-specific CD8+ T cells, which are present at lower frequencies in the circulation, and because the assays are usually optimized for the detection of CD4+ T cells.[1,24,25] As a result, uncertainty may occur about infection- or vaccine-induced CD8+ T-cell responses, whether the (lack of) detected frequencies are biologically accurate or caused by a technical artefact.[6,26,27] In **chapter 5**, the spike-specific CD8+ T-cell frequencies before and during vaccination detected through AIM assay were more variable compared to the CD4+ T cell frequencies, highlighting the need to optimize antigen-specific CD8+ T cell detection methods. In **chapter 4,** we combined the AIM assay with ICS and defined the antigen-specific CD8+ T cells

based on activation markers combined with cytokine production. This resulted in frequency kinetics that were more similar to spike-specific CD4+ T cells. However, spike-specific CD8+ T cells which are unable to produce cytokines might still be important, potentially underestimating the full spectrum of the CD8+ T cell response. Other studies used detection methods for antigen-specific CD8+ T cells that were more complicated than those typically used for CD4+ T cells. They include the use of more activation markers to reduce background noise, stimulating with HLA class I (predicted) epitopes, or the incorporation of a T-cell expansion step to enhance detectable frequencies.[28-31] The fact that each study measures antigen-specific CD8+ T cells differently underlines that a consensus on an optimal detection method is currently lacking. This is a remaining issue, particularly since CD8+ T cells are a key component in the clearance of virus-infected cells and the strong association between SARS-CoV-2-specific T cell responses and the protection against severe disease.[2,4-6]

Apart from the detection method, epitope selection is key to an accurate detection of antigen-specific T cells and affects results obtained through IGRA, ELIspot, and flow cytometry. In the case of the emergence of a new pathogen, this is more challenging since the epitope immunogenicity is unknown. Peptide pools are therefore initially based on covering an immunogenic protein by overlapping peptides, or peptides are selected based on *in silico* predictions. Previous studies have shown that commercialized kits that measure antigen-specific T cells may use suboptimal peptide pools and therefore result in an underestimation of T-cell responses and variable outcomes depending on the kit used.[17,32] In **chapters 4** and **5**, peptide-stimulation assays using 15-mer peptides were complemented using peptide-HLA tetramers for the detection of spike-specific CD8+ T cells. To generate the peptide-HLA tetramers, a selection was made of 23 predicted immunogenic peptide-HLA antigens. The frequencies detected through peptide-HLA tetramers correlated well with the frequencies obtained by AIM assay. Furthermore, peptide-HLA tetramer staining resulted in frequency kinetics that were similar to the frequencies of the antigen-specific CD4+ T cells obtained by AIM assay. Although this indicates that peptide-HLA tetramers could be a preferred method over AIM assays, the frequencies of spike-specific CD8+ T cells as measured by peptide-HLA tetramer frequencies were lower and detected in fewer individuals. This is most likely due to the restricted peptide-HLA combinations present in the tetramer pool, which do not cover the full range of HLA alleles in the population. This exposes the challenge of peptide-HLA tetramers: the ability to include as many immunogenic peptide-HLA complexes as possible. Fortunately, the large focus on measuring T-cell responses during the pandemic has resulted in a fast discovery of T-cell epitopes and therefore improves the accuracy of detection of antigen-specific T cells.[18,28]

To summarize, the measurement of antigen-specific T cells has some challenges to overcome. These challenges are mostly related to the detection method used, limited understanding of how to reliably detect antigen-specific CD8+ T cells, and the complexity of peptide selection. Currently available detection methods are either high throughput but less accurate or more precise yet labor-intensive. Simplifying the measurement of antigen-specific T cells using flow cytometry could pave the way for more accurate measurement of adaptive immune responses to vaccination. The widespread circulation of SARS-CoV-2 has resulted in a boost in optimized detection of antigen-specific T cells. These developments must continue to develop accurate and large-scale detection methods of antigen-specific T cells that can also be applied to other vaccination strategies.

Detection of cross-reactive T cells

T-cell cross-reactivity refers to the ability of a single T-cell receptor (TCR) to recognize different peptide-HLA complexes. This can range from a single amino acid change in the peptide to a completely different peptide and HLA complex. T-cell cross-reactivity is widely studied in different contexts. It is commonly described as beneficial since it can protect against a wider range of pathogens, but it can also be detrimental when it causes autoimmunity. T cell cross-reactivity depends on multiple factors, including sequence similarity, molecular mimicry, hotspot binding, and the structural plasticity of the peptide-HLA complex and/or TCR. In **chapter 2**, we identified CMV-specific CD4+ and CD8+ T cells that were also reactive towards SARS-CoV-2, highlighting an example of such cross-reactivity. Understanding the origin and function of cross-reactive T cells is challenging, but it is vital to expand our understanding of T-cell immunity.

Many research groups have reported the presence of cross-reactive T cells targeting SARS-CoV-2 in samples from SARS-CoV-2-unexposed individuals.[33-37] Since most commonly used assays for detecting antigen-specific T cells have limited sensitivity, the cross-reactivities that are identified tend to be biased toward T cells that are already present at relatively high frequencies in the circulation. In **chapter 2**, we detected and characterized CMV pp65-specific HLA-B*35:01-restricted T cells from multiple SARS-CoV-2 unexposed individuals that were cross-reactive towards a peptide derived from the spike protein of SARS-CoV-2, also presented in the context of HLA-B*35:01. These T cells were likely to have been picked up since CMV-specific T cells are known to be present at high frequencies in a significant portion of the population. Detection methods also vary in their sensitivity to TCR affinity. For instance, peptide-HLA tetramer staining can detect even low-affinity TCR interactions, since the assay relies solely on the physical binding of peptide-HLA complex and the TCR. However, such binding does not always correlate with functional avidity and the ability to

induce a functional T-cell response.[38] Similarly, in peptide-stimulation assays, usually high peptide concentrations are used that also induce activation of low-avidity T cells.[39] This phenomenon can likely have been observed in **chapter 5**, where CD8+ T cell responses after *in vitro* exposure to spike peptide pools were commonly observed before the patients were vaccinated and exposed to SARS-CoV-2. After the detection of cross-reactive T cells, researchers tried to identify their original target peptide-HLA complex. This was commonly only tested against a restricted pool of peptides, based on the assumption that cross-reactivity results from minor peptide sequence changes. However, our data in **chapter 2** demonstrates that a single TCR can be cross-reactive towards peptides that differ in 5 out of 9 amino acids. Therefore, identifying the original antigen of cross-reactive T cells is especially challenging when it involves the recognition of two dissimilar peptides, since the original peptide could originate from any pathogen. Therefore, mapping the antigenic specificity of cross-reactive T cells requires large peptide libraries that cover multiple different pathogens or unbiased peptide discovery approaches. As described in **chapter 2,** applying the combinatorial peptide library enabled an unbiased identification of the original pathogen by testing the T cells against a library of peptides that identify the key amino acids for T cell recognition, independent of known epitopes.[40,41] This expands our understanding of the mechanisms behind T-cell cross-reactivity and their potential implications.

Numerous studies have detected pre-existing SARS-CoV-2-specific CD4+ and CD8+ T cells, but it is currently unclear whether they can play a pivotal role in prevention of severe disease.[28,33,35-37,42-51] Current studies mostly lean towards an important role of cross-reactive T cells during SARS-CoV-2 infection. If these cross-reactive T cells indeed play an pivotal role, this could have implications for the pathogenesis of SARS-CoV-2 infections and could aid in the development of a pan-coronavirus vaccine.[34,36,52-55] However, we propose that the cross-reactive T-cell responses towards SARS-CoV-2 have a high likelihood of being of too low avidity. Pre-existing SARS-CoV-2-reactive T cells are, in most cases, reported to be primed by related common human coronaviruses (229E, NL63, HKU1, and OC43).[56] Despite the relatively high sequence homology with SARS-CoV-2 (65-69%), the sequence similarity is scattered over the genome, resulting in a maximum protein similarity of ~35% and a low amount of predicted shared epitopes.[53,57,58] This is confirmed by the observation that, to our knowledge, none of the identified epitopes of cross-reactive T cells share 100% sequence homology.[33,35-37,42-50] As a result, a limited pool of T cells that are reactive towards the common coronaviruses can recognize SARS-CoV-2, and their avidity appears to be lower due to amino acid changes in the peptide sequence.[37,45,50,53,59] Furthermore, these low-avidity T cells may appear functional in *in vitro* peptide-stimulation assays that use a T-cell optimal environment, but this is likely not

representative of *in vivo* functionality. The data presented in **chapter 2** show that the cross-reactive T cells were SARS-CoV-2-reactive in peptide-stimulation assays, but in a SARS-CoV-2 live virus infection assay, cross-reactive CD8+ T cells were unable to effectively inhibit virus spread. Apart from optimal T-cell conditions, most assays also fail to test if the targeted peptides are effectively processed and presented during infection. This reduces the chances that cross-reactive T cells can form a polyclonal T cell response that plays a major role in protection against severe disease and the ability to develop an effective pan coronavirus vaccine that covers a diverse range of HLA types.

Functionality of T cells in disease and therapy

Vaccination-induced immune responses are commonly measured by the presence of antigen-specific antibodies only, since antibody measurements are standardized and high-throughput. As a result, vaccination guidelines are commonly based on seroconversion. However, not all individuals develop a (measurable) antibody response, which is especially the case for immunocompromised individuals. As illustrated in **chapters 3-5**, it became clear that the absence of antigen-specific antibodies does not correlate with the absence of cellular immune responses and that most immunocompromised patients were able to develop vaccine-induced T-cell responses. This indicates that vaccination should be recommended also in patients where an inability to seroconvert is expected, to increase T-cell-mediated protection against severe disease.

As briefly mentioned, **chapters 4** and **5** show that an absence of a humoral response does not necessarily correlate with an absence of T cell responses: a combined humoral and T-cell response deficiency was rarely observed. This shows that an absence of humoral immunity does not directly indicate a hampered overall immune response. Patients who often have reduced or absent humoral responses are patients with B-cell lymphoma. These patients are usually treated with B-cell-targeting treatments, which explain their variable antibody levels. In contrast to vaccine-induced antibody responses, T cell responses in this patient group were similar to those of healthy individuals, as shown in this thesis in **chapters 4** and **5**, and by others.[60-64] Vaccination schedules should therefore not be based solely on the likelihood of seroconversion. Instead, patients should be vaccinated regardless of treatment status to protect this patient population through T cell immunity.

Patients with CLL are more sensitive to a severe course of infections due to the hampered immune system caused by the disease.[65] This has been particularly well studied for the effect of CLL cells on T cells.[66-68] **Chapters 4-5** of this thesis showed

that while the frequencies of vaccine-induced T-cell responses were similar to healthy controls, the ability to produce cytokines was reduced. Interestingly, when CLL cells were removed from the T-cell stimulation assays, T cells were able to produce normal levels of TNF-α and IL-2. This suggests that CLL cells can hamper cytokine production by T cells when they are in close proximity. Whether this suppression of TNF-α and IL-2 also occurs *in vivo* is unknown and may depend on the local concentration of CLL cells within tissues.[69] After removal of CLL cells, IFN-γ production was still hampered, indicating an intrinsically reduced production of IFN-γ by T cells in patients with untreated CLL. This was likely caused by the presence of CLL cells, since upon inhibition of CLL cells by BTK inhibitors, the cytokine production by *de novo* induced T-cell responses was restored. Although it appears that BTK inhibitors restore T cell immunity, they can negatively affect B cell responses, as presented in **chapters 4-5** and the current literature.[70,71] Therefore, based on the data presented in this thesis and given the risk of viral complications in this patient population, vaccination should be recommended in this patient cohort, independent of their current treatment.[72]

In **chapter 5,** we demonstrate that patients treated with hypomethylating agents (HMA) for AML/MDS had reduced spike-specific antibody concentrations, as well as lower spike-specific CD4+ and CD8+ T-cell frequencies.[73,74] The observation that patients with AML treated with high-dose chemotherapy developed humoral and T-cell responses similar to healthy individuals indicates that the HMA treatment could be the underlying cause of the hampered immune responses. A likely explanation is that HMA, which targets proliferating cells, may impair the expansion of activated, spike-specific T and B cells following vaccination.[73-76] This is supported by the observation that the frequencies of T cells with other specificities (CMV, EBV, flu, and more; CEFX) that are usually at rest during therapy were not reduced. It is important to note that the reduced T-cell frequencies could be attributed to the higher age of patients in the HMA cohort.[62,77,78] Current literature indicates that patients treated with hypomethylating agents have an increased risk of severe infections, independent of age.[79-81] This suggests that the observed reduced immune responses could indeed be caused by hypomethylating agents, urging the need for more elaborate investigation into whether hypomethylating agents indeed can affect vaccine-induced immunity. Investigating the vaccine-induced B- and T-cell responses in a heterogeneous group of patients with different hypomethylating treatment regimens and ages would provide insight into this matter. Until then, the reduced immune function observed in these patients and the continued circulation of SARS-CoV-2 in the population support the use of the SARS-CoV-2 mRNA vaccination in this cohort to provide some protection against severe disease. Since HMA is typically given for a long period, vaccination should not be delayed until after therapy. To protect these patients during therapy,

the vaccination could be scheduled two weeks before the next HMA cycle to allow T cell responses to develop with minimal effect of the HMA. Furthermore, additional booster vaccinations might be necessary to fully protect these patients against a severe course of SARS-CoV-2 infection.

Patient cohorts with low T-cell counts and/or low frequencies of naïve T cells were able to generate vaccine-induced spike-specific CD4+ and CD8+ T cells similar to healthy donors, both based on frequencies and absolute numbers. This includes patients treated with allogeneic stem cell transplantation (SCT) and chimeric antigen receptor (CAR) T cell therapy. Although counterintuitive, the lack of correlation between absolute T-cell counts and vaccine-induced T-cell responses has been reported before.[78,82] It has previously been proposed that T-cell counts in the context of allogeneic SCT could be a better predictor of vaccine immunogenicity than time since transplantation.[12] However, **chapter 5** showed that low T-cell counts and/or percentage of naïve T cells were not indicative of proper T-cell activation and thus should not function as a predictor for adequate *de novo* T-cell responses. Therefore, vaccination should not be delayed based on low lymphocyte counts in circulation, as is often observed shortly after allogeneic SCT and CAR T cell therapy.

The observation that patients with hematological malignancies generated vaccine-induced antibody and/or T-cell responses similarly to healthy individuals supports the use of mRNA vaccination to protect these patients. Compared to other SARS-CoV-2 vaccine modalities, mRNA vaccines appear more effective and can generate stronger humoral and T-cell responses in healthy individuals.[83,84] Of the two mRNA vaccines, the mRNA-1273 (Moderna) induced stronger immune responses than BNT162b2 (Pfizer/BionTech), potentially related to the differences in vaccination dosage, components, or timing between dosages.[84-86] Therefore, mRNA-1273 may be preferred over BNT162b2 for immunocompromised patients. This could change in the near future since BioNTech developed a new SARS-CoV-2 vaccine (BNT162b4) which includes antigens of the membrane, nucleocapsid, and open reading frame 1ab (ORF1ab) genes.[87] This vaccine could further enhance T-cell responses compared to the original spike vaccination only and could thereby outperform mRNA-1273 regarding T-cell responses. At the beginning of the pandemic, major concerns were raised about the waning antibodies after mRNA vaccination. Fortunately, a large study showed that antibody levels quickly decline at first but then stabilized.[88] This supports the use of mRNA vaccines for patients, independent of whether the B cells or T cells may be hampered.

The data presented in this study may have implications for other vaccines as well. Viral complications are one of the major concerns for patients with hematological malignancies, and for this reason, vaccinations against influenza, pneumococcal infection, and herpes zoster virus (VZV) are commonly recommended for patients who are treated with immunosuppressive drugs or stem cell transplantation.[12,89] The vaccination guidelines are based on several factors, including expected vaccine efficacy based on treatment, B- and T-counts in circulation, but also vaccine type.[13-15] One of the issues is that live vaccines are preferably not administered in immunocompromised patients due to the risk of severe side effects.[13,90] Inactivated vaccines are a safer alternative, but they are usually less effective or not yet available.[15] The data presented in this thesis show that mRNA vaccines can induce effective humoral and cellular immune responses in these patients. Furthermore, previous research indicates that mRNA vaccines are more effective compared to other vaccine modalities, supporting their potential as a safe and effective vaccine modality.[84,91] Currently, mRNA vaccines are being developed against multiple infectious diseases, including influenza and VZV.[92] The ability of such vaccines to induce robust humoral and cellular responses will highly depend on the antigen selection and potentially other vaccine modifications.[92]

Concluding remarks

To summarize, in-depth analyses of antigen-specific T cells can provide valuable information to understand protection against severe disease beyond antibody titers. The immune response to SARS-CoV-2 mRNA vaccination was heterogeneous in patients with hematological malignancies. Fortunately, we detected vaccine-specific T-cell responses in most patients, also in the absence of a humoral response. Current vaccination guidelines for immunocompromised patients are frequently based on T-cell counts and/or the predicted ability to develop humoral responses. However, this thesis highlights that this approach is likely unreliable. Importantly, even when vaccine-induced immune responses are diminished compared with those in healthy individuals, immunocompromised patients can still benefit from vaccination, as partial protection is preferable to none. This thesis underscores the importance of investigating the vaccine-induced T-cell responses in patients with hematological malignancies and emphasizes the need for future vaccine development to induce both strong humoral and T-cell immunity to protect vulnerable individuals.

REFERENCES

1. Binayke, A. *et al*. A quest for universal anti-SARS-CoV-2 T cell assay: systematic review, meta-analysis, and experimental validation. *NPJ Vaccines* **9**, 3, doi:10.1038/s41541-023-00794-9 (2024).
2. Sette, A. & Crotty, S. Adaptive immunity to SARS-CoV-2 and COVID-19. *Cell* **184**, 861-880, doi:10.1016/j.cell.2021.01.007 (2021).
3. Tarke, A. *et al*. Early and Polyantigenic CD4 T Cell Responses Correlate with Mild Disease in Acute COVID-19 Donors. *Int J Mol Sci* **23**, doi:10.3390/ijms23137155 (2022).
4. Rydyznski Moderbacher, C. *et al*. Antigen-Specific Adaptive Immunity to SARS-CoV-2 in Acute COVID-19 and Associations with Age and Disease Severity. *Cell* **183**, 996-1012 e1019, doi:10.1016/j.cell.2020.09.038 (2020).
5. Tan, A. T. *et al*. Early induction of functional SARS-CoV-2-specific T cells associates with rapid viral clearance and mild disease in COVID-19 patients. *Cell Rep* **34**, 108728, doi:10.1016/j.celrep.2021.108728 (2021).
6. Sette, A., Sidney, J. & Crotty, S. T Cell Responses to SARS-CoV-2. *Annu Rev Immunol* **41**, 343-373, doi:10.1146/annurev-immunol-101721-061120 (2023).
7. Piechotta, V. *et al*. Effectiveness, immunogenicity, and safety of COVID-19 vaccines for individuals with hematological malignancies: a systematic review. *Blood Cancer J* **12**, 86, doi:10.1038/s41408-022-00684-8 (2022).
8. Wang, K. Y. *et al*. Vaccination efficacy in patients with chronic lymphocytic leukemia. *Leuk Lymphoma* **64**, 42-56, doi:10.1080/10428194.2022.2133538 (2023).
9. Chong, P. P. & Avery, R. K. A Comprehensive Review of Immunization Practices in Solid Organ Transplant and Hematopoietic Stem Cell Transplant Recipients. *Clin Ther* **39**, 1581-1598, doi:10.1016/j.clinthera.2017.07.005 (2017).
10. Kamboj, M. & Shah, M. K. Vaccination of the Stem Cell Transplant Recipient and the Hematologic Malignancy Patient. *Infect Dis Clin North Am* **33**, 593-609, doi:10.1016/j.idc.2019.02.007 (2019).
11. Kim, C., Fang, F., Weyand, C. M. & Goronzy, J. J. The life cycle of a T cell after vaccination - where does immune ageing strike? *Clin Exp Immunol* **187**, 71-81, doi:10.1111/cei.12829 (2017).
12. Tsigrelis, C. & Ljungman, P. Vaccinations in patients with hematological malignancies. *Blood Rev* **30**, 139-147, doi:10.1016/j.blre.2015.10.001 (2016).
13. Lopez, A. *et al*. Vaccination recommendations for the adult immunosuppressed patient: A systematic review and comprehensive field synopsis. *J Autoimmun* **80**, 10-27, doi:10.1016/j.jaut.2017.03.011 (2017).
14. Reynolds, G., Hall, V. G. & Teh, B. W. Vaccine schedule recommendations and updates for patients with hematologic malignancy post-hematopoietic cell transplant or CAR T-cell therapy. *Transpl Infect Dis* **25 Suppl 1**, e14109, doi:10.1111/tid.14109 (2023).
15. Pollard, A. J. & Bijker, E. M. A guide to vaccinology: from basic principles to new developments. *Nat Rev Immunol* **21**, 83-100, doi:10.1038/s41577-020-00479-7 (2021).

16. Groeneweg, L., Loeffen, Y. G. T., Versluys, A. B. & Wolfs, T. F. W. Safety and efficacy of early vaccination with live attenuated measles vaccine for hematopoietic stem cell transplant recipients and solid organ transplant recipients. *Vaccine* **39**, 3338-3345, doi:10.1016/j.vaccine.2021.04.049 (2021).

17. Aiello, A. *et al*. Accuracy of QuantiFERON SARS-CoV-2 research use only assay and characterization of the CD4(+) and CD8(+) T cell-SARS-CoV-2 response: comparison with a homemade interferon-gamma release assay. *Int J Infect Dis* **122**, 841-849, doi:10.1016/j.ijid.2022.07.049 (2022).

18. Yu, E. D. *et al*. Development of a T cell-based immunodiagnostic system to effectively distinguish SARS-CoV-2 infection and COVID-19 vaccination status. *Cell Host Microbe* **30**, 388-399 e383, doi:10.1016/j.chom.2022.02.003 (2022).

19. Mak, W. A., Visser, W., Koeleman, J. G. M. & Ong, D. S. Y. SARS-CoV-2-specific T cell responses: a comparative analysis between QuantiFERON SARS-CoV-2, T-SPOT.COVID, and an in-house Omicron ELISpot. *J Virol Methods* **327**, 114949, doi:10.1016/j.jviromet.2024.114949 (2024).

20. de Vries, R. D. *et al*. Difference in sensitivity between SARS-CoV-2-specific T cell assays in patients with underlying conditions. *J Clin Invest* **131**, doi:10.1172/JCI155499 (2021).

21. Assenmacher, M., Lohning, M. & Radbruch, A. Detection and isolation of cytokine secreting cells using the cytometric cytokine secretion assay. *Curr Protoc Immunol* **Chapter 6**, 6 27 21-26 27 10, doi:10.1002/0471142735.im0627s46 (2002).

22. Ng, D. P. *et al*. Recommendations for using artificial intelligence in clinical flow cytometry. *Cytometry B Clin Cytom* **106**, 228-238, doi:10.1002/cyto.b.22166 (2024).

23. Zandvliet, M. L. *et al*. Detailed analysis of IFNg response upon activation permits efficient isolation of cytomegalovirus-specific CD8+ T cells for adoptive immunotherapy. *J Immunother* **32**, 513-523, doi:10.1097/CJI.0b013e3181a2712c (2009).

24. Kiecker, F. *et al*. Analysis of antigen-specific T-cell responses with synthetic peptides--what kind of peptide for which purpose? *Hum Immunol* **65**, 523-536, doi:10.1016/j.humimm.2004.02.017 (2004).

25. Zhang, W., Moldovan, I., Targoni, O. S., Subbramanian, R. A. & Lehmann, P. V. How much of virus-specific CD8 T cell reactivity is detected with a peptide pool when compared to individual peptides? *Viruses* **4**, 2636-2649, doi:10.3390/v4112636 (2012).

26. Huang, L. *et al*. Herpes zoster mRNA vaccine induces superior vaccine immunity over licensed vaccine in mice and rhesus macaques. *Emerg Microbes Infect* **13**, 2309985, doi:10.1080/22221751.2024.2309985 (2024).

27. Sette, A. & Crotty, S. Immunological memory to SARS-CoV-2 infection and COVID-19 vaccines. *Immunol Rev*, doi:10.1111/imr.13089 (2022).

28. Grifoni, A. *et al*. Targets of T Cell Responses to SARS-CoV-2 Coronavirus in Humans with COVID-19 Disease and Unexposed Individuals. *Cell* **181**, 1489-1501 e1415, doi:10.1016/j.cell.2020.05.015 (2020).

29. Painter, M. M. *et al*. Rapid induction of antigen-specific CD4(+) T cells is associated with coordinated humoral and cellular immunity to SARS-CoV-2 mRNA vaccination. *Immunity* **54**, 2133-2142 e2133, doi:10.1016/j.immuni.2021.08.001 (2021).

30. Oberhardt, V. *et al.* Rapid and stable mobilization of CD8(+) T cells by SARS-CoV-2 mRNA vaccine. *Nature* **597**, 268-273, doi:10.1038/s41586-021-03841-4 (2021).

31. Schnatbaum, K. *et al.* An Overview of Peptides and Peptide Pools for Antigen-Specific Stimulation in T-Cell Assays. *Methods Mol Biol* **2768**, 29-50, doi:10.1007/978-1-0716-3690-9_3 (2024).

32. Phillips, E. *et al.* Comparison of two T-cell assays to evaluate T-cell responses to SARS-CoV-2 following vaccination in naive and convalescent healthcare workers. *Clin Exp Immunol* **209**, 90-98, doi:10.1093/cei/uxac042 (2022).

33. Johansson, A. M. *et al.* Cross-reactive and mono-reactive SARS-CoV-2 CD4+ T cells in prepandemic and COVID-19 convalescent individuals. *PLoS Pathog* **17**, e1010203, doi:10.1371/journal.ppat.1010203 (2021).

34. Kundu, R. *et al.* Cross-reactive memory T cells associate with protection against SARS-CoV-2 infection in COVID-19 contacts. *Nat Commun* **13**, 80, doi:10.1038/s41467-021-27674-x (2022).

35. Le Bert, N. *et al.* SARS-CoV-2-specific T cell immunity in cases of COVID-19 and SARS, and uninfected controls. *Nature* **584**, 457-462, doi:10.1038/s41586-020-2550-z (2020).

36. Loyal, L. *et al.* Cross-reactive CD4(+) T cells enhance SARS-CoV-2 immune responses upon infection and vaccination. *Science* **374**, eabh1823, doi:10.1126/science.abh1823 (2021).

37. Mateus, J. *et al.* Selective and cross-reactive SARS-CoV-2 T cell epitopes in unexposed humans. *Science* **370**, 89-94, doi:10.1126/science.abd3871 (2020).

38. Hombrink, P. *et al.* Mixed functional characteristics correlating with TCR-ligand koff -rate of MHC-tetramer reactive T cells within the naive T-cell repertoire. *Eur J Immunol* **43**, 3038-3050, doi:10.1002/eji.201343397 (2013).

39. Betts, M. R. *et al.* The functional profile of primary human antiviral CD8+ T cell effector activity is dictated by cognate peptide concentration. *J Immunol* **172**, 6407-6417, doi:10.4049/jimmunol.172.10.6407 (2004).

40. Wooldridge, L. *et al.* CD8 controls T cell cross-reactivity. *J Immunol* **185**, 4625-4632, doi:10.4049/jimmunol.1001480 (2010).

41. Bijen, H. M. *et al.* Preclinical Strategies to Identify Off-Target Toxicity of High-Affinity TCRs. *Mol Ther* **26**, 1206-1214, doi:10.1016/j.ymthe.2018.02.017 (2018).

42. Florian, D. M. *et al.* Enhanced and long-lasting SARS-CoV-2 immune memory in individuals with common cold coronavirus cross-reactive T cell immunity. *Front Immunol* **16**, 1501704, doi:10.3389/fimmu.2025.1501704 (2025).

43. Low, J. S. *et al.* Clonal analysis of immunodominance and cross-reactivity of the CD4 T cell response to SARS-CoV-2. *Science* **372**, 1336-1341, doi:10.1126/science.abg8985 (2021).

44. Nelde, A. *et al.* SARS-CoV-2-derived peptides define heterologous and COVID-19-induced T cell recognition. *Nat Immunol* **22**, 74-85, doi:10.1038/s41590-020-00808-x (2021).

45. Dykema, A. G. *et al.* Functional characterization of CD4+ T cell receptors crossreactive for SARS-CoV-2 and endemic coronaviruses. *J Clin Invest* **131**, doi:10.1172/JCI146922 (2021).

46. Stoddard, C. I. *et al.* Epitope profiling reveals binding signatures of SARS-CoV-2 immune response in natural infection and cross-reactivity with endemic human CoVs. *Cell Rep* **35**, 109164, doi:10.1016/j.celrep.2021.109164 (2021).

47. Schulien, I. *et al.* Characterization of pre-existing and induced SARS-CoV-2-specific CD8(+) T cells. *Nat Med* **27**, 78-85, doi:10.1038/s41591-020-01143-2 (2021).

48. Francis, J. M. *et al*. Allelic variation in class I HLA determines CD8(+) T cell repertoire shape and cross-reactive memory responses to SARS-CoV-2. *Sci Immunol* **7**, eabk3070, doi:10.1126/sciimmunol.abk3070 (2022).

49. Jing, L. *et al*. T cell response to intact SARS-CoV-2 includes coronavirus cross-reactive and variant-specific components. *JCI Insight* **7**, doi:10.1172/jci.insight.158126 (2022).

50. Lineburg, K. E. *et al*. CD8(+) T cells specific for an immunodominant SARS-CoV-2 nucleocapsid epitope cross-react with selective seasonal coronaviruses. *Immunity* **54**, 1055-1065 e1055, doi:10.1016/j.immuni.2021.04.006 (2021).

51. Weiskopf, D. *et al*. Phenotype and kinetics of SARS-CoV-2-specific T cells in COVID-19 patients with acute respiratory distress syndrome. *Sci Immunol* **5**, doi:10.1126/sciimmunol.abd2071 (2020).

52. Humbert, M. *et al*. Functional SARS-CoV-2 cross-reactive CD4(+) T cells established in early childhood decline with age. *Proc Natl Acad Sci U S A* **120**, e2220320120, doi:10.1073/pnas.2220320120 (2023).

53. Murray, S. M. *et al*. The impact of pre-existing cross-reactive immunity on SARS-CoV-2 infection and vaccine responses. *Nat Rev Immunol* **23**, 304-316, doi:10.1038/s41577-022-00809-x (2023).

54. Moss, P. The T cell immune response against SARS-CoV-2. *Nat Immunol* **23**, 186-193, doi:10.1038/s41590-021-01122-w (2022).

55. Sagar, M. *et al*. Recent endemic coronavirus infection is associated with less-severe COVID-19. *J Clin Invest* **131**, doi:10.1172/JCI143380 (2021).

56. Vojdani, A., Yaqinuddin, A., Beretta, A. & Reche, P. A. Editorial: Cross-reactive immunity and COVID-19. *Front Immunol* **15**, 1509379, doi:10.3389/fimmu.2024.1509379 (2024).

57. Kaur, N. *et al*. Genetic comparison among various coronavirus strains for the identification of potential vaccine targets of SARS-CoV2. *Infect Genet Evol* **89**, 104490, doi:10.1016/j.meegid.2020.104490 (2021).

58. Lee, C. H. *et al*. Potential CD8+ T Cell Cross-Reactivity Against SARS-CoV-2 Conferred by Other Coronavirus Strains. *Front Immunol* **11**, 579480, doi:10.3389/fimmu.2020.579480 (2020).

59. Bacher, P. *et al*. Low-Avidity CD4(+) T Cell Responses to SARS-CoV-2 in Unexposed Individuals and Humans with Severe COVID-19. *Immunity* **53**, 1258-1271 e1255, doi:10.1016/j.immuni.2020.11.016 (2020).

60. Boerenkamp, L. S. *et al*. Increased CD8 T-cell immunity after COVID-19 vaccination in lymphoid malignancy patients lacking adequate humoral response: An immune compensation mechanism? *Am J Hematol*, doi:10.1002/ajh.26729 (2022).

61. Riise, J. *et al*. Rituximab-treated patients with lymphoma develop strong CD8 T-cell responses following COVID-19 vaccination. *Br J Haematol* **197**, 697-708, doi:10.1111/bjh.18149 (2022).

62. Bitoun, S. *et al*. Rituximab Impairs B Cell Response But Not T Cell Response to COVID-19 Vaccine in Autoimmune Diseases. *Arthritis Rheumatol* **74**, 927-933, doi:10.1002/art.42058 (2022).

63. Keppler-Hafkemeyer, A. *et al*. Potent high-avidity neutralizing antibodies and T cell responses after COVID-19 vaccination in individuals with B cell lymphoma and multiple myeloma. *Nat Cancer* **4**, 81-95, doi:10.1038/s43018-022-00502-x (2023).

64. Zonozi, R. *et al*. T cell responses to SARS-CoV-2 infection and vaccination are elevated in B cell deficiency and reduce risk of severe COVID-19. *Sci Transl Med* **15**, eadh4529, doi:10.1126/scitranslmed.adh4529 (2023).

65. Forconi, F. & Moss, P. Perturbation of the normal immune system in patients with CLL. *Blood* **126**, 573-581, doi:10.1182/blood-2015-03-567388 (2015).

66. van Bruggen, J. A. C. *et al.* Depletion of CLL cells by venetoclax treatment reverses oxidative stress and impaired glycolysis in CD4 T cells. *Blood Adv* **6**, 4185-4195, doi:10.1182/bloodadvances.2022007034 (2022).

67. Riches, J. C. *et al.* T cells from CLL patients exhibit features of T-cell exhaustion but retain capacity for cytokine production. *Blood* **121**, 1612-1621, doi:10.1182/blood-2012-09-457531 (2013).

68. Palma, M. *et al.* T cells in chronic lymphocytic leukemia display dysregulated expression of immune checkpoints and activation markers. *Haematologica* **102**, 562-572, doi:10.3324/haematol.2016.151100 (2017).

69. Camerini, E., Amsen, D., Kater, A. P. & Peters, F. S. The complexities of T-cell dysfunction in chronic lymphocytic leukemia. *Semin Hematol* **61**, 163-171, doi:10.1053/j.seminhematol.2024.04.001 (2024).

70. Solman, I. G. *et al.* Impact of long-term ibrutinib treatment on circulating immune cells in previously untreated chronic lymphocytic leukemia. *Leuk Res* **102**, 106520, doi:10.1016/j.leukres.2021.106520 (2021).

71. Einhaus, J. *et al.* Inhibition of effector B cells by ibrutinib in systemic sclerosis. *Arthritis Res Ther* **22**, 66, doi:10.1186/s13075-020-02153-8 (2020).

72. Morrison, V. A. Infectious complications in patients with chronic lymphocytic leukemia: pathogenesis, spectrum of infection, and approaches to prophylaxis. *Clin Lymphoma Myeloma* **9**, 365-370, doi:10.3816/CLM.2009.n.071 (2009).

73. Loke, J. *et al.* Defective T-cell response to COVID-19 vaccination in acute myeloid leukaemia and myelodysplastic syndromes. *Br J Haematol* **202**, 498-503, doi:10.1111/bjh.18894 (2023).

74. Costantini, B. *et al.* The effects of 5-azacytidine on the function and number of regulatory T cells and T-effectors in myelodysplastic syndrome. *Haematologica* **98**, 1196-1205, doi:10.3324/haematol.2012.074823 (2013).

75. Sato, T., Issa, J. J. & Kropf, P. DNA Hypomethylating Drugs in Cancer Therapy. *Cold Spring Harb Perspect Med* **7**, doi:10.1101/cshperspect.a026948 (2017).

76. Sanchez-Abarca, L. I. *et al.* Immunomodulatory effect of 5-azacytidine (5-azaC): potential role in the transplantation setting. *Blood* **115**, 107-121, doi:10.1182/blood-2009-03-210393 (2010).

77. Vitalle, J. *et al.* Immune defects associated with lower SARS-CoV-2 BNT162b2 mRNA vaccine response in aged people. *JCI Insight* **7**, doi:10.1172/jci.insight.161045 (2022).

78. Demaret, J. *et al.* Impaired Functional T-Cell Response to SARS-CoV-2 After Two Doses of BNT162b2 mRNA Vaccine in Older People. *Front Immunol* **12**, 778679, doi:10.3389/fimmu.2021.778679 (2021).

79. Kirkizlar, T. A. *et al.* Incidence and predisposing factors of infection in patients treated with hypomethylating agents. *Leuk Res* **127**, 107043, doi:10.1016/j.leukres.2023.107043 (2023).

80. Shargian-Alon, L., Gurion, R., Raanani, P., Yahav, D. & Gafter-Gvili, A. Hypomethylating Agents-associated Infections-Systematic Review and Meta-analysis of Randomized Controlled Trials. *Clin Lymphoma Myeloma Leuk* **18**, 603-610 e601, doi:10.1016/j.clml.2018.05.017 (2018).

81. Vilorio-Marques, L. *et al*. Relevance of infections on the outcomes of patients with myelodysplastic syndromes, chronic myelomonocytic leukemia, and acute myeloid leukemia treated with hypomethylating agents: a cohort study from the GESMD. *Ther Adv Hematol* **13**, 20406207221127547, doi:10.1177/20406207221127547 (2022).

82. Janssen, M. J. M. *et al*. Predictive factors for vaccine failure to guide vaccination in allogeneic hematopoietic stem cell transplant recipients. *Bone Marrow Transplant* **56**, 2922-2928, doi:10.1038/s41409-021-01437-0 (2021).

83. Fiolet, T., Kherabi, Y., MacDonald, C. J., Ghosn, J. & Peiffer-Smadja, N. Comparing COVID-19 vaccines for their characteristics, efficacy and effectiveness against SARS-CoV-2 and variants of concern: a narrative review. *Clin Microbiol Infect* **28**, 202-221, doi:10.1016/j.cmi.2021.10.005 (2022).

84. Zhang, Z. *et al*. Humoral and cellular immune memory to four COVID-19 vaccines. *Cell* **185**, 2434-2451 e2417, doi:10.1016/j.cell.2022.05.022 (2022).

85. Greenberger, L. M. *et al*. Anti-spike T-cell and Antibody Responses to SARS-CoV-2 mRNA Vaccines in Patients with Hematologic Malignancies. *Blood Cancer Discov* **3**, 481-489, doi:10.1158/2643-3230.BCD-22-0077 (2022).

86. Heinz, F. X. & Stiasny, K. Distinguishing features of current COVID-19 vaccines: knowns and unknowns of antigen presentation and modes of action. *NPJ Vaccines* **6**, 104, doi:10.1038/s41541-021-00369-6 (2021).

87. Arieta, C. M. *et al*. The T-cell-directed vaccine BNT162b4 encoding conserved non-spike antigens protects animals from severe SARS-CoV-2 infection. *Cell* **186**, 2392-2409 e2321, doi:10.1016/j.cell.2023.04.007 (2023).

88. Srivastava, K. *et al*. SARS-CoV-2-infection- and vaccine-induced antibody responses are long lasting with an initial waning phase followed by a stabilization phase. *Immunity* **57**, 587-599 e584, doi:10.1016/j.immuni.2024.01.017 (2024).

89. Rieger, C. T. *et al*. Anti-infective vaccination strategies in patients with hematologic malignancies or solid tumors-Guideline of the Infectious Diseases Working Party (AGIHO) of the German Society for Hematology and Medical Oncology (DGHO). *Ann Oncol* **29**, 1354-1365, doi:10.1093/annonc/mdy117 (2018).

90. Righi, E. *et al*. A Review of Vaccinations in Adult Patients with Secondary Immunodeficiency. *Infect Dis Ther* **10**, 637-661, doi:10.1007/s40121-021-00404-y (2021).

91. Monslow, M. A. *et al*. Immunogenicity generated by mRNA vaccine encoding VZV gE antigen is comparable to adjuvanted subunit vaccine and better than live attenuated vaccine in nonhuman primates. *Vaccine* **38**, 5793-5802, doi:10.1016/j.vaccine.2020.06.062 (2020).

92. Pardi, N. & Krammer, F. mRNA vaccines for infectious diseases - advances, challenges and opportunities. *Nat Rev Drug Discov* **23**, 838-861, doi:10.1038/s41573-024-01042-y (2024).

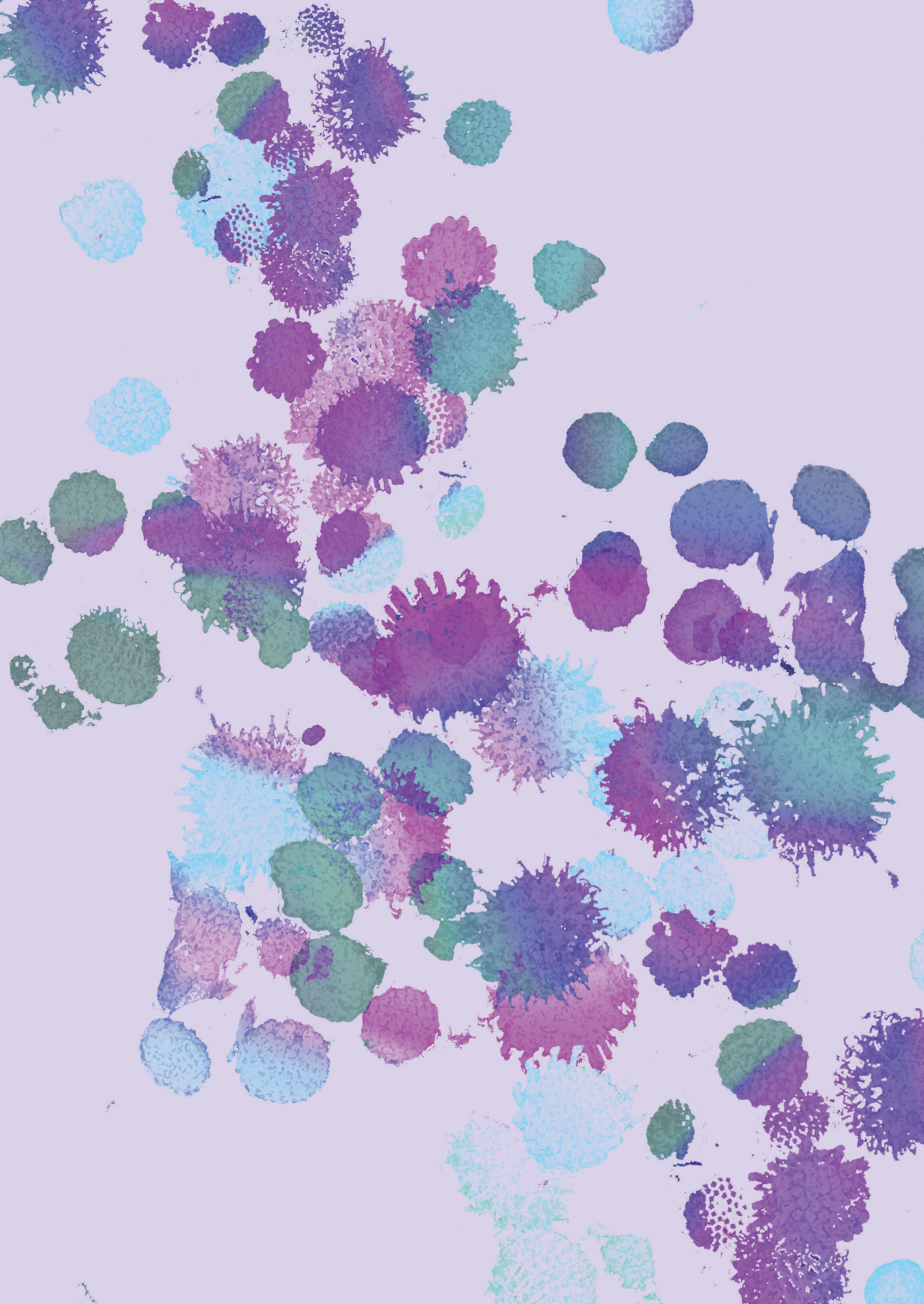

Appendices

NEDERLANDSE SAMENVATTING

CURRICULUM VITAE

LIST OF PUBLICATIONS

ACKNOWLEDGEMENTS

NEDERLANDSE SAMENVATTING

Dit proefschrift met als titel *"Primaire SARS-CoV-2-specifieke T-celresponsen in patiënten met hematologische aandoeningen"*, gaat over hoe goed het immuunsysteem van patiënten met verschillende bloedziekten reageert op de COVID-19-mRNA-vaccinaties. We weten hoe gezonde individuen met een goed functionerend immuunsysteem reageren op de mRNA-vaccinaties tegen het virus dat COVID-19 veroorzaakt, SARS-CoV-2. Dit kunnen we vergelijken met patiënten van wie we verwachten dat zij een verminderd immuunsysteem hebben, zoals vaak het geval is bij patiënten met bloedziekten. De pandemie leent zich goed voor dit soort onderzoek, omdat iedereen voor de eerste keer werd blootgesteld aan SARS-CoV-2 of de vaccinatie. We kunnen daardoor goed in kaart brengen hoe het immuunsysteem van deze patiënten functioneert wanneer het voor het eerst een pathogeen of vaccinatie tegenkomt zonder vertroebeling door immuniteit van eerdere SARS-CoV-2 infecties of vaccinaties. In deze sectie wordt een samenvatting gegeven van het proefschrift, beginnend met achtergrondinformatie over het onderwerp gevolgd door de resultaten van de onderzoekshoofdstukken.

HET IMMUUNSYSTEEM

Het immuunsysteem is een verzameling van verschillende typen immuuncellen met uiteenlopende functies, die gezamenlijk bijdragen aan het effectief opruimen van pathogenen en zieke cellen. Immuuncellen reageren op lichaamsvreemde eiwitten of gevaarsignalen van andere cellen. Grofweg is het immuunsysteem op te delen in twee onderdelen: het aangeboren en het aangeleerde immuunsysteem. Dit systeem is in staat om pathogenen snel en effectief aan te vallen. Lukt dit onvoldoende, dan komt het aangeleerde immuunsysteem in actie. Het aangeleerde immuunsysteem komt trager op gang, maar is specifiek gericht tegen het pathogeen én vormt geheugen. Dit betekent dat als het specifieke pathogeen nogmaals in het lichaam aanwezig is, het aangeleerde immuunsysteem wél snel kan reageren. Daarom verloopt de eerste infectie met een bepaalde bacterie of virus vaak heftiger dan een volgende infectie, die meestal milder is.

HET AANGELEERDE IMMUUNSYSTEEM

Het aangeleerde immuunsysteem, ook wel het adaptieve immuunsysteem genoemd, bestaat uit B- en T-cellen die ontstaan in het beenmerg. De T-cellen gaan vervolgens

naar de thymus (ook wel zwezerik genoemd) voor verdere ontwikkeling. B-cellen produceren antistoffen (ook wel antilichamen genoemd) die sterk kunnen binden aan een virus of bacterie, waardoor het pathogeen niet meer kan infecteren en het zorgt ervoor dat de andere immuuncellen het virus sneller kunnen opruimen. Er bestaan verschillende soorten antilichamen met uiteenlopende functies en bindingsterkte. T-cellen bestaan hoofdzakelijk uit twee soorten, afhankelijk van of ze het eiwit CD4 of CD8 tot expressie brengen. CD4-positieve (CD4+) T-cellen helpen B-cellen optimaal te functioneren en scheiden stimulerende eiwitten uit die andere immuuncellen aansturen. CD8+ T-cellen zijn goed in het direct opruimen van virusgeïnfecteerde cellen. Bij een goed werkend immuunsysteem worden alle drie de componenten van het aangeleerde immuunsysteem geactiveerd bij een infectie of vaccinatie. Zoals eerder aangegeven, duurt het soms enkele dagen voordat het aangeleerde immuunsysteem volledig actief wordt. Dit komt doordat voor het specifieke pathogeen eerst de juiste B- en T-cellen moeten worden geselecteerd, aangepast en vermeerderd. Dit zorgt ervoor dat de immuunreactie effectief is, maar ook specifiek. Zodra de B en T-cellen eenmaal gevonden en aangepast zijn, blijven ze in grotere aantallen aanwezig in het bloed, waardoor bij een tweede infectie deze B- en T-cellen al snel en effectief kunnen reageren. Het pathogeen wordt dan dus veel sneller opgeruimd. Dit fenomeen noemen we immuniteit of immunologisch geheugen.

DE PANDEMIE

Het *severe acute respiratory syndrome coronavirus 2* (SARS-CoV-2) virus circuleerde voor het eerst in de menselijke populatie in 2019 en veroorzaakte in 2020 een pandemie. De ernst van de infectie varieerde van geen symptomen tot ernstige *coronavirus disease 2019* (COVID-19). De verscheidenheid aan symptomen kwam door meerdere factoren, die deels nog onbekend waren omdat nog niemand eerder besmet was geweest met het virus. Hierdoor had nog niemand immunologisch geheugen en moest het aangeleerde immuunsysteem nog worden geactiveerd. De ernst van de symptomen was sterk afhankelijk van de eerste reactie van het aangeboren immuunsysteem en de mate waarin het aangeleerde immuunsysteem reageerde. Gezonde mensen hebben meestal een goed functionerend immuunsysteem, maar mensen met een verzwakt immuunsysteem door ziekte, ouderdom of therapie zijn extra gevoelig voor een ernstig beloop van COVID-19. Gelukkig werden snel effectieve en veilige vaccinaties ontwikkeld tegen SARS-CoV-2, mede doordat de genetische opbouw van het virus snel beschikbaar was, door eerdere ontwikkelingen in mRNA-vaccinatietechnologie, en door het parallel uitvoeren van verschillende fasen van het vaccinatieontwikkelingsproces. Sinds 2021 hebben de meeste mensen een

vaccinatie en/of infectie doorgemaakt en daardoor immunologisch geheugen met het aangeleerde immuunsysteem opgebouwd tegen het virus. Tijdens de pandemie was er grote interesse in het begrijpen waarom het immuunsysteem bij bepaalde groepen mensen anders reageerde tijdens SARS-CoV-2 infectie en na vaccinatie. Om die reden zijn er tijdens de pandemie veel bloedmonsters opgeslagen. Deze monsters vormen uniek materiaal waarmee we kunnen onderzoeken hoe het immuunsysteem reageert als het voor het eerst een pathogeen tegenkomt.

MRNA VACCINATIE

Vaccinatie maakt gebruik van de mogelijkheid van het aangeleerde immuunsysteem om geheugen op te bouwen. Een vaccin bevat meestal onderdelen of een verzwakte versie van het pathogeen waarvoor bescherming gewenst is. Op deze manier wordt het lichaam wel blootgesteld aan het pathogeen, maar zonder de nadelen van een daadwerkelijke infectie. Een vaccinatie wordt in een spier toegediend en het immuunsysteem reageert direct, doordat cellen worden blootgesteld aan lichaamsvreemde eiwitten. Zo wordt immunologisch geheugen opgebouwd tegen het pathogeen. Er bestaan verschillende typen vaccinaties, waarvan de mRNA-vaccinatie, zoals gebruikt voor COVID-19, één van de soorten is. De verschillende typen vaccinaties verwijzen meestal naar de manier waarop de pathogeeneiwitten worden ingebracht. Bij een mRNA-vaccinatie gebeurt dit door middel van mRNA. mRNA is een klein en snel afbreekbaar afgietsel van DNA dat codeert voor hoe een eiwit gemaakt moet worden. In elke cel wordt DNA omgezet in mRNA en vervolgens in eiwit. DNA blijft stabiel aanwezig in de cel, maar mRNA wordt na de aanmaak van het eiwit direct weer afgebroken. In het mRNA vaccin tegen COVID-19 zit mRNA dat codeert voor een belangrijk eiwit van SARS-CoV-2: het spike-eiwit. Dit eiwit is essentieel voor het virus om cellen binnen te kunnen dringen. Het losse eiwit kan gelukkig geen kwaad, maar ons immuunsysteem reageert er wel op omdat wij zelf geen spike-eiwit hebben. Hierdoor bouwt het immuunsysteem immunologisch geheugen op tegen het spike-eiwit, zonder dat er een infectie optreedt. Wanneer SARS-CoV-2 vervolgens het lichaam wil infecteren, herkent het immuunsysteem het spike-eiwit aan de buitenkant van het virus en blokkeert het direct de verspreiding. Tijdens de pandemie en in vele onderzoeken is gebleken dat mRNA-vaccinaties effectief zijn in het activeren van het aangeleerde immuunsysteem en daarmee de symptomen en verspreiding verminderen.

PATIËNTEN MET EEN VERMINDERD IMMUUNSYSTEEM

Patiënten met bloedkanker, zoals leukemie of lymfoom, hebben vaak een minder goed functionerend immuunsysteem. Dit kan veroorzaakt worden door de kanker zelf, maar ook door de therapie. Het is moeilijk om een therapie te ontwikkelen die uitsluitend kankercellen aanvalt en gezonde cellen, zoals immuuncellen, onaangetast laat. Daarnaast kunnen kankercellen gezonde immuuncellen in hun functie belemmeren. Infecties vormen daarom een groter probleem bij deze patiëntengroep. We weten dat deze patiënten een verminderd immuunsysteem hebben, maar welke onderdelen precies minder goed functioneren is nog niet helemaal duidelijk. Dit kan onderzocht worden door te kijken hoe hun immuunsysteem reageert op de mRNA-vaccinaties. Hoe het immuunsysteem reageert op een vaccinatie kan in het laboratorium worden gemeten, zowel oppervlakkig als heel gedetailleerd. Bij grootschalige screenings wordt vaak slechts één type antilichaam gemeten (titerbepaling) om te bepalen of een individu gereageerd heeft op een vaccinatie. Voor de meeste gezonde individuen is dit voldoende. Bij patiënten met bloedkanker wordt echter verwacht dat het immuunsysteem verminderd functioneert, waardoor de aanmaak van de antistoffen na vaccinatie mogelijk beperkt is. Een titerbepaling geeft dan onvoldoende beeld, omdat de T-cellen mogelijk wel goed functioneren. Dit is belangrijke informatie, bijvoorbeeld om te bepalen welk vaccin het meest effectief is, wanneer vaccinatie het meest zinvol is, en om de invloed van ziekte of therapie op het aangeleerde immuunsysteem beter te begrijpen. Idealiter zouden bij screenings dus ook de T-cellen gemeten worden. Het meten van T-cellen is echter arbeidsintensief en kostbaar, en kan daardoor niet routinematig worden uitgevoerd. Hierdoor werd het T-celgeheugen bij gezonde individuen snel in kaart gebracht, maar bij bepaalde patiëntengroepen bleef deze kennis achter.

DIT PROEFSCHRIFT

Dit proefschrift beschrijft onderzoek naar de manier waarop T-cellen reageren op SARS-CoV-2-vaccinatie bij patiënten met verschillende bloedziekten. In **hoofdstuk 2** onderzoeken we kruisreactieve T-cellen: T-cellen die niet op één enkel virus reageren, maar op twee of meer. We ontdekten geheugen-T-cellen die reageerden op SARS-CoV-2, terwijl deze cellen waren afgenomen en ingevroren vóór de pandemie. Deze T-cellen hadden dus geheugen tegen een ander virus, maar reageerden toevallig ook op SARS-CoV-2. Zulke T-cellen kunnen dan mogelijk alvast wat bescherming bieden. Daarnaast maken ze de interpretatie van de resultaten complexer, omdat ze moeilijk te onderscheiden zijn van T-cellen die direct geheugen hebben gevormd tegen SARS-

CoV-2. In hoofdstuk 2 hebben we een deel van deze T-cellen in kaart gebracht en onderzocht tegen welk virus zij oorspronkelijk geheugen hadden gevormd. We hadden als hypothese dat dit door het cytomegalovirus (CMV) komt, onder andere doordat de geheugen T-cellen tegen dit virus in grote hoeveelheden aanwezig zijn in het bloed. Dit was ook het geval voor deze kruisreactieve T-cellen. Deze hypothese was echter controversieel omdat CMV en SARS-CoV-2 weinig op elkaar lijken, waardoor de kans op kruisreactiviteit klein werd geacht. Om dit te onderzoeken, analyseerden we bloed van 67 gezonde individuen om te bepalen of zij degelijke kruisreactieve T-cellen hadden. Bij een aantal van hen werden deze cellen inderdaad gevonden, en hun aanwezigheid correleerde met de aanwezigheid van geheugen-T-cellen tegen CMV. Door deze T-cellen uit het bloed te isoleren en op te kweken, konden we bevestigen dat zij zowel SARS-CoV-2 als CMV herkenden. Vervolgens onderzochten we of deze T-cellen beide virussen even effectief konden opruimen en of ze actief waren bij patiënten met ernstige COVID-19. We zagen dat deze T-cellen minder effectief waren in het opruimen van SARS-CoV-2- en niet actief leken te zijn bij patiënten met ernstige COVID-19. Ze zijn dus minder effectief dan T-cellen die direct geheugen tegen SARS-CoV-2 hebben gevormd. Dit hoofdstuk laat zien dat de kruisreactiviteit tussen twee onverwachte virussen kan optreden, maar dat detectie van zulke T-cellen niet automatisch betekent dat zij functioneel relevant zijn.

In **hoofdstuk 3** hebben we de antilichaamtiters en T-cellen na SARS-CoV-2-vaccinatie onderzocht bij patiënten met aplastische anemie. Aplastische anemie is een auto-immuunziekte waarbij de stamcellen in het beenmerg verdwijnen, wat onder andere leidt tot een slecht functionerend immuunsysteem. Normaal gesproken is het belangrijk dat deze patiënten in een pandemie zo snel mogelijk gevaccineerd worden, maar volgens de destijdse richtlijnen moest men hier voorzichtig mee zijn. Dit was gebaseerd op kleine studies die een mogelijke opleving van de ziekte na vaccinatie aantoonden en op de verwachting dat de vaccinatie bij patiënten weinig effect zou hebben. Dit laatste zou vooral het geval zijn bij vaccineren kort na intensieve behandelingen, maar de richtlijnen maakten daar geen onderscheid in. Onze studie liet zien dat patiënten die in het verleden zware behandelingen hadden ondergaan, inmiddels goed immunologisch geheugen konden opbouwen door vaccinatie. Bovendien zagen we geen aanwijzingen voor een opleving van de ziekte. Onze data ondersteunen dus juist het vaccineren van deze patiëntengroep.

In **hoofdstuk 4** richtten we ons op de antilichaamtiters en T-cellen na SARS-CoV-2-vaccinatie bij een andere groep patiënten, namelijk patiënten met bloedkanker. Dit betrof onder meer patiënten met chronische lymfatische leukemie (CLL), lymfoom, en multipel myeloom (ziekte van Kahler). Deze patiënten maken vaak weinig antistoffen

aan omdat de kankercellen sterk lijken op gezonde B-cellen. Daardoor verdringen zij gezonde B-cellen, of de therapie tast ook deze cellen aan. Slecht functionerende B-cellen leiden tot lage antilichaamtiters. We zagen inderdaad dat vooral patiënten met CLL of lymfoom lage antilichaamtiters hadden na vaccinatie. Wanneer we echter naar de T-cellen keken, zagen we een ander beeld: het merendeel van de patiënten bouwde goede T-celgeheugen op na vaccinatie. Het leek erop dat patiënten die geen antistoffen aanmaakten, juist sterkte T-celgeheugen aanmaakte. Daardoor was het aantal patiënten dat zowel geen antistoffen als geen T-celgeheugen had, zeer klein.

In **hoofdstuk 5** hebben we de onderzoeksgroep uitgebreid naar zestien verschillende subgroepen, onderverdeeld op type bloedkanker en therapie. De behandelingen varieerden van doelgerichte therapie tot stamceltransplantatie en immunotherapie. Ook in deze grotere groep konden we onze eerdere observatie bevestigen: de meeste patiënten met bloedkanker konden nog steeds goed T-celgeheugen aanmaken na SARS-CoV-2-vaccinatie. Slechts zelden zagen we patiënten zonder zowel antistoffen als T-celgeheugen. Daarnaast onderzochten we de functionaliteit van de T-cellen, dus hoe goed zij stimulerende eiwitten kunnen uitscheiden na blootstelling aan viruseiwitten. Zo konden we nauwkeuriger vaststellen in welke patiëntengroepen de T-cellen goed functioneerden en in welke niet. Opvallend was dat sommige patiëntengroepen, ondanks een laag aantal T-cellen in het bloed, toch goed T-celgeheugen konden ontwikkelen. Deze bevindingen helpen verklaren waarom sommige patiënten gevoeliger zijn voor infecties dan anderen, en wat het effect is van bloedkanker of therapie op het adaptieve immuunsysteem. Adviezen over vaccinatie bij patiënten met bloedkanker worden doorgaans gebaseerd op de verwachte antistoftiter en het aantal T-cellen in bloed. Onze resultaten tonen echter aan dat dit geen betrouwbare graadmeters zijn. De meeste patiënten bouwen wél enig van immunologisch geheugen op. Een zekere mate van geheugen is beter dan geen, zeker wanneer het virus actief circuleert in de populatie.

CONCLUSIE

Het immuunsysteem bestaat uit meerdere onderdelen die gezamenlijk bijdragen aan de bescherming tegen ernstige infecties. Immunologisch geheugen kan worden opgebouwd door B-cellen (antistoffen) en T-cellen. Tijdens de pandemie werd de wereldbevolking blootgesteld aan een virus waarvoor niemand immunologisch geheugen had, wat een unieke gelegenheid bood om de opbouw van dit geheugen te bestuderen. In dit proefschrift is dit onderzocht in de context van de COVID-19-mRNA-vaccinaties. Meestal worden alleen antistoffen gemeten als maat voor immunologisch

geheugen, maar dit is vaak onvoldoende bij immuungecompromitteerde patiënten. Daarom zijn in dit onderzoek bij verschillende patiëntengroepen zowel antistoffen als T-celgeheugen na vaccinatie gemeten. We ontdekten dat het ontbreken van antistoffen na SARS-CoV-2-vaccinatie niet automatisch betekent dat er geen T-celgeheugen is. Daarnaast bleek dat slechts weinig patiënten noch antistoffen noch T-celgeheugen ontwikkelden, en dat dit niet kon worden voorspeld op basis van het aantal T-cellen in het bloed. Dit proefschrift laat zien dat patiënten met een verzwakt immuunsysteem baat hebben bij mRNA-vaccinaties. De vaccinaties bieden hen de mogelijkheid om immunologisch geheugen op te bouwen, wat bijdraagt aan een snellere en effectievere opruiming van het virus.

CURRICULUM VITAE

Cilia Rosan Pothast is geboren op 3 augustus 1994 in Almelo en groeide op in Egmond aan den Hoef. Na het afronden van het VWO aan het PCC in Heiloo en Alkmaar, besloot zij de bachelor Gezondheid & Leven te doen aan de Vrije Universiteit Amsterdam. In het laatste jaar van de studie liep zij stage bij het Cancer Center Amsterdam van het VUmc, waar zij onderzoek deed naar induceerbare CD38-CAR T-celtherapie. In 2018 verliet zij Amsterdam om te beginnen aan de Research Master Biomedische Wetenschappen aan de Universiteit Leiden. Tijdens deze opleiding voltooide zij haar eerste stage bij de afdeling Oncologie van het LUMC onder leiding van dr. Ferenc Scheeren, met als doel het ontwikkelen van een genetische modificatiemethode om kankeronderzoek te bevorderen. Vervolgens voltooide zij haar laatste stage bij de afdeling Hematologie onder leiding van dr. Laura Morton, waar zij werkte aan het verbeteren van immuuntherapie door het toepassen van CRISPR-Cas9. Vanuit deze laatste masterstage kreeg zij de mogelijkheid om dit project voort te zetten in de vorm van een promotietraject, onder begeleiding van promotoren prof. dr. Fred Falkenburg en prof. dr. Mirjam Heemskerk. Kort na de start van dit traject begon de COVID-19-pandemie, wat ervoor zorgde dat de werkzaamheden verschoven naar het beter begrijpen van T-cellen tijdens deze ziekte en de vaccinatie tegen SARS-CoV-2, met als resultaat dit proefschrift. In september 2025 is Cilia begonnen aan een gecombineerde postdoctorale functie bij het LUMC, onder begeleiding van prof. dr. Mirjam Heemskerk, en bij het Amsterdam UMC, onder begeleiding van dr. Inger Nijhof, dr. Caroline Rutten, dr. Bram Goorhuis en prof. dr. Mette Hazenberg. In deze functie richt zij zich zowel op onderzoek naar T-cel-immuniteit als op het verbeteren van immuuntherapieën.

LIST OF PUBLICATIONS

Boerenkamp, L. S.*, **Pothast, C. R.***, Dijkland, R. C., van Dijk, K., van Gorkom, G. N. Y., van Loo, I. H. M., Wieten, L., Halkes, C. J. M., Heemskerk, M. H. M., & Van Elssen, C. (2022). Increased CD8 T-cell immunity after COVID-19 vaccination in lymphoid malignancy patients lacking adequate humoral response: An immune compensation mechanism? *Am J Hematol*. https://doi.org/10.1002/ajh.26729

Hanssen, J. L. J., Stienstra, J., Boers, S. A., **Pothast, C. R.**, Zaaijer, H. L., Tjon, J. M., Heemskerk, M. H. M., Feltkamp, M. C. W., & Arend, S. M. (2021). Convalescent Plasma in a Patient with Protracted COVID-19 and Secondary Hypogammaglobulinemia Due to Chronic Lymphocytic Leukemia: Buying Time to Develop Immunity? *Infect Dis Rep*, 13(4), 855-864. https://doi.org/10.3390/idr13040077

Klobuch, S., Lim, J. J., van Balen, P., Kester, M. G. D., de Klerk, W., de Ru, A. H., **Pothast, C. R.**, Jedema, I., Drijfhout, J. W., Rossjohn, J., Reid, H. H., van Veelen, P. A., Falkenburg, J. H. F.*, & Heemskerk, M. H. M.* (2022). Human T cells recognize HLA-DP-bound peptides in two orientations. *Proc Natl Acad Sci USA*, 119(49), e2214331119. https://doi.org/10.1073/pnas.2214331119

Mbow, M.*, Hoving, D.*, Cisse, M., Diallo, I., Honkpehedji, Y. J., Huisman, W., **Pothast, C. R.**, Jongsma, M. L. M., Konig, M. H., de Kroon, A. C., Linh, L. T. K., Azimi, S., Tak, T., Kruize, Y. C. M., Kurniawan, F., Dia, Y. A., Zhang, J. L. H., Prins, C., Roukens, A. H. E., de Vries, J. J. C., Wammes, L. J., Smits, H. H., Adegnika, A. A., Zlei, M., Kuijpers, T. W., Wieske, L., Dieye, A., Mboup, S., Kremsner, P. G., Eftimov, F., Velavan, T. P., Berlin, I., Heemskerk, M. H. M., Yazdanbakhsh, M., Jochems, S. P., consortium, B.-C., & team, C.-L. U. M. C. s. (2024). Immune responses to SARS-CoV-2 in sub-Saharan Africa and western Europe: a retrospective, population-based, cross-sectional study. *Lancet Microbe*, 100942. https://doi.org/10.1016/j.lanmic.2024.07.005

Morton, L. T., Reijmers, R. M., Wouters, A. K., Kweekel, C., Remst, D. F. G., **Pothast, C. R.**, Falkenburg, J. H. F., & Heemskerk, M. H. M. (2020). Simultaneous Deletion of Endogenous TCRalphabeta for TCR Gene Therapy Creates an Improved and Safe Cellular Therapeutic. *Mol Ther*, 28(1), 64-74. https://doi.org/10.1016/j.ymthe.2019.10.001

Pothast, C. R., Dijkland, R. C., Thaler, M., Hagedoorn, R. S., Kester, M. G. D., Wouters, A. K., Hiemstra, P. S., van Hemert, M. J., Gras, S., Falkenburg, J. H. F., & Heemskerk, M. H. M. (2022). SARS-CoV-2-specific CD4(+) and CD8(+) T cell responses can originate from cross-reactive CMV-specific T cells. *Elife*, 11. https://doi.org/10.7554/eLife.82050

Pothast, C. R.*, Hofsink, Q.*, Haggenburg, S., Dijkland, R. C., Van de Meent, M., Van Dijk, K., Bhoekhan, M. S., Haverkate, N. J. E., Van Meerloo, J., Falkenburg, J. H. F., De Groen, R. A. L., Broers, A. E. C., Van Doesum, J. A., Van Binnendijk, R. S., Den Hartog, G., Lissenberg-Witte, B. I., Kater, A. P., Smits, G. P., Wouters, D., van Leeuwen, E.M.M., Bontkes, H. J., Kootstra, N. A., Vogels-Nooijen, S., van Baarle, D., de Vries, R. D., van Meerten, T., Mutsaerts, P. G. N. J., Goorhuis, A., Nijhof, I.S., Hazenberg, M. D., Heemskerk, M. H. M.*, Rutten C. E.*, and COBRA KAI study team. (2025) T-cell and antibody responses in immunocompromised patients with hematologic malignancies indicate strong potential of SARS-CoV-2 mRNA vaccines. *Haematologica*. https://doi.org/10.3324/haematol.2024.287136

Pothast, C. R.*, van Dijk, K.*, Pool, E. S., Halkes, C. J. M., Heemskerk, M. H. M.*, & Tjon, J. M.* (2022). SARS-CoV-2 mRNA vaccination of aplastic anemia patients is safe and effective. *Am J Hematol*. https://doi.org/10.1002/ajh.26780

Prins, M. L. M., Roozen, G. V. T., **Pothast, C. R.**, Huisman, W., van Binnendijk, R., den Hartog, G., Kuiper, V. P., Prins, C., Janse, J. J., Lamers, O. A. C., Koopman, J. P. R., Kruithof, A. C., Kamerling, I. M. C., Dijkland, R. C., de Kroon, A. C., Azimi, S., Feltkamp, M. C. W., Kuijer, M., Jochems, S. P., Heemskerk, M. H. M., Rosendaal, F. R., Roestenberg, M., Visser, L. G., & Roukens, A. H. E. (2024). Immunogenicity and reactogenicity of intradermal mRNA-1273 SARS-CoV-2 vaccination: a non-inferiority, randomized-controlled trial. *NPJ Vaccines*, 9(1), 1. https://doi.org/10.1038/s41541-023-00785-w

Roozen, G. V. T.*, Prins, M. L. M.*, Prins, C., Janse, J. J., de Gruyter, H. L. M., **Pothast, C. R.**, Huisman, W., Koopman, J. P. R., Lamers, O. A. C., Kuijer, M., Myeni, S. K., van Binnendijk, R. S., Hartog, G. D., Heemskerk, M. H. M., Jochems, S. P., Feltkamp, M. C. W., Kikkert, M., Rosendaal, F. R., Roestenberg, M.,...Roukens, A. H. E. (2024). Intradermal delivery of the third dose of the mRNA-1273 SARS-CoV-2 vaccine: safety and immunogenicity of a fractional booster dose. *Clin Microbiol Infect*, 30(7), 930–936. https://doi.org/10.1016/j.cmi.2024.03.028

Roukens, A. H. E., **Pothast, C. R.***, Konig, M.*, Huisman, W.*, Dalebout, T., Tak, T., Azimi, S., Kruize, Y., Hagedoorn, R. S., Zlei, M., Staal, F. J. T., de Bie, F. J., van Dongen, J. J. M., Arbous, S. M., Zhang, J. L. H., Verheij, M., Prins, C., van der Does, A. M., Hiemstra, P. S., de Vries, J. J. C., Janse, J. J., Roestenberg, M., Myeni, S. K., Kikkert, M., Yazdanbakhsh, M., Heemskerk, M. H. M., Smits, H. H.*, Jochems, S. P.*, in collaboration with BEAT-COVID group & COVID-19 LUMC group (2022). Prolonged activation of nasal immune cell populations and development of tissue-resident SARS-CoV-2-specific CD8(+) T cell responses following COVID-19. *Nat Immunol*, 23(1), 23-32. https://doi.org/10.1038/s41590-021-01095-w

Huisman, W., Azimi, S., Nguyen, Y. N., de Kroon, A. C., de Ruiter, K., Tahapary, D. L., Manurung, M. D., **Pothast, C. R.**, Kruize, Y., Heemskerk, M. H. M., Supali, T., Visser, L. G., Roukens, A. H. E., Yazdanbakhsh, M., Jochems, S. P. (2025). Functional screening reveals geographical variation in innate immune capacity and a role for TLR8 in mRNA vaccine responses. *iScience*, 28(11). https://doi.org/10.1016/j.isci.2025.113839

Zlei, M.*, Sidorov, I. A.*, Joosten, S. A., Heemskerk, M. H. M., Myeni, S. K., **Pothast, C. R.**, de Brouwer, C. S., Boomaars-van der Zanden, A. L., van Meijgaarden, K. E., Morales, S. T., Wessels, E., Janse, J. J., Goeman, J. J., Cobbaert, C. M., Kroes, A. C. M., Cannegieter, S. C., Roestenberg, M., Visser, L. G., Kikkert, M., Feltkamp, M. C. W., Arbous, S. M., Staal, F. J. T., Ottenhoff, T. H. M., van Dongen, J. J. M., Roukens, A. H. E., de Vries, J. J. C., in collaboration with BEAT-COVID group & COVID-19 LUMC group (2022). Immune Determinants of Viral Clearance in Hospitalised COVID-19 Patients: Reduced Circulating Naive CD4+ T Cell Counts Correspond with Delayed Viral Clearance. *Cells*, 11(17). https://doi.org/10.3390/cells11172743

Haggenburg, S., **Pothast, C. R.**, Hofsink, Q., Haverkate, N. J. E., Bhoekhan, M.S., Claireaux, M., van Binnendijk, R. S., den Hartog, G., Lissenberg-Witte, B. I., de Vries, R. D., van Tuijn, C., Biemond, B. J., Nur, E., Geurts van Kessel, C. H., Mutsaers, P. G. N. J., Broers, A. E. C., Goorhuis, A., Nijhof, I. S., van Gils, M. J., Heemskerk, M. H. M., Hazenberg, M. D., Rutten, C. E. (2025) Humoral and cellular immunogenicity of COVID-19 mRNA vaccination in patients with sickle cell disease on hydroxyurea. *Accepted for publication in Blood Advances*

Haggenburg, S., van Coillie, J., Reuvekamp, T., **Pothast, C. R.**, Hofsink, Q., Lissenberg-Witte, B. I., Bhoekhan, M. S., Haverkate, N. J. E., van Meent, M., van Binnendijk, R. S., den Hartog, G., van Doesum, J. A., Broers, A. E. C., van Meerten, T., Mutsaers, P. G. N. J., Rots, N. Y., de Vries, R., Visser, R., Wang, W., Nouta, J., Wuhrer, M., van Gils, M. J., Goorhuis, A., Nijhof, I. S., Heemskerk, M. H. M., Rutten, C. E., Vidarsson, G., Hazenberg, M. D. (2025) SARS-CoV-2-specific hybrid immunity in four-dose COVID-19 mRNA vaccinated patients with hematologic malignancies. *Submitted*

Pothast, C. R., Derksen, I., van der Plas-van Duijn, A., el Hebieshy, A., Huisman, W., Franken, K.L., Neefjes, J., Luimstra, J. J., Griffioen, M., Kester, M. G., Vermeer, M. H., Heemskerk, M. H. M., Scheeren, F. A., (2025). Temperature-based MHC class-I multimer peptide exchange for human HLA-A, B and C. Elife. *Under review*

Pool, E. S., **Pothast, C. R.**, Gennesse, S., van Egmond, E. H. M., Giezen, J. M., Veld, S. A. J., Toes, R. E. M., Koning, F., Halkes, C. J. M., Heemskerk, M. H. M., Moes, D. J. A. R., Tjon, J. M-L. (2025) Selective lymphodepletion underlies the efficacy of ATGAM-based immunosuppressive therapy in aplastic anemia. *Under review*

Van Hees, E. P., Rensing, O. W., Hagedoorn, R. S., **Pothast, C. R.**, Wouters, A. K., van Amerongen, R. A., Falkenburg, J. H. F., de Groot, R., Heemskerk, M. H. M. (2025) Overcoming IFN-γ induced resistance in ovarian cancer with a double-hit: NKG2A knockout of PRAME-TCR expressing NK cells. *Under review*

Van Hees, E. P., **Pothast, C. R.**, Pool, E. S., Falkenburg, J. H. F., Melsen, J. E., Heemskerk, M. H. M. (2025) Optimal genetic engineered NK cell products are composed of CD56bright and CD56dim NK cells. *Under review*

** These authors contributed equally*

ACKNOWLEDGEMENTS

Goed wetenschappelijk onderzoek doe je nooit alleen, en is afhankelijk van vertrouwen. Ik wil iedereen bedanken die op wat voor manier dan ook heeft bijgedragen.

Bedankt aan patiënten, clinici en analisten voor de waardevolle samples.

De afdeling Hematologie: het liefst bedank ik iedereen stuk-voor-stuk, want iedereen draagt bij aan de fijne sfeer van de afdeling. We helpen elkaar, regelen zaken goed en zorgen voor gezelligheid. Esther en Ger, jullie hebben alles goed geregeld en we kunnen altijd bij jullie terecht voor (praktische) zaken. Hanny, het is chaos en ongezellig als jij afwezig bent. Bas, je bent een waardevolle ondersteuning van het lab. Michel, de betrouwbare tetrameren en je gedrevenheid zijn ontzettend waardevol. Marian, je bent een duizendpoot en denkt oplossingsgericht, aan jou heb ik altijd wat. Ook iedereen bedankt voor de discussies tijdens meetings, ik leer ontzettend veel van ieders inzichten.

Mirjam, ik ben dankbaar dat ik mijn PhD onder jouw begeleiding mocht doen. Het was een leerzame en leuke tijd, dankzij jouw goede supervisie. Je ziet onze unieke kwaliteiten, bewaakt werk/privé balans, geeft ons groeimogelijkheden en houdt ons met je pragmatische houding gefocust. Fred, als ik de rode draad kwijt was, hielp jij mij die altijd weer te vinden.

Renate, we spreken dezelfde moleculaire taal en enthousiasmeren elkaar daarin. Je legt altijd alles weer helder en geduldig uit, zelfs als het de zoveelste keer is dat ik wat vraag over pre-amplificatie. Je zorgt voor betrouwbaarheid en kennis in onze projecten. Samenwerken is efficiënt én gezellig.

Anne, bij jou is het: go big or go home. Je incubator staat altijd vol en je helpt graag iedereen tegelijk. Met je goede geheugen ben je vaak dé vraagbaak (zoals Janet uit The Good Place). Werken met jou is een feest: foute nummers, vals meezingen, weddenschapjes én een welverdiende koffie achteraf.

De peers van de afdeling: we helpen elkaar graag en bieden mentale steun. Aicha, Dyantha, Eva, Kyra, Rosa, Sietse en Wesley, jullie hebben mij aan het begin van mijn PhD gevormd. Met Els, Emma, Georgia, Ilse, Janneke, Jans, Miranda, Nadine, Neut en Tassilo is ‘collega’ eigenlijk onvoldoende: we delen lief en leed, congressen zijn vriendenuitjes, en we merken het feilloos als iemand niet in zijn/haar hum is. Zo’n hechte groep is allesbepalend.

Laura and Ferenc, I value the interesting scientific discussions, collaborations, and your support throughout my career.

Lara en Janine bedankt voor jullie vertrouwen en efficiënte samenwerking. In de hectiek van de pandemie hebben we een belangrijke boodschap weten te publiceren.

Simon en Anne (Roukens), het is niet te zien in mijn proefschrift, maar we hebben veel samengewerkt en mooie data gegenereerd. Bedankt voor deze kansen en leerzame momenten.

Cobra-Kai studieteam, vooral bedankt Mette, Caroline, Quincy en Sabine. Quincy en Sabine, ik heb ontzettend veel van jullie geleerd en we vulden elkaar goed aan. Jullie klinische kennis, Quincy's nauwkeurigheid en Sabine's projectmanagement skills waren een perfecte aanvulling. Als lotgenootjes konden we klagen en domme vragen aan elkaar stellen.

Mijn studenten: Romy, Kayleigh, Ximaine, Eline, Agnes, Sophie en Merel, ik heb van jullie veel over mijzelf geleerd en hoe ik een betere supervisor moet worden.

Ik wil mijn vrienden buiten werk bedanken voor een luisterend oor, nieuwe perspectieven, de mentale steun en de afleiding. Vooral Evelien, Heidi en Michelle: ik kan mijzelf zijn, mijn frustraties en emoties kwijt en oneindig lol met jullie hebben. Bas, Daniqua, Ilse en Michelle (D2 labratten), onze 'update-rondje' zorgt voor plezier en echte gesprekken. Iris en Natasha, het is fijn om je ei kwijt te kunnen over het PhD-leven zonder dat je collega's bent.

Mijn schoonfamilie: Jaap, Patricia, Manon, Iris, Niek, Menno en Lotte, bedankt dat jullie Joost en mij altijd steunen in wat wij ook doen (zelfs buiten een straal van 5km wonen). Jullie weten ons op de juiste momenten een zetje te geven of juist af te remmen.

Papa, mama, Nic, Femma, Fleur, Floortje en de kinderen Yae, Noa, Brenn, Meesi en Scott: woorden schieten tekort om jullie onvoorwaardelijke steun te beschrijven. Studie of baan keuze maakte nooit uit, als we maar gelukkig waren en gezelligheid belangrijk vonden. Als we elkaar zien dan vliegen dan ook de gezelligheid, grove grapjes, directe opmerkingen, gekibbel, chaos, borrels en toastjes, extreme nuchterheid mij om de oren en ben ik vergeten waarom ik mij druk maakte.

Joost, het is bijzonder dat we beiden een PhD-traject konden gaan doen en het op deze manier samen meemaken. Ik voelde mij door jou minder onzeker, eenzaam en gefrustreerd tijdens dit traject. Door de combinatie van het PhD-leven en de pandemie, moesten we soms nog leren om thuis niet óók over T-cellen en macrofagen te discussiëren. We kennen elkaar inmiddels door-en-door en ik waardeer ontzettend je nieuwsgierigheid, intelligentie, humor, gedrevenheid, zorgzaamheid, scherpzinnigheid, rust, realistische houding, stabiliteit en nog vele andere dingen. Ik heb ontzettend zin in alles wat we nog gaan beleven!